OPTIMISING THE CLINICAL ANALYSIS OF RETINAL IMAGE QUALITY IN THE HUMAN EYE

Alejandro Cerviño Expósito

Doctor of Philosophy

Aston University

January 2007

Aston University
Optimizing the clinical analysis of retinal image quality in the human eye
Alejandro Cerviño Expósito.
Doctor of Philosophy
January 2007

Thesis Summary

Visual perception is dependent on both light transmission through the eye and neuronal conduction through the visual pathway. Advances in clinical diagnostics and treatment modalities over recent years have increased the opportunities to improve the optical path and retinal image quality. Higher order aberrations and retinal straylight are two major factors that influence light transmission through the eye and ultimately, visual outcome. Recent technological advancements have brought these important factors into the clinical domain, however the potential applications of these tools and considerations regarding interpretation of data are much underestimated. The purpose of this thesis was to validate and optimise wavefront analysers and a new clinical tool for the objective evaluation of intraocular scatter. The application of these methods in a clinical setting involving a range of conditions was also explored. The work was divided into two principal sections:

1. Wavefront Aberrometry: optimisation, validation and clinical application
The main findings of this work were:

- Observer manipulation of the aberrometer increases variability by a factor of 3.
- Ocular misalignment can profoundly affect reliability, notably for off-axis aberrations.
- Aberrations measured with wavefront analysers using different principles are not interchangeable, with poor relationships and significant differences between values.
- Instrument myopia of around 0.30D is induced when performing wavefront analysis in non-cyclopleged eyes; values can be as high as 3D, being higher as the baseline level of myopia decreases. Associated accommodation changes may result in relevant changes to the aberration profile, particularly with respect to spherical aberration.
- Young adult healthy Caucasian eyes have significantly more spherical aberration than Asian eyes when matched for age, gender, axial length and refractive error. Axial length is significantly correlated with most components of the aberration profile.

2. Intraocular light scatter: Evaluation of subjective measures and validation and application of a new objective method utilising clinically derived wavefront patterns.
The main findings of this work were:

- Subjective measures of clinical straylight are highly repeatable. Three measurements are suggested as the optimum number for increased reliability.
- Significant differences in straylight values were found for contact lenses designed for contrast enhancement compared to clear lenses of the same design and material specifications. Specifically, grey/green tints induced significantly higher values of retinal straylight.
- Wavefront patterns from a commercial Hartmann-Shack device can be used to obtain objective measures of scatter and are well correlated with subjective straylight values.
- Perceived retinal straylight was similar in groups of patients implanted with monofocal and multifocal intraocular lenses. Correlation between objective and subjective measurements of scatter is poor, possibly due to different illumination conditions between the testing procedures, or a neural component which may alter with age.

Careful acquisition results in highly reproducible *in vivo* measures of higher order aberrations; however, data from different devices are not interchangeable which brings the accuracy of measurement into question. Objective measures of intraocular straylight can be derived from clinical aberrometry and may be of great diagnostic and management importance in the future.

Keywords: wavefront aberrations, intraocular scatter, retinal image quality

A mis padres,

Jose Maria y Ana Isabel

"La página escrita no expresa lo mucho que se ha intentado,
sino lo poco que se ha conseguido"

"The written page does not express how much has been attempted,
but how little has been accomplished"

Antonio Machado

(1875-1939). Spanish writer

ACKNOWLEDGEMENTS

I would like to thank my supervisor Dr. Sarah L. Hosking, for guiding me through this project, for giving me the best advice at the right moment, support, and for being so patient with me and the continuous problems that aroused throughout these years. I am greatly indebted to Prof. Bernard Gilmartin, for being my advisor in previous stages giving me greatly appreciated advice, expertise and support and for being my supervisor in the final stages of the thesis.

I am extremely grateful to my colleagues from the University of Santiago de Compostela, in Spain, particularly with Prof. Eva Yebra-Pimentel and Prof. Manuel A. Parafita Mato, for being so supportive and understanding during my stay in the UK. Their behaviour has been extraordinary.

I am fully indebted to Aston University, and particularly to the School of Life and Health Sciences. The many friends I made here were essential to make my stay and my work come to a good term. Special thanks go to the staff at the Academy of Life Sciences, for their smiles, their great help and for creating the best atmosphere I could wish for in a working environment. I thank Dr. Mark Dunne for letting me use the model eye for some of the studies.

Very special thanks go to my "little sisters", Gurjeet Rai and Sandra Benavente, as well as to Martin Cardall and Parth Shah. This project would have been impossible to accomplish without them.

To the late Neuroscience Research Institute, for giving me the doctoral grant that allowed the consecution of this project.

I'm very grateful to Prof. Jorge L. Alio and all the staff at VISSUM/Instituto Oftalmológico de Alicante for allowing me to stay and collaborate with them and providing with the pseudophakic patients seen for one of the studies.

Very special thanks go to my great friend Dr. Dheeraj Bansal, who allowed me to use his priviledged brains to develop the software tool used in some of the studies of this thesis.

Another very special thanks go to all my life-long friends, as well as my many new friends at Aston, because their friendship has been essential to keep the mood high. I would like to thank specially my best man, Dr. Jose M. Gonzalez-Meijome, for listening to me when I was down and giving the best advice every time I needed it.

And last but not least, to the people I love and care about the most. To my parents for making me the way I am, for doing everything they could to help me reach my targets, and for their love and continuous support regardless the decisions I make. To my sisters for giving me their love and joy, and for being my greatest pride. To Evelyn for taking care of me, for loving me and for accepting the long hours and frequent trips I had to make during the last stages of this project.

CONTENTS

LIST OF ABBREVIATIONS

HOA – Higher order aberrations

PSF – Point spread function

HS – Hartmann-Shack

RMS – Root mean square

HO RMS – higher order root mean square

Log(s) – logarithmic units of straylight

Max_SD - Maximum SD of the pixel values within a lenslet PSF neighbourhood for all the PSFs in the HS image

ESD – Expected standard deviation

CoV – Coefficient of variation

$CoR_{w/in}$ – Intrasession coefficient of repeatability

CoR_{btw} – Intersession coefficient of repeatability

LIST OF EQUATIONS

LIST OF TABLES

LIST OF FIGURES

CHAPTER 1. INTRODUCTION

Visual processing can only begin once light emitted, reflected and transmitted by objects or surfaces from the physical environment reaches the neuroretina. To obtain useful information, the visual system must then classify and codify the many aspects that constitute the visual image resulting in a meaningful visual percept. There are a multitude of physical and physiological aspects of the visual system which limit its performance. These can be categorised in two main areas: first, those anatomical features of the eye itself which limit the transmission of light to the neuroretina before processing can begin, and secondly, the neural transmission of these signals through the remainder of the visual pathway to the visual cortex, resulting in visual perception. Human vision is dependent on both light and neuronal transmission and any diseases or obstacle that precludes either process will result in compromised visual perception.

This thesis is concerned with those aspects of the visual pathway which affect the optical quality of the retinal image prior to neural processing. Specifically, factors which limit light transmission through the eye, including optical defects such as refractive errors and wavefront aberrations, and intraocular light scatter arising from imperfect surfaces or lack of tissue clarity.

1.1. WAVEFRONT ABERRATIONS

Wavefront aberrations are those aspects of optical transmission which result in an image of lesser quality than would be expected from the perfect optical system in which the rays forming the image coincide at a single point. They are a result of the lack of homogeneity of the ocular media as well as local irregularities of the optical surfaces and are specific to each individual. The wave aberration function, $W(x,y)$, is defined as the distance, in optical length from the reference sphere to the wavefront in the exit pupil measured along the ray as a function of the transverse coordinates (x,y) of the ray intersection with a sphere centred on the ideal image point.

The human eye presents numerous refractive defects, including off-axis aberrations, even on the visual axis(Artal, Santamaria, and Bescos, 1988a; He et al., 1998; Iglesias, Berrio, and Artal, 1998; Liang et al., 1994; Liang and Williams, 1997; Mierdel et al., 1997; Navarro and Losada, 1997; Walsh, Charman, and Howland, 1984), and high variability between subjects and eyes(Marcos et al., 2001b) . That is due to the fact that the visual axis does not coincide with the optical axis (this is usually displaced about 5^{o} nasally), and that the optical surfaces do not have revolution symmetry and are decentred and tilted with respect to each other. On the other hand, the retinal radius of curvature makes the eye an almost homocentric system, so the system compensates very well for field curvature aberration.

Aberrations can be classified by their order. The first order aberrations are defocus and longitudinal chromatic aberrations; the third order aberrations (or Seidel's) are spherical, astigmatism, coma, distortion and field curvature; the fifth and higher orders include, besides spherical and astigmatism, combinations between them and other irregularities (in non-centred systems or without revolution symmetry, or defective) (figure 1.1).

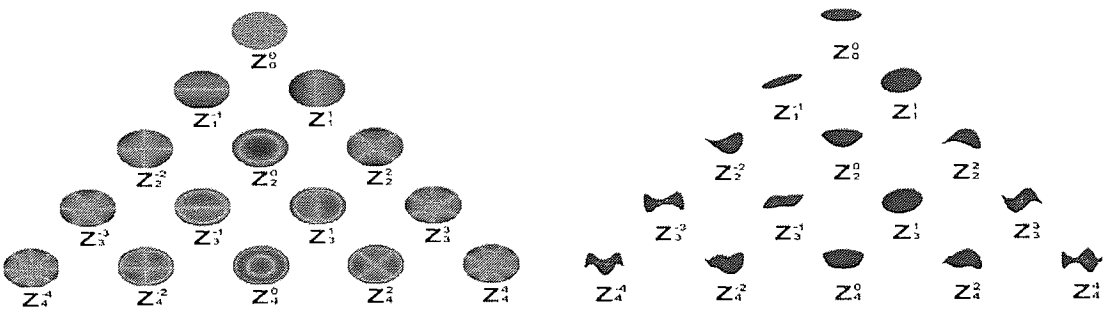

Figure 1.1. *Pyramid of Zernike polynomials up to the fourth order in two (left) and three dimensions (right). Images obtained with Vol-CT software v.6.89 (Sarver and Associates, Inc, USA).*

1.1.I. MONOCHROMATIC ABERRATIONS

Seidel was the first to establish a classification for monochromatic aberrations, although he did not define them mathematically. The usual way of referring to ocular wavefront aberrations, and the one recommended standard by the Optical Society of America(Thibos, 2001), is to classify them according to the Zernike description (see epigraph 1.1.III), as summarised in Figure 1.1. For a detailed review of monochromatic optical aberrations and their representation there are comprehensive reviews by Atchison(Atchison, 2004) and Charman (Charman, 1991), however a brief summary is provided below.

Order 0

- ***Piston.***

Is the lack of aberration, the shape of a wavefront passing through a theoretically perfect eye with no aberrations, i.e. a flat plane.

1st Order

- ***Tilt.***

Is an aberration located on the x or y axis. It is linear, and can be defined using the Zernike polynomials Z_{-1}^{1} and Z_{1}^{1}. Tilt has no impact on the quality of the retinal image.

2nd Order

- ***Defocus.***

This is the most common and can be positive or negative resulting in simple hyperopia or simple myopia respectively. The wavefront is perfectly spherical, but converges before (myopia) or after (hyperopia) reaching the retina. The retinal image is also defocused when the accommodation mechanism fails permanently (presbyopia) or temporally such as in accommodative spasm and other accommodative anomalies. Whereas the effect of defocus on the retinal image is clearly significant in those subjects with ammetropia, inaccurate accommodative responses in emmetropes can affect the quality of the retinal image in near tasks.

Defocus is defined by the Zernike polynomials term Z_{0}^{2}.

- ***Astigmatism***

The presence of astigmatism in both foveal and peripheral vision is well known, although the nature of the aberration is very different in each case. For the fovea, the astigmatism occurs as a result of the lack of symmetry of the optical surfaces of the eye, mostly of the cornea, which generally has a prolate ellipsoidal shape that is of great importance in the optimisation of ocular optical quality, and also from decentration and tilts of optical components. It is relatively rare to find an eye completely free of astigmatism; commonly values are between 0.25 and 1D. This aberration can be compensated with cylindrical lenses.

The Zernike polynomials defining the astigmatism would be those of term Z_{-2}^{2} for the oblique component (corresponding to 45^{0} and 135^{0} meridians) and term Z_{2}^{2} for the horizontal and vertical component (corresponding to 90^{0} and 180^{0} meridians) of the astigmatism.

Peripheral astigmatism is similar to the defect produced in any optical system when working off-axis, increases with retinal eccentricity and is variable between subjects. It eventually appears as a result of surgical procedures, such as cataract removal, penetrating keratoplasty and most other surgeries with corneal intervention, but it is also present as a inherent aberration. This kind of astigmatism would not correspond to 2^{nd} order aberrations, and would be included in the group of higher order aberrations (HOA).

3rd Order

From the 3^{rd} order onwards the aberrations are considered to be HOA, the higher the order the least impact it has on the image quality. The relative impact of HOA is better characterized by their effects on the modulation transfer function (MTF) rather than from their absolute values in the pupil plane (Guirao et al., 2002).

- ***Coma***

Aberration located on the X or Y axis. Coma has a comet-shaped pattern on the emmetropic plane. The wavefront is asymmetric. Its presence would be predictable

though, due to the imperfections of the optical elements of the eye and their lack of symmetry.

Primary coma would be represented by the Zernike polynomials Z_{-1}^{3} (X axis) and Z_{1}^{3} (Y axis).

4th Order

- ***Spherical aberration***

Spherical aberration may be defined as a relative defocus of the rays entering the pupil at different distances from the center (i.e., as a function of the radius). The peripheral wavefront has a different radius of curvature than that formed in the central area, although both may have perfect sphericity. The most common method of measuring spherical aberration is to centre artificial pupils of different radii on the axis and for each pupil determine refraction (objectively or subjectively). If the peripheral rays are brought to focus anterior to the central rays the aberration is positive.

Spherical aberration has been proposed as an explanation for nocturnal myopia, since pupil enlargement at night results in the best image plane being displaced from the retina. Nevertheless, in diurnal vision, a pupil diameter of 2mm or less has a negligible effect on spherical aberration.

Spherical aberration is represented by the Zernike term Z_{0}^{4}.

5th Order and above

Including only aberrations higher than the fourth order, these are an amalgam of irregular aberrations that arise commonly from localized surface variations. In normal eyes they do not significantly degrade the quality of the retinal image.

1.1.II. CHROMATIC ABERRATIONS

Chromatic aberrations arise from the dispersion of light by the refracting elements. There are two types: chromatic variations in the paraxial properties of the optical system, and wavelength dependence of the monochromatic aberrations. Only the first type has been characterized in the human eye and can be classified into two components:

Longitudinal or axial chromatic aberration

Longitudinal, or axial, chromatic aberration results from a relative defocus of the retinal image of wavelengths with respect to each other and is due to differential chromatic dispersion of the ocular media. Due to the similarities in composition of the ocular media both within- and between- populations chromatic aberration exhibits very low variability within populations (Charman and Jennings, 1976; Howarth and Bradley, 1986; Marcos et al., 1999; Rynders, Navarro, and Losada, 1998), being of the order of 2D across the visible spectrum. Short wavelength cones, with peak sensitivity in the blue range, are much less frequent, which reduces the impact of chromatic defocus, whereas cones in the longer wavelengths (red/green), exhibit a chromatic difference of only 0.5D or less. In this way the impact of chromatic aberration is greatly reduced. A potential consequence of this is that vision in the blue range is relatively compromised, however since blue frequently appears as a background in nature, the greater sensitivity is more essential for longer wavelengths providing critical vision.

Transverse chromatic aberration

Transverse chromatic aberration (TCA), also termed *magnification* chromatic aberration, is essentially the distortion between two different wavelengths at the fovea. Using a small diaphragm in front of the eye it is possible to eliminate it by decentring the diaphragm slightly with respect to the pupil. The point at which it is cancelled out is known as the achromatic axis, being the one closest to the optical axis, but not actually coinciding with the axis.

TCA is highly variable between subjects(He et al., 1998; Howland and Howland, 1976; Liang and Williams, 1997; Marcos and Burns, 2000; Marcos et al., 1999; Marcos et al., 2001b; Rynders et al., 1995; Simonet and Campbell, 1990; Thibos et al., 1990) and between eyes (Marcos et al., 2001b). Irregularities in the central corneal region have been proposed as a possible source of TCA (Marcos et al., 2001b).

1.1.III. REPRESENTATION OF ABERRATIONS – ZERNIKE POLYNOMIALS

The Zernike polynomials describe a group of orthogonal functions over a circular pupil with a radius of one unit, and were introduced by Zernike in 1934 (Zernike, 1934).

Often, only a limited number of Zernike modes are necessary to provide a good representation of ocular aberrations. If these modes are corrected by Adaptive Optics an almost diffraction-limited image quality is obtained.

The use of Zernike coefficients is recommended by the Optical Society of America as the standard method for specifying the eye's wavefront aberration (Thibos et al., 2002). They have the advantage that the value of each mode's coefficient represents the root-mean-square (RMS) wavefront error (WFE) attributable to that mode (Thibos, 2001; Thibos et al., 2002)and is valuable for describing and comparing ocular wavefront aberrations in large populations (Porter et al., 2001). Following normalisation (see below), the Zernike polynomials can be described as follows in polar coordinates *(ρ, θ)*, where ρ is the radial coordinate ranging from 0 to 1, and θ is the azimuthal component ranging from 0 to 2π(Thibos, 2001). Each of the Zernike polynomials consists of three components: a normalization factor, a radial-dependent component and an azimuthal-dependent component.

$$Z_n^m(\rho,\theta) = \begin{Bmatrix} N_n^m R_n^{|m|}(\rho)\cos m\theta; \nabla m \geq 0 \\ -N_n^m R_n^{|m|}(\rho)\sin m\theta; \nabla m < 0 \end{Bmatrix} \quad \text{eq.I.1}$$

The radial part, $R_n^{/m/}(\rho)$ is a polynomial, whereas the azimuthal component is sinusoidal. A double indexing scheme is useful for unambiguously describing these

functions, with the index n describing the highest power (order) of the radial polynomial and the index m describing the azimuthal frequency of the sinusoidal component:

$$R_n^m(\rho) = \sum_{s=0}^{(n-|m|)/2} \frac{(-1)^s \cdot (n-s)}{s!\left[\frac{(n+m)}{2}-s\right]!\left[\frac{(n-m)}{2}-s\right]!} \cdot \rho^{n-2s} \qquad \text{eq.1.2}$$

and the normalization component, N_n^m , is written as:

$$N_n^m = \sqrt{\frac{2(n+1)}{1+\delta_{m0}}} \qquad \text{eq.1.3}$$

where δ_{m0} is the Kronecker delta function (δ_{m0}=1 for m=0, and δ_{m0}=0 for $m\neq0$).

From the definition of the polynomials, the radial coordinate ρ varies between 0 and 1. The values of n and m are always whole numbers and fulfils $m \leq n$ and $n-|m| = even$.

In practical applications a finite number of base functions are used. For this reason, the representation of the wavefront is made with an error $\Delta\phi$, which increases as the number of polynomials used for the representation decreases and also with the complexity of the wavefront pattern where other representation methods such as Fourier polynomials would be more adequate (Smolek and Klyce, 2003).

Following the standards recommended by the Optical Society of America (OSA), when describing individual Zernike terms, the two index scheme should be used, although single indexing is often found (see table 1.1 for equivalences). The coordinate system used should be a right handed system: the coordinate origin is at the center of the eye's entrance pupil, the +x axis is horizontal pointing to the right, the +y axis is vertical pointing up, and the +z Cartesian axis points out of the eye and coincides with the foveal line-of-sight in object space as shown in figure 1.2 (Thibos et al., 2002).

Number	n	m	Radial polynomial	Common name
0	0	0	1^(1/2) (1)	Piston
1	1	-1	4^(1/2)(1ρ)sin(θ)	Tilt about y axis
2	1	1	4^(1/2)(1ρ)cos(θ)	Tilt about x axis
3	2	-2	6^(1/2)(1ρ^2)sin(2θ)	Cylinder with axis at ±45°
4	2	0	3^(1/2)(2ρ^2-1)	Defocus
5	2	2	6^(1/2)(1ρ^2)cos(2θ)	Cylinder with axis at 0/90
6	3	-3	8^(1/2)(1ρ^3)sin(3θ)	Trefopil on x axis
7	3	-1	8^(1/2)(3ρ^3-2ρ)sin(θ)	Coma along x axis
8	3	1	8^(1/2)(3ρ^3-2ρ)cos(θ)	Coma along y axis
9	3	3	8^(1/2)(1ρ^3)cos(3θ)	Trefoil on y axis
10	4	-4	10^(1/2)(1ρ^4)sin(4θ)	Tetrafoil on x axis
11	4	-2	10^(1/2)(4ρ^4-3ρ^2)sin(2θ)	Astigmatism
12	4	0	5^(1/2)(6ρ^4-6ρ^2+1)	Spherical aberration
13	4	2	10^(1/2)(4ρ^4-3ρ^2)cos(2θ)	Astigmatism
14	4	4	10^(1/2)(1ρ^4)cos(4θ)	Tetrafoil on y axis

Table 1.1. *Zernike polynomials up to the fourth order with classical description (Z_n^m): n gives the radial order and m the angular frequency.*

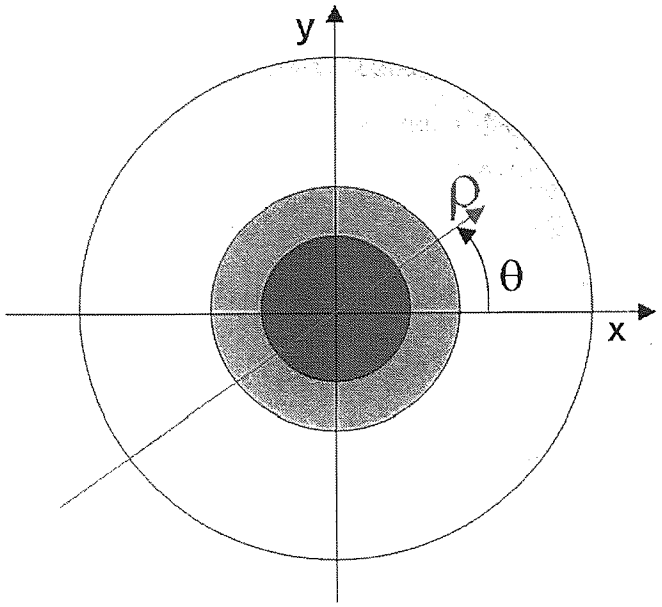

Figure 1.2. *Coordinate system for Zernike polynomials recommended by the OSA for reporting ocular wavefront aberrations (Thibos et al., 2002).*

The RMS is used to describe two different contexts. The first quantifies a fitting error associated with wavefront reconstruction and so describes the quality of the least squares fit. The second relates to how the reconstructed wavefront differs from a perfect wave. Thus, the RMS provides a general estimate of the variation of the wavefront from the ideal. However, for low levels of WFE, RMS values have been reported not to be good predictors of visual acuity (Applegate et al., 2003a; Applegate et al., 2003b; Applegate, Sarver, and Khemsara, 2002) as for an equal amount of RMS not all Zernike coefficients induce equivalent losses in high and low contrast logMAR acuity(Applegate, Sarver, and Khemsara, 2002).

1.2. MEASURING OCULAR WAVEFRONT ABERRATIONS

Two major developments have, in recent years, increased activity in clinical visual optics: refractive surgery and the application of the adaptive optics to the eye. The advance in surgical techniques for modifying the optics of the eye have renewed interest in developing accurate, reproducible techniques for measuring the wavefront aberrations of the human eye as well as for studying changes in the optics of the eye under different conditions such as the effects of ageing, pathology or accommodation. As discussed earlier, the human eye presents a variety of aberrations (Artal, Santamaria,

and Bescos, 1988b; He et al., 1998; Howland and Howland, 1977; Iglesias, Berrio, and Artal, 1998; Liang et al., 1994; Liang and Williams, 1997; Mierdel et al., 1997; Navarro and Losada, 1997; Walsh, Charman, and Howland, 1984) that exhibit high variability between subjects and between eyes(Marcos et al., 2001b). Over recent years several devices have used different design principles to measure these aberrations in clinical settings with the ultimate aim of making aberration measurement a part of everyday clinical practice.

Wavefront aberrations may be defined as anything differing from the perfect optical system in which the rays forming the image of a point in the object plane coincide at a single point in the image plane. They result from a lack of homogeneity in the ocular media, as well as local irregularities of the optical surfaces.

1.2.I. OPTICAL PRINCIPLES OF WAVEFRONT SENSORS

Some of the instruments used for wavefront aberration measurement analyze an image on the retina whereas some others place a source of light on the retina and analyze the wavefront as it leaves the eye.

Almost all the methods used for the clinical determination of wavefront aberrations of the eye are based on ray tracing and the reconstruction of the original wavefront from local slopes (Howland, 2000). The aberrations are derived for various points in the pupil and, typically using least squares, are converted into wave aberration functions. Interferometric methods have the difficulties of stabilization which is the reason they are not used for clinical ocular measurements of aberration.

Original aberrometry techniques used subjective methods of measurement which required the subject to report directly the alterations. These original methods subsequently led to objective methods of measurement. Representative examples of subjective aberrometers are: a) The Tscherning aberroscope (Howland, 2000), b) Howland's cross-cylinder technique (Atchison et al., 1995; Howland and Howland, 1977) and, c) the spatially resolved refractometer (SSR) (Burns, 2000; Marcos et al., 1999); each have well documented use in research (Calver, Cox, and Elliott, 1999;

Collins, Wildsoet, and Atchison, 1995; He, Burns, and Marcos, 2000; Marcos, 2002; Marcos et al., 2001a; Marcos and Burns, 2000; Marcos et al., 1999; Marcos et al., 2001b; McLellan, Marcos, and Burns, 2001; Villegas and Artal, 2003; Walsh and Charman, 1985).

1.2.I.i. TSCHERNING'S ABERROSCOPE

Tscherning's principle was first used by the end of the 19th century with what is known as Tcherning's aberroscope. A grid in the pupil plane was shadowed with a +5.00D lens on the subject's retina while fixating a distant point; the aberrations could be then inferred from the distortion of the grid (Atchison et al., 1995; Howland, 2000; Mrochen et al., 2000). This aberroscope provided the design principle for some modern objective aberrometers currently used in practice and mentioned below.

1.2.I.ii. CROSS-CYLINDER TECHNIQUE

Bradford Howland developed this technique in 1960 initially for testing the quality of camera lenses (Howland, 2000). It is a modification of Tscherning's aberroscope having several advantages such as a sharper grid which clearly indicated a zero defocus point. A cross cylinder of +/- 5.00 diopters was used to shadow a grid on the retina. It was first used to determine subjectively the wavefront aberrations of the human eye (Howland and Howland, 1976; Howland and Howland, 1977) and its first objective version was described in 1984 (Walsh, Charman, and Howland, 1984) and incorporated a second ophthalmoscopic channel to capture the retinal image. The reconstruction algorithms were improved to achieve more reliable results (Smith, Applegate, and Howland, 1996) although the results for detection of variability between eyes were found to be slightly worse than with other objective techniques (Hong et al., 2003).

1.2.I.iii. SPATIALLY RESOLVED REFRACTOMETER

Based on Scheiner's principle and described by Smirnov (Smirnov, 1961), the spatially resolved refractometer (SRR) allows a psychophysical measurement of ocular wavefront aberrations. The principle is relatively simple: a reference centred aperture and a peripheral sub-aperture allow two parallel laser beams to pass through the ocular

media and be projected on the subject's retina. Depending on the aberration at the point measured, the retinal spots will be separated. Changing the angle of the peripheral illumination source allows the retinal spots to be brought together. Measuring the angle needed to have a single retinal spot, the aberration components relative to that pupil location can be calculated. By sampling a number of points the wavefront can be reconstructed (figure 1.3). The results obtained with this subjective technique have been reported to closely match those obtained with other objective methods (Moreno-Barriuso et al., 2001b). Currently, the Emory Vision InterWave scanner (Emory Vision, Atlanta, Ga) is the only clinical wavefront sensor using this principle.

The method requires the patient to align the two points in the presence of local aberrations using a joystick. Although originally it was a psychophysical task that required an input from the subject an objective version has been also described (Webb et al., 2003). The device has been used to plan customised LASIK treatments, as well as to detect corneal ectasiae(Lichter et al., 2002; Randleman, Thompson, and Staver, 2004; Russell, Stulting, and Thompson, 2003; Thompson et al., 2004).

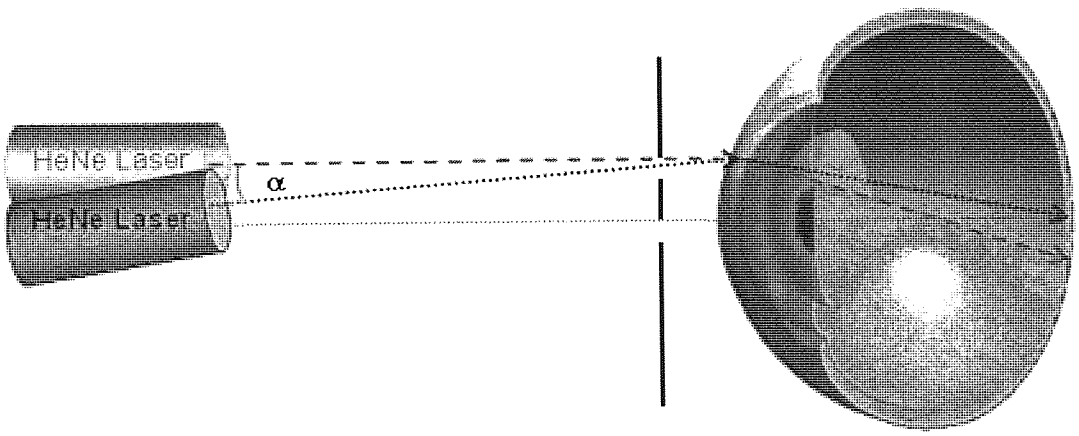

Figure 1.3. *Diagram representing the basic functioning of the principle used by the SRR. When parallel to the axis the incident peripheral beam (dashed line) does not fall on the same retinal spot as the central beam (dotted line). Varying the incident angle α of the peripheral beam until retinal incidence overlaps with that from central beam allows determination of optical behaviour at that particular peripheral location.*

This principle also set the basis for the ray tracing objective aberrometers described later.

The objective methods used currently in clinical practice and resulting from these original techniques are: d) Tscherning's principle-based, e) Laser ray tracing, f) Hartmann-Shack (HS) principle-based, and g) Skiascopy principle-based.

Several classifications have been made to group the systems using different principles according to the direction of the light analyzed (e.g. ingoing or outgoing, as mentioned earlier) or the way the data from the different locations is collected (e.g. sequential or simultaneous). Here, former will be used, depending on whether they analyze the light going into the patient's eye (ingoing), i.e. the retinal image, or the light coming out of the patient's eye (outgoing).

Table 1.2 shows some detailed information pertaining to the sensors currently used by the different commercially available clinical wavefront analyzers.

	Wavescan	Zywave	COAS	Ladarwave	KR-9000 PW	OPD scan	Allegro	Tracey
Manufact	VISX	B&L	Wavefront Sciences	Alcon	Topcon	Nidek	Wavelight	Tracey Tech.
Principle	HS	HS	HS	HS	HS	Dynamic skiascopy	Tscherning	Ray tracing
Min. Pupil Ø	5-6 mm	2.5-8.5 mm 6 mm for Zernike	n/a	2.5 mm 6.5 mm	4mm (up to 4th order) 6mm (up to 6th order)	2.6 mm	n/a	n/a
Dynamic Range	+6.0 to -8.0	+6.0 to -12.0D	+7.0 to -15.0D	+15.0 to -15.0D +8.0 to -14.0D	+15.0 to -15.0D	+22.0 to -20.0D	+6.0 to -12.0D[23]	+15D to -15D SE
Cylinder		≤ 5.0D	≤ 5.0D	≤ 8.0D	≤ 7.0D	≤ 12.0D	≤ 4.0D	n/a
Sampling points (7mm pupil Ø)	240	70-75	800	204-213	85	1440	96	64 95 optionally
Fogging	Auto	Auto	1.5D, fixed	Auto	n/a	n/a	n/a	n/a
Capture time	n/a	n/a	n/a	n/a	n/a	≤ 0.4 sec	≤ 0.4 sec[23]	< 0.5 sec

	Wavescan	Zywave	COAS	Ladarwave	KR-9000 PW	OPD scan	Allegro	Tracey
Repeat. (full pupil size)	n/a	±0.25D SE[†], ±0.29D sphere, ±0.29D cyl[45*]	±0.10D[†] ±0.24D w/o cyclo ±0.12D cyclo[46]	n/a	n/a	n/a	n/a	+/- 0.10D[†]
Accuracy (S,C,A)	n/a	n/a	±0.15D (-14 to +6D, incl. ±3D cyl) ±0.5D (-15 to +7D incl. ±5D cyl)[†]	n/a	n/a	±0.50D (> 10D)[†] ±0.25D (0 to ±10D)[†]	n/a	+/- 0.10D[†]
Chart type	n/a	Scenery	Circular grid	n/a	n/a	Scenery	Star on LED	n/a
Laser λ	785nm	785 nm	830 nm	820 nm	840 nm	808 nm	660 nm	650 nm
HO Ab	Up to 6th order	Up to 5th order	Up to 10th order	Up to 8th order	Up to 6th order	Up to 8th order	Up to 6th	

Table 1.2.- *Details of commercially available wavefront sensors used in clinical devices. Note that only the manufactures of the sensors are listed, some of them are distributed by different companies under different names.*

* Results obtained under cyclopegia.
† Data obtained from the manufacturer

1.2.II. INGOING SYSTEMS

The systems classified into this group measure wavefront data based on retinal imaging, that is, the system measures the position of the laser beam projections on the patient's retina, analyzes a retinal spot distribution and calculates the wavefront.

1.2.II.i. TSCHERNING PRINCIPLE-BASED

This method is based on Tscherning's aberroscope described above although this method is objective. The current clinical devices using this principle employ a dot pattern mask which allows several laser rays from the original beam to reach the eye and be projected on the retina. Five to ten frames of the image formed on the retina are captured and defined through a very small aperture. The degree to which the frames are deformed will depend on the aberrations produced by the eye under examination (Kaemmerer et al., 2000; Mrochen et al., 2000) (figure 1.4).

The deviation of each retinal spot from its equivalent in the ideal reference image is measured and processed to give local slopes and hence the wavefront aberration profile. Provided aberrations are not very high it will be clear which image point coincides with a given pupil position (see advantages and disadvantages section below).

Reports on this method confirm good reproducibility for spherocylindrical refraction and total RMS values for HOA on human eyes(Mrochen et al., 2000).

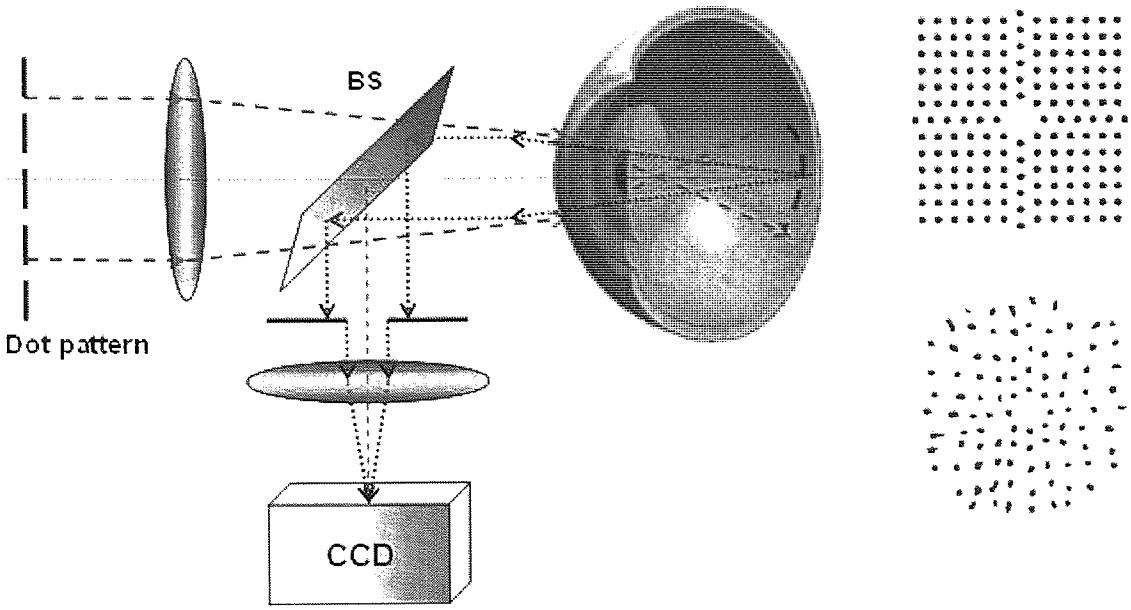

Figure 1.4. *Diagram representing the basic functioning of the aberrometers using Tcherning's principle (left), and an example of a reference grid (top right) and distorted grid on an aberrated eye (bottom right). The dot pattern is projected on the retina (red dashed line) and the image is captured through a small aperture ophthalmoscopic system using a beam splitter (BS)*

Wavelight Laser Technologie AG is, to the author's knowledge, the only manufacturer of sensors using this principle for clinical purposes. It was developed by Mierdel et al.(Mierdel et al., 2001; Mierdel et al., 1997) and successfully used for performing customized ablations (Mrochen, Kaemmerer, and Seiler, 2000; Mrochen, Kaemmerer, and Seiler, 2001).

1.2.II.ii. RAY TRACING

In this technique, a combination of methods from the SRR and Tscherning techniques is used such that the laser beam is projected onto the retina, parallel to the visual axis, at several points on the eye entrance (figure 1.5).

Unlike the Tscherning devices, only one laser beam is projected each time, making a rapid point-by-point scanning by successive laser beams and generating a complete pattern of retinal projections in just a few milliseconds. The system then generates maps showing the optical performance of the visual system. Unlike the SSR, the retinal spot is not displaced towards the reference by modifying the entrance angle, but the distance to the retinal reference, or ideal spot location, is measured and used to compute the aberration(Molebny et al., 2000).

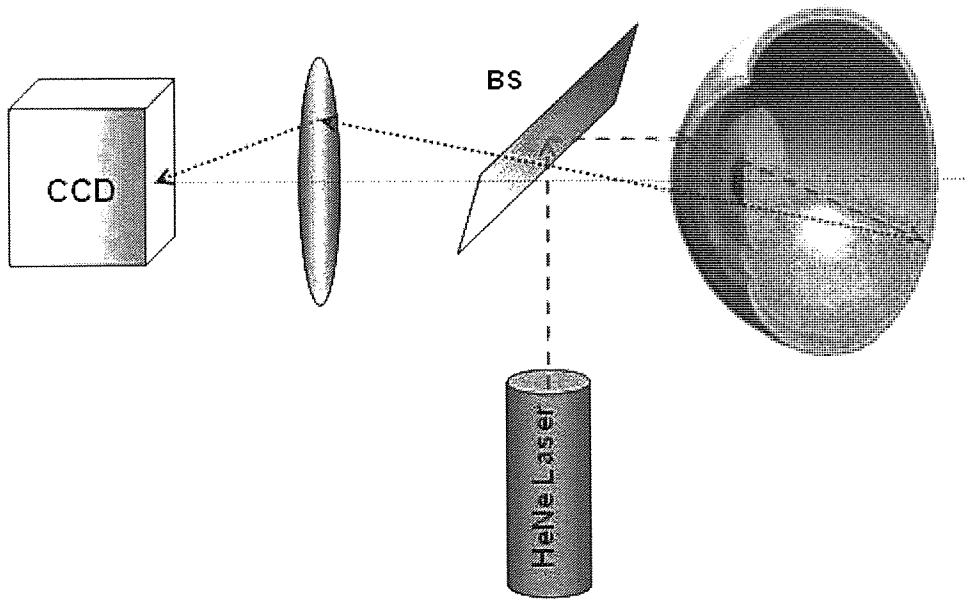

Figure 1.5. *Diagram representing the basic functioning of the aberrometers using laser ray tracing. A laser beam is projected at a specific pupil location each time, the location of the beam reflected back is recorded by a CCD camera to determine the optical behaviour at that pupil location.*

In laboratory settings this method showed results in good agreement with other techniques such as Hartmann-Shack (HS) or SRR(Moreno-Barriuso et al., 2001b) and has proven to be robust and reliable for the evaluation of changes in ocular wavefront following surgery(Moreno-Barriuso et al., 2001a).

The main advantage of the technique is that the sequential projection of the laser beam avoids the possibility of overlapping of neighbouring images, allowing the measurement of relatively high aberrations with a higher level of confidence.

Tracey Technologies Inc is, to the author's knowledge, the only manufacturer of sensors using this principle for clinical purposes. This system has shown good performance for sphero-cylindrical determination, in close match with clinical HS sensors (Wang, Wang, and Koch, 2003). In studies with earlier versions the Tracey device was found to give accurate(Wang et al., 2002) and highly reproducible (Molebny et al., 2000; Pallikaris, Panagopoulou, and Molebny, 2000; Wang et al., 2002) measurements. The same was found with a later version (Wang, Wang, and Koch, 2003). The system has a multiple acquisition mode that allows a rapid screening of aberration changes such as those occurring during dynamic accommodation responses (Pallikaris et al., 2001).

1.2.III. OUTGOING SYSTEMS

1.2.III.i. HARTMANN-SHACK PRINCIPLE BASED

Hartmann-Shack (HS), as it is widely known, is the more popular technology for wavefront analysis. In 1900, Hartmann designed a disc, based on Scheiner's disc, in which he drilled several holes. He used it for measuring the optical quality of lenses by tracing the emerging light rays. Some time later, Shack inserted microlenses in the holes. From that point, the technique was known as Hartmann-Shack (or Shack-Hartmann) method (Platt and Shack, 2001). It has been widely used in the past for astronomical observation and around ten years ago Liang first applied the technology successfully to the human eye (Liang et al., 1994).

If a wavefront is divided spatially then each subdivision can be approximated to a tilted perfect wave (i.e. flat). The reconstruction of the tilts for every division will result in an approximation to the original wavefront (Thibos, 2000). This is the principle on which the HS based wavefront analyzers rely. The sensor consists of a lenslet array, for the wavefront decomposition and focusing of the secondary wavefronts from each subaperture, and a detector. (figure 1.6)

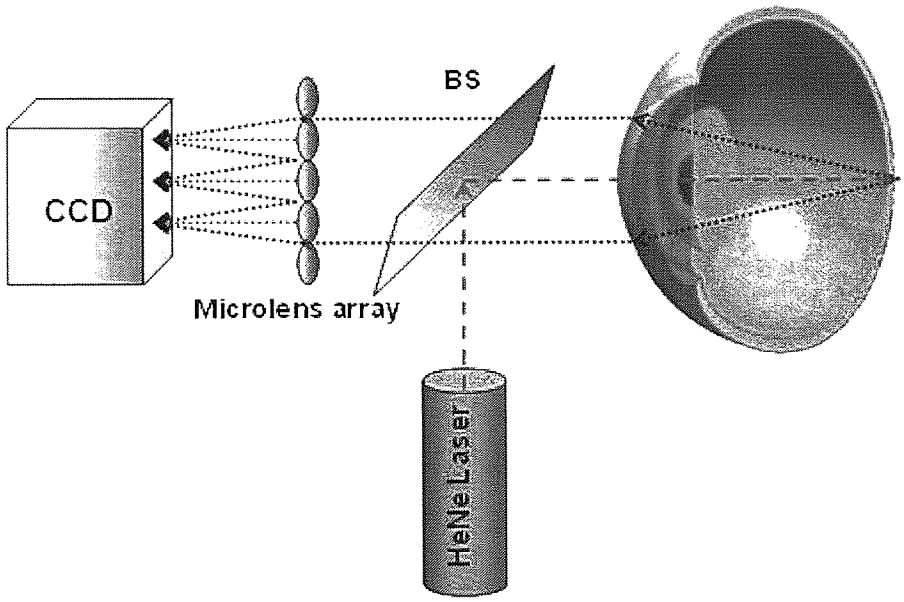

Figure 1.6. *Diagram representing the basic functioning of the aberrometers using HS principle. A laser source is placed on the retina using a beam splitter (BS) (dashed line), and from this point source a wavefront is transmitted through the ocular media, split into small secondary wavefronts by a microlens array and the image then captured by a CCD camera.*

The main difference between the various sensors that use the same principle is spatial resolution which is limited by the microlens size and number and the number of modes used to fit the wavefront (Prieto et al., 2000) (figure 1.7). The physical limitation required for a lenslet array to obtain local slopes, and the cost of manufacturing the microlenses conforming this lenslets make it difficult to establish a balance between

financial outlay and resolution when attempting to optimise performance for clinical purposes.

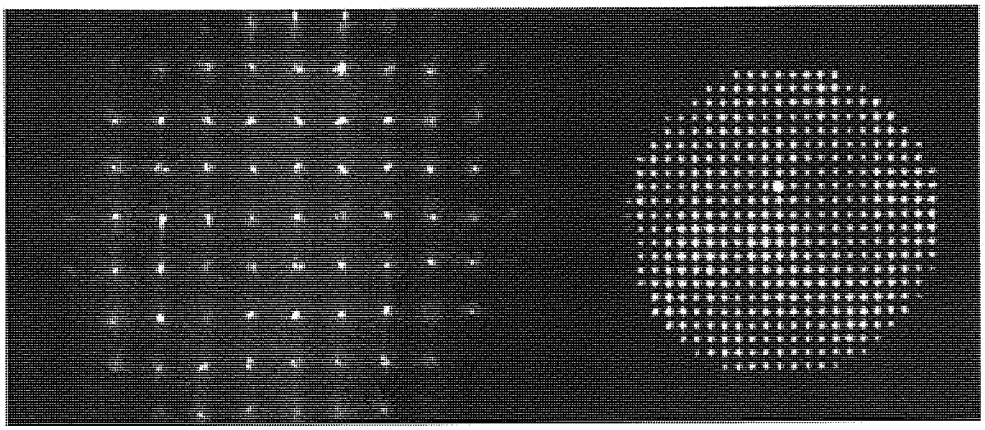

Figure 1.7. *HS pattern obtained from two different clinical sensors commercially available. Note the differences in spatial resolution.*

HS based aberrometers are by far the most commonly used in clinical settings and the most prevalent in research literature. In laboratory settings, the performance of HS sensors has been found to be better in the discrimination of WFE between eyes than the objective cross-cylinder technique(Hong et al., 2003) and to be in good agreement with Smirnov's psychophysical test (Salmon, Thibos, and Bradley, 1998), laser ray tracing (Moreno-Barriuso et al., 2001b; Moreno-Barriuso and Navarro, 2000) and SRR(Moreno-Barriuso et al., 2001b). Also, studies report very good repeatability (Liang and Williams, 1997; Salmon, Thibos, and Bradley, 1998) and accuracy (Liang and Williams, 1997) of HS measures.

There are relatively few studies regarding the performance of clinical HS devices, and these are mainly directed towards the determination of low order aberrations. However, HS based wavefront sensors have been shown to be highly accurate and reproducible in the determination of refractive error (Wang, Wang, and Koch, 2003), and perform similar to, or better than, autorefractors (Hament, Nabar, and Nuijts, 2002; Salmon et al., 2003).

Regarding HOAs, clinical HS sensors show low variability (Cheng et al., 2004b). Nevertheless, these results cannot be applied to all commercially available HS devices since differences between different clinical sensors are evident in the determination of HOAs mainly due to the spatial resolution and reconstruction algorithms. In fact, some of the clinical commercially available sensors have shown poor repeatability for the determination of HOAs, particularly when in small amounts (Mirshahi et al., 2003) suggesting the need for multiple acquisition of measurements to achieve a more reliable result. In the evaluations using model eyes, the performance of just one commercially available clinical aberrometer, the COAS (Wavefront Sciences, USA) is documented and it was found to give highly accurate and reproducible(Cheng et al., 2003) measures of HOA.

To the author's knowledge current manufacturers of sensors using the HS for clinical purposes are Bausch & Lomb Inc., Wavefront Sciences Inc., Topcon Ltd., VISX Inc. and Alcon Inc. Differences between these commercially available sensors can be assessed with reference to table 1.2.

1.2.III.ii. SKIASCOPY PRINCIPLE-BASED

These technologies use the principle of dynamic skiascopy, similar to that used by standard autorefractors, or optical path difference. It could be considered as an objective variant of the SRR. An infrared slit scans across the pupil and measures the time difference, as opposed to position difference, of the light reflected by the retina between a central photodetector and each of several photodetectors on each side from the central(MacRae and Fujieda, 2000). The slit rotates 180°, generating auto-refraction data, as well as calculating wavefront aberration from the difference of refractive power between areas within the pupil area (figure 1.8) (Buscemi, 2004). This system measures longitudinal aberration as opposed to the other systems that compute aberration from local slopes (i.e. transverse aberration).

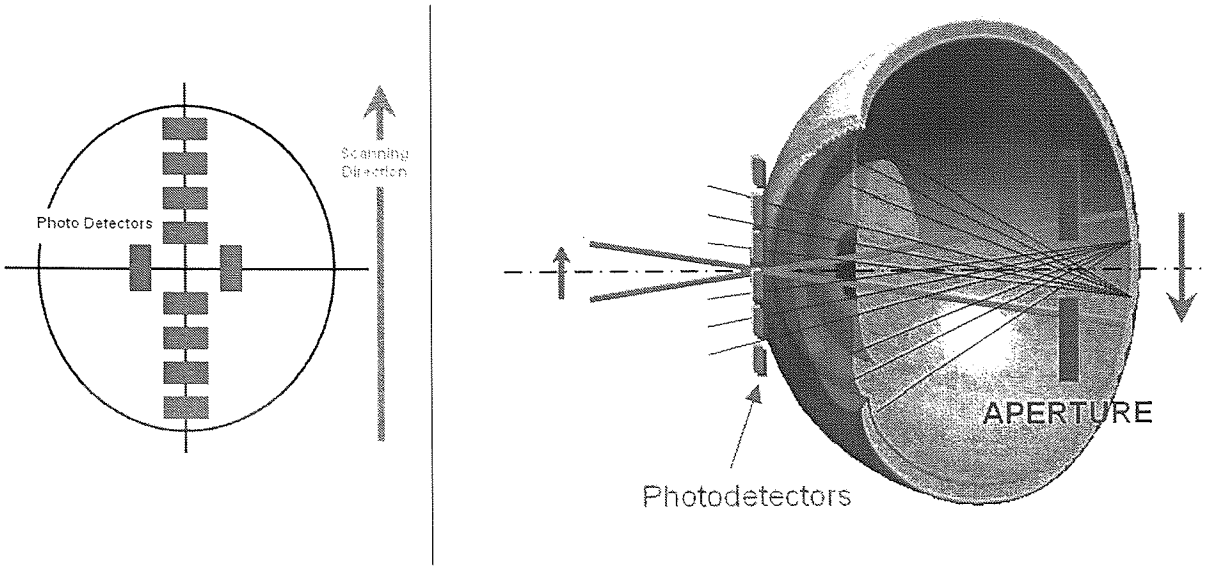

Figure 1.8. *Diagram of the skiascopy-based wavefront sensor arrangement (left), and functioning of the scan (right). The photodetectors are conjugated with the cornea. The aperture is conjugate with the retina in emmetropia, and in front or behind it in myopia and hyperopia respectively. Diagrams redrawn from Buscemi P(Buscemi, 2004).*

Little has been reported on the performance of clinical devices using this principle, although it has been successfully used when coupled to laser systems for customized refractive surgery procedures (Arbelaez, 2001; Gimbel et al., 2003; Gimbel and Stoll, 2001; Nakano et al., 2003; Sarkisian and Petrov, 2002), and the assessment of the optical quality of pathological and post-surgical eyes(Shah et al., 2003). Nidek® Inc. is currently the only manufacturer of this kind of wavefront sensor for clinical purposes.

1.2.IV. ADVANTAGES AND DISADVANTAGES OF ABERROMETERS

Sequential acquisition of wavefront aberrations (i.e. spatially resolved refractometers, laser ray tracing, dynamic skiascopy) has the advantage of avoiding the possibility of "overlapping" or "cross-over" phenomena (figure 1.9). These phenomena represent major drawbacks of simultaneous acquisition measurement system (HS, Tscherning) as they can alter the readings particularly on highly aberrated eyes. These refer to the possibility that, in the case of large distortions of wavefront, focus spots might overlap or cross over to non-corresponding detectors which may result in underestimated readings.

Conversely, simultaneous acquisition measurement allows higher reliability in assessing temporal variation of WFE when taking continuous readings over short periods of time. This characteristic facilitates measurement in the presence of fluctuations in accommodation or micromovements of the eye (Moreno-Barriuso and Navarro, 2000).

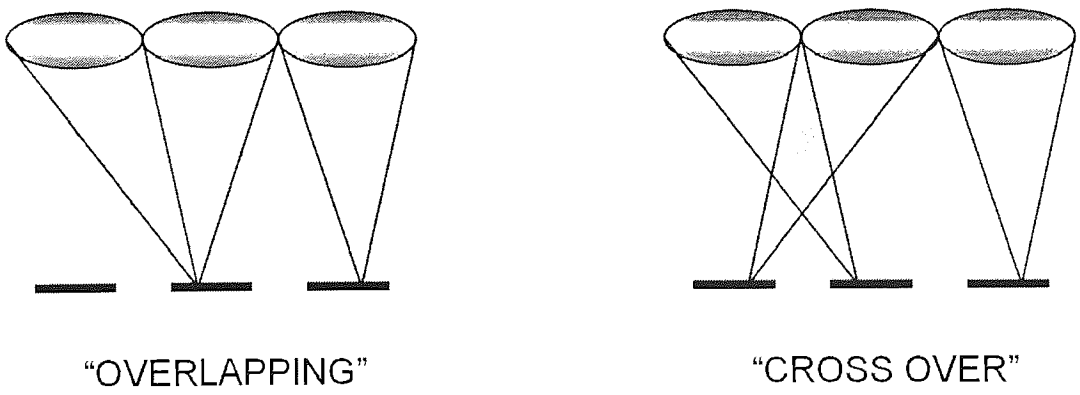

Figure 1.9. *Schematic illustration of two of the main disadvantages of simultaneous measurement of WFE in highly aberrated eyes.*

Ingoing methods measure the retinal image, i.e. first-pass, aberrations, which is more direct and any bias would not be increased by measuring the double-pass, i.e. aerial, image aberrations as the outgoing methods. However, Moreno-Barriuso et al(Moreno-Barriuso and Navarro, 2000) found the same results for both ingoing and outgoing light

analysis thus confirming the reversibility of light and the equivalence of both types of methods.

Simultaneous acquisition methods are more limited by the spatial resolution involving the size of the microlenses (i.e. the HS method) or the mask configuration (i.e. the Tscherning method) making it difficult to adjust the sampling pattern. In sequential acquisition methods, however, there are advantages in that laser ray tracing the sampling pattern can be easily modified and skiascopy-based methods provide the largest spatial resolution of all the systems mentioned (see table 1.2).

1.2.V. IMPORTANCE OF THE PUPIL

Since local aberrations are measured at the pupil plane, and Zernike description depends on the pupil area analyzed. Pupil size is of major importance when using a device for measuring WFE.

With increasing pupil sizes the resolution of the retinal image is altered less by diffraction and more by aberrations in the optical system. Campbell and Green first quantified the impact of pupil size on aberrations (Campbell and Green, 1965). For high magnitudes of spherical aberration, for instance, the refraction will be highly dependent on the pupil size although subjective refraction does not appear to change much with varying pupil sizes (Liang and Williams, 1997).

Light forming the image fills the exit pupil. Since the exit pupil is the image of the aperture (i.e., the iris) as seen from the image space of the optical system of the eye, all the effects of aberrations in the resulting image are contained in the distribution within the pupil. Therefore, the exit pupil is a good location to define, characterize and measure the effects on the light forming the image. Once the light distribution in the exit pupil of the system is known the point spread function (PSF) can be calculated.

Nevertheless, since the representation of the wave aberration using Zernike coefficients is relative to the pupil size, it changes when pupil size changes. This needs to be taken

into account especially when measurements are compared between different situations or devices.

1.3. CLINICAL APPLICATIONS OF WAVEFRONT ANALYSIS

Clinical applications of the wavefront aberration analysis can be grouped into two major fields. First, imaging of the internal structures of the eye, and second, analysis and correction of visual performance. The difference between both fields is based on the direction of the light analyzed. Whereas for imaging purposes the light entering the eye is what needs to be compensated, the opposite happens when the visual performance is the one to be analyzed and/or corrected.

1.3.I. IMAGING OF THE INTERNAL STRUCTURES OF THE EYE

This first application utilizes all the optical improvements in terms of lens design, system filtering, and computing, in order to get optimum results when observing the inner structures of the eye.

Following the great advance in ophthalmoscopic techniques with the invention of the scanning laser ophthalmoscope(Webb and Hughes, 1981) adaptive optics have been combined to provide real time wavefront aberration correction and very high resolution for retinal imaging(Roorda, 2000) (figure 1.10). The wavefront analysis systems give the information needed to make the observation system ideal for the imaging of an individual eye. The HS aberrometer has been described essentially as a modified fundus camera which takes multiple pictures of a single spot of light on the retina (Thibos and Hong, 1999). This description could be similarly extended to all the clinical wavefront analyzers.

The improvement of the systems for non-invasive imaging of the internal structures of the eye has a direct and very important clinical relevance in the early detection of pathological and progressive conditions. The assessment of leukocyte velocity, foveal

dimensions and state, photoreceptors evaluation, can be now performed in real time and non-invasively and consequently retinal anomalies can be detected earlier.

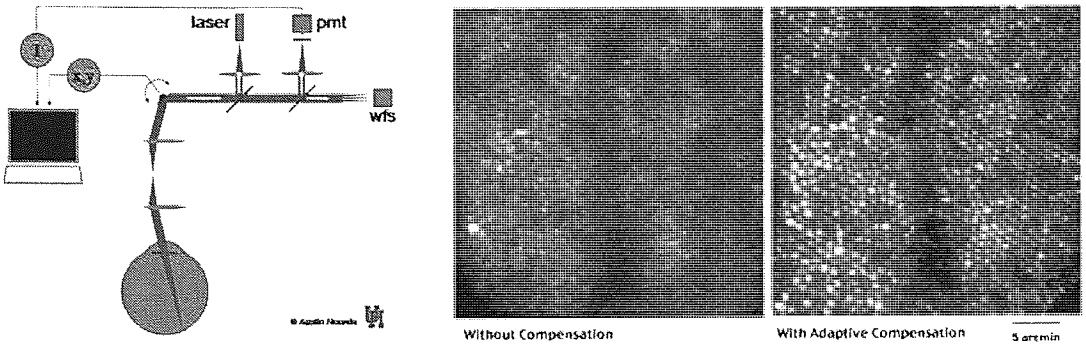

Figure 1.10. *Schematic of the Adaptive Optics Laser Scanning Ophthalmoscope (AOSLO) and the improvement obtained in resolving the image of the retinal mosaic (right). (Images courtesy of Austin Roorda, College of Optometry, University of Houston, TX, USA).*

1.3.II. ANALYSIS AND CORRECTION OF VISUAL PERFORMANCE

This second application comprises all the techniques developed to study and improve the visual performance of the human eye. For this purpose, "aberrometry emerges as the essential clinical instrument for planning sophisticated optical treatments and measuring optical outcome" (Thibos, Applegate, and Marcos, 2003).

1.3.II.i. REFRACTIVE SURGERY

The main reason for the rapid development in ocular wavefront sensing over the last 10 years is the advent and development of refractive surgery. It has been widely reported an increase in the HOA after traditional refractive surgery procedures(Marcos, 2001; Marcos et al., 2001a; Moreno-Barriuso et al., 2001a; Oliver et al., 1997), mainly in spherical aberration, which usually do not affect substantially to the visual performance of the eye under photopic conditions, but being specially manifest with low contrast targets or under scotopic conditions (Applegate and Howland, 1997; Marcos, 2001; Nakamura et al., 2001).

The increase in HOA is mostly due to the reshaping of the anterior corneal surface(Hersh, Fry, and Blaker, 2003; Llorente et al., 2004; Ma, Atchison, and Charman, 2005; Marcos et al., 2001a; Oshika et al., 2002), but also due to changes in the posterior surface(Twa et al., 2005) (mainly in surgery for high myopia where the post-surgery stromal bed after the surgery is significantly thinner) as well as other surgical reasons related to the flap creation and replacement (Potgieter et al., 2005) or laser spot size employed (Huang and Arif, 2002).

The increases in HOA are known to be responsible for complaints of glare, halo and night vision disturbances frequently reported by patients undergoing refractive surgery using traditional tecniques (Chalita et al., 2004; Martinez et al., 1998; Seiler et al., 1994).

Customized excimer laser ablation procedures are the same as traditional techniques, except for the pattern for laser ablation. This pattern is calculated from the WFE measured with the wavefront analyzers. The algorithms used to perform customised ablations, based on the measurements of aberration, are being continuously improved to obtain the best outcomes. The aim is first, to get no increase in aberrations after the surgery and secondly, to be able to reduce higher than normal pre-operative values to closer to more normal values post-operatively.

The direct benefits of customized ablation result from a reduction in HOAs and, therefore, a commensurate increase in contrast sensitivity and visual performance, mainly for scotopic viewing conditions (Kanjani et al., 2004). The benefits are limited by the performance of the wavefront analyzers, the laser precision as well as the surgical planning in terms of the extent or area of correction (Argento et al., 2001; Endl et al., 2001; Seo et al., 2004)).

1.3.II.ii. CONTACT LENS PRACTICE

In theory, contact lenses could be used to correct HOAs and potentially achieve the success evident in the correction of low order aberrations. Customized design of the surfaces would allow modification of the speed of light through every point on the contact lens optical zone which in combination with the eye's optical characteristics would, theoretically, produce an aberration-free system.

Contact lenses have many advantages over surgery particularly in terms of the inability to reverse successfully current surgical procedures. In addition, compensating for wavefront aberrations of the eye with contact lenses allows the parameters to be modified over time and account for time variations in the WFE due to ageing (Chateau, Blanchard, and Baude, 1998; Kuroda et al., 2002c), surgeries, progression of ectasiae(de Brabander et al., 2003), and maintaining a given level of optical performance.

Both rigid gas permeable and soft contact lenses appear to produce an increase in HOAs(Lu et al., 2003) although the increases seem to be relatively predictable, depending on the material and parameters of the contact lens(Dietze and Cox, 2003; Dorronsoro et al., 2003; Hong, Himebaugh, and Thibos, 2001; Lopez-Gil et al., 2002; Patel, Fakhry, and Alio, 2002). It has been shown that there is improvement in performance when the lens design is modified according to the wavefront aberration particularly with respect to spherical aberration. The possibility of predicting and assessing visual performance becomes especially significant in specialist contact lens fitting (Martin and Roorda, 2003). Nevertheless, the rotation of the lens on the eye reduces the predictability of this aberration correction (Lopez-Gil et al., 2002). As these customized contact lenses seek to correct the lower and higher aberrations the translational and rotational movement of the lens should be more accurate and predictable. Wavefront analysis is a useful tool to understand and improve the visual outcomes of contact lens fitting.

Special mention to orthokeratology, a technique that has been used clinically for quite a few years and has to some extent been reborn in the last few years with the better understanding of the corneal biomechanics, new techniques for the assessment and

follow-up of the changes induced, and a increased catalogue of lenses designs and materials. With this technique the cornea is reshaped by a reverse geometry contact lenses fit to reduce myopia (Swarbrick, 2004). It has been reported to induce an increase in HOAs similar to that obtained after refractive surgery (Joslin et al., 2003).

1.3.II.iii. OCULAR PATHOLOGY

Besides the benefits previously mentioned of adaptive optics in imaging intraocular structures wavefront analysis may help in other ways in the diagnosis and evaluation of ocular anomalies.

Much pathology produces a change on the wavefront aberrations of the eye, so knowledge about the wavefront of the eye with pathology may allow an objective assessment of the optical, and therefore visual, consequences of pathology and actuation on the ocular media (Shah et al., 2003).

Anterior segment pathologies especially those that produce morphometric alterations of the cornea, produce a detectable increase in HOAs, worsening the visual function and limiting the options for correction (Maeda et al., 2002; Shah et al., 2003).

Also, crystalline lens pathology may produce an increase in HOAs. It has been reported that cataracts increase the wavefront aberration coefficients, but the polarity has been shown to be negative in nuclear cataract and positive in cortical cataract supporting the potential benefit of wavefront analysis in characterizing eyes with lens pathology (Kuroda et al., 2002a; Kuroda et al., 2002b).

Wavefront aberration analysis systems may also help in other conditions affecting the most anterior optical element of the eye, that is, the tear film. It is known that the tear film has an important role in producing an even surface coating for the anterior corneal surface, so it is clear that the alterations in the tear film will affect the optical quality of the system. Thibos et al. demonstrated that the integrity of the tear film is very important when attempting to image the inner structures of the eye(Thibos and Hong, 1999) and Montes-Mico et al. showed that wavefront aberrations increase to levels of

perceptible degradation of retinal image after periods longer that the normal interblink interval (around 4 seconds)(Montes-Mico et al., 2004). In addition, the HS aberrometer has been recommended as an aid for the assessment and diagnostis of ocular dryness and pathological dry eye (Cervino, McDonald, and Klyce, 2002; Montes-Mico, Alio, and Charman, 2005; Montes-Mico, Caliz, and Alio, 2004b), as well as the effect of treatments to ameliorate the condition(Huang et al., 2004; Montes-Mico, Alio, and Charman, 2005; Montes-Mico, Caliz, and Alio, 2004a)

1.3.II.iv. INTRAOCULAR LENS (IOL) SELECTION AND ASSESSMENT

It has been reported that the implantation of an IOL can produce more HOAs than LASIK increasing mainly the spherical aberration (Miller et al., 2002) and modifying completely the wavefront pattern of the eye previous to surgery. Conversely, clear lensectomy produces smaller aberrations in hypermetropic patients than LASIK in a group of hypermetropic patients of similar age (Ma, Atchison, and Charman, 2005).

Factors, such as lens material, curvature and thickness, may alter the wavefront pattern in a constructive or destructive way. It has been reported that acrylic materials seem to produce more aberrations than silicone or PMMA materials (Vilarrodona, Barrett, and Johnson, 2004) although the reason has not yet been clarified.

The direct benefits of wavefront analysis in terms of IOL design are readily appreciated. IOL design has undergone many improvements in recent years with significant improvement in optical performance. Designing a more prolate anterior surface has, for instance, significantly reduced spherical aberration (Casprini et al., 2005; Holladay et al., 2002; Mester, Dillinger, and Anterist, 2003) especially with large pupil sizes.

1.3.II.v. EVALUATION OF ACCOMMODATION

Although the changes in crystalline lens shape and power during accommodation is the principal means of obtaining clear images for near work in young eyes they also induce substantial changes in the profile of WFE.

It has long been known that most eyes suffer from positive spherical aberration when unaccommodated with a trend towards negative spherical aberration on accommodation (Artal, Fernandez, and Manzanera, 2002; Cheng et al., 2004a; Hazel, Cox, and Strang, 2003; He, Burns, and Marcos, 2000).

These changes in HOAs are of particular importance when a customized correction is being considered, since such correction would only be effective for one state of accommodation (Ninomiya et al., 2002). However, recent reports suggest a high level of predictability for changes in spherical aberration with accommodation and that the typical eye would benefit, for all accommodative states, from correcting aberrations at distance (Cheng et al., 2004a).

Wavefront analysis also has potentially a very useful application in the assessment of accommodation anomalies such as accommodative spasm (Ninomiya et al., 2003) since the optical behaviour in terms of HOAs appears to be different to changes occurring during normal accommodative processes.

1.4. INTRAOCULAR LIGHT SCATTER

Intraocular light scatter arises from light that has reflected, refracted, diffracted, or experienced multiple combinations of all three from particles along the optical path of travel (Bohren, 1995). Due to the roughness of the optical surfaces of the eye and mostly to the local variations in the refractive index, part of the light entering the eye is dispersed as it passes through the ocular media. Intraocular scatter is classified into backscatter and forward scatter depending on the direction of the scattered light.

1.4.I. INTRAOCULAR BACKSCATTER

Backscatter is scattered light travelling up to 90 degrees from the incident light and in a reversed direction. This scattered light does not reach the retina and therefore it does not affect the quality of the retinal image but decreases the amount of light that reaches the retina.

1.4.II. INTRAOCULAR FORWARD SCATTER

Intraocular forward scatter is a phenomenon present in the human eye where the light rays are dispersed to areas other than the focal spot in the retina up to 90° from the PSF center (van den Berg, 1995). This retinal straylight has been defined by the Commission International d'Eclairage as corresponding to "disability glare" (Vos, 1984). There are five major sources that contribute to the total amount of ocular straylight: the cornea, the iris, the sclera, the retina and the lens (de Waard et al., 1992). It is estimated that for young healthy eyes the relative contributions to total amount of straylight are as follows: 1/3 by the cornea, 1/3 by the lens and 1/3 by a combination of the iris, sclera and retina(van den Berg, 1995). As expected, these ratios change with age, pigmentation and specific pathologies (Alexander, Fishman, and Derlacki, 1996; Grover et al., 1998; Ijspeert et al., 1990).

Corneal light scatter is constant with age (Ijspeert et al., 1990; van den Berg, 1995) and intraocular scatter may change with lens opacities (i.e. cataracts) (Ijspeert et al., 1990) or after corneal refractive surgery(Veraart et al., 1993; Veraart et al., 1995; Veraart et al., 1992).

The iris and the sclera scatter light dependent on the patient's pigmentation (van den Berg, JK, and de Waard, 1991), for example, brown irides absorb more light and consequently produce less scatter than light eyes.

Lens scatter increases with age being greater in patients with cataracts (de Wit, 2006).

Finally, the retina produces light scatter which varies across different locations, since not all the incident light is absorbed and some is reflected back, being pigmentation dependent(van den Berg, JK, and de Waard, 1991).

Fan-Paul et al (Fan-Paul et al., 2002) highlighted the fact that glare and disability glare are often confused in the literature. Glare refers to the light source whereas disability glare corresponds to the reduction in visual performance due to a glare source and is the result of forward light scattering. Disability glare corresponds to stray light quantified by means of the external luminance that has the same effect on vision as the glare source (i.e. equivalent luminance).

1.4.III. VISUAL IMPLICATIONS OF INTRAOCULAR SCATTER

Intraocular backscatter does not affect the quality of the retinal image but decreases the amount of light reaching the retina.

The impact of straylight on the contrast sensitivity function is relatively weak. Contrast is reduced by retinal straylight, but this decrease is much smaller than the increase in straylight itself, for example a five times increase in straylight decreases contrast only by 20%. Despite this, reduction in contrast sensitivity is still the main effect of straylight. The effect of straylight would be better understood when glare sources, i.e., sources of light of different intensities, are added in (figure 1.11).

The parameter related to the effect of straylight on contrast sensitivity would be the decrease in contrast sensitivity due to a certain glare source. This sets the basis for the different attempts made to measure retinal straylight that will be reviewed below.

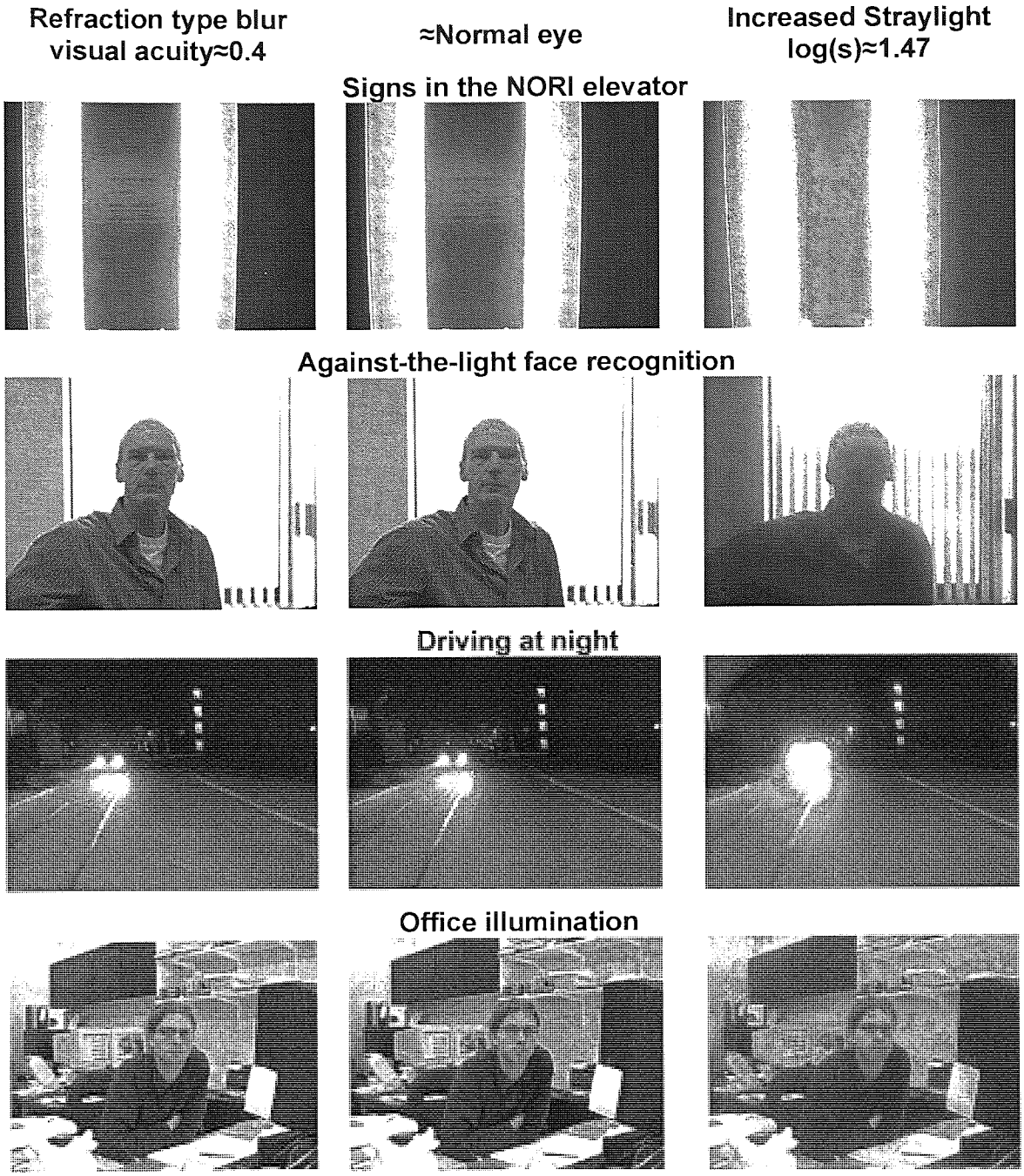

Figure 1. 11. *Comparison between refraction type blur (visual acuity around 0.4) and early straylight disturbance (log(s) around 1.47) for different daily life situations. (Images courtesy of Dr. Tom Van den Berg, Netherlands Ophthalmic Research Institute, Amsterdam)*

1.5. MEASUREMENT OF INTRAOCULAR SCATTER

Most of the methods for determining scatter were developed to determine the effects of cataract onset and progression on both the quality of the retinal image and the visual function. Therefore, many methods are focused on the changes occurring on the lens and their results extrapolated to the whole ocular optical system.

The measurement of intraocular scatter has to be divided into those methods that measure backscatter and those that measure forward scatter. Among the latter, there are two groups of interest: objective and subjective methods.

1.5.I. MEASUREMENT OF OCULAR BACKSCATTER

In contrast to forward scatter, backscatter can easily be quantified using a range of subjective and objective methods to do so.

1.5.I.i. SLIT-LAMP MICROSCOPY

Standardized retroillumination of the different ocular media provides useful information about backscatter. Optical sections using the widest observation angle possible enables visualization of the different optical elements of the eye by means of the light backscattered. Simple observation has been used by many authors to grade crystalline lens capsule opacification (see section 1.6.I.iii) fibrosis or Elschnig pearls (Aslam and Patton, 2004; Sacu, Menapace, and Findl, 2006).

O'Donell and Wolffsohn reviewed different methods for grading corneal transparency and concluded that the measurement of intensity variation across an optical section performed with a slit lamp is the best method for the quantification of corneal oedema and transparency (O'Donnell and Wolffsohn, 2004).

1.5.I.ii. SCHEIMPFLUG IMAGING

A Scheimpflug camera can be regarded as a modified slit lamp in which the image plane, lens plane, or both planes are tilted to obtain a sharp image of the cornea and the lens simultaneously (Scheimpflug, 1906).

The resulting image using the Scheimpflug technique is very similar to an optical section obtained with a slit lamp. The difference between them is that, whilst with the slit lamp we can only see one of the structures focused at a time, Scheimpflug principle allows the observation of all the structures along the axis in focus simultaneously. The principle, illustrated in figure 1.12, is based on the relative positions of the subject plane, the lens plane and the image plane. Whereas in a normal system the three planes will be parallel with each other, in a Scheimpflug camera the planes are tilted with respect to each other and intersect at one straight line.

When the film plane and the subject plane intersect to form 90 degrees and this angle is halved by the lens plane then a 1:1 image-to-subject ratio is achieved.

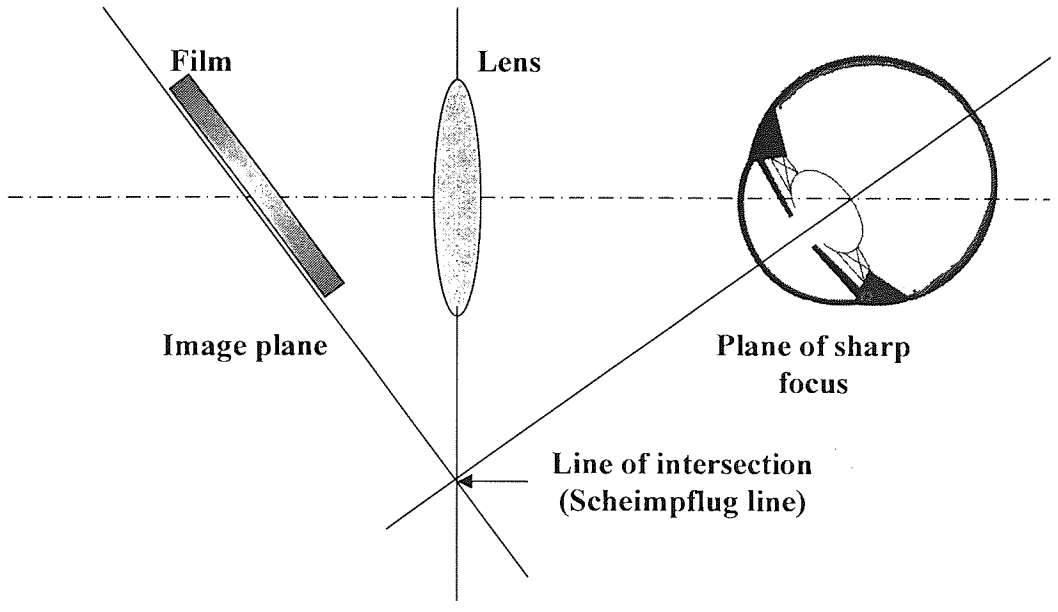

Figure 1.12. *Diagram representing the Scheimpflug principle*

1.5.I.iii. LENS OPACITIES CLASSIFICATION SYSTEM III (LOCS III)

The LOCS III system is possibly the most widely used method for the classification and evaluation of cataract. It is based in the clinical findings obtained by slit lamp observation using optical section and retroillumination of lens structures. It has been used in a number of studies for the classification and grading of cataract(Bencic et al., 2005; Freeman and Pesudovs, 2005; Stifter et al., 2006) as well as for assessing the performance of other methods of cataract grading (Donnelly et al., 2004; Siik et al., 1999; van den Berg and Coppens, 1999). Some approaches have also been made to apply this classification to clear lenses (van den Berg and Coppens, 1999).

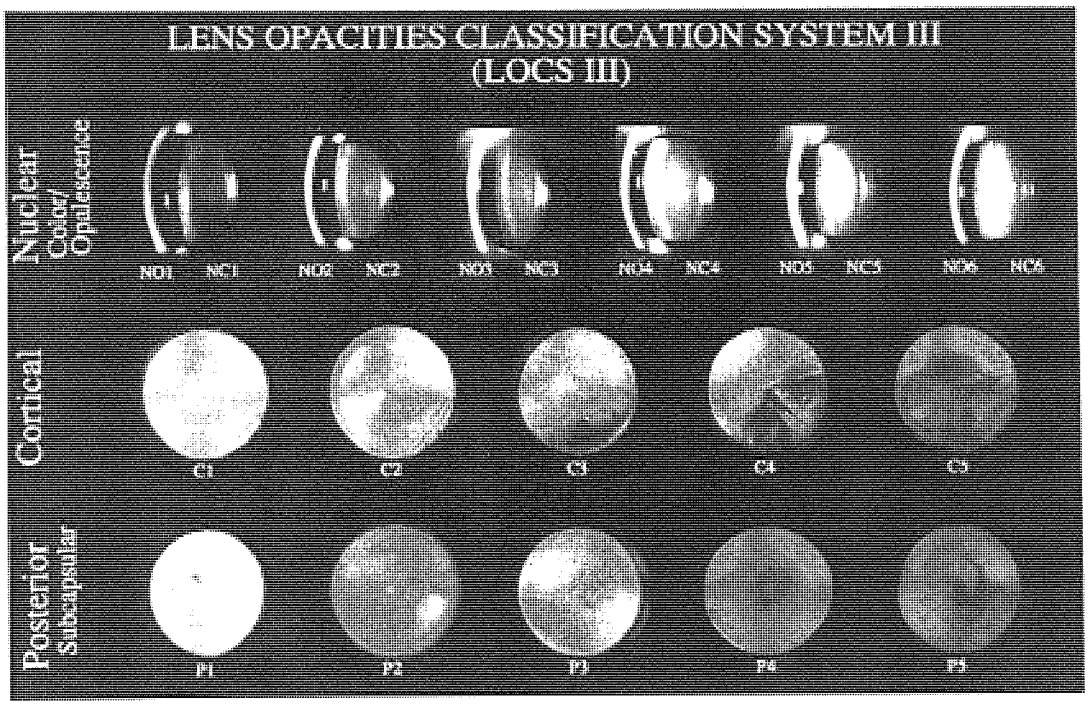

Figure 1.13. *Lens opacities classification system III (LOCS III) (Chylack et al., 1993)*

1.5.I.iv. CONFOCAL MICROSCOPIC IMAGE ANALYSIS

Confocal microscopy allows the *in-vivo* observation of corneal tissue at microscopic level. Despite not being designed or intended for the assessment of corneal scatter, the analysis of the extracellular matrix from images of the stroma can provide an indicator of corneal transparency (figure 1.14). It has been used for that purpose to assess corneal scatter in contact lens wearers (Patel et al., 2002).

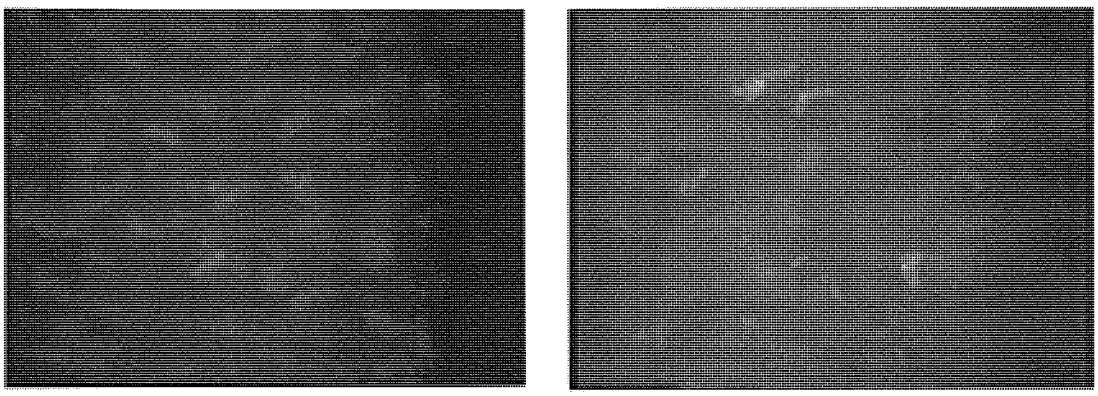

Figure 1.14. Example of two confocal microscopy images corresponding to a normal healthy eye (left) and the eye of a patient with surgical complications from a corneal surgery procedure (right). Note the difference in extracellular matrix reflectivity (i.e. amount of grey tissue).

1.5.II. SUBJECTIVE MEASUREMENT OF OCULAR FORWARD LIGHT SCATTER

The term ocular stray light is typically used to denote large angle stray light (> 1 deg), which means that the major contributor is scattered light.

Straylight causes a veiling luminance over the retina reducing the contrast of the retinal image. Van den Berg introduced a psychophysical method of determining intraocular light scatter by attempting to overcome the low correlation between the values observed and other methods previously implemented measuring intraocular straylight by means of equivalent luminance. This psychophysical method was called the "direct comparison

method" and involved a flickering, ring-shaped, light source presented at a specified angular distance (van den Berg, 1986).

1.5.II.i. CONTRAST SENSITIVITY

Traditionally, human spatial vision is characterised by the minimum size of a test figure of high contrast that a subject was capable of detecting or recognizing, i.e., the visual acuity (VA). Besides the minimum luminance difference that is possible to detect between an extensive and well defined object and its surrounding uniform field previously this was everything known about the sensitivity of the spatial vision of an observer. Nevertheless, this kind of information just determines limits to vision, but does not indicate fully what happens within these limits.

The contrast sensitivity function (CSF) reflects the sensitivity of the visual system not just to the smallest detail, but all the other details, regardless of size.

Although the CSF was first determined in 1956 by Schade (Schade, 1956)use in characterizing the visual system was not generalised until the 70's, when the Fourier techniques were proved to be of value in vision science(Westheimer, 1973).

Since the main effect of intraocular scatter is a decrease in the CSF, it is clear that CSF can be used as an indirect indicator of intraocular scatter. However, care must be taken to ensure that the defect is due to a reduction in optical quality and not to a neural deficit.

1.5.II.ii. GLARE TESTERS

There are currently on the market a number of instruments to measure the effect of glare on visual function (Babizhayev et al., 2003). These instruments do not assess straylight nor disability glare, but a more loosely related score(van den Berg, 1991; Van den Berg, 1994). The components common to all of these systems are a glare source and a target for the subject to exercise discrimination judgements (figure1.15). These instruments normally allow control of the intensity of the source as well as the wavelength used.

Although the different glare testers show reasonably good repeatability, CSF or VA in the presence of glare has been reported as more valid and of better discriminative value than the "disability glare scores" from glare testers when assessing patients with cataract (Elliott and Bullimore, 1993). Despite the similarities between the different glare testers, they each perform differently. The Regan low-contrast chart with the brightness acuity test (BAT) and the Berkeley test have been shown as reliable and valid (Elliott and Bullimore, 1993). Similar to CSF, the usefulness of glare testers for assessing scatter is limited to subjects with good VA and therefore it can be assumed that the defect is due to optical factors rather than to neural deficits.

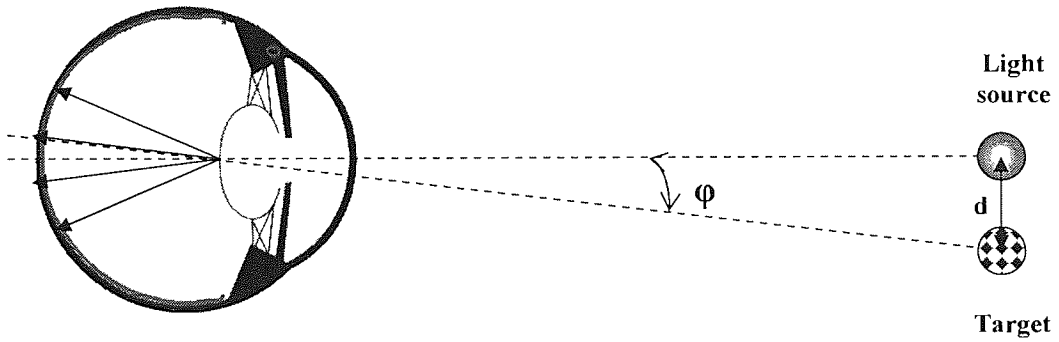

Figure 1.15. *Schematic representation of the principle used by the Halometer glare test. The target is brought towards the source until the patient no longer sees the target; then the incident light angle φ between the source and the target is measured. The measured glare radius is defined as a target image projection from the vector of light scatter (indicatrix of light scatter $I=I_0\cos^2\varphi$) when the glare source is activated and the patient asked to identify the target during illumination of the eye with a glare source (after Babizhayev et al(Babizhayev et al., 2003)).*

1.5.II.iii. DIRECT COMPENSATION METHOD

Intraocular scatter results in that part of the light from the source that is projected onto the tested part of the retina to flicker; this can then be extinguished using counterphased compensation light presented at the retinal test field. The amount of compensation needed to do so is recorded as a measure of straylight.

This method has provided excellent results in laboratory settings and has been used as the gold-standard for assessing the performance of other glare testers. Nevertheless, the method had some drawbacks away from laboratory settings, as stated by Franssen et al (Franssen, Coppens, and van den Berg, 2006). These limitations are:

1.- the difficulty for some patients to judge the weaker flicker in the test field.

2.- The task is to identify the moment when the flicker disappears, as opposed to most tests where the task is to indicate when they are able to see flicker.

3.- The accuracy seems to depend highly on an appropriate explanation of procedures and strategy which may differ considerably between observers.

4.- There is no control over the reliability of the measurement.

5.- The subjects had the ability to influence the outcomes, which is a major drawback for a clinical procedure.

To overcome for these limitations a recent modification of the original direct comparison method has been proposed. It is called the "compensation comparison" method and has been described in detail elsewhere (Franssen, Coppens, and van den Berg, 2006) and validated for clinical use (Franssen, Coppens, and van den Berg, 2006) (see Chapter 5). A clinical device manufactured by Oculus AG, the C-Quant straylightmeter, has recently been introduced to the market and is now being used on a large scale for research and clinical purposes.

1.5.II.iv. COMPENSATION COMPARISON METHOD

In contrast to the original direct comparison method, the test field of the compensation comparison method is now divided into two halves as shown in figure 1.16. The subject fixates and responds to which of the two halves' flicker is stronger. The two halves will be perceived as flickering but with a different modulation since one of them has added compensation light intensity.

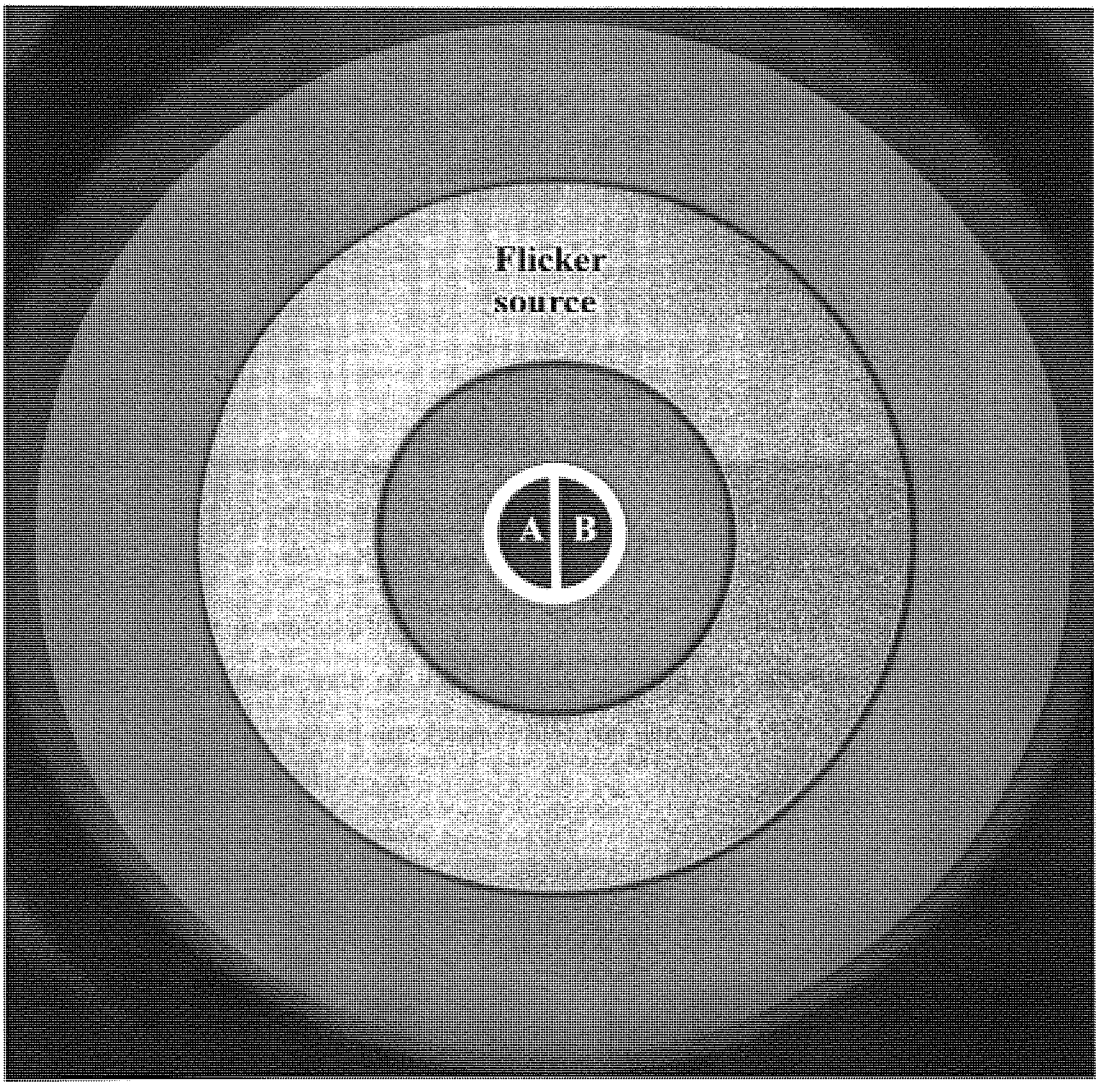

Figure 1.16.- *Target for the Straylightmeter. A and B represent the two halves of the test field, one of which will have a compensation light added to the flicker.*

As described in previous reports (Franssen, Coppens, and van den Berg, 2006) the examination process consists on two phases: a dark phase and a bright phase (i.e. maximum light intensity of the straylight source). The first phase has a double task: to give an initial estimate of the psychometric function (figure 1.17), and therefore of the straylight value, and make the task accessible to the patient in order to get familiar with the procedure. The second phase serves to define this first estimate and give the final straylight value.

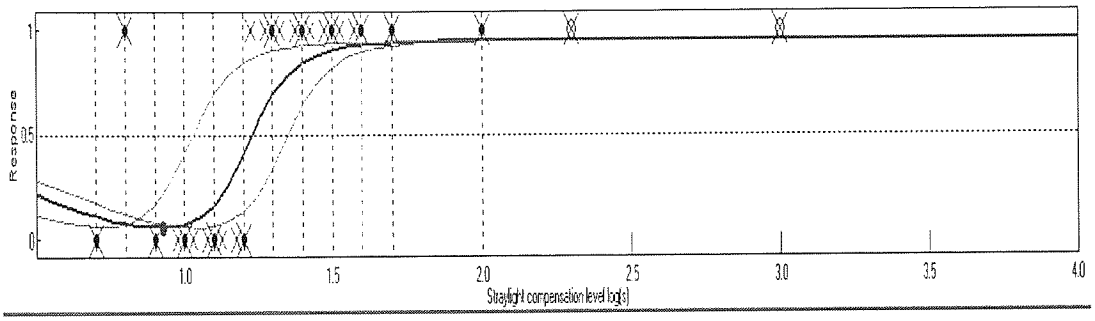

Figure 1.17. *Psychometric function given by the C-Quant straylight meter, which represents the probability of achieving a score of 1 (i.e. compensation test field flickers the most) as function of the strength of the counterphase compensation light.*

The task consists of comparing the flickering of the two halves of the test field. The probability of choosing one of the halves as having the stronger flicker is given by (Franssen, Coppens, and van den Berg, 2006; van den Berg, 1995):

$$P = \frac{1}{1 + e^{-[MDC/MDC_c]}} \quad \text{eq.1.4}$$

The modulation depth contrast (MDC) describes the contrast between the two flickers. MDCc describes the contrast with compensation light.

As mentioned earlier, the light originating from scatter corresponds to an outside luminance, the equivalent luminance, given by the equation (van den Berg, 1995):

$$L_{eq} = 0.0013 \cdot s \cdot L_{src} \quad \text{eq.1.5}$$

Where L_{src} is the luminance of the straylight ring and s is the straylight parameter of the eye under examination.

The system uses reliability parameters to ensure reliability of measurements.
Expected standard deviation (ESD) corresponds to the width of the likelihood function calculated from the psychometric function divided by the number of standard deviations it represents measured at four different levels of confidence (68, 95, 99.7 and 99.99%) and then the four values obtained are averaged. The ESD is based on a single assumed shape of the psychometric function yet the system provides a shape factor (Q) for the psychometric function which must be higher than 1 in order to be acceptable. The ESD limiting value for reliable measurements in the C-Quant straylightmeter, the only commercially available clinical straylightmeter, is set at an ESD value of 0.08. This parameter has been shown as a good reliability measure in this instrument (Coppens et al., 2006).

Van Rjin et al(van Rijn et al., 2005) found very similar repeatability values between most of the devices used for the measurement of ocular straylight and glare. They also found low discriminative ability for the Nykotest and Mesotest for detecting cataract as well as high discriminative ability for the Straylightmeter.

1.5.III. OBJECTIVE MEASUREMENT OF OCULAR FORWARD SCATTER

The objective measurement of *in vivo* forward scatter in the human eye has been, and still is, a challenge for scientists. The advent of ocular wavefront analysis has introduced new ways of detecting the point spread function (PSF). Stray light can be quantified by means of the PSF (Thibos and Hong, 1999). When a point light source is imaged onto the retina (or any other image plane) the resulting image will not be a point but will be a function in which the energy is spread out (figure 1.18).

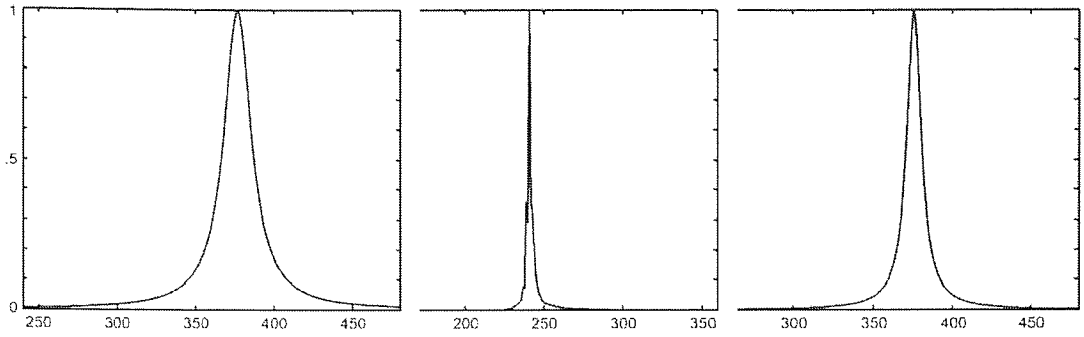

Figure 1.18. *Line spread function of a human eye representing the contribution of wavefront aberrations and intraocular scatter to the resulting function (from Shahidi et al(Shahidi et al., 2005))*

Reasons for this spread are:

- Optical aberrations
- Diffraction of light
- Ghost images (spurious reflections inside the eye)
- Scattered light.

The Stiles-Holladay approximation for this angular range (θ, in degrees) is given by the relation:

$$PSF(\theta) = 10 \cdot \theta^{-2} \qquad \text{Eq.1.6}$$

Based on research data of human PSFs, this so-called "glare" equation has recently been updated to include age (A in years) and pigmentation dependence (p: 0 for dark eyes to 1.2 for blue eyes) as well as an extension of the valid angular region from 0.1^{o} to 100^{o} (Ijspeert et al., 1990):

$$PSF(q, A, p) = \frac{10}{q^3} + \left(\frac{5}{\theta^2} + \frac{0.1 \cdot p}{\theta} \right) \cdot \left(1 + \left(\frac{A}{62.5} \right)^4 \right) + 0.0025 \cdot p \qquad \text{Eq.1.7}$$

Cox et al(Cox, Atchison, and Scott, 2003) suggested that it should be possible to assess narrow-angle forward light scatter from wavefront analyzers' calculated PSF by removing any confounding effect of wavefront aberration.

1.5.III.i. MEASUREMENT OF POLARIZED LIGHT AS AN INDEX OF SCATTER

Bueno et al described in 2004 (Bueno et al., 2004)a method to measure intraocular scatter as a function of the amount of polarized light exiting the eye with a double-pass method that quantifies simultaneously polarization and wavefront aberrations(Bueno, Berrio, and Artal, 2003). Evaluation using ceramic plates with variable amounts of induced scatter showed high correlation between the amount of polarized light and the amount of scatter.

1.5.III.ii. COMBINED WAVEFRONT SENSING AND OPTICAL SECTION

By modifying a HS wavefront sensor, Shahidi and Yang(Shahidi and Yang, 2004) measured simultaneously wavefront aberrations and light scatter. Their method consisted first by measuring the wavefront aberration by HS wavefront sensing and then by introducing a cylindrical lens in the laser beam path in order to obtain a laser slit. This slit would provide a line spread function containing information of both wavefront aberrations and intraocular scatter. By calculating the area underneath both curves, that is the one obtained from the wavefront aberrations by HS sensing and the line spread function obtained from the slit, the difference will give a metric of forward light scatter. This method has been applied to both normal (Shahidi and Yang, 2004) and diseased eyes(Shahidi et al., 2004; Shahidi et al., 2005).

1.5.III.iii. ANALYSIS OF HARTMANN – SHACK PATTERNS TO MEASURE SCATTER

Fujikado et al used the diameter of the HS spots as a measure of forward scatter (Fujikado et al., 2004) to evaluate cataract.

Donnelly et al (Donnelly et al., 2004) used the HS patterns provided by a custom-made wavefront analyzer to objectively quantify ocular scatter in order to evaluate nuclear cataract and predict its severity. The scatter metrics were calculated from the brightness of pixels within an area of the PSF tail of each lenslet, i.e. the area surrounding the centroid of each lenslet. After determining several different metrics from the brightness of the pixels within an area containing each lenslet's PSF tail in order to bring all the scatter information down to one number, they found the maximum standard deviation for all the PSF in the HS pattern (Max_SD) to be the one that better explained the contribution of forward scatter to the variance in visual performance in patients with cataract, being up to 51%.

1.6. CLINICAL APPLICATIONS OF INTRAOCULAR SCATTER MEASUREMENT

Clinical applications of intraocular scatter measurements are similar to those previously reported in this chapter for wavefront analysis. Most of the systems developed have aimed to assess the progression and visual consequences of cataract. For this reason, most of research studies apply these methods to investigations of cataract onset, classification and progression.

1.6.I. CATARACT EVALUATION

The crystalline lens has been reported as the major contributor to light scatter (Chylack et al., 1993; de Waard et al., 1992). With the progression of cataract, forward light scatter becomes more important than backscatter (Bettelheim and Ali, 1985). The assessment of backscatter is the main tool clinicians have for the assessment of onset and progression of cataract. The assessment of forward scatter allows assessment and

monitoring of the visual effects of cataract. The role of scatter evaluation in cataract assessment and follow-up is fundamental. For that reason, most of the clinical tools devised to measure backscatter and forward scatter were designed specifically for the assessment of cataractous processes, even though they were applied later to other conditions.

1.6.II. REFRACTIVE SURGERY

Besides the corneal alterations mentioned in section 1.3.II.i. of this chapter, which affect both wavefront aberrations and intraocular scatter, the corneal healing processes following refractive surgery may imply variable amounts of haziness being frequently observed by clinicians in the stromal bed, an observation that suggests an increase in backscatter and forward scatter. Verrart et al did not however find any correlation between haziness and forward scatter (Veraart et al., 1993). Harrison et al did not find a significant increase of forward scatter 1 month after PRK using several methods of straylight measurement (Harrison et al., 1995) although in the same year Veraart et al reported significant increases after PRK using one of the same measurement systems (Veraart et al., 1995).

1.6.III. OCULAR PATHOLOGY

Changes in any of the ocular media will induce changes in the amount of light scattered. Therefore, any ocular pathology which involves changes to the ocular refracting surfaces and media and/or an increased number of particles (e.g. pigments, proteins, inflammatory cells) floating in the aqueous or vitreous will induce increased amounts of light scattered.

Increased light scatter has been reported in pathologies such as retinitis pigmentosa (Alexander, Fishman, and Derlacki, 1996), choroidemia (Grover et al., 1998; Grover et al., 2002) and glaucoma(Horn, Junemann, and Korth, 2001).

1.6.IV. CONTACT LENS PRACTICE

Elliott et al showed the straylightmeter to be more sensitive than CSF or VA acuity measures but similar to slit lamp assessment for the determination of contact lens induced oedema (Elliott et al., 1993). Straylight values of soft contact lens wearers after removal of the contact lens (CL) were significantly higher than those for rigid gas permeable contact lens wearers after removal, suggesting subclinical corneal oedema (Elliott, Mitchell, and Whitaker, 1991).

Patel et al used images obtained from confocal microscopy to evaluate backscatter by calculating the mean grayscale after removing the keratocyte nuclei from the images of the corneal stroma (Patel et al., 2002). Using this method they found no significant differences between non-wearers and long-term CL wearers.

1.6.V. EVALUATION OF VISUAL LIMITATIONS IN GENERAL

Considering that forward scatter causes contrast loss in the final retinal image, the estimation of this parameter becomes very useful for testing driving abilities under glare conditions such as night driving, which is widely supported in the literature (Babizhayev, 2003; Puell et al., 2004; Theeuwes, Alferdinck, and Perel, 2002; West et al., 2003) Recently, an important multicentre study assessed the impact of glare in drivers (van den Berg and van Rijn, 2005).

CHAPTER 2. RESEARCH RATIONALE

When considering limitations to visual performance, the first physical limitation is the optical quality of the retinal image, limited by wavefront aberrations, diffraction, scatter and chromatic aberration(Bettelheim and Ali, 1985; Charman, 1991; Charman and Jennings, 1976; Gilmartin and Hogan, 1985; Ijspeert et al., 1990; Porter et al., 2001; Schwiegerling, 2000; Thibos, 1987; Thibos, Bradley, and Zhang, 1991).

Whilst current clinical devices have evolved substantially to provide measurements of wavefront aberrations in clinical settings, the quality and quantity of the information has not been fully explored.

The main goal of this research is to optimise the information pertaining to retinal image quality in clinical settings provided by commercially available wavefront analysers. This will be achieved by:

1. Determining sources of error in the clinical determination of higher order aberrations and their implications for interpretation of the values obtained
2. Using the information provided by the wavefront analyser to measure objectively the amount of intraocular light scatter.
3. A further aim of the research is to determine the relationships between wavefront aberrations, ocular biometric parameters and ethnicity and investigate differences between eyes corrected with monofocal and multifocal intraocular lenses in terms of subjective and objective measures of intraocular scatter.

The experimental chapters of the thesis will be structured as follows:

Chapter 3 will investigate the sources of error arising from the manipulation of the wavefront analyser by the clinician and from the fixation errors by the subject examined. In order to achieve this, model eyes will be used to reduce the number of variables inherent with human observers and determine the performance of the instrument in several situations: realigning the system between measurements, not

realigning or angularly misaligned. A second study will compare the aberration values obtained with Hartmann-Shack based and skiascopy based wavefront analysers to determine the variance of wavefront aberration measurements obtained with each on human eyes and the validity and correlation of data provided by instruments using these different optical principles.

Chapter 4 will study a phenomenon present in many closed-field clinical instruments that may have a significant impact on the values of wavefront aberration obtained, that is, instrument myopia. In a preliminary study the presence or otherwise of instrument myopia when using clinical wavefront analysers will be studied in a population of non-cyclopleged young adult subjects using three different wavefront analysers that use different optical principles to measure aberration. The impact of instrument myopia on the wavefront aberration measurement will be subsequently studied in a smaller sample of subjects that is required to fixate at designated intermediate and near distances in real space while measuring wavefront aberrations.

Chapter 5 will elucidate the potential relationships between ocular biometric parameters, wavefront aberrations and ethnicity. Human ocular wavefront aberrations have been shown as variable between individuals (Paquin, Hamam, and Simonet, 2002; Porter et al., 2001; Zadok et al., 2005), and this study aims to identify patterns or models that would explain such variability in terms of ethnic differences in ocular components and behaviour reported previously in the literature (Hanna et al., 2004; Hyman et al., 2005; Riley et al., 2001).

Chapter 6 will examine further the concept of intraocular scatter measurement. In order to provide a gold standard against which to compare the methodology to be developed for the objective determination of intraocular scatter using data from wavefront analysers, the C-Quant straylightmeter (Oculus, Germany), the only clinical straylightmeter available and ostensibly the most reliable instrument for the subjective clinical determination of intraocular scatter (Coppens et al., 2006; Elliott and Bullimore, 1993; Franssen, Coppens, and van den Berg, 2006; van der Heijde, Weber, and Boukes, 1985), will be further assessed to determine the impact of continuous measurements on the reliability of the measurements and, therefore, determine the optimum number of measurements required in a clinical setting. In a second experiment the C-Quant

straylightmeter will be used to determine the effect of contact lens tints on straylight values by comparing straylight measures with spectral tinted contact lenses intended for contrast enhancement with a clear contact lens of the same design specifications and material.

Chapter 7 will evaluate and validate a novel dedicated software for the objective measurement of intraocular scatter measurements using images from Hartmann-Shack patterns obtained from a clinically available wavefront analyser. This analysis technique is derived from a method previously described by Donnelly et al(Donnelly et al., 2004), but has not previously been applied to commercially available wavefront analysers. Validation will be performed by comparing the values obtained from this objective image analysis technique to those obtained with the previously validated subjective straylightmeter in a population of young adult subjects.

Chapter 8 will apply both methodologies for intraocular scatter determination (i.e. subjective straylightmeter and objective Hartmann-Shack analysis) to analyse differences in optical quality between monofocal and multifocal intraocular lenses in a population of pseudophakic patients. Differences between monofocal and multifocal lenses and relationships between objective and subjective measures of scatter will be assessed.

Chapter 9 will present a summary of findings and suggestions for future work, as well as a discussion of the implications of the conclusions reached following the research studies presented in the thesis.

CHAPTER 3. MONOCHROMATIC WAVEFRONT ABERRATIONS IN HUMAN AND MODEL EYES

CHAPTER SUMMARY

Purpose: To investigate factors influencing the reproducibility of measurements from clinical wavefront aberrometers.

Methods: Two studies were conducted: 1. A model eye study investigating the effect of possible operator errors on the reproducibility of wavefront measurements with the WASCA wavefront analyser. 2. A human eye study of the reproducibility of Hartman-Shack and dynamic skiascopy- based aberrometers.

Results: 1. In the model eye study, repeatability of the WASCA was excellent in all the situations tested. However, realignment by the observer between measurements increased the standard deviations by a factor of 3; angular misalignment resulted in significant errors, particularly in the determination of coma. 2. In the human eye study, the WASCA wavefront analyzer showed good repeatability; however, the data spread shows great variability for those Zernike coefficients more relevant to visual outcomes, i.e., coma, trefoil and spherical aberration.

Conclusions: Data from both model and human eye studies show good reproducibility of wavefront measures. Operator errors increase variability and particular care should be observed when acquiring data from highly aberrated eyes. Wavefront data obtained from different wavefront analyzers are not interchangeable. Differences between measurements with different wavefront analyzers on non-cyclopeged human eyes may occur due to different accommodative response to the different fixation targets

3.1. INFLUENCE OF OPERATOR ERRORS IN WAVEFRONT SENSING WITH A HARTMANN-SHACK (HS) SENSOR: A MODEL EYE STUDY

3.1.I. ABSTRACT

Purpose: To evaluate the effects of instrument realignment by the clinician and angular misalignment of the patient during the clinical determination of wavefront aberrations simulated using model eyes.

Methods: Six model eyes were constructed and examined with the WASCA in 4 sessions of 10 measurements each. In 2 sessions, the readings were obtained consecutively without realigning the system; in the third session, the instrument was realigned after every measurement; in the final session, the readings were consecutive, without realignment, but the model eye was angularly shifted 6 degrees from the optimum alignment position. Intersession repeatability, effects of realignment and 6 degrees misalignment were obtained by comparing the measurements in the different sessions for coma, spherical aberration and HOA. Intra-class correlation coefficients (ICCs) were calculated as a measure of intra-session repeatability for each of the sessions.

Results: Realignment by the observer between measurements increased the standard deviations by a factor of 3 compared to the first session without realignment. Mean differences between the 2 sessions without realigning the system were -0.014 ± 0.076 μm for Z_3^{-1}, p=0.551, 0.009 ± 0.139 μm for Z_3^1, p=0.877, 0.004 ± 0.037 μm for Z_4^0; p=0.820 and 0.005 ± 0.01 μm for high order RMS, p=0.301. Differences between non-realigned and realigned after each measurement were -0.017 ± 0.026 μm for Z_3^{-1}, p=0.159 **Conclusions:** Repeatability of the WASCA was excellent in all the situations tested. Realignment of the instrument by the clinician substantially increases the variance of the measurements. Angular misalignment such as may arise due to poor fixation can result in significant errors, particularly in the determination of coma. These findings are of importance when assessing highly aberrated eyes during follow-up or prior to surgical treatment.

Paper published in J Cataract Refract Surg: See Appendix II

3.1.II. INTRODUCTION

Numerous studies have evaluated the performance of clinical wavefront analyzers in both the determination of low- (Hament, Nabar, and Nuijts, 2002; Salmon et al., 2003; Wang, Wang, and Koch, 2003) and high-order aberrations(Cheng et al., 2003; Mirshahi et al., 2003; Rodriguez et al., 2004; Zadok et al., 2005). They all agree on the capabilities of wavefront analysis systems to determine low order aberrations with high accuracy, although the different studies yield discrepant conclusions for the determination of HOA with different instruments.

When performing a clinical examination with any instrument, there are always a number of sources of error that needs to be accounted for before interpretation of the data. There are currently several instruments that automatically capture data only when the system is properly aligned (e.g. corneal topography analyzers like the Medmont, or wavefront analyzers like the OPD-scan); however, most systems require observer judgement of the best alignment position followed by image capture. This alignment is therefore strongly dependent on the skills of the practitioner to judge the specific optimum position, as well as the ability of the patient to hold a proper fixation.

Davies et al (Davies, Diaz-Santana, and Lara-Saucedo, 2003) assessed the repeatability of HS wavefront sensing on nine human eyes using pupil centration and a dental bite bar. With this arrangement they showed that repeated measurement of ocular wavefront leads to significant differences in the Zernike coefficient values obtained as a result of small misalignment errors, short-term variations in aberration and drifts in the equipment position. In the present study, model eyes remove the inherent physiological short-term variations in wavefront aberration associated with human eyes, as well as enabling the quantification of the degree of misalignment and its impact on the values obtained.

When wavefront analysis is performed in clinical settings, as with many other clinical instruments, it is advisable to take several readings due to the temporal variations of wavefront error (Cheng et al., 2004), small errors in the measurement due to the

instrument, as well as small axial and lateral misalignments due to the manipulation of the instrument during the focusing procedure (Cheng et al., 2003; Davies, Diaz-Santana, and Lara-Saucedo, 2003). When taking a measure, the ability of the observer to choose the right moment to take the reading may be crucial for the reliability of the values obtained. In the same way, small shifts in the fixation of the patient may also affect the final readings. This is of particular importance when high values of aberration are to be quantified and/or treated as, for example, when a customized ablation is considered.

Cheng et al. reported different aspects of the performance of the Complete Ophthalmic Analysis System (COAS, Wavefront Sciences ltd.) for the determination of low and HOA on human and model eyes (Cheng et al., 2003). They also showed that measurements with the COAS tolerate axial and lateral misalignments within a range greater than that in which the system appears aligned to the clinician. The sensor has been shown to be highly accurate and repeatable, with very low variability, and robust to lateral and axial misalignment. The WASCA (Zeiss/Meditec, Germany) is essentially the same wavefront sensor as the COAS, so the results obtained by Cheng et al. could be extrapolated to this system.

There are three main aims for this study:

1. To evaluate objectively the repeatability (intra-session) and reproducibility (inter-session) of the WASCA wavefront analyzer.

2. To assess how the observer's judgement when locating the optimum alignment prior to data capture, i.e. small lateral and axial misalignments, affects the values obtained and the performance of the instrument in terms of intra- and intersession repeatability.

3. -To assess the effect of small angular misalignments with respect to the instrument axis such as would happen with small changes in fixation by the patient during the image acquisition, on the values obtained and the performance of the instrument,.

In order to achieve these aims, all the variables introduced by the patient's eye are eliminated by using a model eye.

3.1.III. MATERIALS AND METHODS

3.1.III.i. Model Eye

The sample eyes were constructed from an artificial eye with a set of removable elements of known parameters as shown in table 3.1. The artificial eye comprises a brass body with four segments on which the optical components are mounted (figure 3.1). It has been described in detail elsewhere (Kirschkamp et al., 1998), and has been used widely in research studies such as the simulation of Purkinje reflections for determining radii of curvature and position of the crystalline lens (Kirschkamp et al., 1998), and phakometric measurement of ocular surface radius of curvature and alignment (Barry, Dunne, and Kirschkamp, 2001; Dunne et al., 2005). Six of the possible eyes resulting from the combination of these elements were used in this study. The model eyes used were chosen to have relatively high values of coma and spherical aberration as summarised in Table 3.2. Note that the model eyes used did not permit the absolute callibration of the instrument, since the removable elements fit in such a way that coupling of the different parts prior to measurement can be variable; equally, once the model eye was set up for each set of experiments, it was not moved between measurements or between sessions.

CORNEA			
Anterior surface radius	**Thickness**	**Posterior Surface radius**	
8.84 ± 0.02	0.8 ± 0.002	8.45 ± 0.01	
7.83 ± 0.02	0.8 ± 0.002	7.44 ± 0.01	
ANTERIOR CHAMBER DEPTH	**LENS**		
3.67 ± 0.003	**Anterior surface radius**	**Thickness**	**Posterior Surface radius**
4.18 ± 0.003	13.6 ± 0.02	3.5 ± 0.01	8.32 ± 0.01
5.19 ± 0.003	**VITREOUS CHAMBER DEPTH**		
	20.52 ± 0.18		

Table 3.1.- *Parameters of the different elements used in the different model eyes examined. All the values are in mm*

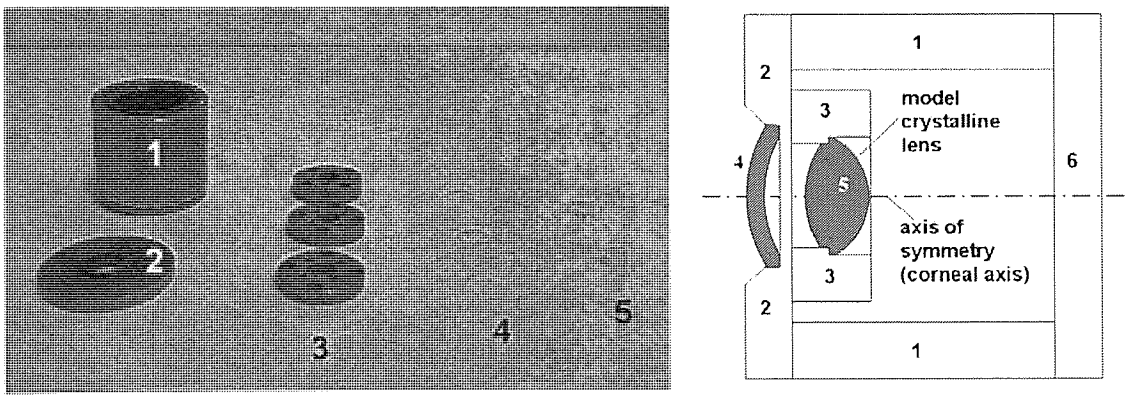

Figure 3.1.- *Cross section of brass segments of the elements used:*
1 – Outer casing, 2 – Anterior segment mounting designed to hold model cornea, 3 – Interior segment mounting designed to hold model crystalline lens, 4 – Model corneas, 5.- Model crystalline lens, 6.- Posterior cap of outer casing. (Redrawn with permission from Kirschkamp et al (Kirschkamp et al., 1998))

3.1.III.ii. Wavefront Analyser

The WASCA uses a source diode, emitting at a wavelength of 850 nm, and a 44x33 lenslet array (i.e. a total of 1452 lenslets) which measures the tilt of the wavefront over several pupil locations. It gives information of the HOA up to the fifth order. The diameter of each lenslet is 144 μm.

According to the manufacturer the pupil magnification factor is about 0.685, which means that the lenslet array samples the exiting wavefront every 210 μm in the pupil plane. This allows approximately 500 sample points within the 5.0 mm diameter pupils that will be analysed in this study.

The model eye was coupled to the wavefront analyser to take all the measurements (figure 3.2).

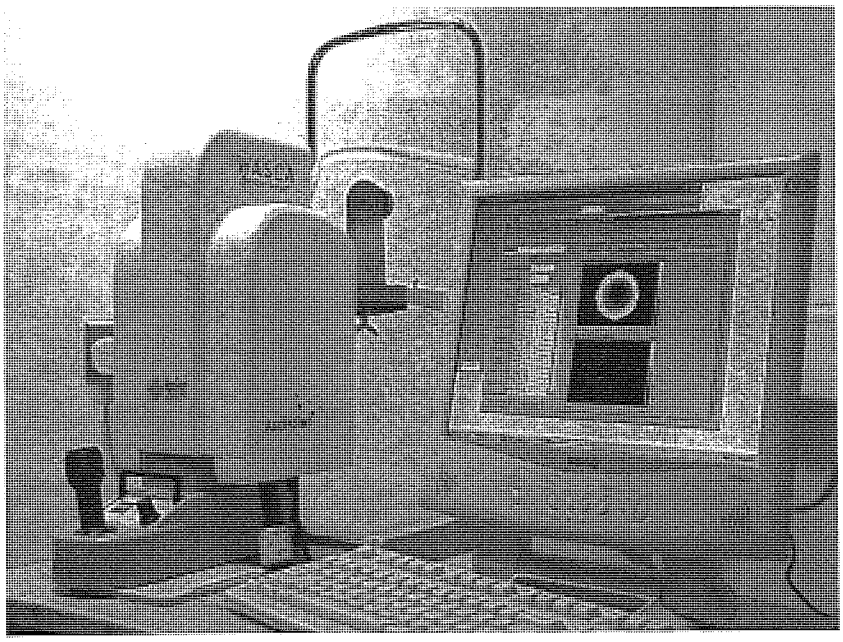

Figure 3.2.- *Image of the model eye coupled to the WASCA analyzer.*

3.1.III.iii. Experimental design

Ten consecutive measurements without realignment of the system were obtained on the different model eyes in each of two sessions. Additionally, 10 further measurements were taken after inducing an angular misalignment of 6 degrees of the model eye with respect to the instrument and 10 taken after realigning the system before each measurement (joystick displacement in the x-y-z directions out of focus after each reading). Note that all measurements were taken by an experienced operator (AC).

3.1.III.iv. Data analysis

Data were obtained, and analyzed, as Zernike coefficients, complying with the recommended standards by the Optical Society of America (Thibos et al., 2002). Due to physical limitations of the model eye, data were obtained and analyzed for a 5mm pupil size. Analysis was performed for primary coma and spherical aberration coefficients, the main off-axis and axial wavefront errors and, therefore, the most compromising for visual performance.

Intrasession repeatability was assessed by determination of the intraclass correlation coefficient (ICC), a reliability coefficient calculated from variance estimates obtained through an analysis of variance(Lam, Chan, and Chiu, 2004) using the statistical package for social sciences SPSS (SPSS 12.0, SPSS Inc, USA) (eq. 3.1), and by the graphical representation of the variations of the standard deviation with the number of measurements analyzed.

$$ICC = \frac{\sigma_{between} - \sigma_{w/in}}{\sigma_{between} + \sigma_{w/in}} \quad \text{(eq. 3.1)}$$

In eq. 3.1. $\sigma_{between}$ represents variance between the different eyes and $\sigma_{w/in}$ the variance within the model eyes.

Intersession variation, differences with realignment and effect of angular misalignment were assessed by Pearson's correlation coefficient, Bland-Altman plots of the differences against the mean, repeated measures analysis of variance (ANOVA) and

paired t-tests. Because of the multiple comparisons, a Bonferroni adjustment for repeated measures was applied (for an alpha level of 0.05 and 4 comparisons) resulting in $p \leq 0.012$ for statistical significance.

3.1.IV. RESULTS

The mean values of spherocylindrical error and the Zernike coefficients for primary coma (Z_3^{-1}, Z_3^1), primary spherical aberration (Z_4^0), and high order root mean square (HO RMS) for each of the model eyes studied as measured in the first session are displayed in table 3.2.

	Eye 1	Eye 2	Eye 3	Eye 4	Eye 5	Eye 6
Sphere	-10.07 (±0.00)	-9.39 (±0.00)	-7.45 (±0.01)	-5.74 (±0.00)	-4.86 (±0.00)	-3.16 (±0.01)
Cylinder	-0.30 (±0.00)	-0.15 (±0.00)	-0.23 (±0.00)	-0.46 (±0.00)	-0.43 (±0.00)	-0.43 (±0.01)
Axis	85.0 (±0.0)	17.3 (±0.5)	61.1 (±0.3)	94.0 (±0.0)	150.4 (±0.0)	135.9 (±0.3)
Z_3^{-1}	-0.464 (±0.003)	-0.182 (±0.009)	-0.553 (±0.008)	-0.170 (±0.004)	0.018 (±0.004)	0.008 (±0.008)
Z_3^1	-0.141 (±0.012)	0.216 (±0.009)	0.441 (±0.013)	0.170 (±0.008)	0.138 (±0.005)	0.241 (±0.003)
Z_4^0	-0.760 (±0.004)	-0.838 (±0.008)	-0.719 (±0.006)	-0.644 (±0.002)	-0.641 (±0.002)	-0.628 (±0.004)
HO RMS	0.382 (±0.004)	0.383 (±0.005)	0.414 (±0.007)	0.308 (±0.010)	0.290 (±0.000)	0.290 (±0.005)

Table 3.2.- *Mean value (± SD) of spherocylindrical refractive error (in dioptres) and the Zernike coefficients for coma (Z_3^{-1}, Z_3^1, Z_4^0 and HO RMS, in microns).*

3.1.IV.i. Intrasession repeatability

ICCs were used to determine the intrasession repeatability for all data sets and are shown in table 3.3.

	Session 1	Session 2	Refocusing	Misaligned
Z_3^{-1}	0.999	1.000	0.991	0.998
Z_3^{1}	0.997	0.992	0.970	0.996
Z_4^{0}	0.999	1.000	0.971	1.000
HO RMS	0.989	1.000	0.981	0.992

Table 3.3.- *Intraclass correlation coefficients for the measurements of HOA on each of the sessions*

Figure 3.3 shows the plots of the mean standard deviations obtained within each of the experimental sessions for the third and HOA calculated for repeated measurements up to ten. These plots show that in most instances the standard deviation of three readings does not differ significantly from that for ten repeated measures.

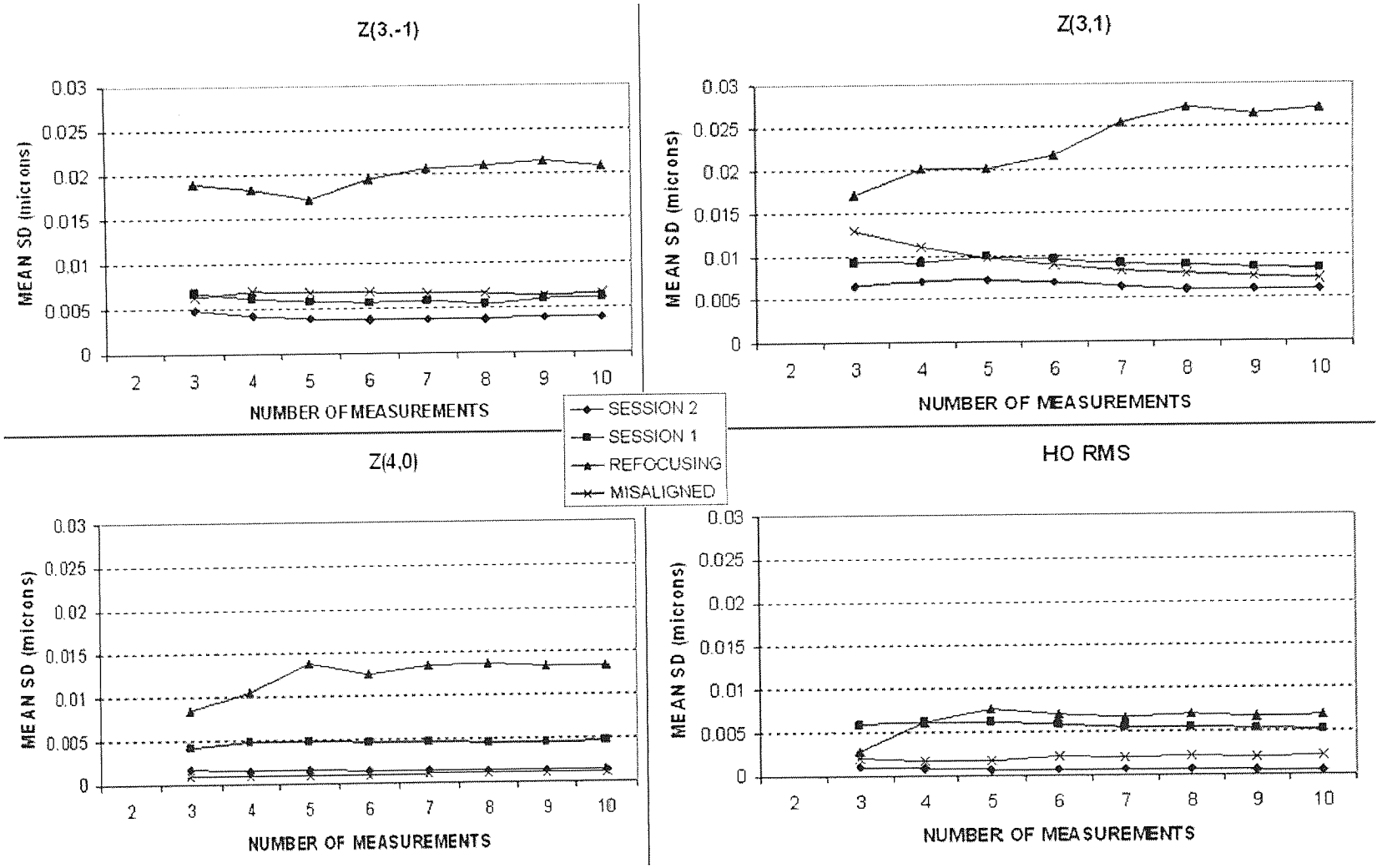

Figure 3.3.- *Plots of mean SD against the number of measurements for the Zernike coefficients measured.*

3.1.IV.ii. Intersession repeatability

Bland and Altman plots of mean difference against mean for the Zernike coefficients obtained for the eye models between all the different sessions are displayed in figures 3.4-3.7. The mean difference in all cases was very close to zero, with the exception of coefficient Z_3^{-1} when misaligned with respect to the instrument axis. It is interesting to note that the 95% confidence intervals were broader for the comparisons of the two sessions without realignment than for the comparison of realignment versus non-realignment. This finding could be due to the fact that in the non-realignment sessions, once the system was aligned and focused, it was locked and the measurements were taken consecutively. Hence the initial difference in the values, due to a minor movement of the eye or a single outlier in one data set, would be maintained throughout the session, whereas when refocusing one measurement could possibly compensate for the error of the previous one.

As shown in table 3.4, two-tailed paired t-tests demonstrated that, with the exception of HO RMS, there were no statistically significant differences between the first two sessions with high correlation between the values obtained. For HO RMS there was a significant difference between values at the first two sessions ($p=0.002$), however the measures were still highly correlated.

3.1.IV.iii. Realignment

As can be seen in table 3.4, For the most part there were no significant differences between the values obtained realigning the system between measurements compared to those without realignment, with high correlation between the respective values obtained. Only the differences between the values of Z_3^{-1} obtained in the two situations reached significance ($p<0.001$) despite the mean of the differences being low (0.017 ± 0.033 μm) and the presence of a positive, significant correlation (Pearson's correlation coefficient = 0.991, $p<0.001$).

3.1.IV.iv. Angular misalignment

Angular misalignment of the model eye induced statistically significant differences in the values obtained for Z_3^{-1} and HO RMS ($p<0.001$ in both cases), although the values are well correlated (Pearson's correlation coefficient =0.778 and 0.938, respectively; $p<0.001$ in both cases). The mean difference for Z_3^{-1} is however quite high (mean difference ± SD = -0.355 ± 0.137, $p<0.001$; table 3.4).

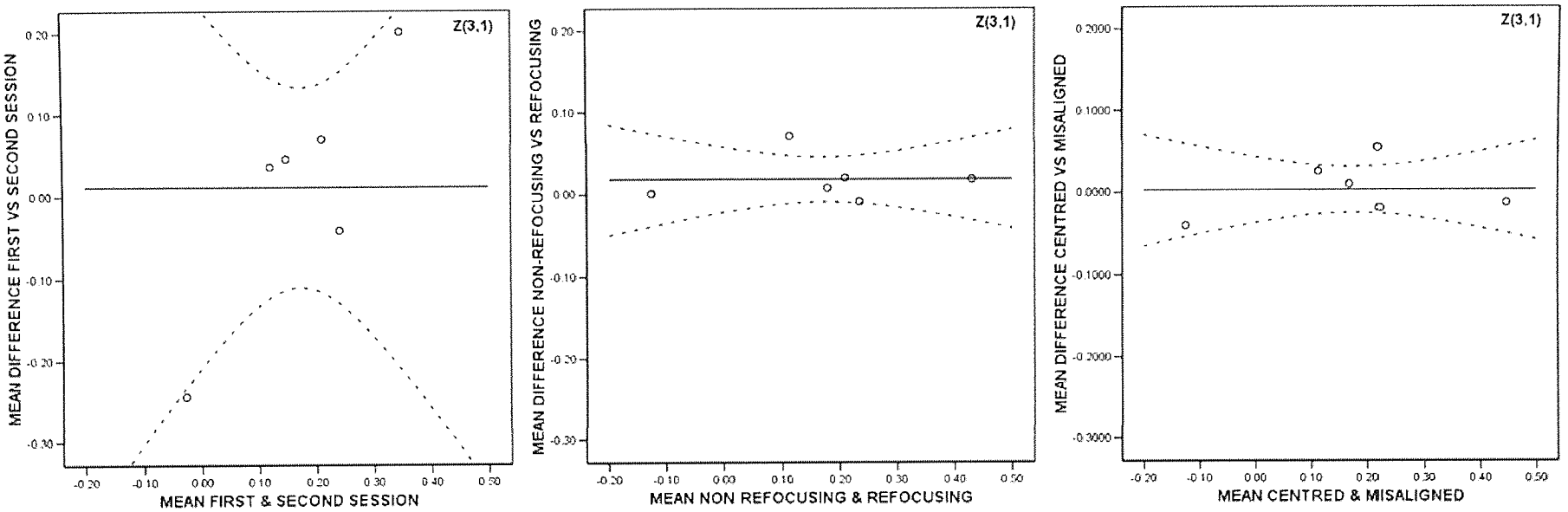

Figure 3.4.- *Bland-Altman plots of difference versus mean of the values obtained for different the Zernike coefficient Z(3,1) in all the conditions measured. All values are in microns.*

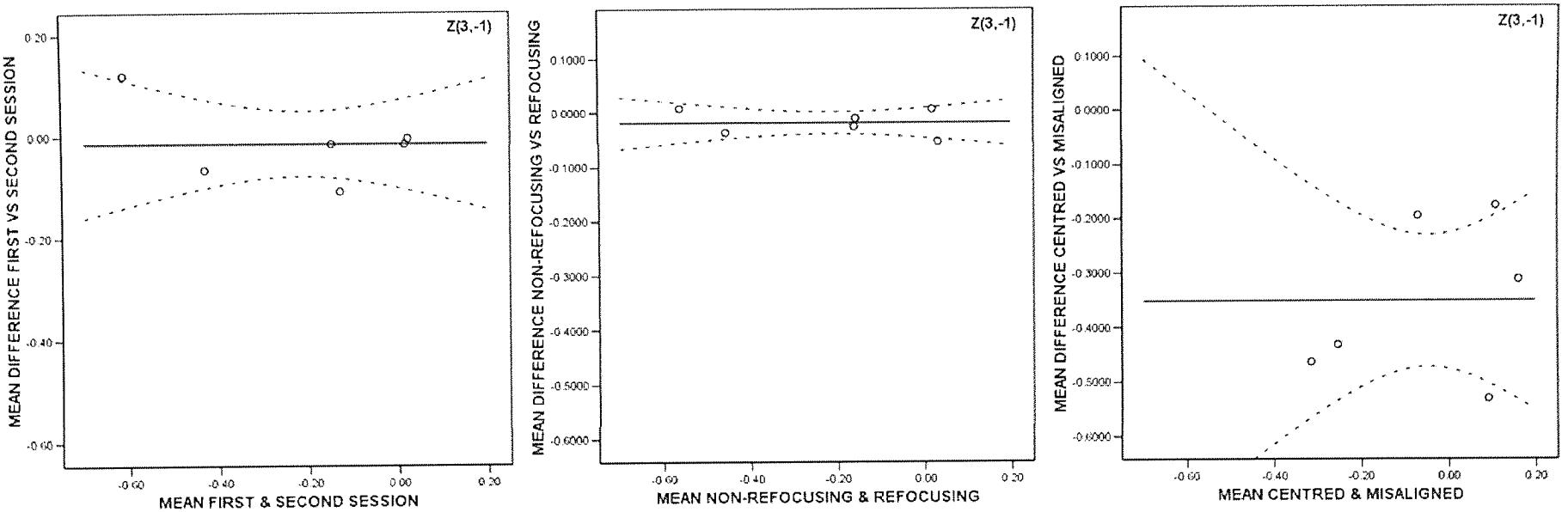

Figure 3.5.- *Bland-Altman plots of difference versus mean of the values obtained for different the Zernike coefficient Z(3,-1) in all the conditions measured. All the values are in microns.*

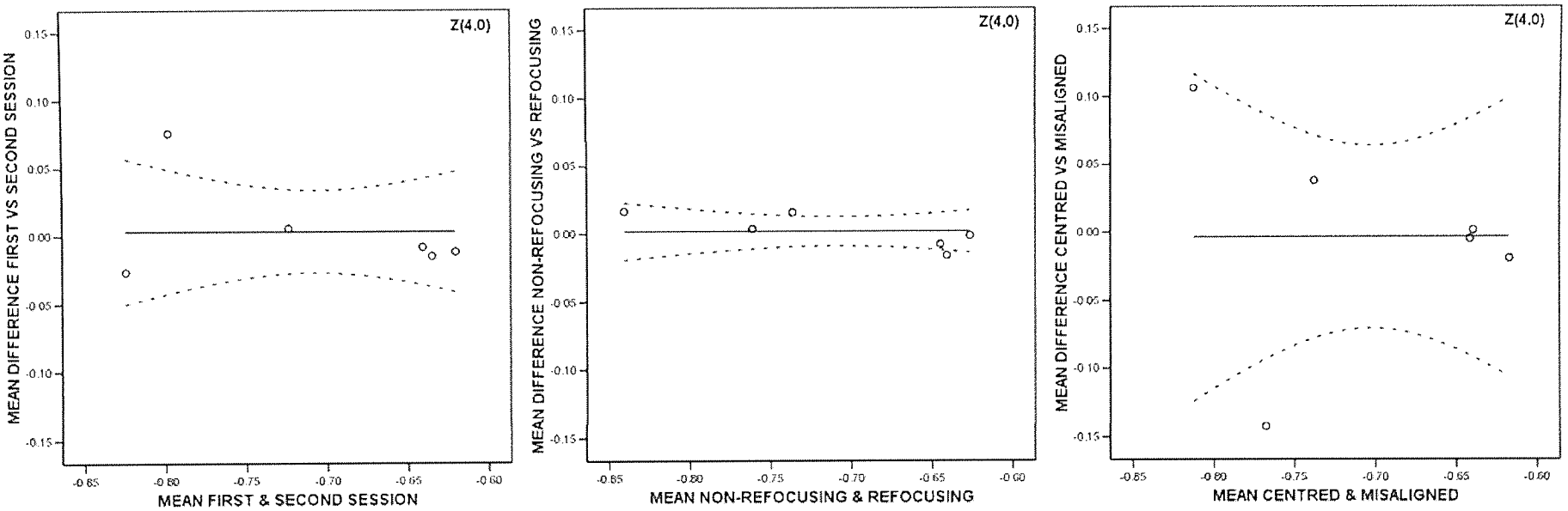

Figure 3.6.- *Bland-Altman plots of difference versus mean of the values obtained for different the Zernike coefficient Z(4,0) in all the conditions measured. All the values are in microns.*

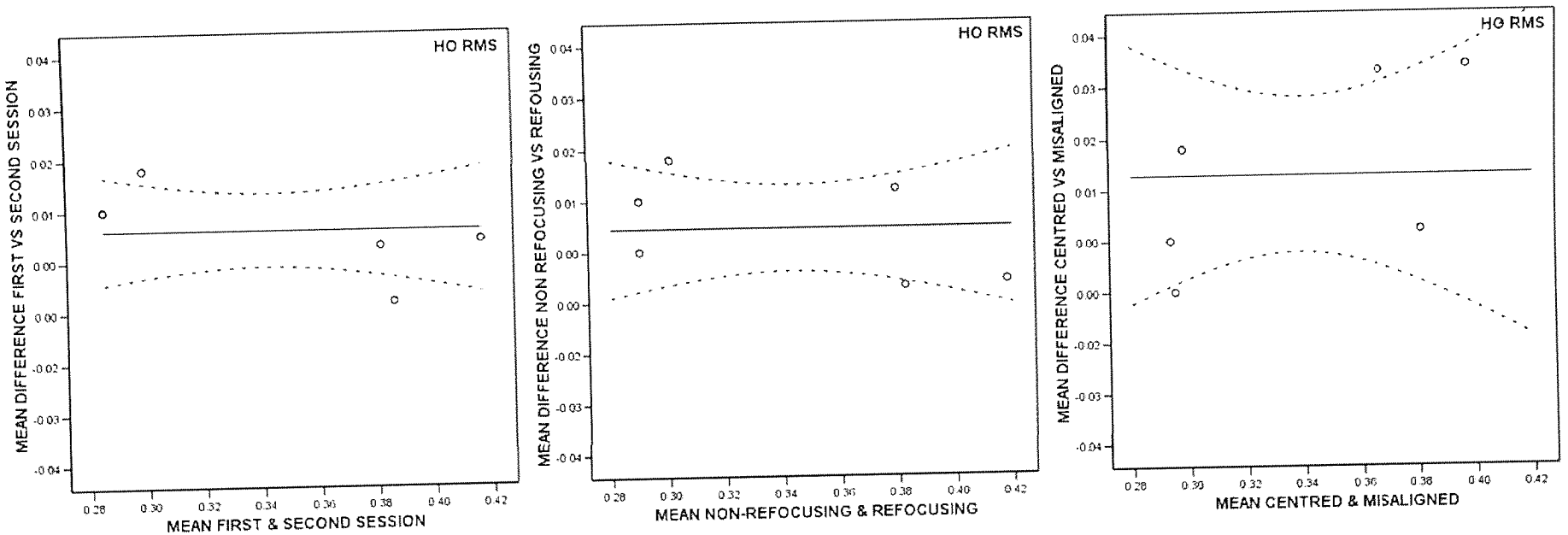

Figure 3.7.- *Bland-Altman plots of difference versus mean of the values obtained for different values of HO RMS obtained in all the conditions measured. All the values are in microns.*

	SESSION 1 Vs SESSION 2 NO REALIGNMENT					NO REALIGNMENTvs REALIGNMENT					CENTERED Vs MISALIGNED NO REALIGNMENT				
	Mean Diff	SD	p	Pearson's Correlation	p	Mean Diff	SD	p	Pearson's Correlation	p	Mean Diff	SD	p	Pearson's Correlation	p
Z_3^{-1}	-0.014	0.070	0.119	0.967	<0.001	-0.017	0.033	<0.001	0.991	<0.001	-0.355	0.137	<0.001	0.778	<0.001
Z_3^{1}	0.009	0.128	0.579	0.761	<0.001	0.009	0.038	0.072	0.977	<0.001	0.007	0.035	0.109	0.979	<0.001
Z_4^{0}	0.004	0.034	0.417	0.927	<0.001	0.007	0.021	0.015	0.966	<0.001	-0.005	0.074	0.603	0.605	<0.001
HORMS	0.005	0.011	0.002	0.989	<0.001	0.002	0.012	0.193	0.977	<0.001	0.012	0.019	<0.001	0.938	<0.001

Table 3.4.- *Results from the two-tailed paired t-tests comparing the results obtained in the four different sessions. For each comparison, mean difference between the two sessions, along with the corresponding SD and p-value, and Pearson's correlation coefficient, also with its corresponding p-value, are shown. Units are microns.*

3.1.V. DISCUSSION

This study confirmed the WASCA to be a highly repeatable instrument for measurements of all the Zernike coefficients studied. Further, intrasession repeatability did not decrease when the model was angularly misaligned with respect to the instrument axis. These findings are consistent with those of a previous study which demonstrated good repeatability, low variability and measures that were robust to axial and lateral misalignments (Cheng et al., 2003). The present study did demonstrate that with highly aberrated eyes, angular misalignment results in a significant change in the degree of coma.

A particular feature of the methodology in this study was to assess the impact of the type of operator errors that might be induced during normal clinical evaluation, that is, the clinician performing a normal realignment between measurements (combination of small axial and lateral misalignments), and with a small fixation error by the patient (angular misalignment of six degrees of the model eye). It is of interest that there is a substantial increase in the variability of measures acquired during the session in which the system was realigned after each measurement. This increase accounts for small differences in lateral and axial misalignments that occur between the measurements and are highly dependent on how capable the observer is in finding the right focusing position each time. The reference for focusing of the COAS/WASCA consists of six light circles that the observer has to focus and centre on the cornea (figure 3.8). The observer's perception of these lights as being focused will depend on factors such as the patient's corneal curvature, the observer's own refractive error, and the corresponding depth-of-focus, resulting in a range of conditions within which a particular observer may see the reference lights as equally focused. These clinically important factors should be taken into consideration, especially if it is intended to monitor or treat patients based on a single data measurement; therefore, it is recommended to take at least two consecutive measurements.

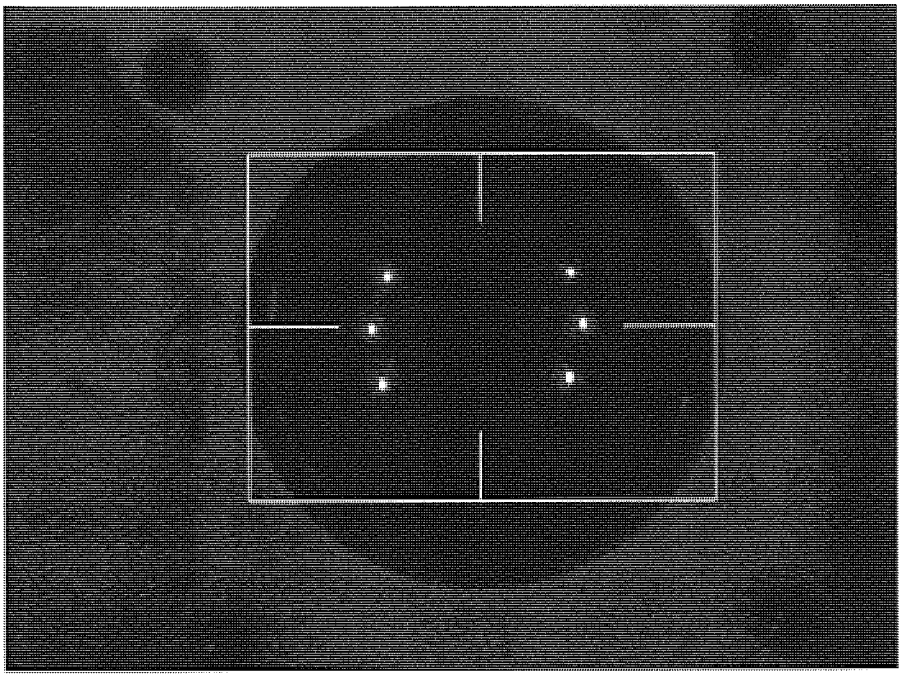

Figure 3.8.- *Image of the alignment and focusing reference for the observer with the WASCA analyzer.*

As shown in figure 3.3, the mean standard deviation did not vary widely with increasing numbers of readings in the model eyes, suggesting that the reported variation in repeated measures associated with data from human eyes (Davies, Diaz-Santana, and Lara-Saucedo, 2003) is most likely associated with a physiological variation in human wavefront aberrations over time. It is possible that any such variability is related to the ocular pulse, and pulse synchronisation of data acquisition may need to be considered to improve clinical wavefront measures in future iterations of the technology.

A further aim of this study was to assess the impact that an angular misalignment, as would occur when the patient is not fixating properly, would have in the determination of the wavefront aberration pattern. The results show that, perhaps expectedly, the vertical component of coma was significantly affected by misalignment suggesting that it is more greatly affected by misalignment in the clinical setting. The extent of any error will of course depend on the degree to which an eye is aberrated, and importantly, since the model eye utilised a spherical model for the cornea, it is possible that the aspheric nature of the human eye will result in further errors in a human system. Therefore, variations in horizontal coma and spherical aberrations may also be expected

when measuring a misaligned human eye with respect to the values obtained when aligned. This should be a subject for future study.

In summary, this study reaffirms previous findings that the WASCA is a highly repeatable instrument for the measurement of ocular wavefront aberrations both inter- and intra-session. However, the study also shows that the manipulation of the instrument during the realignment process between measurements increases the variance of the values, being likely dependent on the clinician skills to realign the system, and thus repeated measures such as those acquired in the follow-up of patients should be measured and interpreted with caution(Cervino, 2006). None the less, the repeatability after realignment is still very high. Angular misalignment of the eye during the image acquisition leads to significant differences in the values of coma obtained, mainly its vertical component. It is likely that the impact of this in the aspheric human cornea may be greater. These findings are of particular importance in the assessment of highly aberrated eyes, which are perhaps those most likely to benefit from customised ablation procedures (Mastropasqua et al., 2006). Careful repositioning of the instrument and alignment of the patient will therefore provide the best data for treatment or follow-up. Automated acquisition protocols with pulse synchronisation may benefit the accuracy and repeatability of measures in the future.

3.2. PERFORMANCE OF A HARTMANN-SHACK SENSOR IN HUMAN EYES. COMPARISON WITH SKIASCOPY-BASED ABERROMETRY.

3.2.I. ABSTRACT

Purpose: To compare the measurement of wavefront aberrations in non-cyclopleged human eyes with HS (SH), and dynamic-skiascopy based wavefront analyzers.

Methods: Eighty eyes from 40 healthy young adults (19 men, 21 women; mean age 20.8 ± 2.5 years) with refractive errors ranging from +1.5 D to -9.75 D sphere and up to 1.75D cylinder (total mean spherical equivalent MSE -2.12 ± 2.69 D) were examined with the WASCA and OPD wavefront analyzers and with the SRW5000 binocular, infrared, open-field autorefractor without the instillation of dilating = cycloplegic eyedrops. Three consecutive measurements were taken with each of the systems, in a randomized sequence. In order to avoid differences due to instrument myopia, eyes were excluded if the MSEs obtained with any of the wavefront analyzers were more than 1D more negative than those obtained with the SRW5000; 13 eyes were excluded from the analysis. Coefficient of repeatability (CoR) was determined for the WASCA as the confidence interval (CI) for the differences between the repeated measures. Comparison between values obtained with the two wavefront analyzers was performed by paired t-tests with Bonferroni adjustment for multiple comparisons. Correlation was assessed by Pearson's correlation coefficient. Bland Altman plots of difference versus mean were also produced.

Results: The CoR for the values obtained with the WASCA ranged from 0.008 to 0.022 μm. Data distribution was normal for all Zernike coefficients measured with WASCA, but only for Z_3^{-1}, Z_3^1, Z_4^0 measured with the OPD. Mean differences in coefficients Z_3^{-3}, Z_3^1, Z_3^3, Z_4^0 and Z_4^2 and HO RMS reached statistical significance (Mean difference ± CI were -0.054 ± 0.021, -0.056 ± 0.022 and 0.030 ± 0.016, respectively, $p<0.05$ in all cases). Correlation coefficients were significant only for HO RMS (Spearman's rho =0.777; $p>0.001$).

Conclusion: The WASCA wavefront analyzer shows good repeatability on human eyes without cycloplegia. Although mean differences are close to zero, the data spread shows

great variability for those coefficients more relevant to visual outcomes, i.e., coma, trefoil and spherical aberration. Aberration values obtained with dynamic skiascopy and Hartmann Shack systems on non-cyclopleged human eyes are not well correlated with each other, although good correlation of HO RMS might lead one to think differently.

3.2.II. INTRODUCTION

The need for greater accuracy of wavefront analysis performed preoperatively, and postoperatively during follow-up, will optimise the outcomes of customised refractive surgery procedures and is a common topic of discussion in studies assessing the performance of the different instruments involved. This is particularly important when measuring the aberrations of the eye in normal viewing conditions (Cervino, 2006).

There are a number of reports which investigate the agreement between different wavefront sensors on model and cyclopleged human eyes for both lower and HOA, showing good agreement overall (Hong et al., 2003; Moreno-Barriuso et al., 2001; Moreno-Barriuso and Navarro, 2000; Salmon, Thibos, and Bradley, 1998; Wang, Wang, and Koch, 2003) and indeed being consistent with the results reported in the study 3.1 of this thesis.

Wavefront analysis aims to measure ocular aberrations with the eye in its natural state, often in the pre- and post-operative setting. Therefore, it is of particular importance to know if the different techniques available for measuring ocular optical quality in these conditions are interchangeable, since this would allow direct comparison of results obtained in different studies with different instruments.

The main aim of this study is to evaluate the performance of the WASCA wavefront analyzer against an alternative commercial device also widely used for research and clinical purposes in terms of measuring the optical quality of young healthy human eyes under normal viewing conditions, namely, without the instillation of any pharmacological agent for pupil dilation and cycloplegia.

3.2.III. METHODS

3.2.III.i. Sample description

Eighty eyes from 40 healthy young adults (19 men, 21 women; mean age 20.5 ± 2.6 years) with refractive errors ranging from +1.5 D to -9.75 D sphere and up to 1.75D cylinder (mean spherical equivalent -2.11 ± 2.69 D) were examined with two clinical wavefront analyzers, the WASCA and the OPD, and with the SRW5000 binocular, infrared, open-field autorefractor (Shin-Nippon, also branded as Grand Seiko 5000), without the instillation of any dilating cycloplegic eyedrops.

Subjects were recruited from the student and staff population of Aston University. Exclusion criteria involved ocular pathology observed by slit lamp and ophthalmoscopy examination, a history of ocular disease or having worn CL less than 24 hours prior to examination. Those cases in which there was more than 1D difference between the mean spherical equivalent obtained with the autorefractor and any of the wavefront analyzers were removed from the sample in order to avoid individual differences in instrument myopia (Cervino, 2006), which will be investigated further in chapter 4.

There were no specific requirements or restrictions pertaining to refractive error, ethnicity, gender or age.

3.2.III.ii. Ethics approval

Informed consent was obtained from each participant after explanation of procedures. The protocol followed the tenets of the Declaration of Helsinki and was approved by the Ethics Committee of Aston University.

3.2.III.iii. Experimental procedures

Three consecutive measurements were taken with each of the systems, alternating for instrument sequence and always measuring right eye first. Patients were instructed to

fixate the internal target provided by each of the analyzers and a distant Maltese cross when measuring with the SRW5000.

The OPD-scan®/ARK-10000® (Nidek Co, Gamagori, Japan) is a device for the determination of wavefront aberration using the principle of dynamic skiascopy, described previously in Chapter 1 (section 1.2.1.vii). In brief, the device uses an infrared system of slit scans across the pupil to measure the time difference of the light reflected by the retina between the centre and each of several photodetectors on each side from the centre(Buscemi, 2004; MacRae and Fujieda, 2000). Relatively, little has been reported on the performance of clinical devices using this principle. However poor repeatability for higher order aberration values in non-cyclopeged eyes has been demonstrated (Zadok et al., 2005), in contrast with close agreement with HS wavefront sensors in determining RMS values in model and human eyes with induced mydriasis(Hieda and Kinoshita, 2003). It has also been successfully coupled to laser systems for customized refractive surgery procedures(Arbelaez, 2001; Gimbel et al., 2003; Gimbel and Stoll, 2001; Nakano et al., 2003; Sarkisian and Petrov, 2002), and for the assessment of the optical quality of pathological and post-surgical eyes(Shah et al., 2003).

3.2.III.iv. Data analysis

In this study, values for Zernike coefficients Z_3^{-1}, Z_4^{-4}, Z_4^{-2} , Z_4^4 , Z_3^{-3}, Z_3^1, Z_3^3, Z_4^0 and Z_4^2, as well as for high order RMS (HO RMS), were obtained with both systems. Statistical analysis was performed with the SPSS v.12.0.1 (SPSS Inc.) Assessment of the repeatability of WASCA measurements was determined from the calculation of the coefficient of repeatability (COR), calculated as twice the 95% confidence interval for the differences between measurements. Assessment of the repeatability of the OPD was not performed since the instrument automatically averages the three readings.

In order to assess differences between both instruments the Zernike coefficients obtained by each device were compared through two-tailed paired t-tests.
Bland-Altman plots of difference versus mean between the two analyzers were also made for each of the Zernike coefficients analyzed.

3.2.IV. RESULTS

A total of 13 eyes were excluded from the analysis due to a discrepancy in refractive error between any of the wavefront analyzer and the autorefractor greater than 1D, resulting in 67 eyes for analysis.

Table 3.5 shows the descriptive statistics of the sample included in the analysis (n=67).

	Minimum	Maximum	Mean	SD
Age (years)	18	31	20.8	2.7
MSE (D)	-9.88	2.19	-2.44	2.74
Difference WASCA – SRW5000 (D)	-0.82	0.98	0.36	0.39
Difference OPD –SRW5000 (D)	-0.55	0.94	0.16	0.32

Table 3.5. *Descriptive statistics of the sample included in the analysis (15 men, 17 women).*

Table 3.6 shows details on the sub sample excluded from the analysis (n=13).

For the remaining sample, the COR for the values obtained with the WASCA are shown in table 3.7, and ranged from 0.008 to 0.022 μm for the different coefficients analyzed.

Data distribution was normal for all coefficients measured with the WASCA. However, distribution was normal only for coefficients Z_3^{-1}, Z_3^1, Z_4^0 measured with the OPD, therefore Wilcoxon signed ranks test was applied to all the coefficients, including those three coefficients with normal distribution, in order to make interpretation of the results easier to follow.

Patient n°	Age (years)	Gender (M/F)	Eye (R/L)	MSE (D)	Difference WASCA – SRW5000 (D)	Difference OPD -SRW5000 (D)
4	19	M	R	0.75	1.28	0.75
			L	1.00	1.17	1
5	20	M	R	-6.18	1.28	0.25
17	19	F	R	-0.25	0.48	3
			L	-0.19	0.08	3.31
26	19	M	R	-0.31	1.19	1.82
			L	-0.50	1.31	2.5
34	19	M	R	-5.81	0.88	1.07
35	19	F	R	0.32	2.52	3.45
			L	0.37	2.11	2.12
39	19	F	R	-0.43	1.46	1.2
			L	-0.62	1.64	0.76
44	18	F	R	0.00	1.24	0.62

Table 3.6. *Details of the sample excluded from the analysis. Note that, except for 3 eyes, all the cases correspond to the right and left eyes of 5 subjects who are on the youngest end of the age range examined, and have a low refractive error.*

	Z_3^{-3}	Z_3^{-1}	Z_3^{1}	Z_3^{3}	Z_4^{-4}	Z_4^{-2}	Z_4^{0}	Z_4^{2}	Z_4^{4}
COR	0.020	0.022	0.017	0.014	0.008	0.009	0.015	0.012	0.010

Table 3.7.- *Mean COR obtained for the WASCA for the different Zernike coefficients analyzed here.*

Mean differences, confidence intervals and significance are shown in table 3.8.

Differences in coefficients Z_3^{-3}, Z_3^{1}, Z_3^{3} and Z_4^{2} and HO RMS reached statistical significance ($p<0.005$).

	95% Confidence Interval			
	Mean diff.	Lower	Upper	p
Z_2^{-2}	-0.054	-0.076	-0.033	**< 0.001**
Z_2^{0}	0.030	-0.009	0.069	0.095
Z_2^{2}	-0.056	-0.078	-0.034	**< 0.001**
Z_3^{-2}	0.018	0.002	0.033	**0.039**
Z_3^{-1}	-0.005	-0.015	0.004	0.280
Z_3^{1}	0.001	-0.010	0.011	0.617
Z_4^{0}	0.017	0.001	0.034	0.064
Z_4^{2}	0.030	0.013	0.046	**0.001**
Z_4^{4}	0.007	-0.001	0.015	0.089
HO RMS	0.031	-0.006	0.067	**0.018**

Table 3.8.- *Mean difference, 95% confidence intervals for the difference and significance between Zernike values obtained with WASCA and OPD-scan. Units are microns (μm). Bold p-value represents statistical significance..*

Correlation coefficients (Spearman's rho since non-parametric tests are applied) and significance levels are shown in table 3.9. The values obtained with both systems were not significantly correlated for any of the Zernike coefficients measured.

	Spearman's rho	p
Z_3^{-3}	-0.080	0.520
Z_3^{-1}	0.069	0.577
Z_3^{1}	0.069	0.578
Z_3^{3}	-0.165	0.181
Z_4^{-4}	0.098	0.430
Z_4^{-2}	0.187	0.130
Z_4^{0}	0.182	0.140
Z_4^{2}	0.131	0.292
Z_4^{4}	-0.214	0.082
HO RMS	0.034	0.786

Table 3.9.- *Correlation coefficient and level of statistical significance between Zernike values obtained with WASCA and OPD-scan..*

Bland Altman plots of difference against mean for the different coefficients are displayed in figures 3.9 through 3.18. It can be seen that, although mean differences are close to zero, the data spread shows great variability for the differences on those coefficients more relevant to visual outcomes, i.e., coma, trefoil and spherical aberration(Applegate et al., 2003).

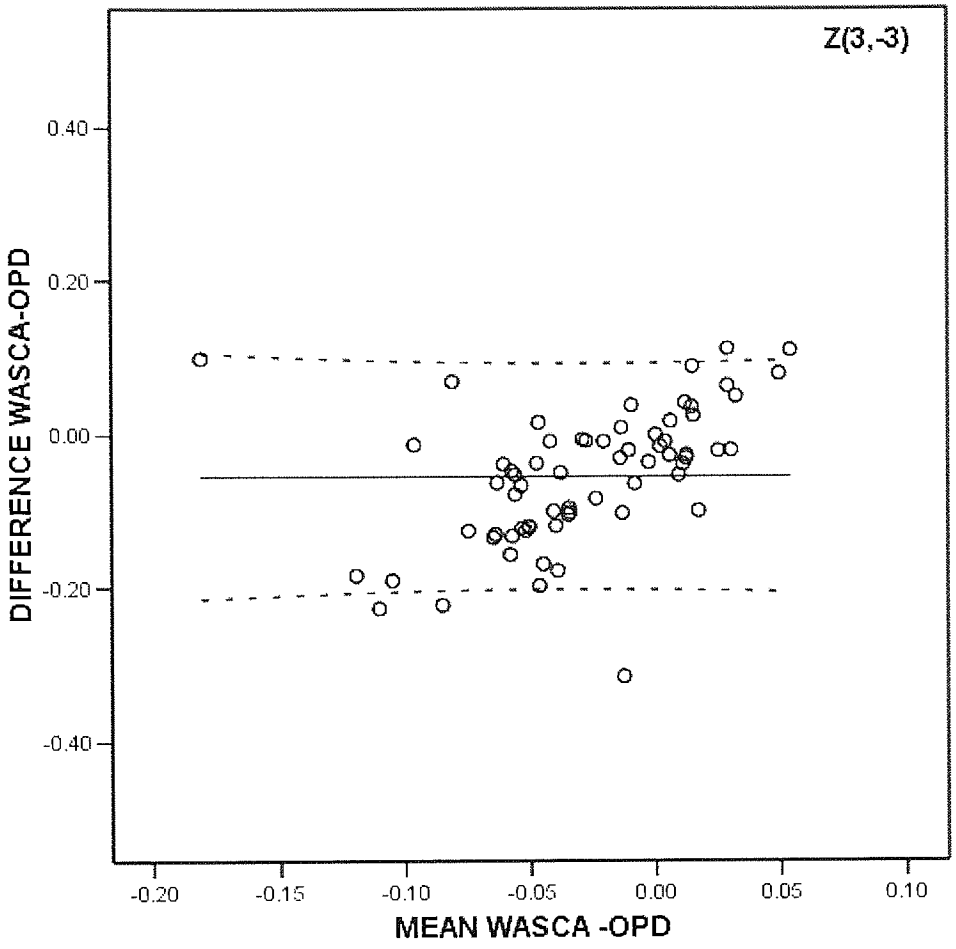

Figure 3.9.- *Bland-Altman plots of difference against mean between the Zernike values obtained with the WASCA and OPD-scan for coefficient* Z_3^{-3} *(trefoil component). Units are microns.*

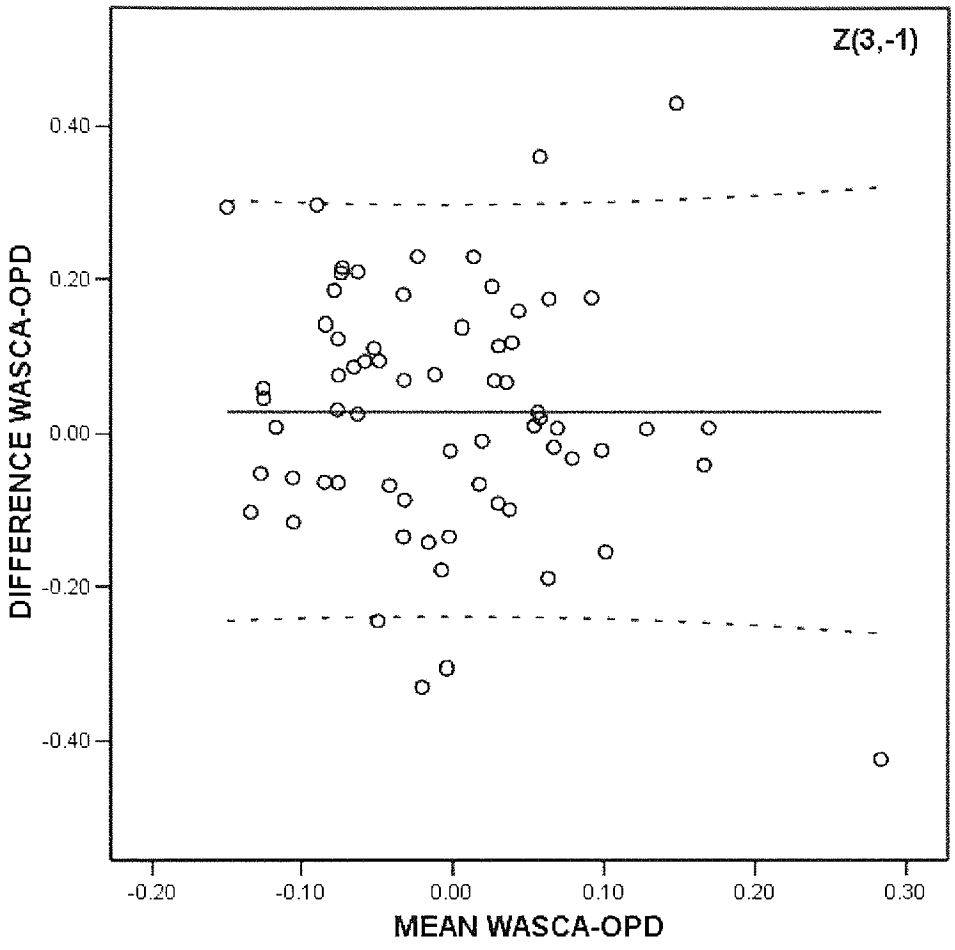

Figure 3.10.- *Bland-Altman plots of difference against mean between the Zernike values obtained with the WASCA and OPD-scan for coefficient* Z_3^{-1} *(vertical coma component). Units are microns.*

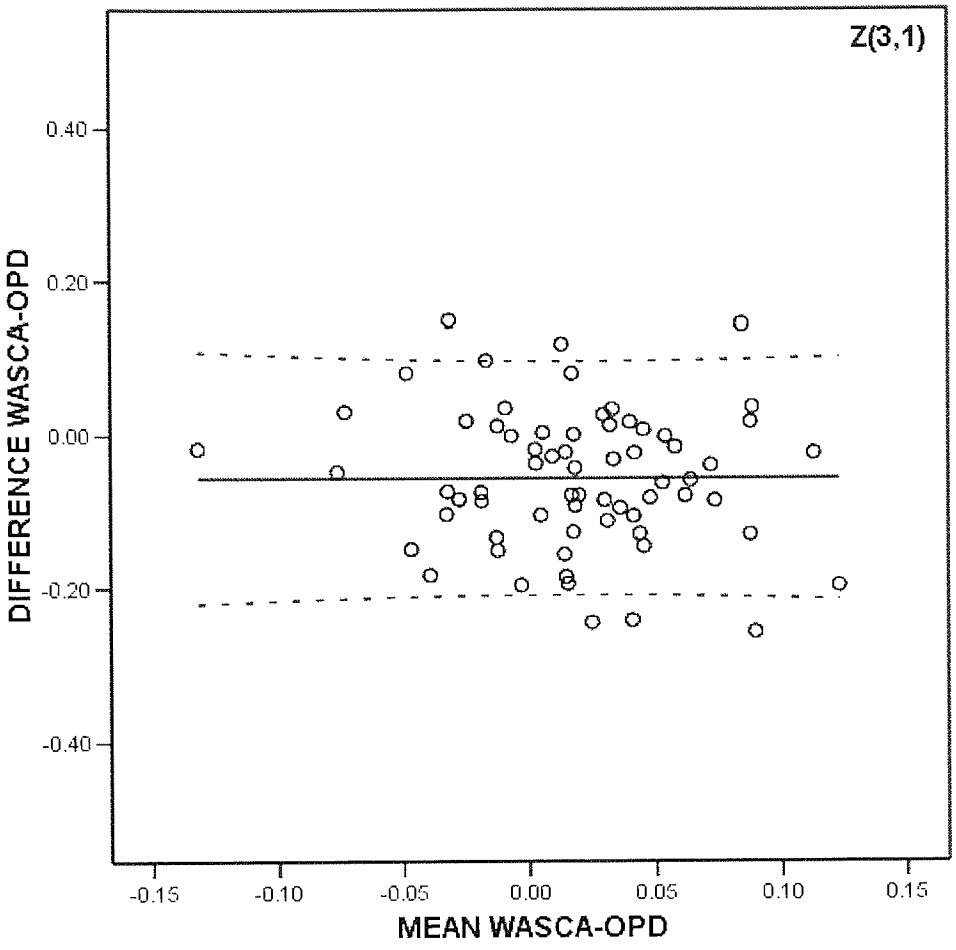

Figure 3.11.- *Bland-Altman plots of difference against mean between the Zernike values obtained with the WASCA and OPD-scan for coefficient* Z_3^1 *(horizontal coma component). Units are microns.*

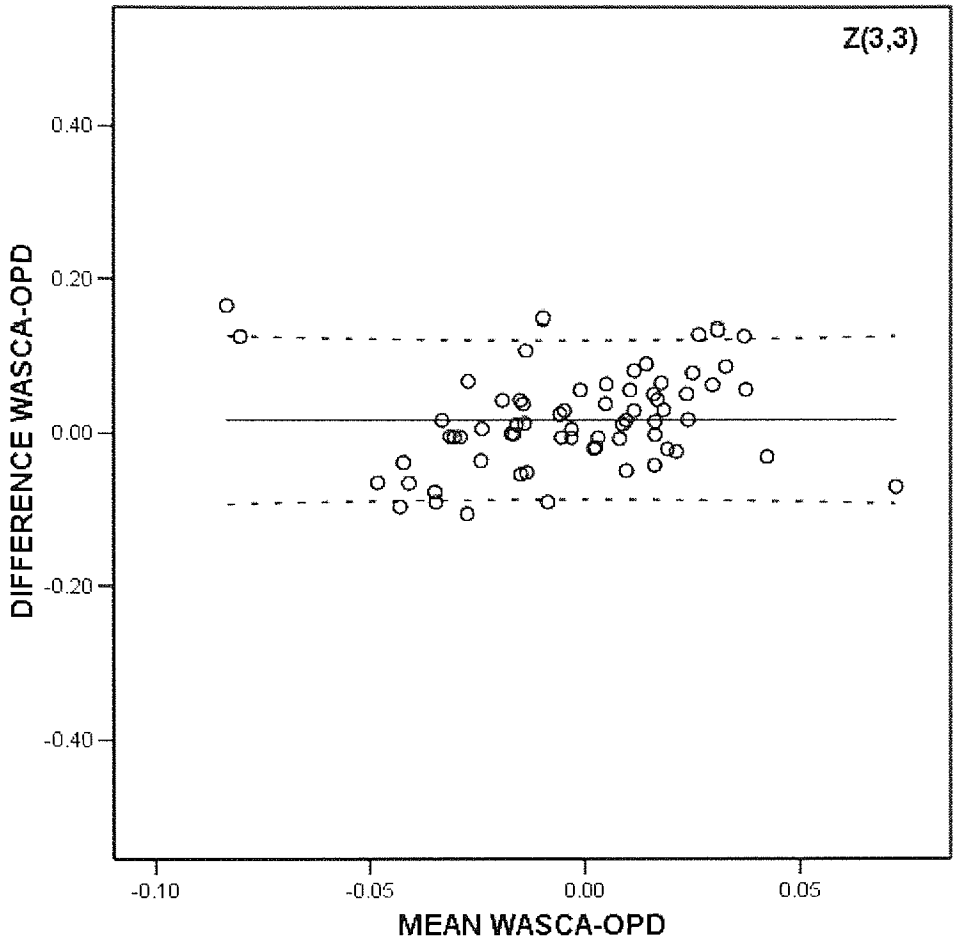

Figure 3.12.- *Bland-Altman plots of difference against mean between the Zernike values obtained with the WASCA and OPD-scan for coefficient* Z_3^3 *(trefoil component). Units are microns.*

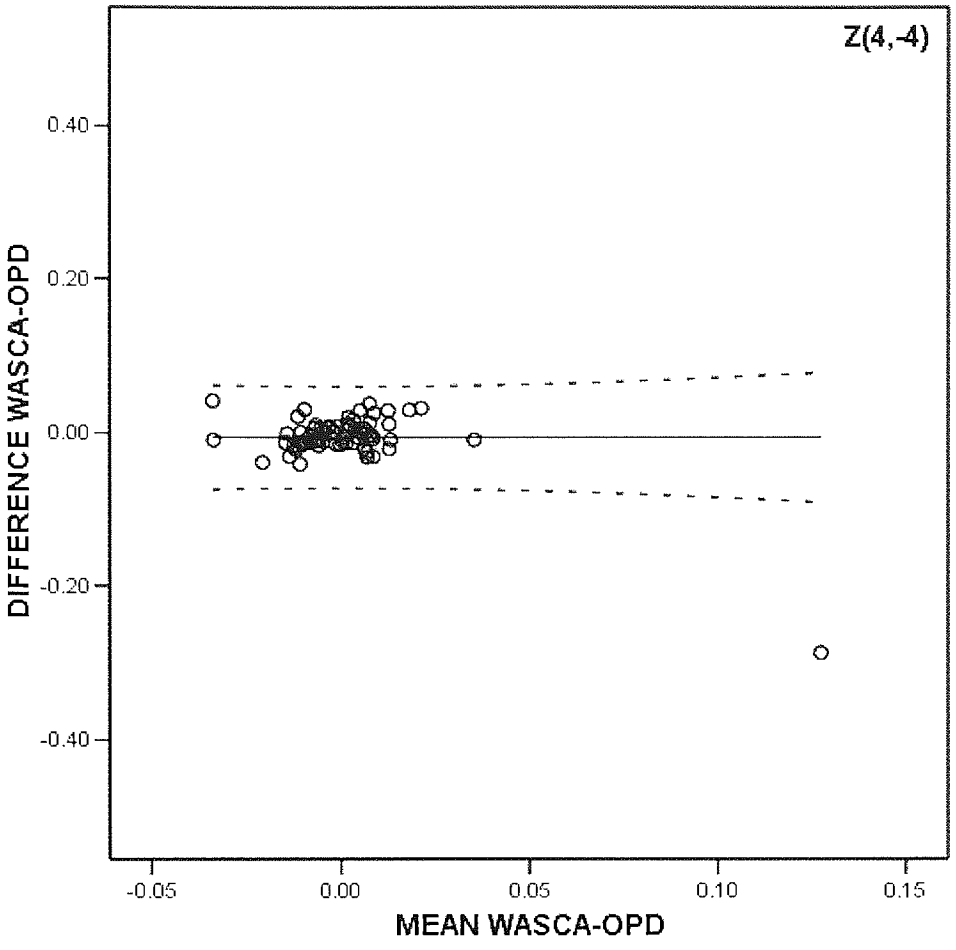

Figure 3.13.- *Bland-Altman plots of difference against mean between the Zernike values obtained with the WASCA and OPD-scan for coefficient* Z_4^4. *Units are microns.*

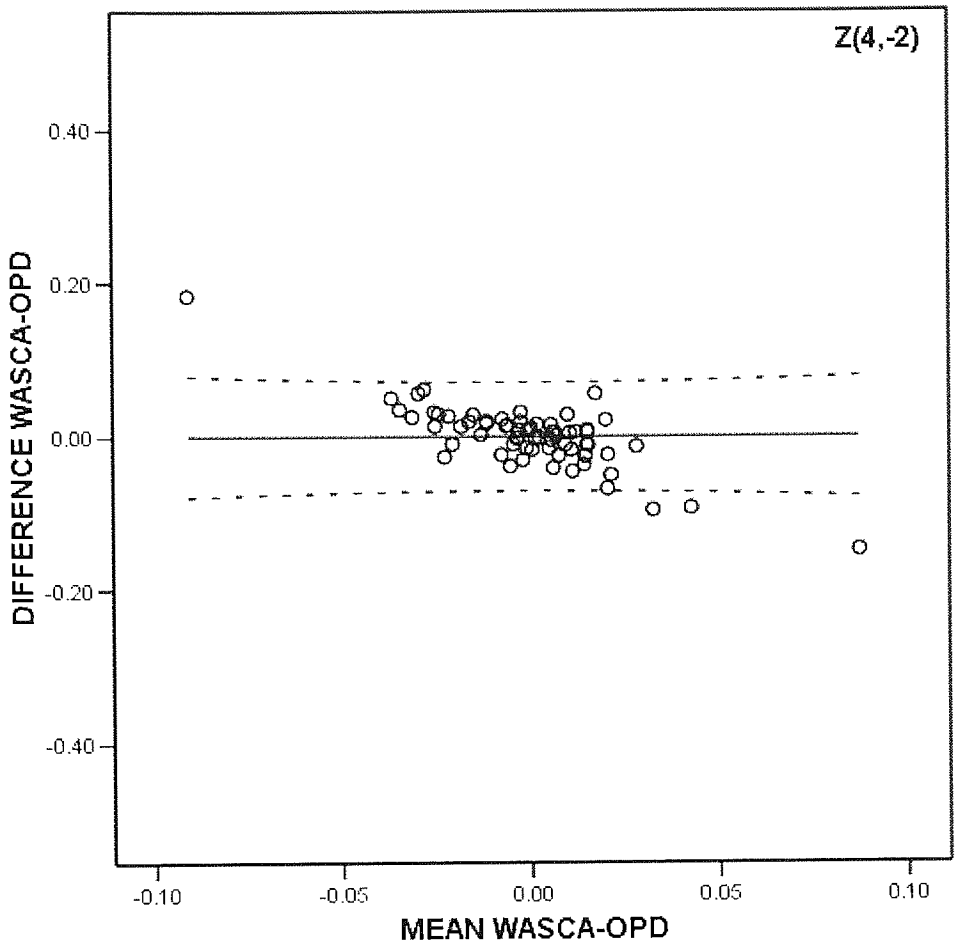

Figure 3.14.- *Bland-Altman plots of difference against mean between the Zernike values obtained with the WASCA and OPD-scan for coefficient* Z_4^{-2}. *Units are microns.*

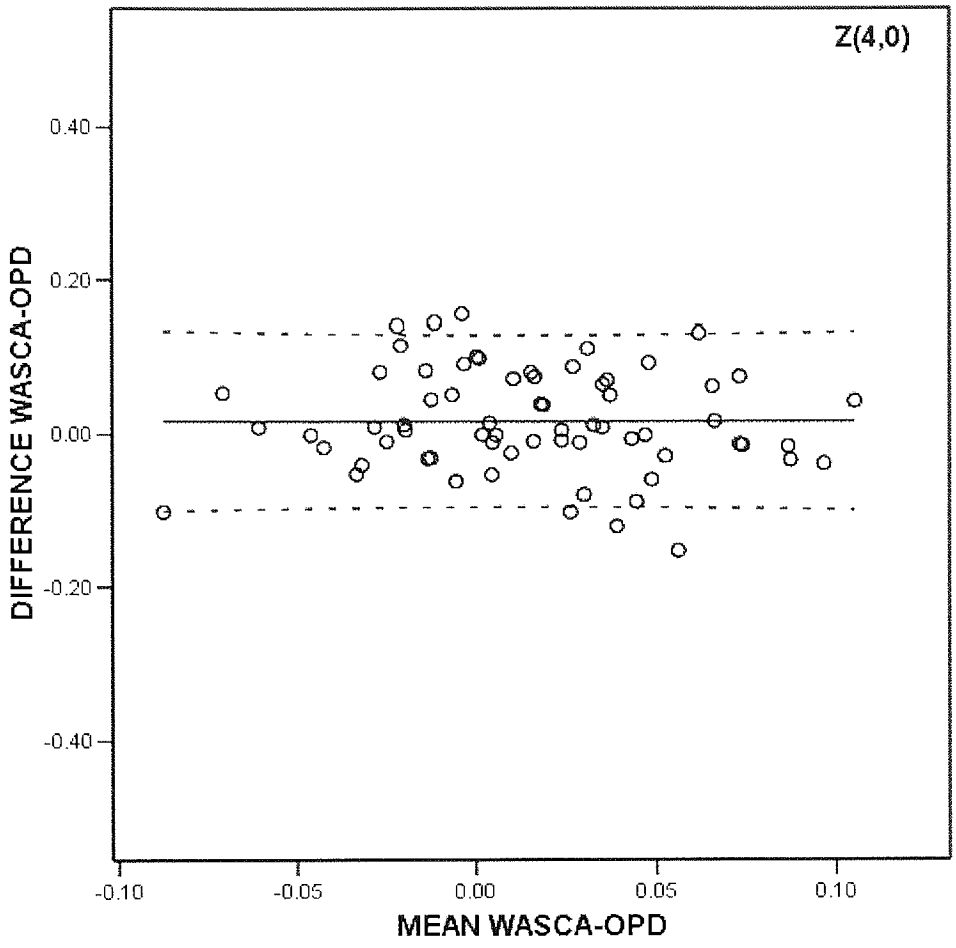

Figure 3.15.- *Bland-Altman plots of difference against mean between the Zernike values obtained with the WASCA and OPD-scan for coefficient* Z_4^0 *(primary spherical). Units are microns.*

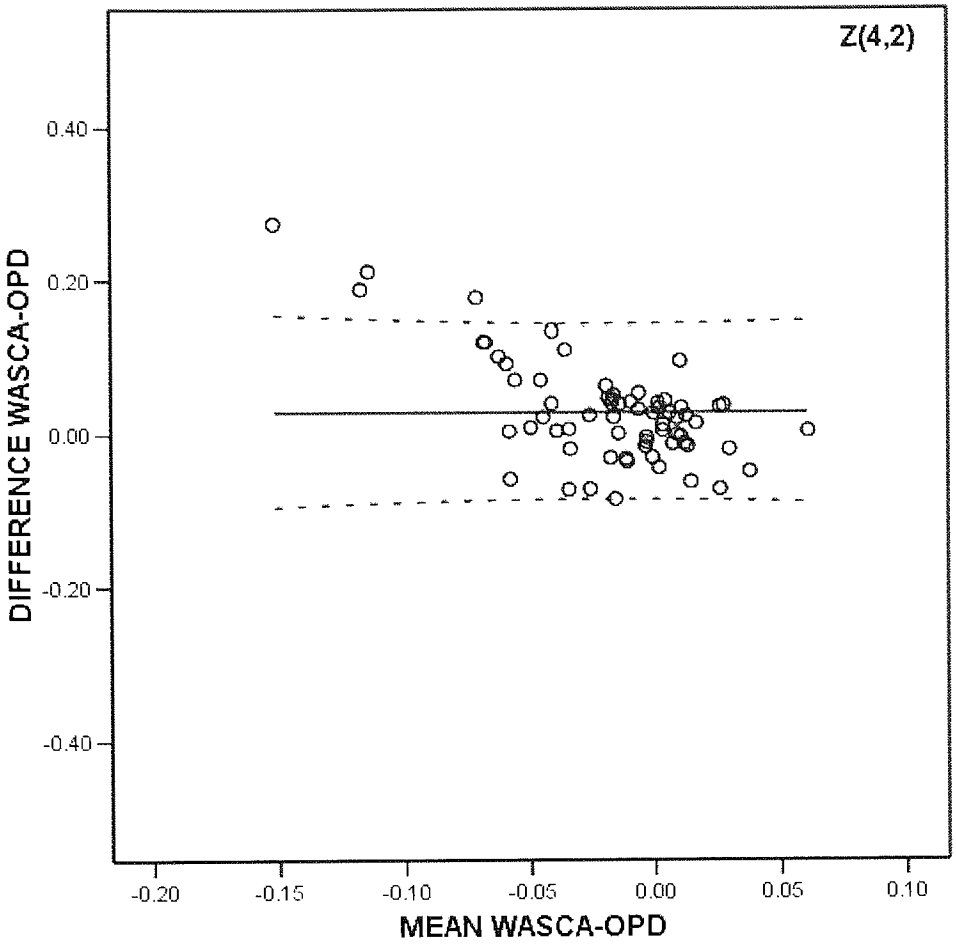

Figure 3.16.- *Bland-Altman plots of difference against mean between the Zernike values obtained with the WASCA and OPD-scan for coefficient* Z_4^2. *Units are microns.*

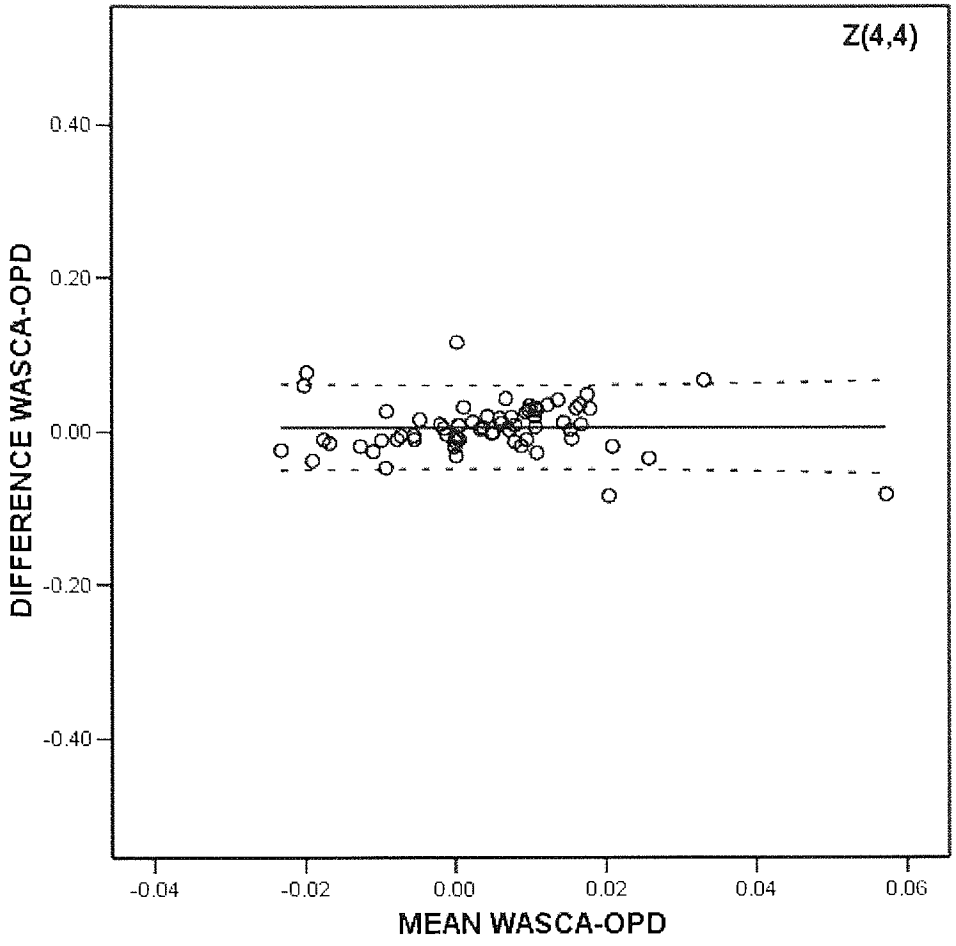

Figure 3.17.- *Bland-Altman plots of difference against mean between the Zernike values obtained with the WASCA and OPD-scan for coefficient* Z_4^4. *Units are microns.*

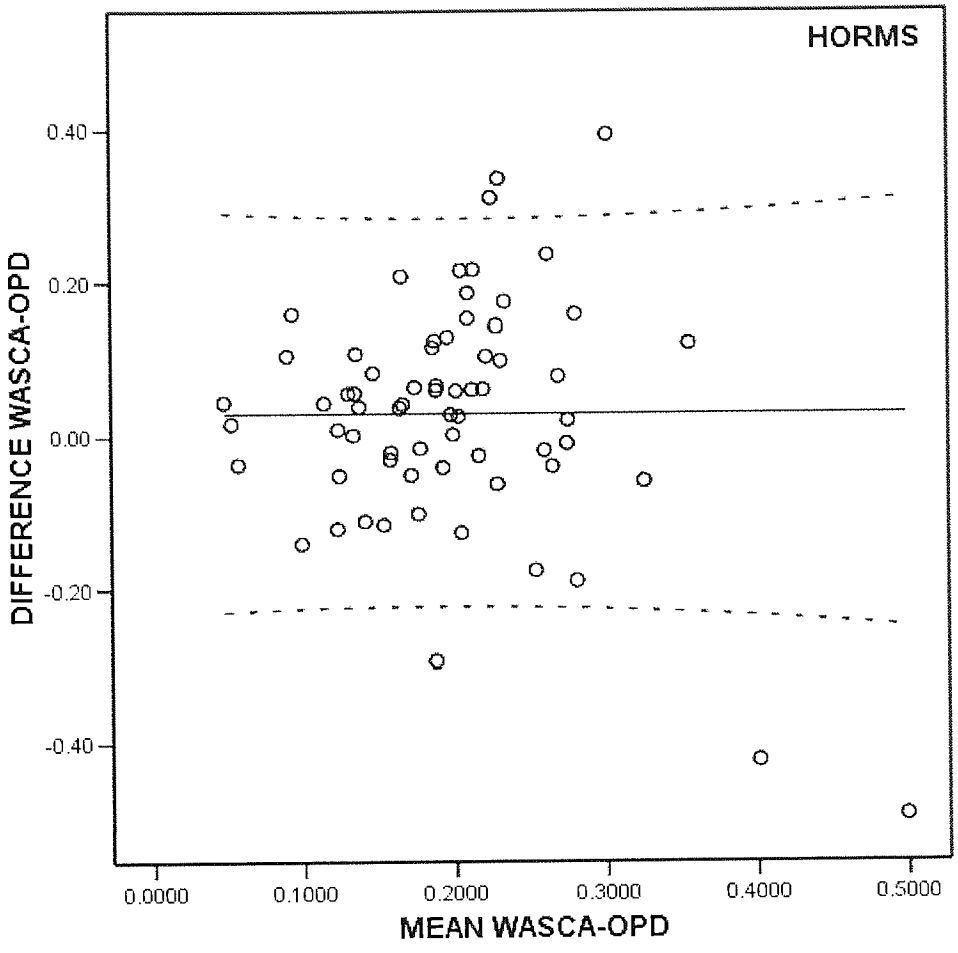

Figure 3.18.- *Bland-Altman plots of difference against mean between the values obtained with the WASCA and OPD-scan for HORMS. Units are microns.*

3.2.V. DISCUSSION

The results obtained in the present study for 5 mm pupil size in non-cyclopleged eyes did not show any correlation for any of the Zernike values obtained with both HS and skiascopy-based wavefront analyzers. In a previous study comparing the OPD and the Zywave (another HS aberrometer), Hieda and Kinoshita reported similar values for both instruments on model eyes, significant correlation for second, third and fourth order aberrations in 6mm pupil size of pharmacologically dilated human eyes and significant correlation for second and fourth order when 4mm pupil were considered (Hieda and Kinoshita, 2003). They suggested as a reason for the discrepancies found that the OPD has no information within 2.3 mm, since that is the distance of smallest photodetectors, as well as differences in spatial resolution.

The reason for the disagreement with the results reported by Hieda and Kinoshita (2003) could be that, in the present study, there is no induced cyclopegia or mydriasis and a different aberration profile to the different fixation targets offered by the instruments used could account for some of the differences shown as a result of the different accommodative response (Cervino, 2006); this will be studied further in Chapter 4.

Agreement between different wavefront sensors is an important issue that has been addressed before in several studies for sensors using a different measurement principle (Moreno-Barriuso et al., 2001; Moreno-Barriuso and Navarro, 2000; Salmon, Thibos, and Bradley, 1998), and using the same principle (Liang, Juo, and Chang, 2005). Moreno-Barriuso and Navarro concluded in their comparison between laser ray tracing and HS that both methods are equally valid (Moreno-Barriuso and Navarro, 2000) and then later found a close match between the Zernike coefficient values obtained by HS, laser ray tracing and spatially resolved refractometry (Moreno-Barriuso et al., 2001) although both studies were performed in laboratory settings and not with clinical wavefront analyzers such as those used in the present study.

Liang, Juo and Chang recently compared three different clinical HS wavefront analyzers on 34 cyclopeged human eyes, finding significant discrepancies between the

three aberrometers in the measurement of HOA (Liang, Juo, and Chang, 2005). This is an important finding as measurement of HOA is not interchangeable between instruments, even when using the same principle. Although the instruments used for these comparisons were different from those used in the present study it is important to point out that they reached the same conclusion regarding the agreement between commercial devices even though the subjects in their sample were cyclopeged at the time of measurement.

Equally important is to address the agreement on human eyes when cyclopegia is not induced, since the response of the eye to different fixation targets in closed-field environments has been proven to involve changes in the refractive error measured and, therefore, could affect the HOA obtained(Cervino, 2006)(see Chapter 4). Thus it might be expected that examining an older subject population would yield different results for the repeatability of the WASCA and possibly for the agreement between instruments.

Both wavefront analyzers evaluated here have been previously studied. The WASCA is the wavefront sensor that has attracted most attention in the literature showing that it provides high reliability in its measurements (Cheng et al., 2003; Cheng et al., 2004) although there may be some accommodative response when used in non-cyclopeged human eyes particularly with low refractive errors (Cervino, 2006).

In this study, the repeatability of the WASCA in the determination of HOA was found to be high, in agreement with the values reported previously on human eyes (Cheng et al., 2004; Salmon and van de Pol, 2005), and just slightly worse than those found on model eyes (Cheng et al., 2003). The variability found has been previously attributed mainly to accommodation fluctuations; tear film disruption or misalignment between the eye and the instrument rather than to the instrument itself (Cheng et al., 2003; Cheng et al., 2004).

There is considerably less supporting literature regarding the performance of the OPD. It has been recently shown to have poor repeatability in studies on human eyes (Zadok et al., 2005).

In the results reported here, those Zernike coefficients more relevant to visual function (coma, spherical aberration, and trefoil)(Applegate et al., 2003) are those for which differences between instruments are statistically significant, besides HO RMS. Plots of difference *vs.* mean show that mean difference approaches zero, however the data spread is considerably wide, demonstrating that the agreement between both systems is poor on a case-by-case analysis. This finding is particularly evident from the poor correlation between the values obtained with both systems, showing that, on a case-by-case basis, there is no relationship between the values obtained with both systems for any of the Zernike coefficients analyzed, even though on a group-wise analysis differences were not statistically significant for certain Zernike coefficients, and HO RMS are very significantly correlated between both instruments.

In summary, the results of HOA obtained with the OPD and the WASCA wavefront analysers are not interchangeable and, therefore, direct comparison between the results obtained in different studies using them would be of limited value. These results imply, therefore, that wavefront analysis without cycloplegia, although desirable since it corresponds to more natural viewing conditions, should be performed carefully. Further study would be needed in order to establish the level of agreement between the two methods on cyclopleged and non-cyclopleged human eyes, to determine the extent of differences attributable to the accommodative response and/or microfluctuations triggered by the fixation targets used by the wavefront analyzers. It is interesting to note that in this respect the subsample excluded from analysis corresponded mostly to the right and left eyes of a few subjects that were also very young and functionally emmetropic. The implications of these variations will be studied further in the next experimental chapter (Chapter 4).

3.3. CONCLUSIONS

The aim of this chapter was to explore repeatability issues that at the time of the study had received little attention, and to provide a methodological basis for investigations in subsequent chapters of the thesis. Two areas of importance were identified.
First, the WASCA has been shown to be a repeatable and realiable tool for the determination of wavefront aberrations on model eyes. Care must be taken, however, when the subjects examined are not cyclopleged. The extent and implications of the variations observed in non-cyclopleged subjects will be studied further in the next experimental chapter (Chapter 4).

Second, the results obtained by two different wavefront analyzers on non-cyclopleged human eyes are not interchangeable. This suggests the need for further research measuring wavefront aberrations with different devices on the same sample with and without dilation and cycloplegia in order to establish the variability attributed to the eye with each system.

The instrument of choice for the subsequent chapters was the WASCA system for a number of reasons.

First, this is the clinical wavefront analyzer about which there is more information available in the literature. It has been the reference for HS aberrometry for a number of years and has been used by the principal researchers in the field for both improving the instrumentation and learning more about the optical properties of the human eye.

Second, the other main area of interest in terms of optical quality of the retinal image is light scatter. There are instruments that measure retinal straylight in a number of ways (see Chapter 1, epigraph 1.4 onwards for a review), and the most recent and reliable one will be used later in the following chapters, but they mostly require a response from the observer. Although there has been ongoing research that has investigated objective ways of measuring intraocular light scatter *in vivo*, there is no clinical device yet capable of the measurement. Following previous work from Applegate and co-workers, a software tool was developed to obtain a scatter value from the raw data obtained from

the wavefront analyzer (see Chapters 6 and 7 for details of this analysis). For this purpose we needed a HS system.

The conclusions of this chapter are:

1.- The WASCA is a repeatable and reproducible instrument for the assessment of wavefront aberrations of the human eye.

2.- There are some operator-induced errors that may affect the readings. For example, the operator's realignment between measurements increased the SD by a factor of 3, although the differences are not statistically significant.

3.- From the analysis of repeatability it can be concluded that 3 measurements would suffice to get a reliable value.

4.- Small shifts in patient fixation (i.e. angular misalignment) can lead to significant changes in the aberrations measured, mainly those pertaining to coma.

CHAPTER 4. EFFECT OF ACCOMMODATION ON HIGHER ORDER ABERRATIONS

CHAPTER SUMMARY

Purpose: To investigate the influence of instrument myopia on wavefront analysis and its effect of wavefront aberration values obtained.

Methods: Two studies were conducted 1. Evaluation of the existence and magnitude of instrument myopia when examining non-cyclopleged young human subjects. 2. The effect of intermediate levels of accommodation to real distance targets on ocular wavefront aberrations.

Results: 1. Wavefront analyzer refraction resulted in the recording of 0.30D more myopia in eyes without cycloplegia as a result of instrument myopia. 2. With accommodation levels up to 3D, a strong trend for spherical aberration to move towards more negative values was observed, and also in comatic aberration components although in a less predictable way. Different responses in emmetropic eyes compared to myopic eyes suggests a role for spherical aberration in driving the retinotopic accommodative response to achieve an optimum balance between defocus and performance.

Conclusions: Wavefront analysis without the use of any antimuscarinic agent will allow an accommodative response due to the closed field environment of current clinical wavefront analyzers (i.e. instrument myopia). Although the response is, on average, around 0.30 D (0.33±0.11D), some patients may have an induced response of up to 3D. Even for lower levels of accommodation i.e. less than 3D the changes in measured wavefront aberrations may reach significance which is of particular importance when measurements obtained are to plan a customized refractive surgical procedure.

4.1. INSTRUMENT MYOPIA WITH WAVEFRONT ANALYZERS

4.1.I. ABSTRACT

Purpose: To assess the accuracy of three wavefront analysers versus a validated binocular open-view autorefractor in determining refractive error in non cyclopleged eyes.

Methods: Eighty eyes were examined using the SRW5000 open-view infrared autorefractor, and, in a randomised sequence, with three wavefront analyzers: 1)OPDscan (Nidek), 2)WASCA (Zeiss/Meditec) and 3)Allegretto (Wavelight). Subjects were healthy adults (19 men, 21 women; 20.8±2.5 years old). Refractive errors ranged from +1.5D to -9.75D (mean -1.83±2.74D) with up to 1.75D cylinder (mean 0.58±0.53D). Three readings were collected per instrument, by one examiner, without antimuscarinic agents. Refraction values were decomposed into vector components for analysis, resulting in mean spherical equivalent (M), and J_0 and J_{45} being vectors of cylindrical power at 0 and 45 degrees, respectively.

Results: Positive correlations were observed between wavefront analyzers and SRW5000 for M (OPD,r=0.959,p<0.001; WASCA,r=0.981,p<0.001; Allegretto,r=0.942,p<0.001). Mean differences and limits of agreement showed more negative M with wavefront analyzers (OPD, 0.406±0.768D, 0.235 to 0.580,p<0.001; WASCA, 0.511±0.550D, 0.390 to 0.634,p<0.001; Allegretto, 0.434±0.904D, 0.233 to 0.635,p<0.001). A second analysis eliminated outliers and showed the same trend but lower differences: OPD, 0.24±0.41D, 0.15 to 0.34D,p<0.001 (n=75); WASCA, 0.46±0.47D, 0.36 to 0.57D,p<0.001 (n=78); and Allegretto, 0.30±0.62D, 0.16 to 0.44D,p<0.001 (n=77). There were no statistically significant differences for J_0 and J_{45}.

Conclusion: Wavefront analyzer refraction resulted in 0.30D (0.33±0.11D) more myopia compared to SRW5000 refraction in eyes without cycloplegia. It is suggested that this is the result of the accommodation excess attributable to instrument myopia. For the relatively low degrees of astigmatism in this study (<2D) there was good agreement between wavefront analyzers and SRW5000.

Published in J Refract Surg: See Appendix II

4.1.II. INTRODUCTION

Although autorefraction *per se* is commonly used as a starting point for subjective refraction, or for refractive screening purposes (Saw et al., 2005; Zadnik et al., 2004), Wavefront analyzers may be used to establish both higher and lower order aberrations prior to refractive surgical techniques, and appropriate interpretation of their output is therefore critical to a successful surgical outcome.

In customized refractive surgery procedures, greater accuracy of wavefront analysis preoperatively should translate into better results of the surgery itself, as well as the assessment of these results in subsequent follow-ups. This is particularly important when measuring the aberrations of the eye in normal viewing conditions. Currently, the assessment of wavefront aberrations with clinical wavefront analyzers is commonly performed after instillation of antimuscarinic dilating drops to ensure a pupil size sufficient to facilitate collection of wavefront readings. Pharmacologically-induced dilation of the pupil prior to wavefront aberration assessment is currently the subject of debate, since it would offer an aberration profile that is less relevant to the natural pupil view normally experienced by the patient (Carkeet et al., 2003). A balance exists between the need for a sufficiently large pupil to provide reliable aberrometry data and the desire to establish the impact of aberrations as they affect the patient in the natural viewing state. It therefore follows that the acquisition of clinically relevant, stable refractive/aberrometry data without the use of dilating agents would provide an ideal baseline for treatment.

Shack-Hartmann sensors exhibit good agreement with open field autorefractors, both centrally and peripherally in cyclopleged eyes(Atchison, 2003). Since cycloplegic refraction invariably differs from manifest refraction, it follows that the corresponding wavefront error will differ from that found in the non-cyclopleged state due to the effect on the tone of the ciliary muscle. Pupil dilation with antimuscarinic agents typically has a modest effect in reducing distance refraction, particularly in adults, however it can reduce the range of near accommodation by up to 6 dioptres, which will in turn help to reduce the impact of instrument myopia(Gilmartin, Amer, and Ingleby, 1995).

Instrument myopia is attributed to a relatively low level surfeit of accommodation and variations in accommodation have been widely reported to induce variations in higher order aberrations(Cheng et al., 2004a; He, Burns, and Marcos, 2000; Pallikaris et al., 2001) as was observed in the previous study (see section 2.1). Therefore, where patients are not dilated pharmacologically, it is imperative to know that excessive instrument myopia is not being induced.

The OPD-scan®/ARK-10000® (Nidek Co, Gamagori, Japan) determines wavefront aberration using the principle of dynamic skiascopy, as mentioned earlier. The system then generates automatically composite refraction data, as well as wavefront aberrations from the difference in refractive power across the pupil area.

The WASCA® (Zeiss/Meditec Inc, Germany), also described earlier, gives highly accurate and reproducible measures of both low and higher order aberrations up to the fourth order in human and model eyes(Cheng et al., 2003) with low variability(Cheng et al., 2004b).

The Allegro Wave® analyzer (Wavelight Laser Tech. AG, Germany), developed by Mierdel et al.(Mierdel et al., 2001; Mierdel et al., 1997), is an objective version of the Tscherning aberroscope, as detailed in the introductory chapter. This method uses a dot pattern mask which allows several laser rays from the original beam to be projected on the retina. Five to ten frames of the image formed on the retina are first captured and defined through a very small aperture and then deformed to greater and lesser extents depending on the aberrations produced by the eye(Kaemmerer et al., 2000; Mrochen et al., 2000). The deviation of each retinal spot from its equivalent in the ideal reference image is measured and processed to give local slopes and, therefore, the corresponding wavefront aberrations. Good reproducibility has been demonstrated for this technique for measures of spherocylindrical refraction and total RMS values for higher order aberrations in human eyes (Mrochen et al., 2000).

All three wavefront analyzers use a closed field internal fixation target, imaged at infinity to minimise accommodation during measurements. In the case of the OPD, the

internal target consists of a road receding into the distance. In comparison, a high contrast circular web-like grid and an orange LED with a central star are the fixation targets for the WASCA and Allegretto, respectively.

Closed field autorefractors are sometimes considered less suitable as a starting point for subjective refraction than other procedures, such as retinoscopy (Jorge et al., 2005a; Jorge et al., 2005b). The Shin-Nippon SRW-5000®, also marketed as Grand Seiko WV500®, (Shin-Nippon Ltd, Japan) is an infrared, open-view, objective autorefractor. Its open-view arrangement allows an unimpeded 63.4 degrees horizontal (33.7 degrees either side of fixation) by 31.5 degrees vertical (14.8 degrees above fixation and 16.7 degrees below fixation) binocular view and thus minimises instrument myopia. It has been shown to compare favourably with subjective refraction being reliable in both adults (mean difference for the spherical equivalent 0.16 ± 0.44D) (Mallen et al., 2001) and children (mean difference for the spherical equivalent 0.24 ± 0.34D, cyclopleged)(Chat and Edwards, 2001), and can be converted to measure continuously the accommodative response with high precision(Wolffsohn et al., 2001; Wolffsohn et al., 2004). For these reasons it will be used here as the gold standard against which to assess the performance of the OPD-scan, WASCA and Allegretto in the determination of spherocylindrical refractive error without cycloplegia.

The clinical application of wavefront analysis is generally to measure ocular aberrations with the eye in its natural state, often in the pre- and post-operative setting. The efficacy of the closed field targets used in wavefront analyzers to relax a patient's accommodation during the measurement process in eyes without cylcoplegia is unknown. By comparison to a validated objective refractive technique, this study aims to show whether wavefront analyzer readings taken with physiological mydriasis only is a reliable method by which to perform wavefront analysis. The performance of the OPD-scan, WASCA and Allegretto wavefront analyzers as clinical autorefractors for the determination of non-cycloplegic refractive error is examined in a group of young adult subjects.

4.1.III. MATERIAL AND METHODS

4.1.III.i. Sample details

The refractive errors of eighty eyes of forty young subjects (19 men, 21 women; mean age 20.8 ± 2.5 years) with refractive errors ranging from +1.5 D to -9.75 D sphere (mean -1.83 ± 2.74 D) and up to 1.75D cylinder (mean 0.58 ± 0.53 D) were examined with the Shin-Nippon SRW-5000 autorefractor, the OPD-scan, WASCA and Allegro wavefront analyzers under similar low illumination conditions (0.75 cd/m^2).
Subjects were recruited from the student population of Aston University. Exclusion criteria included history of ocular pathology or abnormal findings on slit lamp and ophthalmoscope examination or having worn contact lenses less than 24 hours prior to examination.

4.1.III.ii. Ethical approval

This study was approved by the Ethical Committee of Aston University. All procedures follow the agreement of the Declaration of Helsinki. Measurements were performed after informed consent was obtained from all volunteers.

4.1.III.iii. Experimental procedures

The examinations were performed by a single examiner (AC). Three readings of spherocylindrical refractive error were obtained for the central 5 mm from each of the wavefront analyzers.

Wavefront and refraction data were obtained for the central 5 mm with all three wavefront analyzers since it would be the closest diameter to the 3mm analyzed by the SRW5000 while still offering clinically useful wavefront aberrations data.

4.1.III.iv. Data analysis

Initially, right and left eyes were plotted separately (as Bland-Altman's difference *versus* mean plots), but since no differences were found, both eyes were included in the analysis. Mixing of eyes did not bias the results since the pattern of aberrations is in general non-symmetric (Marcos and Burns, 2000).

Refraction data in conventional clinical notation present a problem for analysis and comparison due to the variance in astigmatic power and axis and consequently need to be transformed to be analyzed in dioptric power space for more accessible comparison (Bullimore, Fusaro, and Adams, 1998; Harris, 2001). For this reason, data were converted into power vector representation as a spherical component M, equal to the mean spherical equivalent of the refraction (eq. 4.1); and a cylindrical component being represented by a Jackson cross cylinder at 0°, with a power J_0 (eq. 4.2), and a Jackson cross cylinder at 45°, with power J_{45} (eq. 4.3)(Thibos, Wheeler, and Horner, 1997).

$$M = Sphere + \frac{Cylinder}{2} \qquad \text{(eq. 4.1)}$$

$$J_0 = \frac{cylinder}{2} \cdot \cos(2 \cdot axis) \qquad \text{(eq. 4.2)}$$

$$J_{45} = \frac{cylinder}{2} \cdot \sin(2 \cdot axis) \qquad \text{(eq. 4.3)}$$

The bias was assessed statistically (SPSS 12.0, SPSS Inc, USA) as the mean of the differences compared to zero. The hypothesis of zero bias was assessed by two-tailed paired t-tests with the Bonferroni adjustment for repeated comparisons (alpha level set at 0.05 and 4 comparisons), so that $p<0.012$ was the criterion for statistical significance.

Plots of difference against mean were used to represent the agreement between methods (Bland and Altman, 1986).

4.1.IV. RESULTS

The descriptive statistics for the vectorial components M, J_0 and J_{45} given by the four instruments, shown in table 3.1, indicate slightly higher negative values for the three wavefront analyzers for the M, J_0 and J_{45} components compared to the autorefractor.

		Minimum	Maximum	Mean	SD
SRW-5000	M	-9.88	2.19	-2.1158	2.6923
	J_0	-0.82	0.80	-0.0080	0.2440
	J_{45}	-1.77	1.04	0.0008	0.3120
OPD/ARK10000	M	-9.88	1.75	-2.5219	2.5864
	J_0	-1.31	0.37	-0.0478	0.2540
	J_{45}	-0.45	1.54	0.0471	0.2479
WASCA	M	-9.44	1.28	-2.6270	2.4739
	J_0	-0.60	1.05	-0.022	0.1904
	J_{45}	-0.28	0.71	0.0156	0.1329
ALLEGRO	M	-9.00	2.58	-2.5501	2.4583
	J_0	-1.48	0.47	-0.0612	0.28941
	J_{45}	-7.49	0.81	-0.0745	0.87241

Table 4.1.- *Descriptive statistics for the different components of the power vectors corresponding to the measurements obtained with Shin-Nippon SRW-500 and the three wavefront analyzers. Values are in diopters.*

Good correlation for the spherical equivalent M between the readings obtained with the three wavefront analyzers and the autorefractor was evident (Pearson's correlation coefficients were 0.959, 0.981 and 0.942 for the OPD, WASCA and Allegretto, respectively).

However, as shown in table 4.2, the mean differences, level of significance and limits of agreement for the three components yield, for each of the wavefront analyzers, more negative power for the M component: OPD, 0.41±0.79D (0.23 to 0.58), $p<0.001$; WASCA, 0.51±0.55D (0.39 to 0.63), $p<0.001$; and Allegretto, 0.43±0.77 (0.23 to 0.63)

$p<0.001$; but no statistically significant differences for the astigmatic components J_0 and J_{45} (-0.01 ± 0.29; p=0.832 and -0.03 ± 0.32; p=0.474, for OPD, WASCA and Allegro, respectively).

		Mean	SD	p	Limits of agreement	
					Mean − 1.96*SD	Mean + 1.96*SD
OPD-scan	M	0.41	0.77	0.000	0.23	0.58
	J_0	0.04	0.38	0.358	-0.05	0.13
	J_{45}	-0.05	0.48	0.388	-0.15	0.06
WASCA	M	0.51	0.55	0.000	0.39	0.63
	J_0	-0.10	0.28	0.747	-0.07	0.05
	J_{45}	-0.01	0.37	0.723	-0.10	0.07
Allegro	M	0.43	0.90	0.000	0.23	0.63
	J_0	0.053	0.40	0.240	-0.04	0.14
	J_{45}	0.07	0.98	0.495	-0.14	0.29

Table 4.2.- *Mean difference, significance level, and 95% limits of agreement between Shin-Nippon SRW-500 and the three wavefront analyzers for the components M, J_0 and J_{45} in diopters.*

Bland-Altman dispersion plots show that each of the three wavefront analyzers give around 0.50 D more myopia than the SRW5000 ($p<0.001$) and a positive bias towards smaller refractive errors, showing less differences between the wavefront analyzers and the SRW5000 for more myopic eyes. The WASCA shows the smallest confidence intervals, and fewer outliers, whereas the OPD shows the lowest mean difference compared to the SRW5000 (figures 4.1-4.3).

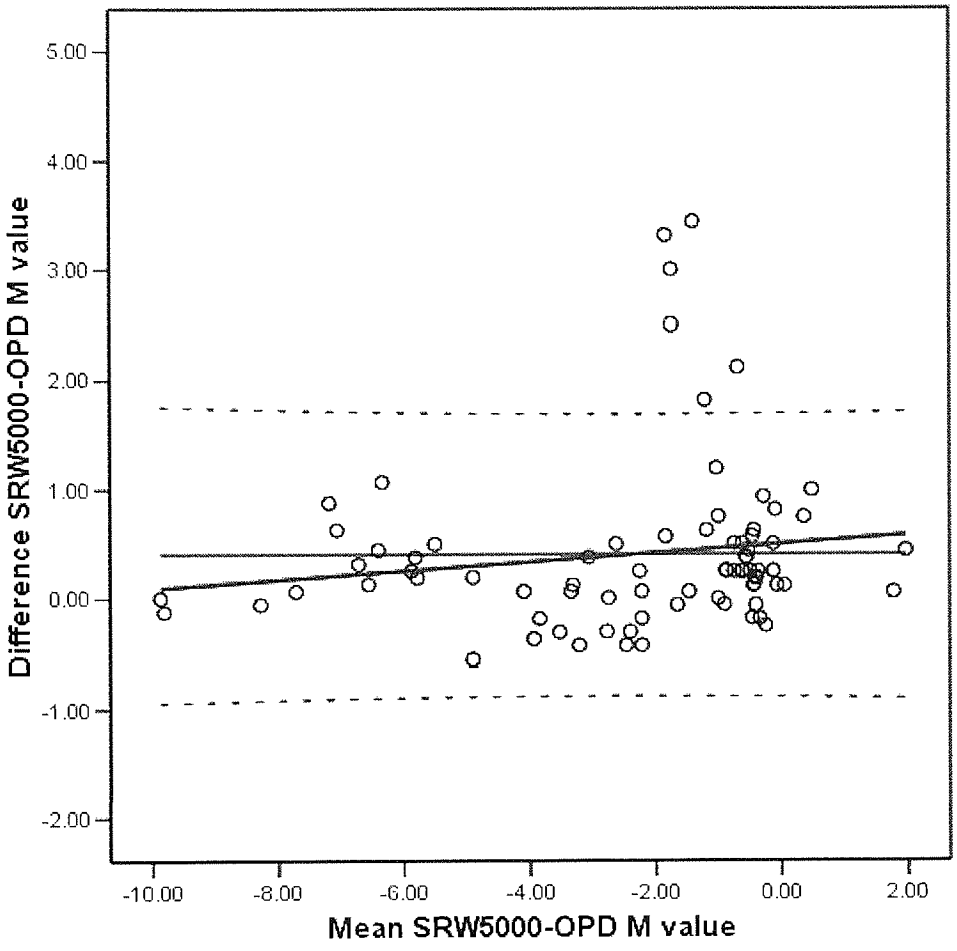

Figure 4.1.- *Bland-Altman plot for differences against mean (and 95% confidence intervals) and regression line between the SRW-5000 and the OPD for the spherical component M in diopters.*

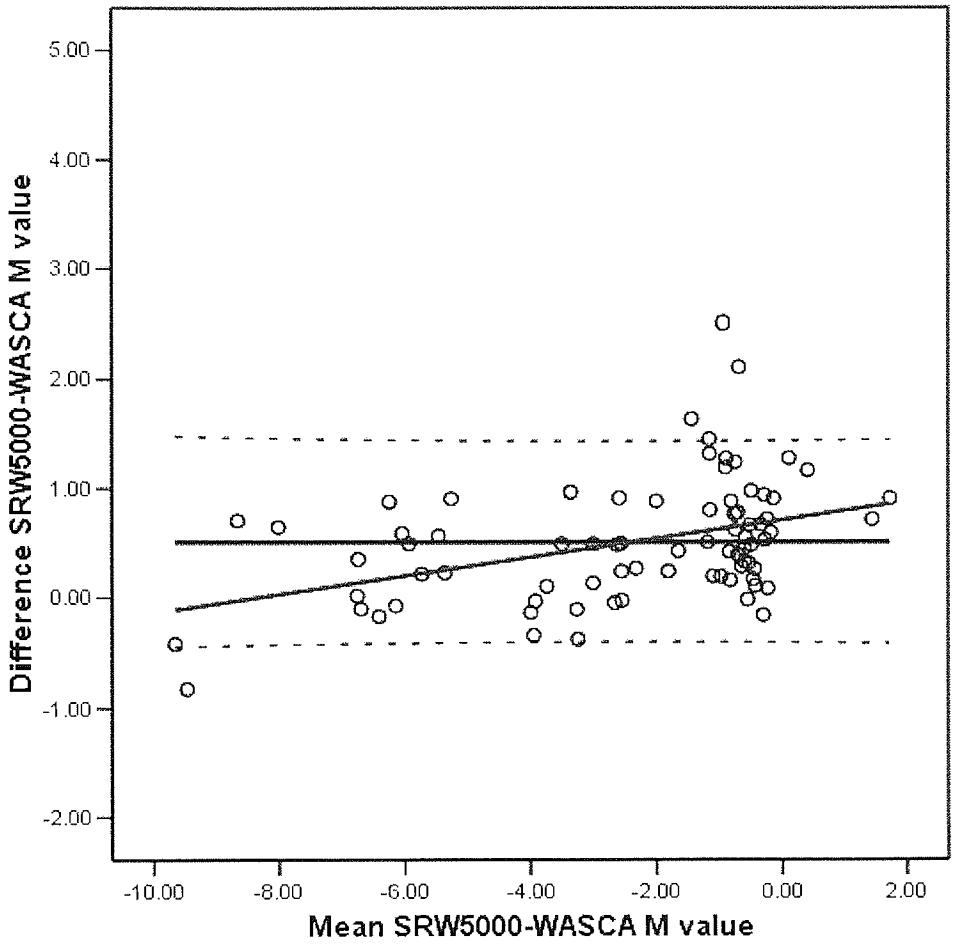

Figure 4.2.- *Bland-Altman plot for differences against mean (and 95% confidence intervals) and regression line between the SRW-5000 and the WASCA for the spherical component M in diopters.*

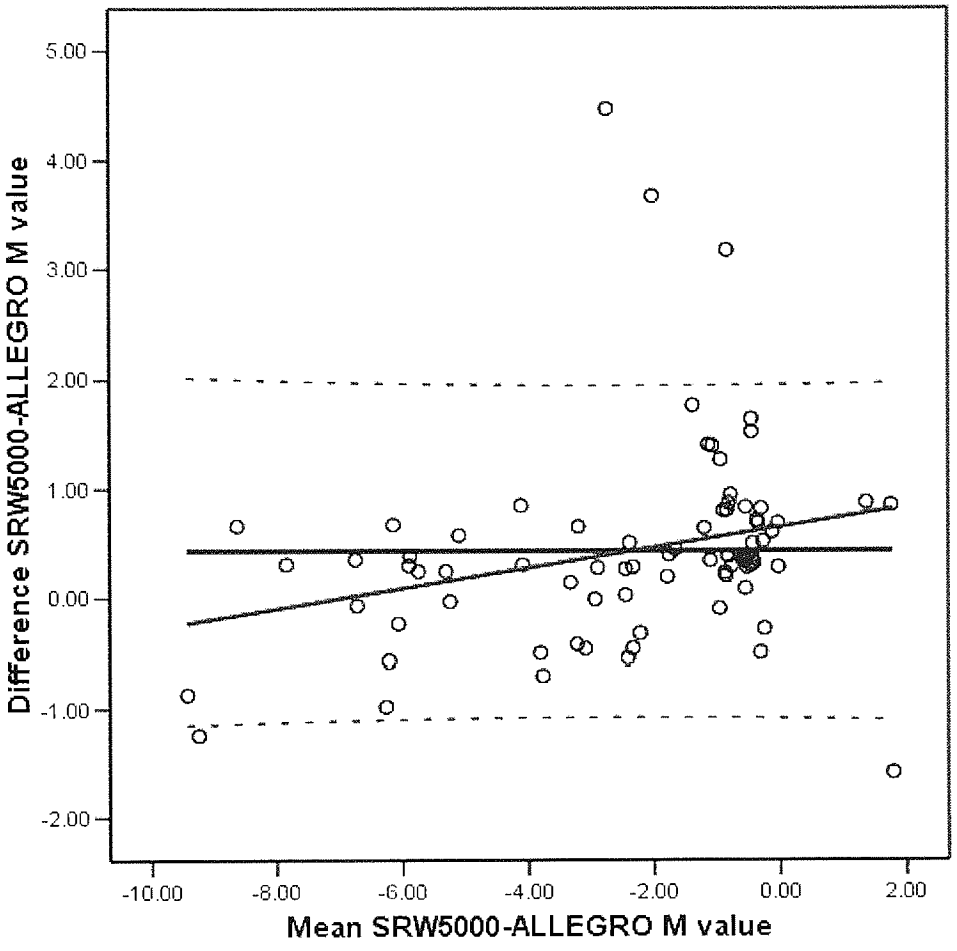

Figure 4.3.- *Bland-Altman plot for differences against mean (and 95% confidence intervals) and regression line between the SRW-5000 and the Allegretto for the spherical component M in diopters.*

When the outliers observed in figures 4.1-4.3 are removed, stating a criteria of differences equal or less than 2D, and a new analysis performed (see table 4.3), the mean differences and confidence intervals for the M component are reduced to: OPD, 0.24 ± 0.41 D, 0.15 to 0.34D, $p<0.001$ (n=75); WASCA, 0.46 ±0.47 D, 0.36 to 0.57D, $p<0.001$ (n=78); and Allegretto, 0.30 ±0.62D, 0.16 to 0.44D, $p<0.001$ (n=77), although the same trend line can be observed in the corresponding Bland-Altman dispersion plots (figures 4.4-4.6).

	N	Mean	SD	p	Limits of agreement	
					Mean – 1.96*SD	Mean + 1.96*SD
OPD	75	0.24	0.41	0.000	0.15	0.34
WASCA	78	0.46	0.47	0.000	0.36	0.57
Allegretto	77	0.30	0.62	0.000	0.16	0.44

Table 4.3.- *Sample analyzed (N), mean difference, significance level, and 95% limits of agreement between Shin-Nippon SRW-5000 and the three wavefront analyzers for the M component, in dioptres, after removing the outliers.*

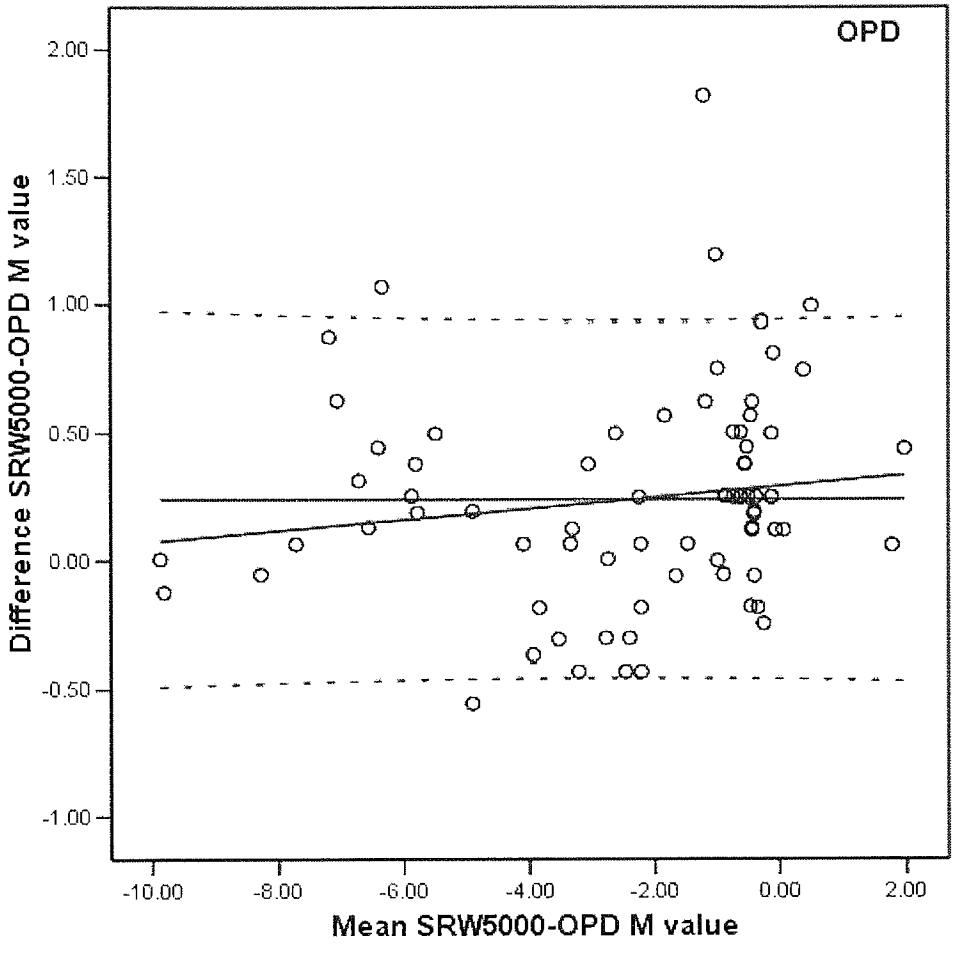

Figure 4.4.- *Bland-Altman plot for differences against mean (and 95% confidence intervals) and regression line between the SRW-5000 and the OPD for the spherical component M in diopters after removing the outliers.*

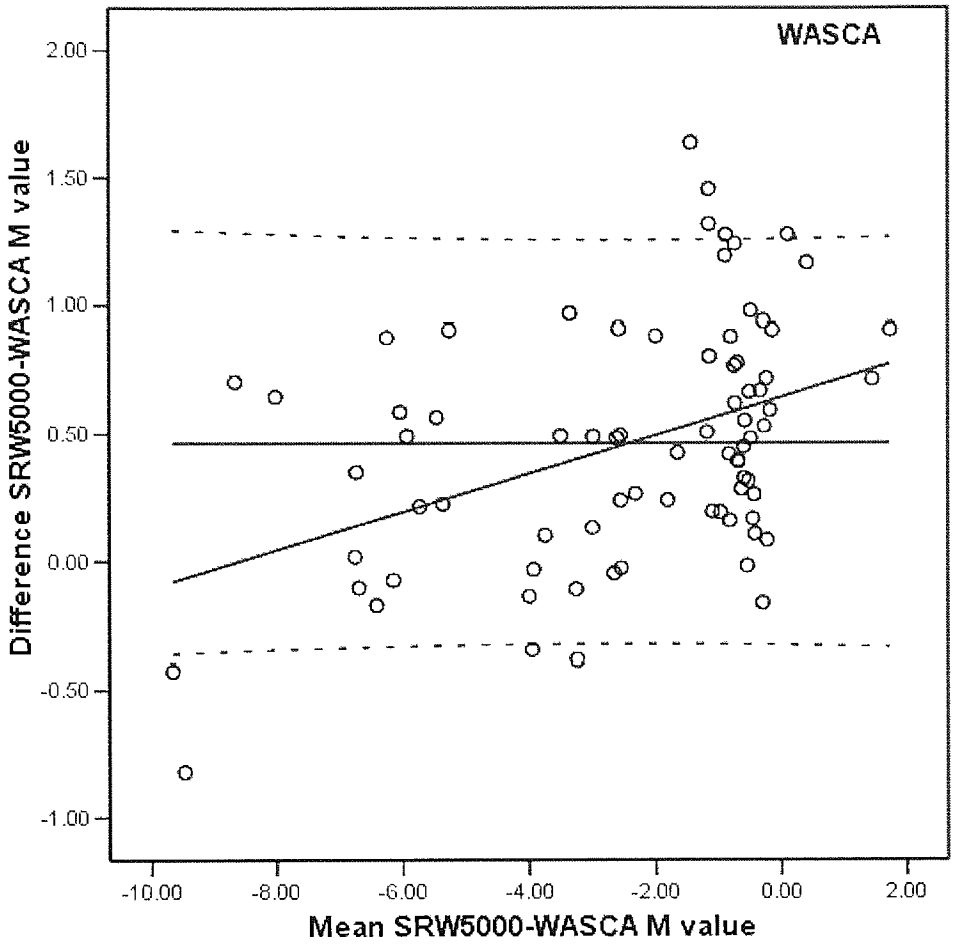

Figure 4.5.- *Bland-Altman plot for differences against mean (and 95% confidence intervals) and regression line between the SRW-5000 and the WASCA for the spherical component M in dioptres after removing the outliers.*

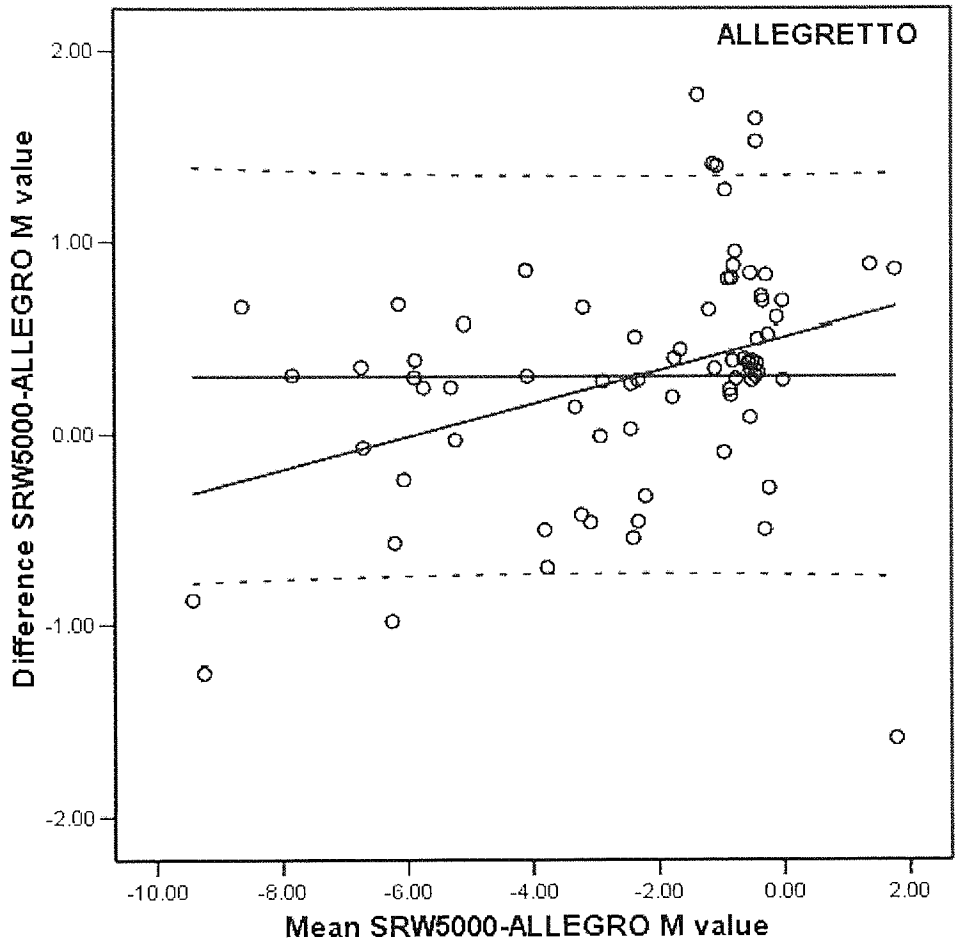

Figure 4.6.- *Bland-Altman plot for differences against mean (and 95% confidence intervals) and regression line between the SRW-5000 and the Allegretto for the spherical component M in diopters after removing the outliers.*

The astigmatic components J_0 and J_{45} show mean differences close to zero, and not statistically significant, compared to the SRW5000. Confidence intervals are smaller for the WASCA and OPD, and considerably wider for the Allegretto (figure 4.7).

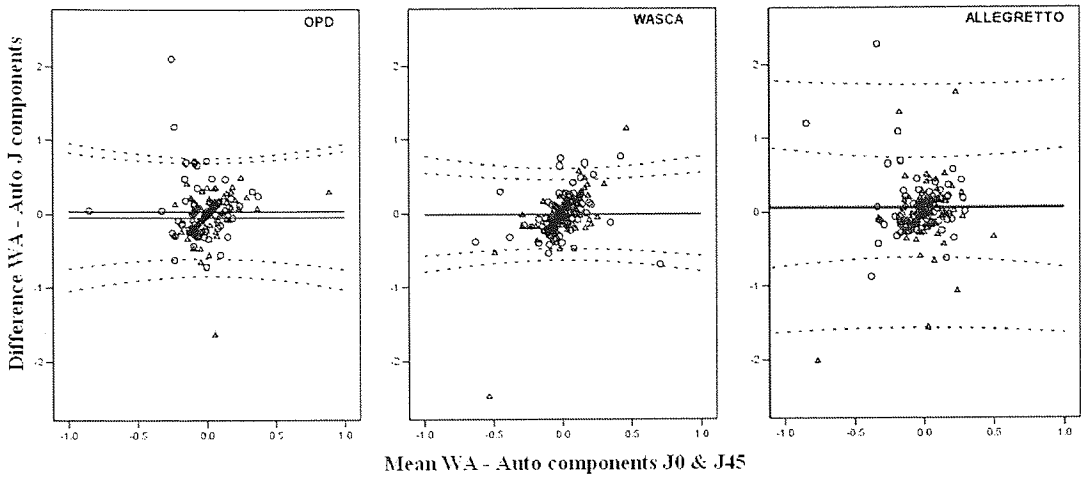

Figure 4.7.- *Bland-Altman plots for differences against mean (and 95% confidence intervals) between the SRW-5000 and the three wavefront analyzers for the astigmatic components J0 (o) and J45 (Δ) in diopters.*

4.1.V. DISCUSSION

The results of this study show statistically significant differences between the wavefront analyzers and the Shin Nippon autorefractor for the spherical component M of the power vector. Specifically, the mean value of M is 0.30D more myopic when measured using wavefront analysis technology. It is proposed that this finding is the result of instrument myopia induced by these instruments. This finding is consistent with the differences obtained by Jorge et al. when comparing closed-field auto-refraction, retinoscopy, subjective refraction, and eyes without cylcoplegia (Jorge et al., 2005a). Retinoscopy was found to be a better start-point for subjective refraction than close-field autorefraction since the latter was approximately 0.50D more myopic, possibly due to instrument myopia (Jorge et al., 2005a). In a study comparing refraction in young myopic eyes with and without cycloplegia as measured with the COAS (Complete Ophthalmic Analysis System) aberrometer (a Shack-Hartmann aberrometer, with the same sensor as the WASCA) the Nidek ARK-2000 autorefractor and subjective refraction, the wavefront analyzer and autorefractor each showed a vector error of 0.3-0.4D without cycloplegia; under cycloplegia, the vector error for the COAS remained unchanged (Salmon et al., 2003). As suggested in a more recent study the lower values of instrument myopia found by Salmon et al could possibly be due to the range of refractive errors sampled; while the later study showed results in close agreement with

those reported here (Salmon and van de Pol, 2005). In a more recent study, Zadok *et al* (Zadok et al., 2005) reported low repeatability for the OPD in non-cyclopleged eyes, and suggested disruptions in the tear film and accommodative microfluctuations as possible causes.

The confidence intervals indicated from the Bland and Altman plots indicate the variability of the data with respect to the SRW-5000, such that a narrow interval indicates better agreement. The confidence intervals in this sample were ± 0.171 for OPD, ±0.201 for Allegretto and ±0.121D for WASCA, suggesting that the agreement was slightly better for WASCA and slightly worse for Allegretto. After removing the outliers from the analysis and plots, the confidence intervals were ± 0.096 for OPD, ± 0.140 for Allegretto and ± 0.106D for WASCA, making it slightly better for OPD and slightly worse for Allegretto.

Compared to the SRW-5000 there was a trend for the myopic overcorrection measured using the wavefront analyzers to be greater in low degrees of myopia or hypermetropia, as demonstrated by the positive regression line on each graph. This regression line was shallow for the OPD scan suggesting only a mild effect of absolute power, whereas the Allegretto exhibited a steeper regression line indicating that the effect was greater with this device. In addition, inspection of the Bland-Altman plots shows a number of data points falling outside the limits of agreement. This suggests that in each case, some patients differ in measurement from the SRW-5000 by an amount which is outside the normal variability of the device. Typically, these outliers arise when the actual refraction is less then -2.00DS and the wavefront analyzer errors in these cases can be as high as -3.50D (OPD) or even -4.50D (Allegretto). It is important to note that comparison of the data shows that the outliers obtained in the three data sets can be attributed to both eyes of the same few patients in each case, suggesting that this is a finding that arises only in certain patients, and will affect all devices to some lesser or greater extent. These outliers account principally for the positive regression line and suggest that the interpretation of myopia less than -2.00D when measured with all three devices, but particularly with the OPD scan and Allegretto, is not reliable on a case-wise basis when cycloplegia is not used.

Differences in the cylindrical components were not statistically significant. This suggests that for the mild to moderate degrees of astigmatism present in the sample all three methods provided reliable cylindrical data. Conclusions should not be drawn regarding the determination of astigmatism of values greater than those included in this study.

Overall, the three wavefront analyzers perform simillarly as regards accuracy and repeatability of measurement although particular differences arise in relation to the effects of absolute refraction, limits of agreement and the presence of outliers. The different fixation targets used by the three devices contribute to these differences. For example, the OPD uses a natural scene similar to that used in closed-field autorefractors, whereas the WASCA uses a high contrast web-like pattern and the Allegretto uses an orange LED with a central star pattern (figure 4.8).

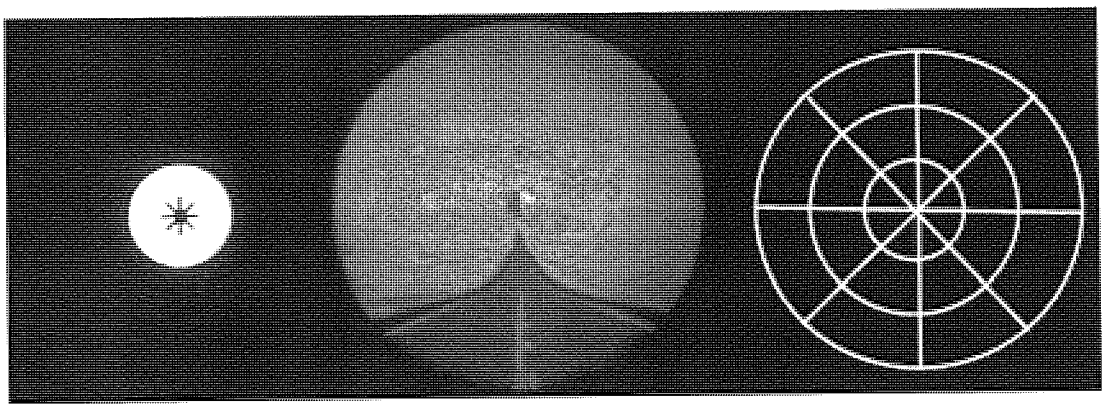

Figure 4.8. *Different targets used by the different wavefront analyzers used in this study: Allegretto (left), OPD (center) and WASCA (right).*

Equally, the differences in the wavelengths used by the different fixation targets may result in a different response by the accommodation system due to the presence of chromatic aberration (Seidemann and Schaeffel, 2002); human subjects tend to accommodate less for shorter wavelengths and more for longer wavelengths. The relatively narrower limits of agreement and more moderate outliers observed in the WASCA device would suggest that, if the target is a factor, it may have the better target for the purpose, particularly in eyes with lower degrees of myopia.

It is possible that the mathematical derivations of refractive error affect the agreement with the autorefractor findings. For small pupil sizes, second order coefficients may be sufficient for calculating the spherocylindrical refraction. However, as the pupil size increases, higher order aberrations (mainly spherical aberration) also increase their contribution to these refraction values and should, therefore, be considered in the calculation (Thibos et al., 2004). In this study, natural pupils were examined with all instruments using similar illumination levels, and the wavefront and refraction data were obtained for the central 5 mm with all three wavefront analyzers since it would be the closest diameter to the 3mm analyzed by the SRW5000 but still offering clinically useful wavefront aberrations data. The open field, binocular, infrared character of the SRW5000 makes instrument myopia very unlikely when using it for the determination of refractive error.

All the values of refraction were obtained from the default settings of the wavefront analyzers.
According to the manufacturers, both the OPD and Allegretto give an integral 'best fit' refraction which includes higher order aberrations. The WASCA, however, gives the default refraction values from the low order aberrations only, having been found to give better repeatability (Salmon and van de Pol, 2005). The system gives also the option of using a Seidel sphere fit that includes spherical aberration in the computation of refractive error.

In this respect the acquisition protocols were consistent suggesting that the contribution of spherical aberration to the incident image would be similar for the three devices; any variability would therefore be due to differences in the optical setup and image analysis.

In summary, the determination of mean spherical power obtained with the three clinical wavefront analyzers used in this study, without the instillation of antimuscarinic drops, resulted in a myopic overestimation of around 0.30D, which varied to some extent with the degree of myopia (being less with higher degrees of myopia), and in some individuals was seen to be excessive (Cervino, 2006). The relatively frequent finding of outliers in the data suggest that on a case-wise basis preoperative data must be interpreted with caution if optimal post-surgical results are to be achieved. With respect

to wavefront aberrations *per se*, it has previously been shown that myopic shifts associated with relatively small amounts of excess accommodation have little impact on the RMS value (Cheng et al., 2004a; He, Burns, and Marcos, 2000), however the implications for those patients exhibiting large amounts of over-accommodation (greater than 3D) may be profound.

4.2. MEASUREMENT OF CHANGES IN OPTICAL QUALITY OF THE RETINAL IMAGE WITH ACCOMMODATION TO TARGETS LOCATED IN REAL SPACE

4.2.I. ABSTRACT

Purpose: To assess changes in quality of the retinal image with accommodation to real distance targets in two refractive groups.

Methods: Twenty right eyes from twenty young adults (10 men and 10 women; 10 emmetropic and 10 myopic; mean age 20.8 ± 2.5 years), with refractive errors ranging from +0.13 D to -10.88 D spherical equivalent (mean -2.53 ± 3.26 D), were examined with the WASCA wavefront analyzer when focusing targets set in real space at distances corresponding to accommodative stimuli of 0.17, 0.33, 0.5, 1 and 3 D. Three measurements were taken at each distance. Repeated measures ANOVA was performed between the mean of the three measurements of HOA obtained for each of the 5 distances. Correlation analysis was done between the HOA values and the accommodative response when fixating each of the targets, and between accommodation error (lag) and change in spherical aberration by refractive group.

Results: Significant correlations were found for the comatic components Z_3^{-1} (Pearson's correlation coefficient 0.234, p=0.048) and Z_3^1 (r= 0.365, p=0.002), spherical aberration Z_4^0 (Pearson's -0.812, p<0.001) and tetrafoil component Z_4^4 (Pearson's -0.315, p=0.007) with the accommodative response. ANOVA showed significant changes in Z_4^0 when fixating closer than 1m (p<0.001 at 1 m and p<0.001 at 33 cm), as well as in Z_3^1 (p=0.021 at 1 m and p=0.001 at 33 cm) and Z_3^{-1} (p=0.028 at 1 m and p=0.005 at 33 cm). The decrease in spherical aberration with accommodative response

was similar for both emmetropic and myopic patients, however the change in spherical aberration was correlated to accommodation error in emmetropic (Pearson's 0.338, p= 0.044) and not in myopic subjects (Pearson's -0.045, p=0.794).

Conclusion: With accommodation levels up to 3D a strong trend for spherical aberration to move towards more negative values was observed, A similar trend was found in comatic aberration components, although in a less predictable way. Different responses in emmetropic eyes compared to myopic suggests a role for spherical aberration in driving the retinotopic accommodative response. Instrument myopia may have a significant effect on the wavefront aberration values obtained.

4.2.II. INTRODUCTION

In the process of accommodation, when the crystalline lens changes its power for focusing objects at near distance, the zonular fibres relax allowing the crystalline lens to recover its natural shape. This effect will alter not just the spherocylindrical power of the lens, but also the higher order aberrations and the quality of the resulting retinal image. Cheng et al(Cheng et al., 2004a) showed that wavefront RMS does not change for accommodation up to 3D, although there is a large individual variation. RMS would reach a minimum around 2D accommodative level. A systematic decrease in spherical aberration with accommodation has been strongly supported (Cheng et al., 2004a; Hazel, Cox, and Strang, 2003; He, Burns, and Marcos, 2000; Ninomiya et al., 2002; Plainis, Ginis, and Pallikaris, 2005; Vilupuru, Roorda, and Glasser, 2004). Conversely, astigmatism and coma increase with accommodation (Cheng et al., 2004a; Plainis, Ginis, and Pallikaris, 2005; Vilupuru, Roorda, and Glasser, 2004), possibly due to a change in crystalline lens tilt, although the extent of these changes is not predictable due to large individual variations.

The accommodative response of the eye, which is generally not coincident with the accommodative demand of the target, is responsible for degradation of the retinal image, producing accommodation errors (i.e. lag of accommodation for high dioptric demand and lead of accommodation for low dioptric demand). Buehren and Collins showed that the combination of higher order aberrations with accommodation errors improved the retinal image quality (Buehren and Collins, 2005). They also reported the

importance of changing pupil size and higher order aberrations in the accommodation-response function; for larger pupil sizes, the higher order aberrations influence the lag and lead of accommodation. Pupil area was also found to decrease linearly with accommodation until the accommodative system can no longer respond (Plainis, Ginis, and Pallikaris, 2005).

Although changes in accommodation can be attributed largely to changes in the internal optics of the eye, He *et al.* have shown that there is a statistically significant increase in both the mean corneal radius at the vertex and the corneal shape factor when accommodating for a stimulus at 20 cm, which in turn translated into significant changes for both horizontal coma and spherical aberration (He et al., 2003).

Lags of accommodation are more pronounced in myopes than emmetropes (Gwiazda et al., 1993; Rosenfield and Gilmartin, 1988), being larger for lens-induced accommodation than distance-induced accommodation(Gwiazda et al., 1993; He et al., 2005). He *et al.* also found that those myopic eyes with greater lag of accommodation showed the poorest image quality, a finding not replicated in the emmetropic group (He et al., 2005). They explain these discrepancies either as different wavefront profiles for emmetropes and myopes, producing different image quality with similar RMS and Sthrel ratios, or as underlying differences in the sensitivity to accommodative cues, with adult myopes showing reduced sensitivity to defocus(Rosenfield and Abraham-Cohen, 1999) and a reduced effect of defocus on visual performance tasks.

4.2.III. MATERIAL AND METHODS

4.1.III.i. Sample details

Twenty right eyes from 20 young adults (10 men, 10 women; mean age 20.8 ± 2.5 years) with refractive errors ranging from +0.13 D to -10.88 D spherical equivalent (mean -2.53 ± 3.26 D).were examined with the WASCA wavefront analyzer under similar low illumination conditions (0.75 cd/m^2) when focusing targets located in real space set at different fixation distances.

Subjects were recruited from the student population of Aston University. Exclusion criteria included history of ocular pathology or abnormal findings in slit lamp and ophthalmoscope, or having worn CL less than 24 hours prior to examination.

4.1.III.ii. Ethical approval

This study was approved by the Ethical Committee of Aston University. All procedures follow the agreement of the Declaration of Helsinki. Measurements were performed after informed consent was obtained from all volunteers.

4.1.III.iii. Experimental procedures

The fixation targets were several high-contrast Maltese crosses of different sizes, one for each distance, so that the angular size was kept constant (around 7', equivalent to 4.40 cpd) for the subjects when focusing at the different distances. The reason for the chosen size was arbitrary, requiring only that the subjects were capable of seeing the center of the Maltese cross clearly and to maintain it sharply focused during data acquisition.

The targets were self illuminated by a diffuse backlight to make it easier for the subject to focus the centre in mesopic room illumination (0.75 cd/m^2) and varying the intensity of the target illumination for the different distances to allow a minimum pupil diameter of 5 mm without the instillation of any mydriatic agent.

Stimuli were set at distances from the subject that were equivalent to accommodative demands of 0.17 D (6 m), 0.33 D (3 m), 0.5 D (2 m), 1 D (1 m) and 3 D (33 cm) D. Since the purpose of the study was not to evaluate the stimulus-response function, it was not necessary to apply effectivity formulas to correct for apparent stimulus for patients corrected with spectacles (Buehren and Collins, 2005; Mutti et al., 2000). Care was taken in placing the target such that the non-fixating eye, the one being examined with the WASCA, was centred for data acquisition.

Three measurements were taken at each distance while instructing the subject to fixate the central portion of the fixation target, and taking the measurements after the subjects ensured they could see and maintain the target sharply focused.

4.1.III.iv. Data analysis

Data were obtained for 5mm pupil diameters and analyzed as Zernike coefficients, complying with the standards set by the Optical Society of America for reporting wavefront aberration of human eyes (Thibos et al., 2002).

Measurement of the accommodative response was obtained from the wavefront analyzer. WASCA has been shown as an accurate and reliable autorefractor in previous studies (Salmon and van de Pol, 2005; Salmon et al., 2003). However, all measurements were checked against an open field, infrared autorefractor (SRW5000) as used in the previous chapter with the subjects fixating the same targets located at the same distances to ensure consistency of measurement conditions.

For some analyses subjects were subdivided by refractive error into emmetropes (MSE > -0.50D; mean MSE -0.02 ± 0.16D) and myopes (MSE < -2.00 D; mean MSE -3.16 ± 2.95 D).

SPSS statistical package (v. 12.0.1, SPSS Inc.) was used for data analysis. Correlations between accommodative stimuli and responses were determined although that was not an aim of the study. Repeated measures ANOVA was done to identify change from baseline of all Zernike coefficients following accommodation to the different targets and to determine which level of accommodation induced significant changes in aberrations. Correlation analysis between accommodative response and degree of change in Zernike coefficients was assessed by Pearson's correlation coefficient.

4.2. IV. RESULTS

Figure 4.9 displays the correlation plot between accommodative stimulus and accommodative response for both emmetropic and myopic subjects. As expected, the accommodative response was lower for the myopic subjects.

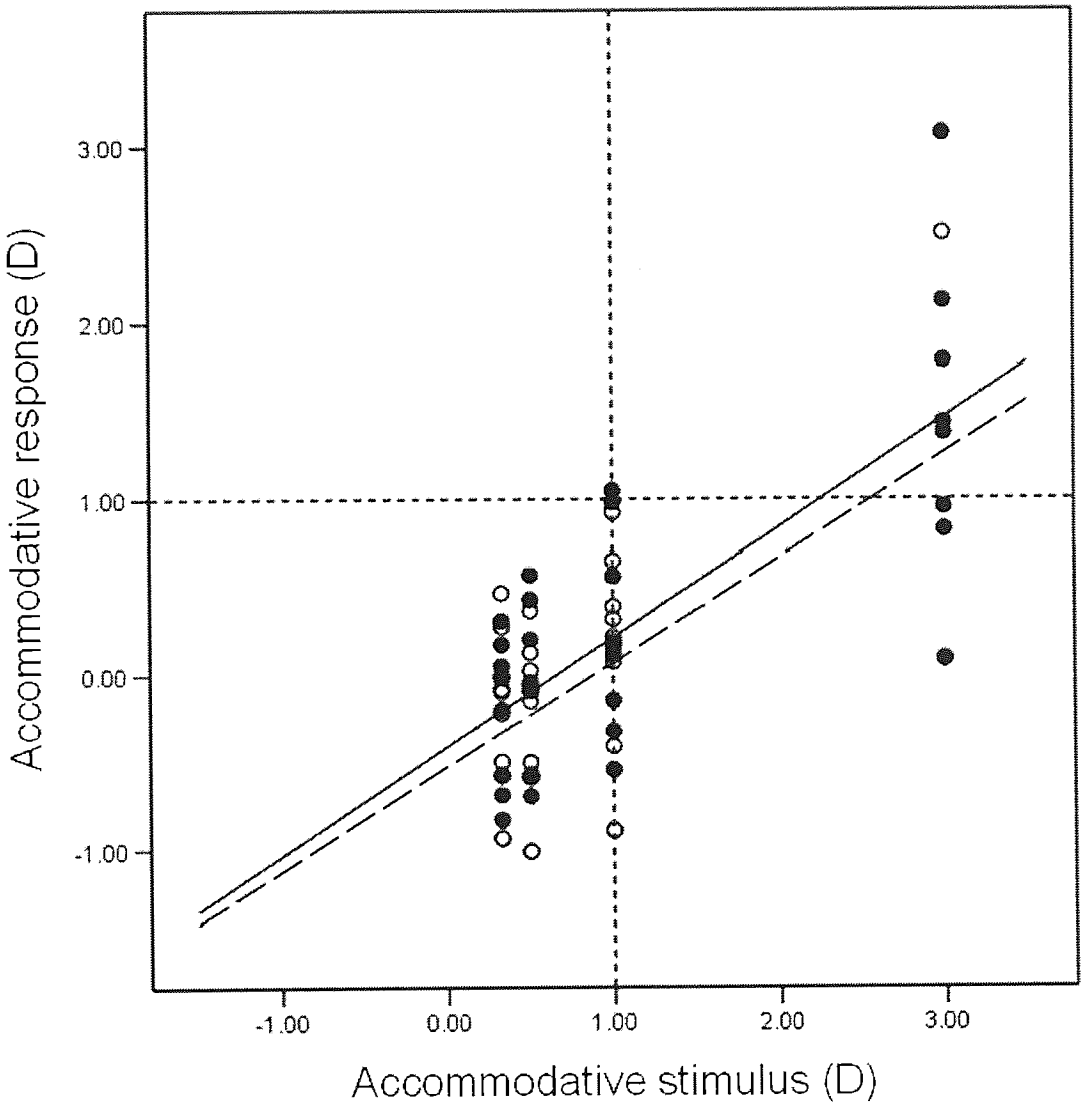

Figure 4.9.- *Correlation plot for the accommodative stimulus-response function for both emmetropes (empty bins, solid line) and myopes (full bins, dashed line)). Note that some bins overlap.*

Figure 4.10 shows the histogram of mean changes in the different Zernikes analyzed for the whole sample while fixating the different accommodation stimuli. Note the

systematic increase of primary spherical aberration (Z_4^0) towards more negative values with decreasing distance to stimuli from 0.50 D and the increase in vertical and horizontal primary comatic components Z_3^{-1} and Z_3^1.

Repeated measures ANOVA showed significant differences for spherical aberration values when fixating 1 m and 33 cm compared to baseline at 6m fixation (mean difference ± CI= 0.20 ± 0.08 μm, $p<0.001$ and 0.093 ± 0.021 μm, $p<0.001$, respectively) (see Appendix I for tables).
Univariate test did not show an effect of the refractive condition (emmetropia or myopia) in the change of spherical aberration when accommodating to targets at different distances ($p=0.167$).

The coma components Z_3^1 and Z_3^{-1} also showed significant differences compared to baseline when fixating target at 1 m and 33 cm (mean diff ± CI = -0.027 ± 0.022, $p=0.021$ at 1 m and -0.073 ± 0.037, $p=0.001$ at 33 cm for Z_3^1; mean diff ± CI = -0.015 ± 0.014, $p=0.021$ at 1 m and -0.052 ± 0.033, $p=0.001$ at 33 cm for Z_3^{-1}). None of the other Zernike coefficients analyzed were significantly different against baseline following ANOVA.

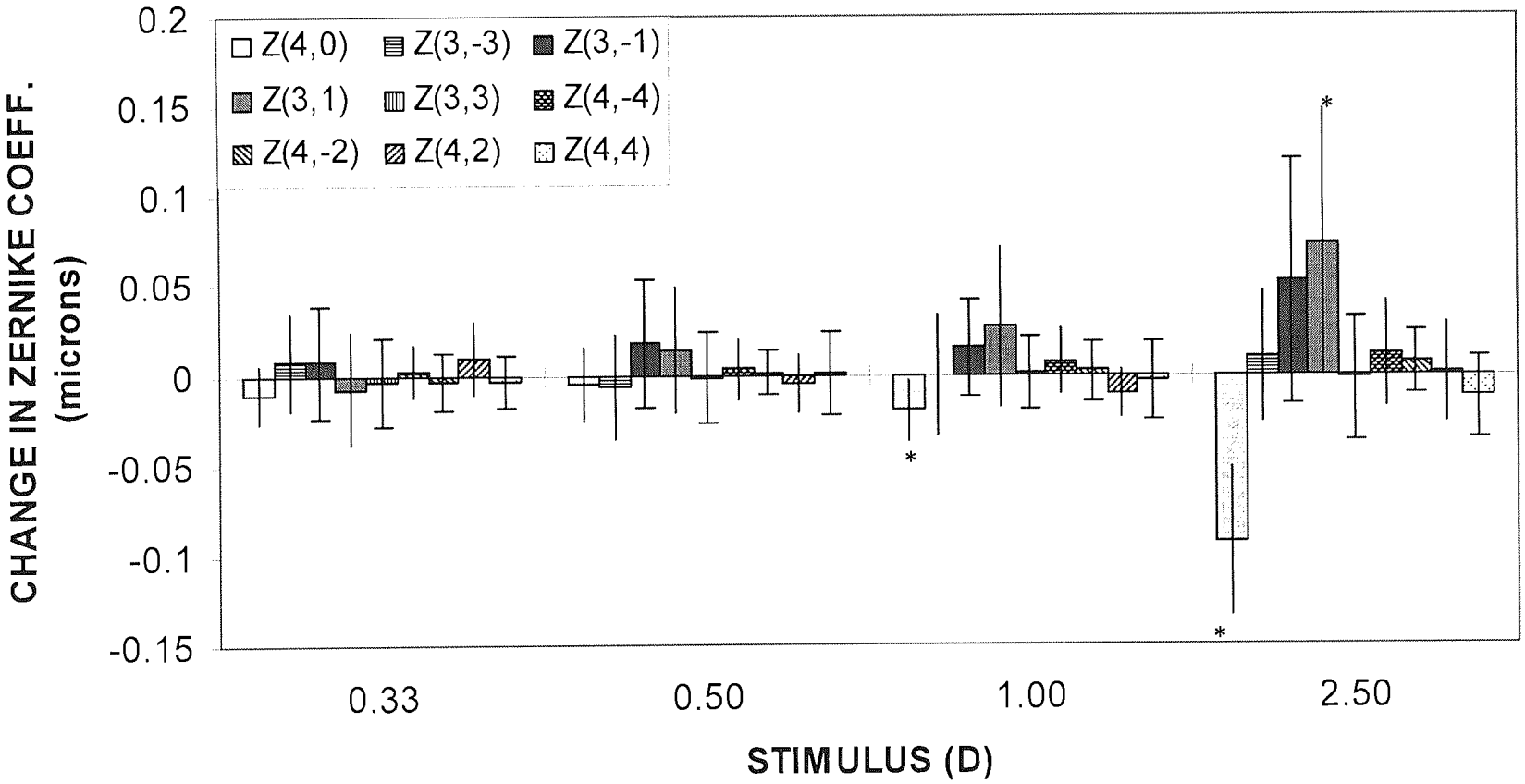

Figure 4.10.- *Histogram representing the mean change for each of the Zernike coefficients analyzed when fixating at the different target distances. Error bars represent ±1SD. Asterisks (*) represent statistical significance through ANOVA ($p \leq 0.001$)*

Figure 4.11 represents the correlation plots showing the accommodative response and the values of the comatic components Z_3^{-1} and Z_3^1.

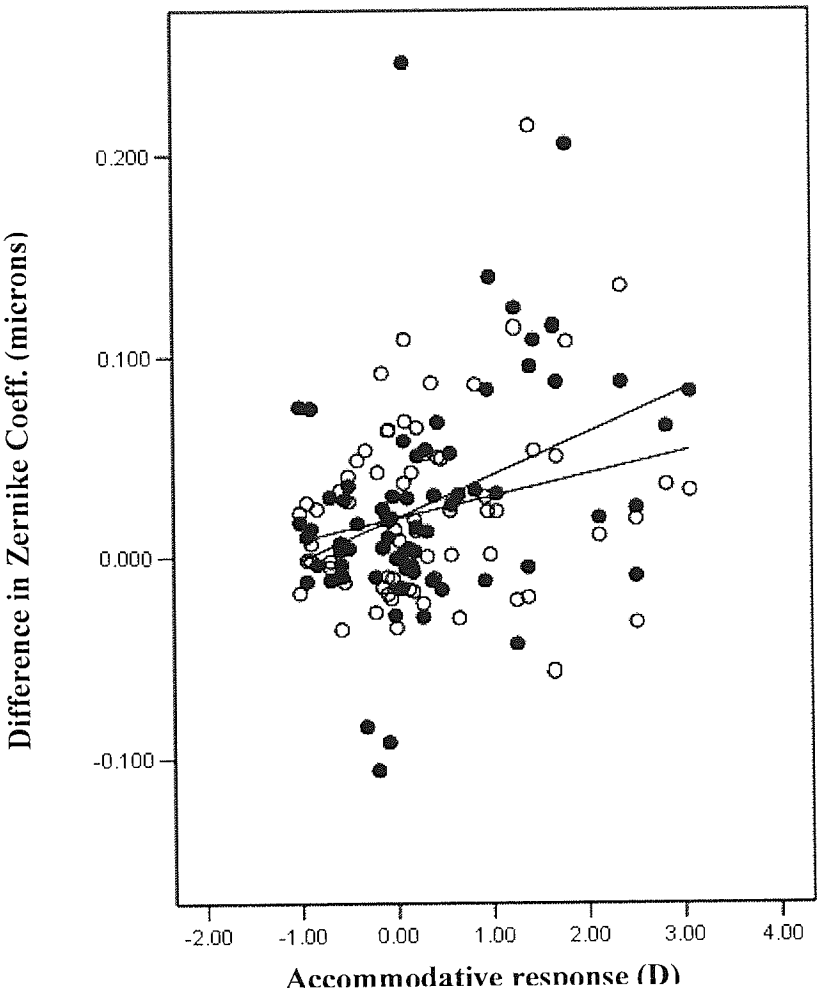

Figure 4.11.- *Scatterplot representing the change in the amount of primary coma Zernike coefficients Z_3^{-1} (empty circles) and Z_3^1 (full circles) with the accommodative response.*

Significant correlations were found for the comatic components Z_3^{-1} (Pearson's correlation coefficient 0.234, p=0.048) and Z_3^1 (Pearson's 0.365, p=0.002), spherical aberration Z_4^0 (Pearson's -0.812, p<0.001) and tetrafoil component Z_4^4 (Pearson's -0.315, p=0.007) with the accommodative response.

The decrease in spherical aberration with accommodative response was similar for both emmetropic and myopic subjects, as shown in figure 4.12.

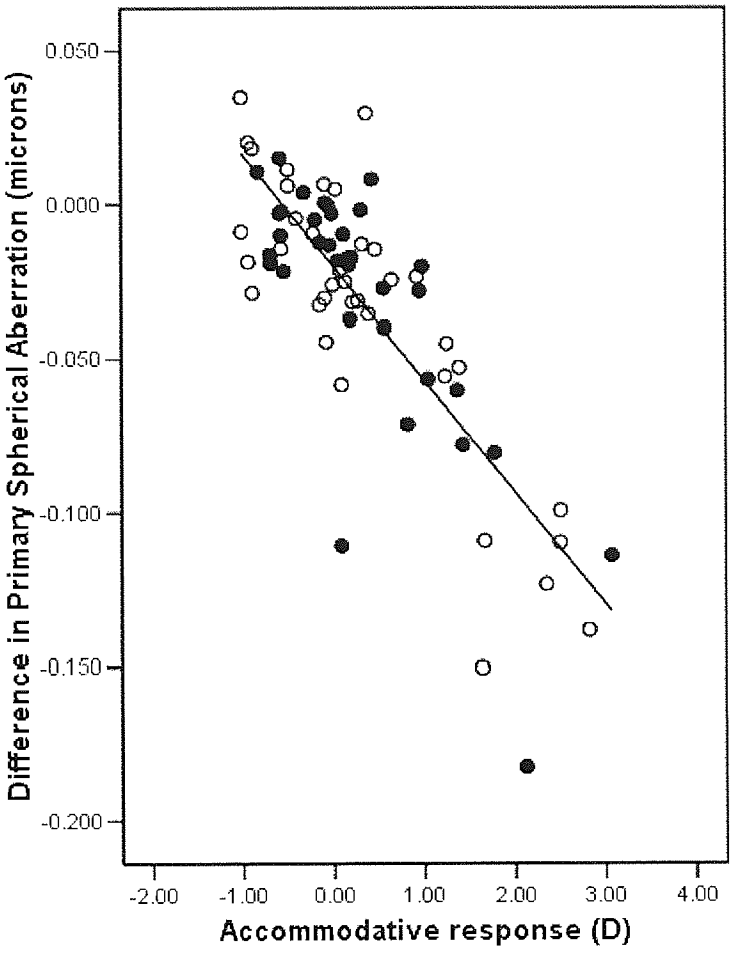

Figure 4.12. *Plot of difference in primary spherical aberration Z_4^0 with accommodative response for each refractive error group. Empty bins represent emmetropic subjects (less than ±0.50D MSE), full bins represent myopes.*

Correlation analysis between the accommodation error and change in spherical aberration showed statistically significant correlation for emmetropic subjects (Pearson's correlation coefficient=0.338; p=0.044) but not for myopes (Pearson's correlation coeff.= -0.045; p=0.794).

4.2.V. DISCUSSION

The results of this study corroborate previously reported findings such that with accommodation levels up to 3D there is a strong trend for spherical aberration to move towards more negative values. Horizontal and vertical coma components also changed significantly with accommodation, although in a less predictable way, and with more individual variations.

Because the accommodation stimuli were targets located in real space, and one eye was used for fixation while the other was measured, account could not be taken of the synergistic convergence response even though care was taken to center the system before data acquisition. Therefore some of the changes observed could be due to variable amounts of misalignment between the subject's ocular axis and the instrument axis. As described in chapter 3.1, small misalignments can induce changes principally in comatic aberrations while not affecting significantly the other coefficients. Therefore conclusions should not be drawn from these results regarding coma or off-axis aberrations. Some effect might also be expected with misalignment in spherical aberration although this is likely not to be significant in relation to the substantial effects induced by accommodation.

Looking at figure 4.9 it can be seen that the accommodation stimulus-response function showed a greater accommodation lag for myopes, and a resting point for accommodation between 0.5 and 1D fixation distance. It must be noted, however, that correcting formulas for spectacle correction were not applied. The data in fig. 4.10 above show that, when fixating targets closer than 2 m (0.5 D), changes in certain aberrations are statistically significant. Specifically, spherical aberration is strongly linked to the degree of accommodation. This strong link between change in spherical aberration and accommodation has been previously reported by different studies using both real distance and Badal system-induced accommodation(Plainis, Ginis, and Pallikaris, 2005).

In a recent paper, Buehren and Collins(Buehren and Collins, 2005) reported best subjective visual acuity at intermediate accommodation levels, and that accommodation

errors combined with spherical aberration could actually improve the quality of the final retinal image. The optimum proportionate combination of aberrations that can improve the quality of the retinal image has been previously reported (Applegate et al., 2003; Chen et al., 2005) (figure 4.13). In fact, significant amounts of aberrations have been reported for eyes with supernormal vision, even higher than those in emmetropic subjects with normal vision (Levy et al., 2005).The difference in accommodative response between emmetropes and myopes was examined in the present study principally with reference to the change in spherical aberration. The modest (i.e. only explains 13% of the variance) but significant correlation between the accommodation error, when looking at different real distance targets, and the change in spherical aberration from distance viewing in the emmetropic subjects suggests that those emmetropic subjects that exhibit different amounts of spherical aberration during accommodation need different amounts of accommodative defocus to see the target focused, i.e., a balance between spherical aberration and defocus to see the target focused is the aim of accommodation rather than a certain amount of accommodative defocus only. This correlation was not found in the myopic subjects. The reason for this difference could lie on the myopic eyes being less sensitive to retinal blur (Rosenfield and Abraham-Cohen, 1999) reducing the retinotopic accommodative response, or differences in peripheral refraction between myopic and emmetropic subjects (Charman, 2005). Fernandez and Artal reported a role for higher order aberrations in driving the accommodative response; finding a systematic increase in accommodative response times when correcting aberrations in real time (Fernandez and Artal, 2005). The hypothesis suggested here needs, however, to be studied further with larger sample sizes, better control of accommodation and convergence levels and more specific differentiation between and within refractive groups.

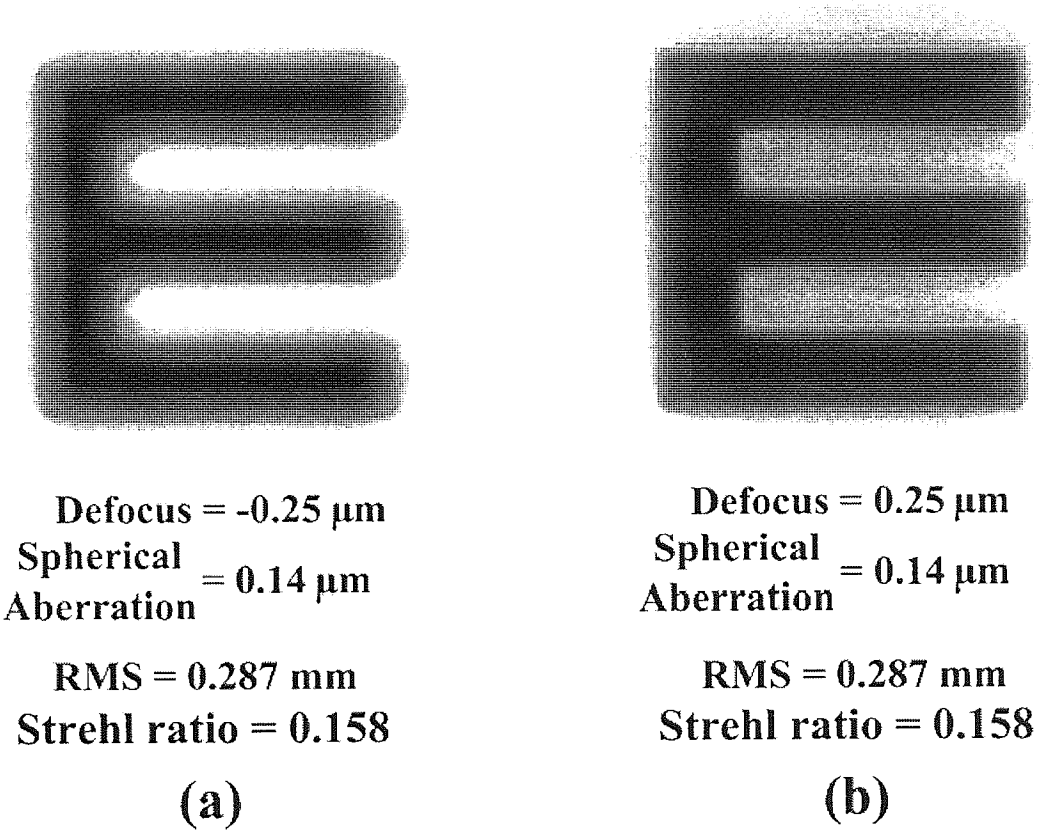

Figure 4.13. *Simulation of a Snellen E as seen through two eyes with the same amount of total RMS and Strehl ratio, but different amounts of defocus, i.e. different balance between defocus and spherical aberration. Reproduced from Chen et al (Chen et al., 2005) (permission requested).*

These findings also imply and that the presence of instrument myopia shown in study 3.1 may have a significant effect on the wavefront aberration values obtained mainly for amounts of instrument myopia higher than 1D.

4.3. CONCLUSIONS

It is shown that instrument myopia when performing wavefront analysis in young non-cyclopleged human subjects is likely to occur and that it will alter significantly the readings of wavefront aberrations compared to actual unaccommodated values.

The results obtained in this chapter show that since the 13 eyes excluded from the analysis in study 2.2 of chapter 2 were, in fact, experiencing over-accommodation of 1D and higher, significant departures of measured against real higher order aberrations are likely to have occurred. This is an important finding for clinical reasons as it indicates the need for higher order aberrations to be interpreted with caution when patients over-accommodate, and for any study of aberrations in which we would recommend exclusion of patients with excessive accommodation. For the purpose of achieving clinical accuracy, higher order aberrations should be assessed only after establishing that the wavefront aberration-derived refraction does not exceed by more than 1D the refractive error determined by other techniques.

Previous findings reported by other authors stating that accommodation significantly changes wavefront error have been corroborated in the present experiments. Wavefront aberrometry intended for clinical use aims to achieve values for optical quality as close to natural viewing conditions as possible. It has been demonstrated here that:

1.- Wavefront analysis without the use of an antimuscarinic agent may trigger an accommodative response due to the close field environment of the current clinical wavefront analyzers in the form of instrument myopia. Although this value is, on average, around 0.30 D (0.33±0.11D), some patients may trigger a response up to 3D (Cervino, 2006).

2.- Not detecting instrument myopia results in wavefront data that are erroneous since accommodation modifies wavefront aberration values, mainly spherical aberration and coma, which are the most relevant in visual performance. Even for lower levels of accommodation, less than 3D, the changes in measured wavefront aberrations may

reach significance, what would be of great importance mainly if the measurements obtained are to plan a customized refractive surgical procedure.

Changes in wavefront aberrations occurring with age(Brunette et al., 2003), and specifically the increasing spherical aberration towards more positive values with age (McLellan, Marcos, and Burns, 2001), as well as the well-known effect of age on accommodation, suggest that different results would be expected for different age groups. Further studies with broader age ranges, control of accommodation-induced convergence, refractive error and accommodation levels would be desirable.

CHAPTER 5. FACTORS INFLUENCING THE DISTRIBUTION OF WAVEFRONT ABERRATIONS IN YOUNG ADULTS

5.1. ABSTRACT

Purpose: To determine relationships between wavefront aberrations and biometric measures, gender, ethnicity and visual performance.

Methods: 74 right eyes from 74 young healthy subjects were assigned to two racial groups A. Caucasian: n= 30, MSE = -1.28 ± 2.24 D (-8.31 to 0.75 D), age =24.8 ± 4.4 years (18 to 34 years), 16 women; B. British Asian: n=44, MSE = -2.37 ± 3.08 D (-10.88 to 2.19 D), age = 20.73 ± 2.37 years (18 to 17 years), 22 women. Both groups were examined for higher order aberrations (WASCA wavefront analyzer) and ocular biometric characteristics (IOLMaster). The relationship between ethnicity, gender, axial length (AL), anterior chamber depth (ACD), mean spherical equivalent (MSE), mesopic low CS and wavefront HO RMS and aberration components were assessed by multiple regression and correlation analysis.

Results: AL on its own accounted for 4.7% of the variance in trefoil component Z_3^{-3} ($F_{1,72}$=4.602; p=0.035), 13.7% of coma component Z_3^1 (F1,72=12.536; p=0.001) and 6.1% of trefoil component Z_3^3 ($F_{1,72}$=5.705; p=0.020) and 9.8% of coefficient Z_4^{-2} ($F_{1,72}$=8.908; p=0.004). MSE, AL, CS and gender were not different between the two ethnic groups Asian and Caucasian (independent t-test, p>0.05). A significant model emerged ($F_{2,71}$=6.164; p=0.003) accounting for 12.4% of variance in primary spherical aberration. Ethnicity accounted for 8.4% of the variance. Estimated marginal means give, for an AL of 24.14 mm, a value for spherical aberration 0.032 μm higher for Caucasian than British Asian subjects. For Caucasian subjects a significant correlation was found between AL and Z_3^1 (Pearson's correlation coefficient -0.500; p=0.005) and Z_4^0 (Pearson's correlation coefficient -0.423; p=0.020). For British Asian subjects, AL

was only correlated with coefficient Z_4^{-2} (Pearson's correlation coefficient -0.358; p=0.017). Gender, ACD and MSE were not found to be good predictors of spherical aberration in the sample analyzed.

Conclusion: Ethnicity is a factor to be considered in the variability of wavefront aberration, particularly spherical aberration. It is suggested that compensation of corneal aberrations by internal optics may account for these differences. If higher order aberrations play a role in the emmetropization process, this may be different for different populations.

5.2. INTRODUCTION

The human eye is an optical imaging system that is far from perfect suffering from chromatic and monochromatic wavefront aberrations, light scattering and diffraction as previously outlined in the introduction. It is widely accepted that spherical refractive error is due primarily to an AL that is either too long or too short (Gwiazda et al., 2002; Strang, Schmid, and Carney, 1998), although there is some equivocal evidence that the optical components may also vary with refractive error (Carney, Mainstone, and Henderson, 1997; Horner et al., 2000; Mainstone et al., 1998; Strang, Schmid, and Carney, 1998). The role of higher-order aberrations is equally unclear. It has been suggested that high levels of HOA could play a role in myopia development (He et al., 2002). On the one hand, increased coma and spherical aberration has been found in some myopic eyes (He et al., 2002) but it has been also reported that lower average spherical aberrations occur in high myopes compared with emmetropes (Collins, Wildsoet, and Atchison, 1995). Nevertheless, all studies agree that great variability in wavefront aberration occurs with little, if any, relationship with refractive error.

Hyman et al (Hyman et al., 2005) found in a 3-year follow-up of children involved in the Correction of Myopia Evaluation Trial (COMET) that progression in myopia varied among different ethnic groups, showing Afro-American children as those having slowest myopia progression.

The aim of the present study is to determine whether the relationships between the different ocular parameters and ethnic groups are influenced or related to determined aberrometric patterns.

5.3. MATERIAL AND METHODS

5.3.I. Sample details

Seventy-four young adult volunteers were examined in this study (36 men, 38 women; mean age 22.51±3.89 years old). Subjects were recruited from the student population of Aston University. Exclusion criteria included history of ocular pathology or abnormal findings in slit lamp and ophthalmoscope examination. Only data obtained from the right eyes were used for analysis.

MSE averaged -1.90±2.76 D (range -10.88 to +2.19 D) with astigmatism up to 1.75 D (mean 0.49 ± 0.49 D).

Measurements of refractive error (MSE), axial length (AL), anterior chamber depth (ACD), mesopic contrast sensitivity (CS) and wavefront aberrations were taken using the different instruments described below. Descriptive statistics for the whole sample and divided by ethnic group are shown in table 5.1 and 5.2, respectively.

5.3.II. Ethical approval

Informed consent was obtained from each participant after explanation of procedures. The protocol followed the tenets of the Declaration of Helsinki and was approved by the Ethics Committee of Aston University.

5.3.III. Measurement of refractive error

Refractive error was assessed using the Shin-Nippon SRW5000 autorefractor used previously in Chapters 2 and 3. The system provides an objective measure of refractive error using an infrared, open-field, binocular autorefraction, hence avoiding the risk of

instrument myopia as described previously (Chat and Edwards, 2001; Mallen et al., 2001).

5.3.IV. Measurement of ocular biometry

The IOLMaster was used to assess AL and ACD. It is known to provide highly accurate and reproducible data (Connors, Boseman, and Olson, 2002; Gobin, 2002; Lam, Chan, and Pang, 2001; Santodomingo-Rubido et al., 2002; Vogel, Dick, and Krummenauer, 2001). The system has been described in detail elsewhere (Santodomingo-Rubido et al., 2002), however in brief, it uses a dual-beam version of partial coherence laser interferometry. The front surface of the cornea serves as the reference; therefore the measurements are independent of longitudinal eye movements during the scan. When the optical length in the eye equals the difference in arm length of the interferometer, interference fringes can be seen. This is detected by a photodetector. A scan of the eye can be displayed in the form of an A-scan. This is similar to the A-scan in ultrasound; however, the peaks are much slimmer, resulting in the higher precision for this technique (Lam, Chan, and Pang, 2001; Santodomingo-Rubido et al., 2002).

5.3.V. Measurement of contrast sensitivity

CS was measured best-corrected under mesopic conditions (0.75 cd/m^2) using the low contrast (10%) Bailey-Lovie chart.

Pesudovs et al. reported low contrast visual acuity testing under mesopic conditions as the visual performance test of choice and to be the one that correlates best with wavefront aberrations (Pesudovs et al., 2004).

The logMAR value for each subject was determined as the point where the subject failed all five letters on a size level or if they could not identify any letter at a given size level (Pesudovs et al., 2004). Measurements were taken on a single session.

5.3.VI. Measurement of wavefront aberrations

Wavefront aberration was measured using the WASCA wavefront analyzer described in the previous chapters. Three consecutive measurements were taken on each eye by a single examiner. Data was obtained for natural pupils and analyzed using the central 5mm. Dilating eyedrops were not instilled for the purposes of data acquisition.

5.3.VII. Study design and data analysis

After data acquisition, the analysis was made for the whole sample first, and then divided by ethnic group. For that reason the results and discussion sections will be divided into two epigraphs.

Correlations between the different parameters (biometric, refractive, CS, gender and ethnicity) and HOAs were determined for the whole sample first, and then by ethnic group. Multiple regression analysis was applied to examine the validity of models to account for the variability of the Zernike coefficients.

Differences between both ethnic groups for each of the parameters measured were assessed by independent samples t-test with a Bonferroni adjustment for multiple comparisons. As a result of the Bonferroni adjustment (for an alpha level of 0.05 and 13 comparisons), significance level was set at $p=0.003$.

5.4. RESULTS

5.4.I. Biometry, gender, MSE and ethnicity against HOAs

Descriptive statistics for the sample analyzed are shown in table 5.1.

n = 74	Mean	SD	Min.	Max.
AL (mm)	24.14	1.32	21.30	27.89
ACD (mm)	3.42	0.40	2.25	3.88
MSE (D)	-1.93	2.81	-10.88	2.19
CS (LogMAR)	0.37	0.19	0.08	1.10
Z_3^{-3} **(μm)**	-0.052	0.068	-0.200	0.137
Z_3^{-1} **(μm)**	0.013	0.113	-0.247	0.363
Z_3^{3} **(μm)**	0.001	.0580	-0.165	0.206
Z_3^{1} **(μm)**	0.014	0.057	-0.101	0.157
Z_4^{-4} **(μm)**	0.004	0.019	-0.092	0.039
Z_4^{-2} **(μm)**	-0.001	0.016	-0.034	0.046
Z_4^{0} **(μm)**	0.033	0.053	-0.052	0.228
Z_4^{2} **(μm)**	-0.002	0.031	-0.087	0.056
Z_4^{4} **(μm)**	0.006	0.024	-0.053	0.089
RMS (μm)	0.167	0.070	0.048	0.455

Table 5.1.- *Descriptive statistics for the whole sample used in the study. Distribution of Zernike coefficients across the population studied is shown in figure 4.1.*

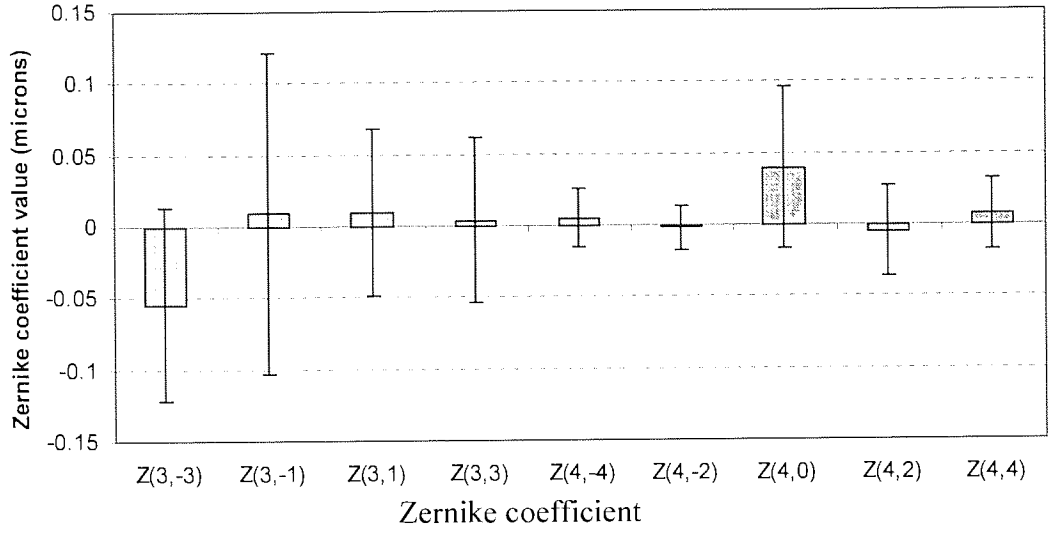

Figure 5.1. *Distribution of Zernike coefficients across the population studied. Error bars represent ±1SD.*

A strong correlation was found between AL and MSE (Pearson's correlation coefficient = -0.841; $p<0.001$) (Figure 4.2)

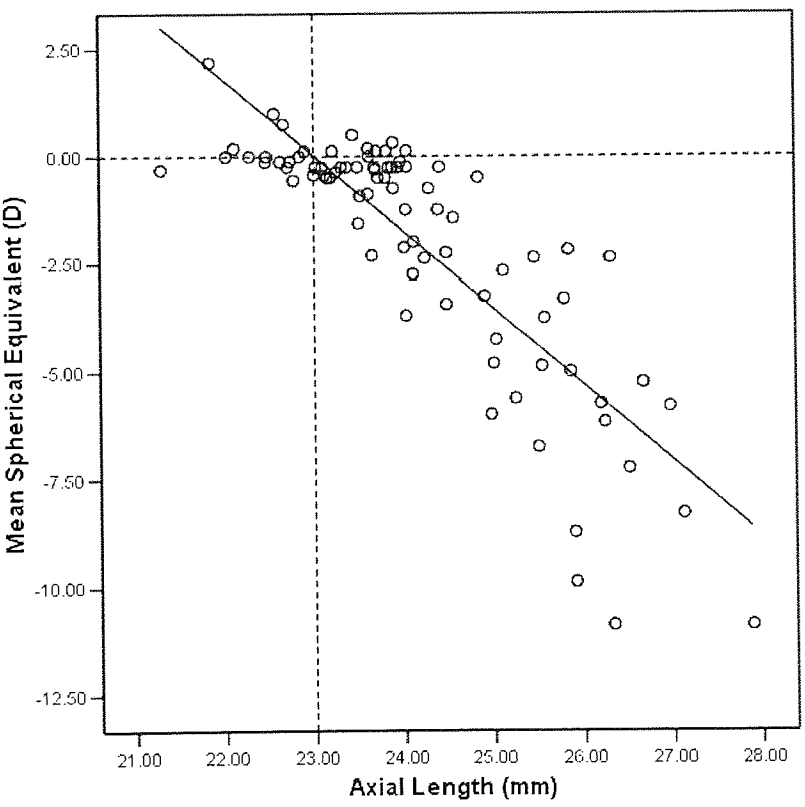

Figure 5.2. *Scatterplot showing the variation in MSE with AL.*

Multiple regression analysis using the stepwise method has shown significant models. AL on its own accounted for 4.7% the variance in trefoil component Z_3^{-3} ($F_{1,72}$=4.602; p=0.035), 13.7% of coma component Z_3^1 ($F_{1,72}$=12.536; p=0.001), 6.1% of trefoil component Z_3^3 ($F_{1,72}$=5.705; p=0.020) and 9.8% of coefficient Z_4^{-2} ($F_{1,72}$=8.908; p=0.004).

A significant model emerged ($F_{2,71}$=6.164; p=0.003), accounting for 12.4% of variance in primary spherical aberration. Ethnicity accounted for 8.4% of the variance, whereas AL added the remaining 4.0%.

Gender, ACD and MSE were not found as good predictors for the variability of spherical aberration in the sample analyzed.

Mesopic CS was not correlated to any other biometric or aberrometric component but trefoil component Z_3^3 (Pearson's correlation coefficient = 0.274, p=0.020)

5.4.II. Analysis by ethnic group

Since one of the aims of the study is to address if there are significant differences in the distribution of wavefront error among different racial groups, the sample was also divided by ethnicity. Descriptive statistics by ethnicity are shown in table 5.2.

Adjusted mean spherical aberration scores suggest that Caucasian young adults have larger values of spherical aberration than British Asian eyes (0.052±0.009 and 0.020±0.007 μm, respectively, adjusted for a 24.14 mm long eye), although as can be observed in figure 5.2, both racial groups have considerable variability (see Appendix I for tables).

Differences in the distribution of wavefront error between both ethnic groups can be observed in figure 5.3.

	Difference	Asian (n=44: 22 men, 22 women)				Caucasian (n=30:14 men, 16 women)			
	p-value	Min.	Max.	Mean	SD	Min.	Max.	Mean	SD
Age (years)	<0.001	18	27	20.73	2.37	18	34	24.80	4.40
AL (mm)	0.486	21.84	27.89	24.23	1.32	21.30	27.12	24.01	1.34
ACD (mm)	0.108	2.39	3.87	3.4795	0.36	2.25	3.88	3.32	0.45
CS (LogMAR)	0.991	0.10	1.10	0.37	0.18	0.08	0.90	0.37	0.19
MSE (D)	0.100	-10.88	2.19	-2.37	3.08	-8.31	0.75	-1.28	2.24
Z_3^{-3} (μm)	0.437	-0.196	0.137	-0.058	0.069	-0.200	0.053	-0.045	0.066
Z_3^{-1} (μm)	0.844	-0.187	0.363	0.010	0.113	-0.247	0.301	0.016	0.114
Z_3^{1} (μm)	0.341	-0.096	0.106	0.009	0.050	-0.101	0.157	0.022	0.065
Z_3^{3} (μm)	0.031	-0.081	0.206	0.012	0.054	-0.165	0.107	-0.017	0.061
Z_4^{-4} (μm)	0.964	-0.092	0.039	0.004	0.021	-0.041	0.034	0.004	0.017
Z_4^{-2} (μm)	0.075	-0.022	0.046	0.002	0.015	-0.034	0.045	-0.005	0.017
Z_4^{0} (μm)	0.007	-0.052	0.135	0.020	0.042	-0.045	0.228	0.053	0.061
Z_4^{2} (μm)	0.546	-0.087	0.053	-0.001	0.031	-0.081	0.056	-0.005	0.031
Z_4^{4} (μm)	0.154	-0.053	0.089	0.009	0.026	-0.046	0.043	0.001	0.020
RMS (μm)	0.567	0.048	0.430	0.163	0.063	0.093	0.455	0.173	0.079

Table 5.2.- *Descriptive statistics of the sample used in the study by ethnic group. The second column displays the p-values showing which parameters were statistically significant between both ethnic groups (independent samples t-test, p=0.003 after Bonferroni adjustment for multiple comparisons)*

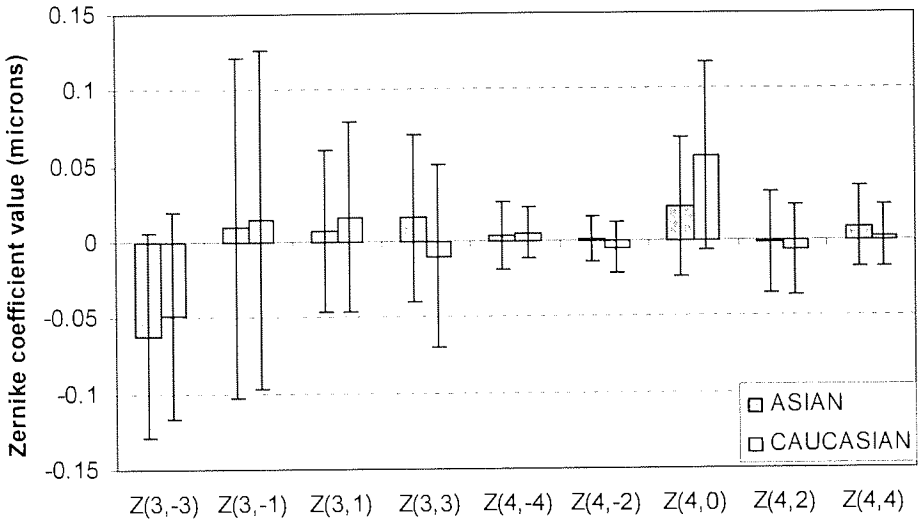

Figure 5.3. *Distribution of Zernike coefficients as a function of ethnicity. Error bars represent ±1SD.*

For Caucasian subjects a significant correlation was found between AL and Z_3^1 (Pearson's correlation coefficient -0.500; p=0.005) and Z_4^0 (Pearson's correlation coefficient -0.423; p=0.020) (figure 5.4).

For British Asian subjects, AL was only correlated to coefficient Z_4^{-2} (Pearson's correlation coefficient -0.358; p=0.017).

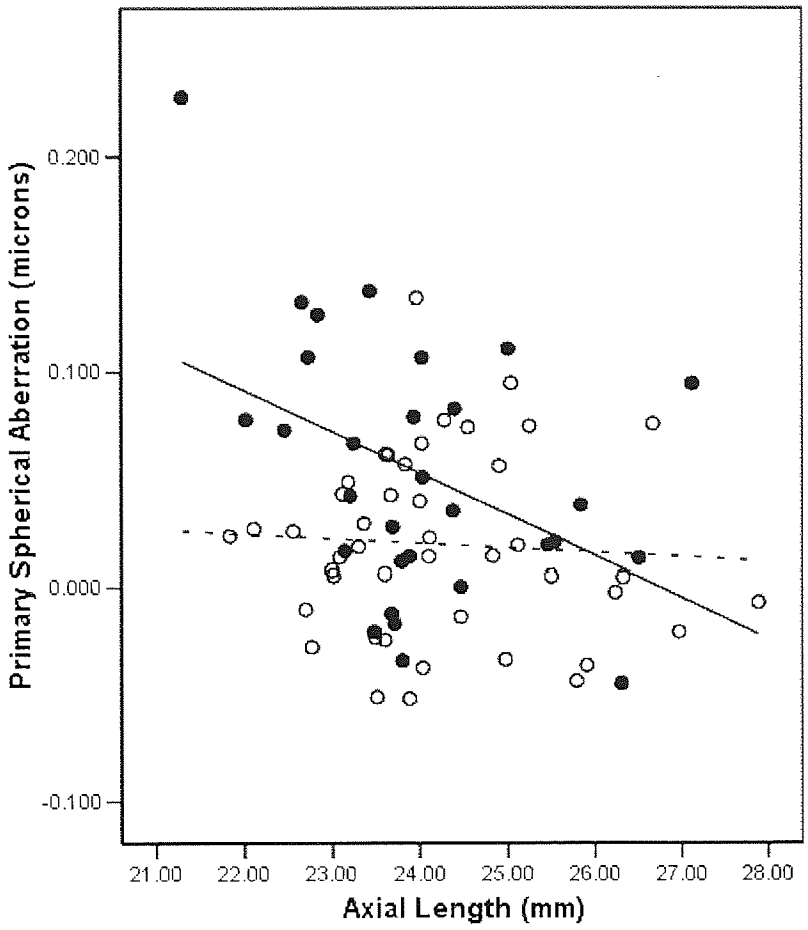

Figure 5.4.- *Scatterplot showing the variation in spherical aberration with AL for the two ethnic group studied: British Asian (empty bins, dashed line; r^2=0.004) and Caucasian (full bins, solid line; r^2=0.179).*

5.5. DISCUSSION

It has been postulated that high levels of axial ocular aberration might have a role in the development of myopia due to the retinal blur induced (Marcos, Barbero, and Llorente, 2002; Smith, Hung, and Harwerth, 1994). As discussed by Charman (Charman, 2005), it could be hypothesized that high levels of aberration could produce an excessively blurred PSF which, through form deprivation, could lead to the development of myopia. Animal experiments supported the hypothesis of higher levels of image degradation inducing greater final levels of myopia (Bartmann and Schaeffel, 1994). He et al (He et al., 2002) also found greater values of aberration RMS in myopes than emmetropes, supporting this hypothesis. Carkeet et al (Carkeet et al., 2002) found, however, decreased values of spherical aberration in low myopes compared to high myopes, emmetropes and hyperopes in Singaporean children. Cheng et al(Cheng et al., 2003) examined the relationship between ametropia and optical aberrations but did not find significant differences in spherical aberration with AL, even though theory and experiments on model eyes had previously predicted this to be the case. The results found in the present study agree with those reported by Carkeet et al, since HO RMS was found not to be correlated with the level of myopia or the AL of the eye. AL has been found, in the present study, to correlate to a more or less extent to most of the aberration components studied, including spherical aberration. The results reported here agree with the great variability in aberration values observed previously (Iglesias, Berrio, and Artal, 1998; Porter et al., 2001). The relative lack of hyperopes in the sample analyzed in the present study constitutes a limitation for the extrapolation of this results to the overall population, although it does represent a real population of University students.

Brunette et al(Brunette et al., 2003) analyzed monochromatic aberrations as a function of age and were able to fit their data to a quadratic model. RMS, third, fourth and fifth to seventh orders decreased progressively until early adulthood, and increased progressively with age after the fourth decade of life. Their results suggest a possible role of higher order aberrations in the emmetropization process.

The results obtained by Brunette et al suggest that the period of optimal optical quality of the human eye is between the third and fourth decade of life. According to this, subjects examined in the present study were in the period of "wavefront error improvement".

Although there were not significant differences in HO RMS between the two ethnic groups, ethnicity has been found in this study to be strongly linked to Z_4^0, with British Asian subjects having less primary spherical aberration than Caucasian. When doing a correlation analysis by ethnicity, AL is correlated significantly to spherical aberration only for Caucasian eyes. Hyman et al. found, on a three year evaluation, evidence of differences in the progression of myopia with ethnicity (Hyman et al., 2005). Despite the differences found in the aberrometric patterns of both ethnic groups, the visual performance was not significantly different. Due to the cross-sectional character of the present study, all the variables affecting visual performance could not be accounted for. For instance, individual variations in intraocular light scatter could have an effect in the variability of the visual response outcomes observed.

Differences in corneal thickness have been reported between different ethnicities (Aghaian et al., 2004; Hanna et al., 2004), although differences in corneal curvature and other ocular biometric components between British Asian and Caucasian subjects were not found to be significant in previous studies(Logan et al., 2005). Evidence of compensation of corneal aberrations by internal optics of the eye has been reported (Artal et al., 2001; Fraenkel et al., 2004), and spherical aberration did not show individual compensation, suggesting that it is a genetically determined physiological result(Kelly, Mihashi, and Howland, 2004). This evidence, along with the results reported in the present study, suggest that the difference between ethnic groups may lie in the compensation of corneal aberrations by the internal optics.

Further studies on larger sample sizes and accounting for more sources of variability would be needed to better establish ethnic differences in optical quality and their effect in visual performance. If ocular aberrations have an effect on the onset and progression of myopia, this finding is relevant to give another step towards a better understanding of the mechanisms underlying the onset and progression of refractive defects.

CHAPTER 6. VALIDATION OF CLINICAL SUBJECTIVE LIGHT SCATTER MEASUREMENTS: THE EFFECT OF SPECTRAL TINTS ON CONTACT LENS WEAR

CHAPTER SUMMARY

Purpose: To determine the repeatability of the C-Quant straylight meter for the determination of retinal straylight and apply the methodology to determine the effect of lens tint of the new spectral CL for contrast enhancement.

Methods: Two studies were conducted 1. Repeatability study of retinal straylight measurements with the C-Quant, determining intra- and intersession repeatabilities; 2. A study on the effects of the tint of the new Maxsight® spectral CL for contrast enhancement in retinal straylight values.

Results: 1. Repeatability of the C-Quant was excellent, although as an effect of repeated measures, standard deviation increases with increasing number of readings, suggesting that three consecutive measurements is the optimum number for clinical use; 2. Grey/green contact lenses induce an increase in perceived straylight, which may be deleterious when performing certain activities such as driving at night.

Conclusions: Retinal stray light measurement using the C-Quant is a useful parameter that is repeatable and reliable and suitable for the clinical determination of visual implications of intraocular scatter.

6.1. VALIDATION OF SUBJECTIVE MEASUREMENTS OF RETINAL STRAYLIGHT

6.1.I. ABSTRACT

Purpose: Assessment of repeatability and reproducibility of retinal stray light measurements with the C-Quant stray light meter (Oculus AG, Germany) in young healthy human eyes.

Methods: Twenty eyes of 20 normal healthy subjects (mean age 26.9 ± 2.7 years, mean refractive error -1.34 ± 2.72 D) were examined with the C-Quant stray light meter, taking 10 consecutive readings per eye. Measurements were repeated on five of the subjects, who were also examined at the same time on 5 consecutive days for the assessment of reproducibility. The number of images required was determined from the plateau of standard deviations of multiple readings; within-visit repeatability was determined from the coefficient of repeatability; between-visit reproducibility was determined from the coefficient of repeatability and intraclass correlation coefficient (ICC).

Results: ANOVA did not show significant differences between the consecutive readings within sessions ($p=0.267$). $COR_{w/in}$ was 7.8% for 10 consecutive measurements decreasing to 5.9% when only the 3 first measurements were considered. Differences between mean values of stray light obtained in consecutive sessions were not different following ANOVA ($p=0.126$). ICC was 0.669. Mean COR_{btw} was 6.7%. Some individual intersession variability was found.

Conclusion: The C-Quant straylight meter is a repeatable, reliable tool for the assessment of retinal stray light in young healthy eyes. Three consecutive measurements are suggested as the optimum number to avoid increasing variability due to factors related to the acquisition procedure or patient compliance.

6.1.II. INTRODUCTION

Intraocular light scatter is light that has been reflected, refracted, diffracted, or experienced multiple combinations of all three from particles along the optical path of travel (Bohren, 1995). There are five major sources that contribute to the total amount of ocular stray light: the cornea, the iris, the sclera, the retina and the lens (de Waard et al., 1992). It is assumed that for young healthy eyes the total amount of stray light is comprised as follows: 1/3 by the iris, 1/3 by the lens and 1/3 by the iris, sclera and retina. Clearly these ratios change with age, pigmentation and specific pathologies. Corneal light scatter is constant with age (Ijspeert et al., 1990; van den Berg, 1995), and may change with lens opacities (i.e. cataracts)(Ijspeert et al., 1990) or after corneal refractive surgery(Veraart et al., 1993; Veraart et al., 1995; Veraart et al., 1992). The iris and the scleral light scatter depend on an individual's pigmentation (van den Berg, JK, and de Waard, 1991) for example, brown irides absorb more light and consequently produce less scatter than light irides. Lens scatter increases with age being greater in patients with cataracts (de Wit, 2006). Finally, the retina produces light scatter in different locations being pigmentation dependent (van den Berg, JK, and de Waard, 1991).

A clinical application of stray light measurement is to diagnose patients with complaints caused by substantial light scatter in the eyes as a result of lens opacities or corneal turbidity after laser corneal surgery. As scattered light causes loss of contrast in the final retinal image, the estimation of this parameter becomes very important in cataract and refractive surgery procedures. Several clinical devices have been developed to evaluate stray light and glare (i.e. nyktotest, mesotest and the straylight meter) (van Rijn et al., 2005). A recent modification of the original direct compensation method for the measurement of retinal stray light has been introduced in order to make it more suitable for the measurement of stray light in large scale clinical setting. This method has been described in detail in the introduction chapter, and has been shown as repeatable and reliable (Coppens et al., 2006; Franssen, Coppens, and van den Berg, 2006).

Since the measurement of retinal stray light is a subjective procedure, this study will evaluate the effect of continuous repeated measures of stray light, the possible existence of a subjective learning curve, and the optimum number of measurements to maximize the reliability of the value obtained using the C-Quant device.

6.1.III. METHODS

6.1.III.i. Sample details

Twenty eyes from 20 young adults (mean age 26.9 ± 2.7 years, mean refractive error -1.34 ± 2.72 D), were examined using the C-Quant stray-light meter.
Subjects were recruited from the student and staff population of Aston University.

Exclusion criteria involved ocular pathology observed through slit lamp and ophthalmoscopy, or history of ocular disease nor corneal refractive surgery, or having worn CL less than 24 hours prior to examination.

6.1.III.ii. Ethical approval

This study was approved by the Ethical Committee of Aston University. All procedures follow the agreement of the Declaration of Helsinki. Measurements were performed after informed consent was obtained from all volunteers.

6.2.III.iii. Retinal straylightmeter

The C-Quant is a newly developed instrument to measure the retinal stray light using the "compensation comparison" method. In essence, this method presents exactly the same stimuli to the subject as the direct compensation method described in previous reports(van den Berg, 1986), and implemented in previous versions of the instrument(van den Berg, 1992) (Chapter 1). In contrast, in the compensation comparison method, two stimuli of the direct compensation method are presented to, and compared by, the subject simultaneously (Franssen, Coppens, and van den Berg, 2006).

6.2.III.iv. Experimental procedures

Ten consecutive measurements were taken on each eye without any compensation for refractive error. All measurements obtained were considered reliable by the system, that is, the estimated standard deviation (ESD) and shape factor (Q) values were lower than 0.08 and higher than 1.00, respectively (see details in chapter 1). A time interval of between 30 seconds and 1 minute was allowed between measurements for the patient to rest from the task. Each single measurement lasted about 1.5-2 minutes.
Additionally, 5 emmetropic subjects from the sample were measured three times on each of 5 sessions. These sessions were taken at the same time on five consecutive days in order to assess the reproducibility of the measurements.

6.2.III.v. Data analysis

The optimum number of measurements to perform in order to increase reliability was obtained by plotting the mean SD against the number of measurements.

Repeated-measures ANOVA was used to assess differences between the consecutive measurements obtained within the same session. Intrasession repeatability was assessed by determining the coefficient of repeatability ($CoR_{w/in}$), defined as the SD of the difference between each measurement from the mean of the repeated measures, divided by the average response (eq.6.1).

$$CoR_{w/in} = \frac{SD_{diff}}{Average} \quad \text{Eq. 6.1}$$

A repeated measures ANOVA was also performed to assess the significance of the differences between the measurements obtained in the 5 sessions. Intraclass correlation coefficient, defined as the proportion of relevant variance that is associated with differences among measured subjects, was calculated, as described in eq. 3.1, using the SPSS reliability tool as a measure of intersession repeatability, as well as intersession CoR (CoR_{btw}) (eq. 6.2)

$$CoR_{btw} = \frac{SD_{diff}}{Average_{mn}} \quad \text{Eq. 6.2}$$

Where SD_{btw} is the SD of the differences between pairs of measurements and $Average_{mn}$ is the average of the means of each pair.

6.1.IV. RESULTS

6.1.IV.i. Intrasession repeatability

Figure 6.1 shows little variation of the mean standard deviation (SD) throughout the 10 consecutive readings. However, SD increases with the number of measurements, possibly due to tiredness of the subject examined due to the subjective character of the test and its duration (around 2 minutes each measurement).

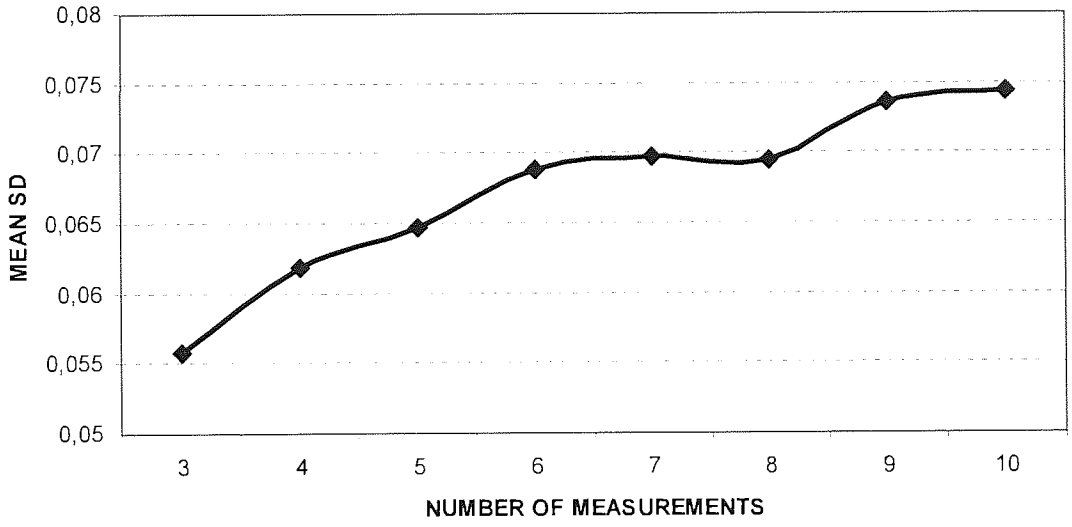

Figure 6.1.- *Graphical representation of the variation of the mean SD with the number of measurements taken on the 20 eyes of 20 subjects.*

Table 6.1 shows the mean and standard deviation of the stray light parameter, in logarithmic units of stray light, obtained for the sample in the 10 consecutive measurements, along with the $CoR_{w/in}$. obtained from the 10 consecutive readings as well as the $CoR_{w/in}$ obtained from the 3 first consecutive readings. Analysis of variance

(ANOVA) did not show statistically significant differences between the measurements taken within the same session (p=0.267) (see Appendix I for tables).

Patient	Mean Log(s)	SD	$CoR_{w/in}10$ (%)	$CoR_{w/in}3$ (%)
1	0.91	0.12	11.3	11.0
2	1.06	0.10	8.6	4.0
3	0.69	0.06	8.1	2.5
4	0.92	0.09	9.1	2.9
5	0.62	0.07	9.5	7.9
6	0.89	0.05	5.8	3.9
7	0.72	0.05	6.1	7.9
8	1.25	0.08	7.1	7.1
9	0.80	0.06	7.4	5.4
10	0.99	0.08	7.1	5.2
11	0.99	0.09	10.3	8.6
12	0.81	0.07	8.7	10.9
13	1.05	0.07	6.5	4.1
14	1.14	0.05	4.8	4.0
15	0.91	0.05	6.6	1.2
16	1.09	0.09	7.6	3.7
17	1.00	0.04	3.7	0.6
18	0.92	0.07	7.8	10.1
19	1.05	0.13	13.3	12.0
20	0.76	0.05	6.0	4.8

Table 6.1.- *Mean logarithmic straylight value, log(s) and standard deviation (SD) obtained from 10 measurements for each of the 20 patients within the same session, along with the corresponding $CoR_{w/in}$ for 10 and 3 measurements.*

Mean $CoR_{w/in}$ was 7.8% for the 10 consecutive readings and decreased to 5.9% when only the 3 first consecutive measurements were considered.

6.1.IV.ii. Intersession repeatability

Table 6.2 shows the stray light values and SD throughout the 5 sessions. Analysis of variance (ANOVA) did not show statistically significant differences between the measurements obtained in the 5 sessions (p=0.126), although some degree of variability up to 0.22 log(s) units can be seen in figure 6.2, which could possibly be attributed to normal individual variations (see Appendix I for tables).

	Session 1		Session 2		Session 3		Session 4		Session 5	
Patient	Log(s)	SD	Log(s)	SD	Log(s)	SD	Log(s)	SD	Log(s)	SD
1	0.84	0.05	0.86	0.04	0.81	0.02	0.85	0.04	0.90	0.08
2	0.78	0.01	0.79	0.07	0.81	0.03	0.79	0.01	0.78	0.08
3	0.76	0.02	0.78	0.02	0.81	0.05	0.81	0.04	0.95	0.03
4	0.90	0.03	0.94	0.04	0.95	0.04	1.12	0.03	1.04	0.04
5	0.88	0.03	0.84	0.02	0.77	0.03	0.90	0.04	0.86	0.03

Table 6.2.- *Mean logarithm of the stray light value, log(s), and standard deviation (SD) from the 3 measurements obtained on the 5 sessions taken on consecutive days.*

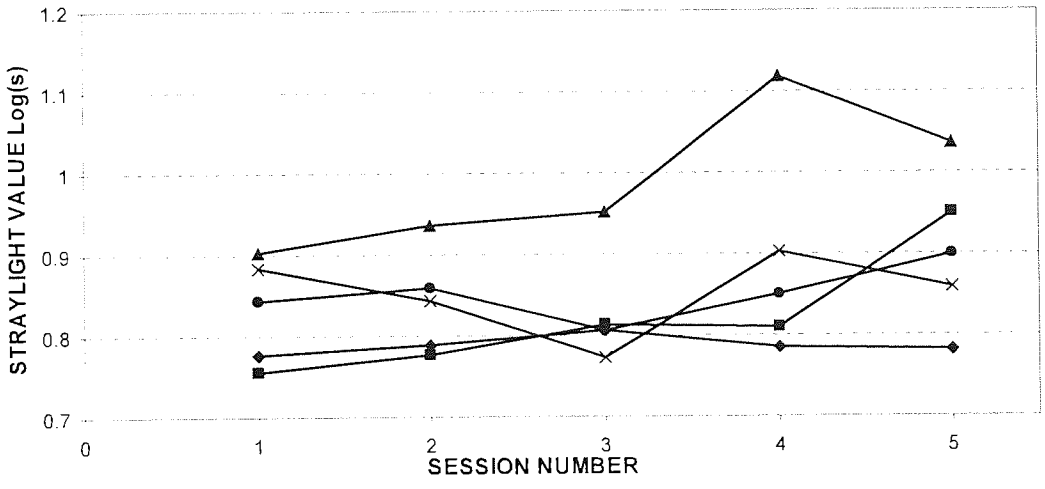

Figure 6.2.- *Variation of the mean straylight value for each of the subjects throughout the five consecutive sessions.*

ICC for the 5 consecutive sessions was 0.669. Mean CoR_{btw} was 6.7%. Table 5.3 shows the CoR_{btw} for the different subjects.

	Subject 1	Subject 2	Subject 3	Subject 4	Subject 5
CoR_{btw} (%)	5.3	2.1	8.5	9.1	8.7

Table 6.3. *CoR_{btw} for the different subjects examined across the five different sessions*

6.1.V. DISCUSSION

Direct compensation method for the determination of retinal straylight has been successfully used in a number of studies, and has been widely reported in literature as an useful approach in the study of optical performance in cataract (de Waard et al., 1992; Meacock et al., 2003), corneal distrophies(van den Berg, Hwan, and Delleman, 1993), retinal disease(Alexander, Fishman, and Derlacki, 1996; Grover et al., 1998; Grover et al., 2002) the effects of ocular lubricants(Veraart and van den Berg, 1992), laser refractive therapy(Harrison et al., 1995; Veraart et al., 1993; Veraart et al., 1995) and radial keratotomy(Veraart et al., 1992). Recently, a modification to the original method has been made in order to make it more suitable for clinical use on a large scale. This new method was named the compensation comparison method, and has also been described in detail in literature (Franssen, Coppens, and van den Berg, 2006), resulting in a reliable instrument for the measurement of retinal straylight in clinical settings and has been successfully used in large scale studies (van den Berg and van Rijn, 2005). However, all the studies reported have to the authors' knowledge been done taking no more than 2 repeated measurements on each of the subjects. The aim of the present study was to assess the effect that repeated measurement of retinal stray light had on the final values and determine the number of measurements needed to achieve optimum reliability.

When repeated measures are carried out in a subjective test in which a bright light flickers at different intensity levels, some kind of "bleaching" effect is expected that would affect the values obtained, i.e., the last readings would be less reliable than the first ones due to saturation of the retinal receptors that would make the task more difficult to perform. In a previous study describing and assessing the procedure used here, Franssen *et al.*(Franssen, Coppens, and van den Berg, 2006) found an overall SD

of repeated measures between 0.06 and 0.1 log units, which agrees with the findings of the present study i.e. SDs between 0.04 and 0.13 log units. This high repeatability suggests that the system is reliable and useful for detecting clinically significant stray light values.

The C-Quant relies on reliability parameters to identify whether the measurement can be considered reliable or whether another measurement should be taken. The expected standard deviation (ESD), which the system designates as reliable when lower than 0.08 and is based on a single assumed shape factor for the psychometric function obtained which depends itself on the critical modulation depth contrast and a parameter describing the lapse rate. Both parameters and the reasoning behind them have been described in detail elsewhere (Coppens et al., 2006) and Chapter 1. In a recent publication assessing the reliability of the method, Coppens et al. showed ESD to be efficient for detecting unreliable measurements (Coppens et al., 2006).

In summary, the C-Quant stray-light meter is a very intuitive, easy to use clinical tool that provides reliable, repeatable measurements of retinal stray light in young healthy eyes. More measurements do not necessarily increase reliability of the values obtained, and a balance between number of measurements and time required for the patient to perform the test is crucial. From the results obtained in the present study, it is proposed that 3 consecutive measurements may be the optimum number in order to provide higher reliability.

6.2. SUBJECTIVE RETINAL STRAYLIGHT IN PATIENTS WEARING SPECTRAL TINTED CONTACT LENSES

6.2.I. ABSTRACT

Purpose: To measure the retinal stray light induced by tinted contact lenses (CLs) commercially available for outside sport activity, compared to a clear lens of the same material.

Methods: Thirteen emmetropic patients were fitted with two CLs, one to each eye, in normal room illumination: 1. A tinted sports lens (Nike Maxsight®,Bausch & Lomb), 2. A clear lens made of the same material (Optima 38 –polymacon–, Bausch & Lomb). The tinted lens was randomly assigned to one eye, and alternately fitted in each of two colours, amber Maxsight (CL AM) or grey-green Maxsight (CL GGM); the clear lens was fitted in the fellow eye. Two stray light measurements were taken on each eye before (baseline) and then 5 minutes after lens insertion to allow stabilization of the lens and tear film.

Results: Mean stray light values were 0.90±0.09 at baseline (no lens) and 0.95±0.1 with the clear lens. Stray light values with tinted lenses were 0.97±0.1 logarithmic units of stray light (log(s)) with CL AM and 1.0±0.1 log(s) with CL GGM. Differences between baseline and clear CL were not significant (mean diff. ± 95%CI: -0.05 ± 0.06 log(s); p=0.066), nor was the difference between baseline and CL AM (mean diff. ± 95%CI: -0.065 ± 0.07 log(s); p=0.052). Conversely, CL GGM showed a statistically significant increase in retinal straylight compared to baseline (mean diff. ± 95%CI: -0.098 ± 0.05 log(s); p=0.002).

Conclusions: Clear contact lenses and some tinted lenses do not significantly increase perceived retinal straylight. However, a further lens (grey-green Maxsight) resulted in significant increases in retinal straylight. These findings have implications for lens choice during certain activities such as driving.

6.2.II. INTRODUCTION

The direct compensation method, described in Chapter 1, for the determination of retinal straylight has been successfully used in a number of studies, and has been widely reported in the literature as a useful approach in the study of optical performance in patients with cataract (de Waard et al., 1992; Meacock et al., 2003), corneal distrophies(van den Berg, Hwan, and Delleman, 1993) or retinal disease(Alexander, Fishman, and Derlacki, 1996; Grover et al., 1998; Grover et al., 2002), as well as the effects of ocular lubricants(Veraart and van den Berg, 1992), laser refractive therapy(Harrison et al., 1995; Veraart et al., 1993; Veraart et al., 1995) or radial keratotomy(Veraart et al., 1992).

A clinical application of straylight measurement is to diagnose and quantify the extent of change in patients with any disease in which the optical ray path is interfered with, when increased scatter is to be expected. Lens opacities and evaluation of intraocular lens implants or corneal turbidity after laser corneal surgery are good examples of potential clinical applications. Several clinical devices have been developed to evaluate straylight and glare (i.e. nyktotest, mesotest and the straylight meter)(van Rijn et al., 2005). The recently introduced computer version of the straylight meter, used in study 6.1 has been designed to improve the clinical measurement of ocular straylight (Franssen, Coppens, and van den Berg, 2006). This instrument has proved to be sensitive and repeatable for systematic application in research and clinical activities.

A further field of application of straylight measurements is in assessing the ocular response to contact lens wear, particularly the evaluation of oedema (Elliott et al., 1993; Elliott, Mitchell, and Whitaker, 1991). Tinted contact lenses could also affect this function, by their very presence on the eye's surface, even in the absence of significant levels of oedema.

Measurements of retinal stray light have been shown to be highly dependent on age and pigmentation (Coppens, Franssen, and van den Berg, 2006) and affected by changes in corneal hydration due to contact lens wear (Elliott, Mitchell, and Whitaker, 1991). The new Bausch & Lomb "performance-enhancing" tinted soft contact lens (MaxSight™) approved by the Food and Drug Administration (FDA) in 2005 is designed for athletes engaging in outdoor sports. The lens (Polymacon, Bausch & Lomb) selectively filters blue and red wavelengths and reduces glare to provide, it is claimed, the wearer with enhanced clarity of vision. The Maxsight is available in two tint colours: amber (AM) and grey-green (GGM), both having different absorption spectra, as shown in figure 6.3. Amber lenses absorb yellow wavelengths and is intended to allow the wearer to see the ball better in fast-moving sports (e.g., baseball, softball, soccer, tennis, and football). Grey-green lenses are intended for bright sun activities, including golf and running. The wearer has reduced reflection and glare.

As discussed previously, whereas retinal stray light has been shown to be highly dependent on, among other things, age and pigmentation of the eye (Hennelly et al., 1998; Ijspeert et al., 1990; van den Berg, 1995; van den Berg, JK, and de Waard, 1991; Whitaker, Steen, and Elliott, 1993), a low wavelength dependency has been reported in particular in eyes with low pigmentation (e.g. Caucasian eyes) such as those used in the present study(Coppens, Franssen, and van den Berg, 2006; Whitaker, Steen, and Elliott, 1993). For that reason, we would expect a change in the retinal stray light following the insertion of these tinted lenses.

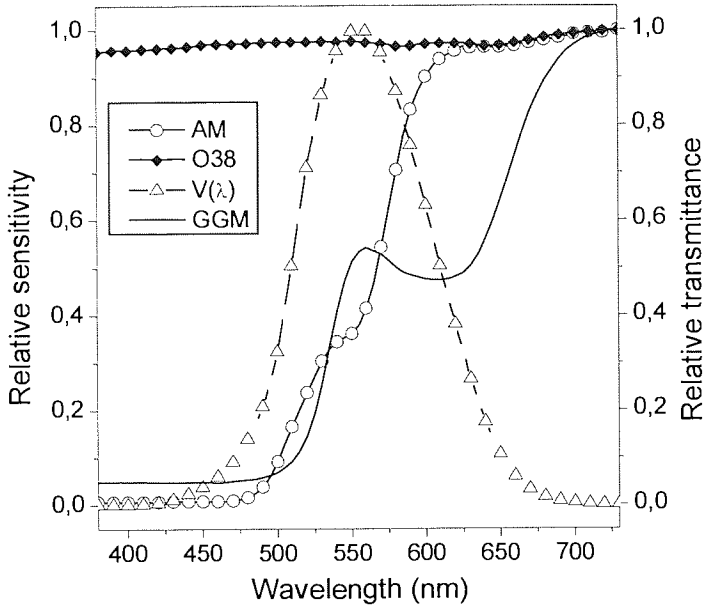

Figure 6.3. *Normalized CIE (1924) Photopic spectral luminous efficiency function (open-triangles line, adapted from CIE,2004) plotted against the normalized mean transmittance of two AM (open-circles line) and two GGM (solid line) CL, and the transmittance of O38 CL (black diamonds line).*

The aim of the present study is to investigate the effect of new spectral contact lenses on retinal straylight as measured using the C-Quant device validated in study 6.1.

6.2.III. MATERIAL AND METHODS

6.2.III.i. Sample details

Thirteen emmetropic subjects (10 men, 3 women; mean age 25.4 ± 4,4 years old) were recruited for the study. Refractive and ocular examination was carried out before entering the study. No contact lens wearers were admitted to take part in the study because of the potential confounding effect of chronic corneal oedema.

6.2.III.ii. Ethical approval

The study protocol followed the tenets of the Declaration of Helsinki and was reviewed and approved by the Scientific Committee of the University of Minho, where the study took place. After the nature of the study was explained, a signed consent form was obtained from each patient.

6.2.III.iii. Determination of retinal straylight

The procedure for stray light measurement was the same as that used in study 6.1, described in detail in Chapter 1. Subjects looking at a circle divided in two halves are required to indicate which of the halves flickers more clearly (more intense) by pressing one of two buttons, left or right. The 1 and 0 answers are plotted giving a psychometric function from which a logarithmic value of straylight, log(s), is obtained. Two coefficients defined previously in chapter 1 and in study 6.1 of the present chapter, ESD and shape factor Q, give a measure of the reliability of the values obtained. As discussed in relation to the results obtained in study 6.1, three measurements are the optimum number for reliability of the values.

6.2.III.iv. Contact lens application

After baseline measurements of light scatter, patients were fitted contra-laterally with a clear hydrophilic CL Optima® 38 (O38) and one of two tinted hydrophilic CL Nike

Maxsight®, amber (AM) and grey-green (GGM), made of the same material and manufactured by Bausch & Lomb Inc. (Rochester, NY). The assignment of right and left eye to a clear or tinted lens was made according to a randomization table. Further technical details of the CLs used in the study are provided in table 6.4. Figure 6.3 provides further details on light transmittance of the used clear and tinted contact lenses measured with a scanning spectrophotometer (UV-3101PC Shimadzu Corporation, Kyoto, Japan) along with the spectral luminous efficiency function of the human eye for photopic vision(adapted from CIE, 2004(CIE, 2004)).

	Optima 38	Nike Maxsight®
Manufacturer	Bausch & Lomb	Bausch & Lomb
Material (USANC)	Polymacon	Polymacon
Manufacturing	Spin-cast/Lathe-cut	Spin-cast/Lathe-cut
Hydration (FDA)	38.6% (group I)	38.6% (group I)
Dk	8.5 barrer	8.5 barrer
BC	8.7 mm	8.7 mm
Diameter	14.2 mm	14.3 mm
Power	-0.25	-0.25
Tint	No	Amber / Grey-green

Table 6.4. *Technical details of the lenses used in the study*

After lens insertion, lens stabilization was allowed for a 5 minute period, after which the straylight was measured again. The tinted lens was removed and replaced with the alternate colour lens and the measurement procedure was repeated. Retinal straylight was therefore measured twice in each eye for each combination of clear and tinted lens. The order in which each tinted lens was applied (to the same eye) was also randomized. The measurement of retinal straylight was performed monocularly. The non-examined eye was covered and the system has an ocular that couples directly onto the eye, minimizing the external light coming from the room illumination. Despite this, the room was kept under ambient scotopic conditions, the procedure described in detail elsewhere was followed (Franssen, Coppens, and van den Berg, 2006).

6.2.III.v. Data Analysis

Data were analyzed using the statistical package SPSS version 14.0. Normal distribution of variables was assessed by the Kolmogorov-Smirnov normality test and homogeneity of variances was assessed by the Levene test. Differences between log values obtained under different experimental conditions were assessed statistically by paired t-test and the Wilcoxon non-parametric test for variables with normal and non-normal distribution, respectively. Bi-variate correlations between the stray light values obtained with the different contact lenses against baseline were assessed by parametric (Pearson) and non-parametric (Spearman) correlations depending on the normal or non-normal distribution of the variables involved, respectively. Regression analysis was also used in order to illustrate graphically the nature of the correlations. The level of statistical significance was established at p=0.05.

6.2.IV. RESULTS

Descriptive statistics of the stray light values obtained with the different lenses are shown in table 6.5. To illustrate the increase in retinal stray light with the different contact lenses, a histogram showing the mean values and SDs of retinal stray light is shown in figure 6.4.

			95% CI	
	MEAN	SD	UPPER	LOWER
BASELINE	0.902	0.086	1.071	0.732
OPTIMA 38	0.950	0.010	1.146	0.754
AMBER MAXSIGHT®	0.970	0.103	1.170	0.764
GREY/GREEN MAXSIGHT®	0.999	0.098	1.191	0.808

Table 6.5.- *Descriptive statistics of stray light values obtained on thirteen eyes. Values are presented as logarithmic units of stray light.*

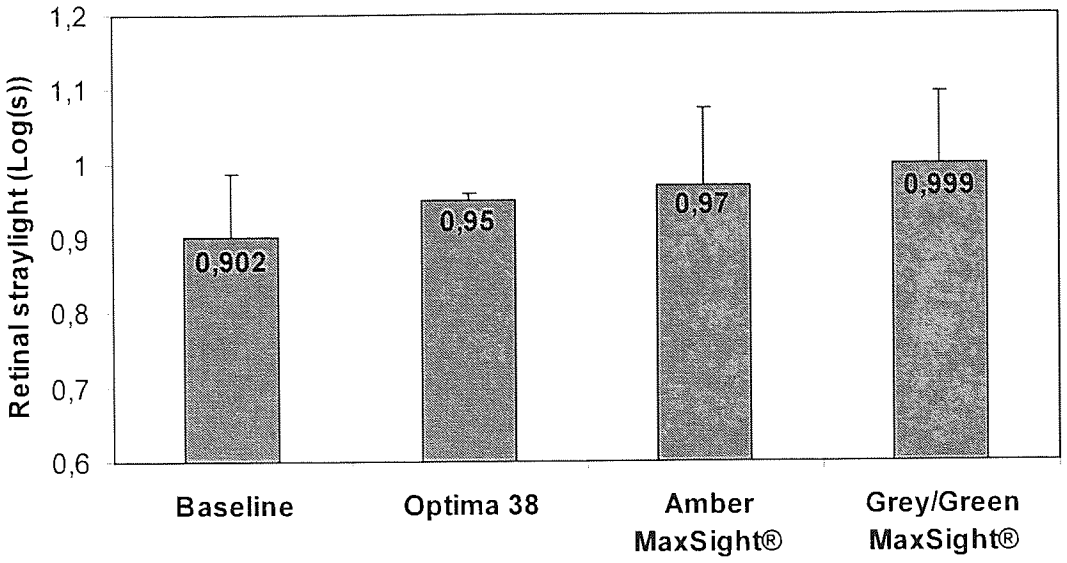

Figure 6.4.- *Histogram representing the descriptive statistics of table 2. Error bars represent 1 SD. Note the increase in the mean stray light value from baseline with all tested contact lenses. Values are presented as logarithmic units of stray light.*

Distribution was normal for the values obtained for baseline, O38 and AM tinted CL but not for GGM. Therefore non-parametric tests were applied to the values obtained with the GGM. Paired sample t-tests did not show significant differences between the stray light baseline values and those obtained with AM (mean diff: -0.065 ± 0.110; p=0.052). Wilcoxon signed-rank tests showed significant differences between the stray light baseline values and those obtained with the GGM (mean diff: -0.098 ± 0.091; p=0.002).

Figure 6.5 represents the increments in stray light values from baseline with the clear lens and with both tinted lenses for each one of the thirteen subjects enrolled in the clinical study. It shows a trend towards an increase in stray light values from baseline for O38, AMB and GGM with the latter presenting the higher levels of perceived stray light. Despite this general trend there is some variability in the response to the two tinted lenses at an individual level.

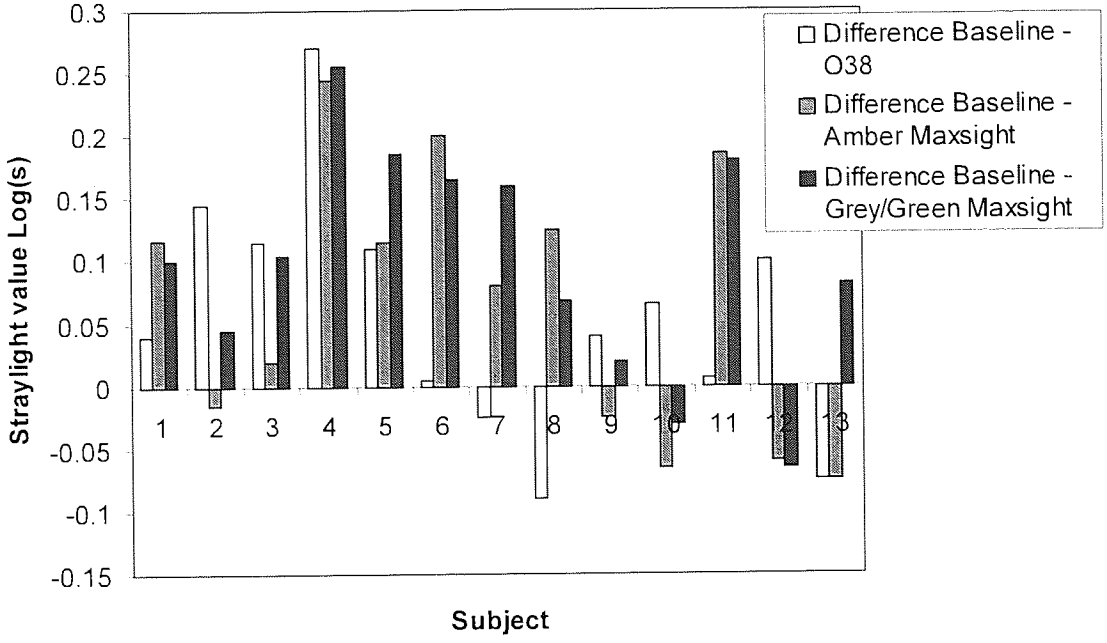

Figure 6.5.- *Mean difference from baseline in stray light value, log(s),for each of the 13 patients fitted with the O38 and AM and GGM tinted lenses. Values are presented as logarithmic units of stray light.*

6.2.V. DISCUSSION

All the subjects examined in this study were functionally emmetropic and, therefore in terms of refractive correction were not seeking contact lens wear. Figure 6.4 is evidence, although not significant, for the presence of a short-term effect of lens insertion in a non-contact lens wearer. This effect would be due to some extent, to the changes in hydration of the cornea as well as effectively a new refracting surface placed on its surface (Elliott et al., 1993; Elliott, Mitchell, and Whitaker, 1991). Retinal stray light measurement with the stray light meter is reported to be as sensitive as slit lamp evaluation in the assessment of contact lens induced corneal oedema (Elliott et al., 1993). Contact lens wearers were shown to give higher values of stray light after lens removal compared to non-wearers and in particular soft contact lens wearers (Elliott, Mitchell, and Whitaker, 1991). In order to discriminate the possible influence of corneal hydration changes in retinal stray light due to contact lens wear and, therefore, evaluate the effect of the contact lens tint, a clear contact lens of the same material and parameters (as shown in table 1) was fitted on the fellow eye and used as control. All

the subjects employed reported that they felt comfortable with all the contact lenses used after a few minutes post-fit and in the period prior to data acquisition.

The addition of a coloured filter to the eye not only modifies the amount of veiling luminance but also decreases the capability of the eye to detect the test stimulus used. In a previous study that used short- and long- wavelength pass filters, Steen et al. did not find measurable differences in disability glare (Steen et al., 1993) (corresponding to retinal stray light according to the CIE Commission International d'Eclairage).

This study has demonstrated that spectral tinted contact lenses can significantly affect the perception of retinal stray light when compared with the control clear lens condition. The results suggest that the benefits of tinted contact lenses are subject to individual differences in performance and that they may limit the capabilities of the wearers to perform certain activities such as night driving (Babizhayev, 2003), and possibly increasing reaction times due to decreased target visibility (Plainis and Murray, 2002). Further studies should be performed to confirm this hypothesis and to evaluate the subjective and objective impact of such lenses on visual performance under different illumination conditions. Since there are currently many intraocular lenses using tinted UV radiation filters(Harris, Haririfar, and Hirano, 1999) (Hayashi and Hayashi, 2006; Rodriguez-Galietero et al., 2005a; Rodriguez-Galietero et al., 2005b), other fields of application for retinal straylight measurement with the C-Quant straylightmeter could be the evaluation of post-surgical effect of different IOL types in retinal straylight values.

CHAPTER 7. OBJECTIVE MEASUREMENT OF INTRAOCULAR FORWARD LIGHT SCATTER USING HARTMANN-SHACK PATTERNS. VALIDATION ON MODEL AND HUMAN EYES

7.1. ABSTRACT

Purpose: To validate a new software-based image analysis tool for the objective determination of intraocular light scatter determined from clinically-derived Hartmann-Shack patterns.

Methods: Bespoke image analysis software was developed in conjunction with a programmer (DB) to quantify objectively aberrations measured using a Hartmann-Shack based wavefront analyser, the WASCA used in the previous studies. Three values of scatter, as maximum SD within a lenslet for all the lenslets in the Hartmann-Shack pattern (Max_SD), were obtained on each of 6 model eyes and 10 healthy human eyes. On the model eye sample, Hartmann-Shack patterns were obtained in four sessions: 2 without realigning between measurements, 1 with realignment between measurements, and one with the model eye angularly shifted 6 degrees from the instrument axis. Three measurements were made on the human eyes with the C-Quant stray light meter to obtain subjective as well as objective measures of retinal stray light. ANOVA, intraclass correlation coefficients ($ICC_{w/in}$), coefficient of repeatability (CoR) and correlation analysis were used to determine intra-session and inter-session repeatabilities and relationship between subjective and objective measures of scatter.

Results: No significant differences were found between the four image-acquisition sessions with the model eye ($p= 0.234$). Mean CoR was less than 10% in all sessions with both model eyes and human eyes. After removal of incomplete Hartmann-Shack patterns, a good correlation was achieved between subjective retinal stray light and objective scatter measurements despite the small residual sample size ($n=6$; $r= -0.831$, $p=0.040$).

Conclusion: The methodology was repeatable on model and human eyes. Realignment and misalignment had no effect on the values obtained. Optimising the Hartmann-Shack images obtained from the wavefront analyzer is crucial to increase the reliability of the method.

7.2. INTRODUCTION

The objective determination of intraocular light scatter has, in historical terms, proven difficult. The broad range of options for refractive correction, such as LASIK, phakic IOLs, as well as the increasing knowledge of the retinal image quality and the factors affecting it has renewed interest in an objective method for determining the extent of ocular light scatter in clinical settings. As previously discussed in chapter 1 most of the current methods for determining intraocular scatter are based on subjective assessment by the patient, which apart from the need for subject compliance also involves neural factors.

Procedures to obtain objective measures of scatter have been discussed in Chapter 1. The most recent methods aim to obtain objective measures of scatter using modified HS wavefront analyzers. Shahidi and Yang (Shahidi et al., 2004) designed an instrument for the simultaneous acquisition of wavefront aberration data and forward intraocular scatter. The operational basis of the instrument is that the measurement of intraocular scatter can be determined from the difference between the wavefront aberrations alone and the combination of wavefront aberrations and scatter.

Bueno et al. also used a modified HS aberrometer, referred to as the aberro-polariscope (Bueno, Berrio, and Artal, 2003), to determine wavefront aberrations and intraocular scatter. In this instance the measure of scatter was determined from a measure of the polarized light exiting the eye after a double-pass analysis. Bueno et al. obtained good reliability measuring ceramic plates of varying amounts of scatter.

Donnelly et al. (Donnelly et al., 2004) developed a method for extracting scatter values from the Hartmann-Shack patterns obtained from a customized wavefront analyzer. The basis for this method is the image analysis of the HS patterns and calculation of the

pixel intensities of the tails of the PSF of each lenslet. A scatter-free optical system measured with a HS analyzer provides a diffraction-limited HS pattern, as illustrated in figure 7.1. Any source of scatter will widen the PSF points.

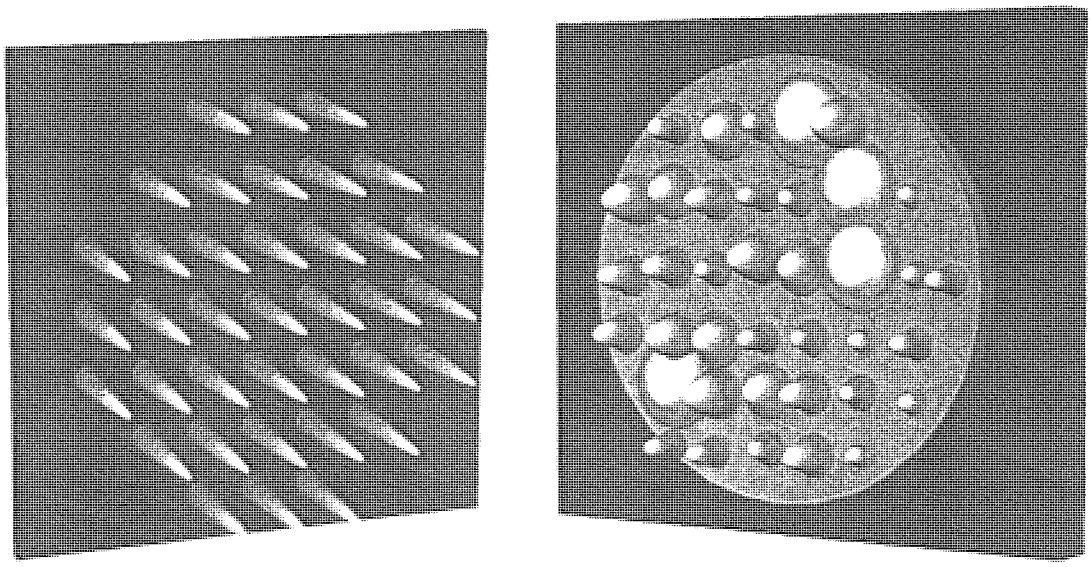

Figure 7.1.- *Intensity profiles of simulated HS images representing a perfect diffraction limited HS image (left) and a simulated cataract with local PSF spreading (right). From Donnelly et al.(Donnelly et al., 2004)*

Donnelly et al. also devised several metrics to collapse scatter within a given area down to a single number. It was concluded that the maximum standard deviation (i.e. Max_SD) of all point spread functions (PSF) of the lenslets in the Hartmann-Shack image is the metric that best characterises the intraocular forward scatter. This method is described in detail in Chapter 1. A similar more basic and less accurate method was used by Fujikado et al. (Fujikado et al., 2004) and involved measuring the diameter of the spots in the Hartmann-Shack patterns.

The aims of this chapter are:

- To test the applicability of the methodology described by Donelly *et al* to a commercially-available clinical WA by developing a software tool for the analysis of HS patterns. There were several reasons to choose the method:
    - It should be easy to implement into commercially-available HS wavefront analyzers since it is based on image analysis and does not require, in principle, hardware modifications.

- It is the most in-depth studied from a clinical point of view(Donnelly and Applegate, 2005; Donnelly et al., 2004), and has given results that explain convincingly variance in the visual performance of subjects with cataract.

- To validate the measurements of scatter obtained with this procedure on the HS pattern obtained in the model eyes used in Chapter 2 and, in addition explore the possible sources of variability on the measurements.

- To validate the measurements of scatter on human eyes by comparing them with the subjective stray light values obtained using the C-Quant straylightmeter, validated in Chapter 6, on a small human sample.

7.3 MATERIAL AND METHODS

7.3.I. Image Analysis for Intraocular Light Scatter

An *MS Windows*-based software tool was developed and based predominantly on the methodology previously reported by Donnelly et al (Donnelly, 2004), in which scatter information was extracted from HS patterns in order to characterise the effect of cataract on intraocular light scatter. This method was described in detail in Chapter 1 (section 1.6.III.iii). Although the same image used by WAs to extract aberration data is used to extract scatter information it will not be related to the magnitude of high order aberrations (HOA), since the determination of HOA and scatter from the same image is completely different. As described in chapter 1, the HOAs from Hartmann-Shack patterns are measured as the displacement of the centroid from an ideal position, whereas for scatter the software will measure the "spread" of the centroid.

For the purposes of this study software was devised in conjunction with a computer programmer (DB) and has potential applications which are commercially sensitive. Since a detailed computational description is considered to be beyond the scope of this thesis, only a description of the methodological principles and objectives will be included.

The Hartmann-Shack patterns obtained were analysed with a clinical Hartmann-Shack analyzer used in the previous chapters (WASCA, Zeiss/Meditec, Germany). The procedure was as follows:

1. An examination with the wavefront analyzer was performed following the same procedure as that used for the determination of wavefront aberrations.
2. A bitmap image of the Hartmann-Shack pattern was extracted with an image capture software tool (Hypersnap v.2.70, Hyperionics).
3. The image was then analyzed using the Hartmann-Shack analyzer software tool so that all the scatter distribution across the area analyzed was brought down to one number. The metric obtained was the maximum SD of the pixel values within a lenslet PSF neighbourhood for all the PSFs in the HS image (Max_SD), as described previously by Donnelly et al (Donnelly, 2004) (eq. 7.1).

$$Max\_SD = \max\left[\sqrt{\frac{\sum_{i,j} P(i,j)^2}{M} - \left(\frac{\sum_{i,j} P(i,j)}{M}\right)^2}\right] \qquad \text{(eq. 7.1)}$$

for all neighbourhoods n (1-N) where N is the number of PSFs in the HS pattern. A pixel neighbourhood is a square perimeter surrounding the centroid of each PSF of total pixel M (figure 7.2). Each pixel has a value P given by the number of photons captured at a pixel location (i,j).

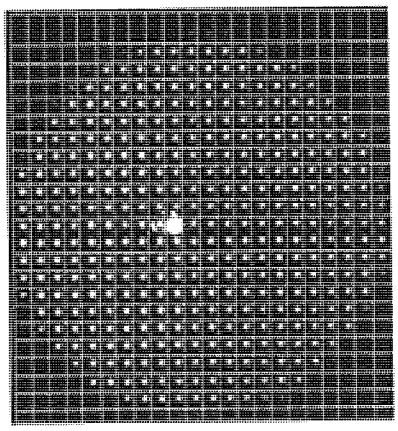

Figure 7.2. *Example of the grid division of a HS pattern into the different neighbourhoods for analysis.*

Max_SD has been shown to be the best metric for forward scatter obtained from HS images. Pixel intensities have a value between 0 and 255, where 0 is zero intensity and 255 is maximum intensity, therefore Max_SD values will range from 0 to 255 being 0 for maximum amounts of scatter and 255 for minimum amounts of scatter. A colour coded scatter map showing the distribution of scatter across the different areas was also obtained (figure 7.3).

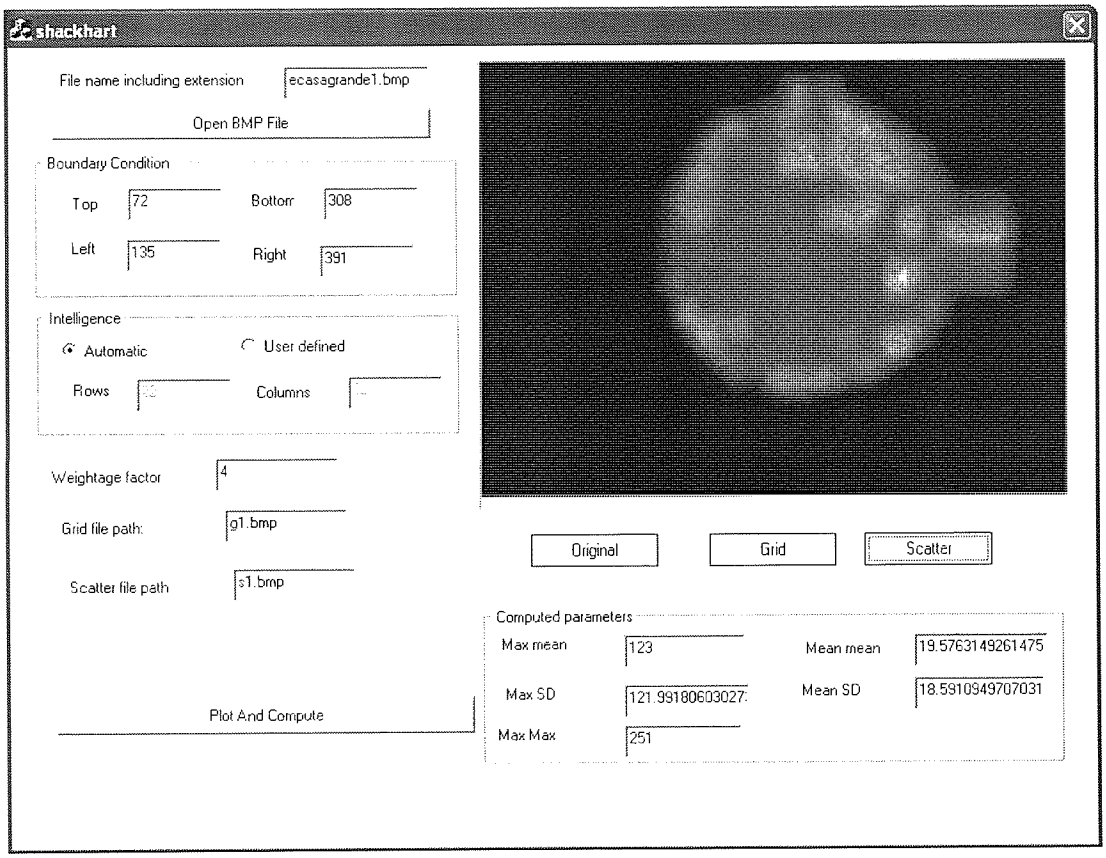

Figure 7.3. *Example of the scatter map obtained from the software tool representing the differences in scatter in the different areas. Colours represent relative pixel intensity, warmer colours (reds) show areas of increased scatter compared to colder colours (blues).*

7.3.II. Model eye sample

Since it is possible to analyse scatter on a retrospective basis from WA data already acquired, images from the model eye already described in study 3.1 were used for this study, and the model eye characteristics can therefore be found in tables 3.1-3.2 and figures 3.1-3.2. In order to determine whether the scatter data are robust to operational variables such as refocusing and misalignment and also whether the data can be differentiated from HOAs *per se*, the images from all four sessions in chapter 3 were included in the analysis. As such, three Max_SD values were obtained for each model eye in four different sessions: two sessions taking consecutive readings without realignment, one session realigning between measurements, and one session with the model eye misaligned 6 degrees with respect to the instrument axis.

7.3.III. Human eye sample

In order to evaluate the relationship between light scatter measured objectively and the subjective perception of light scatter, 10 right eyes from 10 healthy young adults (8 men, 2 women; mean age 27.5 ± 2.9 years old) were examined with the C-Quant stray light meter and the HS WA. MSE was -1.61 ± 2.59 D. Subjects were recruited from the student and staff population of Aston University.

Exclusion criteria involved ocular pathology observed through slit lamp and ophthalmoscopy examination, history of ocular disease or having worn CL less than 24 hours prior to examination.

Three measurements were made with each instrument. The HS patterns obtained from the WASCA were then analyzed with the HS analyzer and a Max_SD value was obtained for each of them.

7.3.IV. Ethics approval

Informed consent was obtained from each participant after explanation of procedures. The protocol followed the tenets of the Declaration of Helsinki and was approved by the Human Ethics Committee of Aston University.

7.3.V. Data analysis

7.3.V.i.Model eyes

Mean and SD of the three measurements of Max_SD obtained for each eye were calculated. Intraclass correlation ($ICC_{w/in}$) coefficients were calculated as a measure of intrasession repeatability as described in previous chapters. Intersession variation, differences with realignment and effect of angular misalignment were assessed by Pearson's correlation coefficient and Bland-Altman plots of the differences against the mean and repeated measures analysis of variance (ANOVA). Because of the multiple comparisons, a Bonferroni adjustment for repeated measures was applied, resulting in $p \leq 0.012$ for statistical significance.

7.3.V.ii. Human eyes

Coefficient of repeatability (COR) of objective scatter measures was determined as the SD of the difference between each measurement from the mean of the repeated measures, divided by the average response, as in previous chapters. The relationship between retinal stray light values obtained with the C-Quant and Max_SD obtained from HS image analysis was tested using correlation analysis.

SPSS v.12.0.1 (SPSS Inc) and Excel (Microsoft Inc.) were used for all statistical analyses.

7.4. RESULTS

7.4.I. Model eyes

Mean and SD of scatter value Max_SD obtained in the four different sessions are shown in table 7.1.

	First session		Second session		Realigning		Misaligned	
Eye	Mean	SD	Mean	SD	Mean	SD	Mean	SD
1	79.993	0.000	76.493	2.121	74.989	2.642	74.986	1.733
2	74.987	0.000	76.987	0.00	72.655	4.160	70.489	0.702
3	71.660	0.577	68.657	0.582	75.991	8.888	72.993	0.000
4	74.653	0.578	74.326	2.082	75.489	2.126	69.988	0.004
5	69.989	0.005	70.989	1.419	67.985	0.000	68.489	2.117
6	91.992	7.553	76.486	4.950	68.321	1.527	72.991	1.997

Table 7.1. *Mean and SD of the Max_SD values obtained for the different sessions on each model eye.*

Repeated measures ANOVA did not show significant differences between the values obtained within the same sessions (p=0.462, 0.471, 0.384 and 0.436 for sessions 1, 2, realigning and misaligned, respectively) (see Appendix I for tables).

Mean coefficients of variation (CoV) ranged from 1.5 to 5.2% for the four sessions (table 7.2).

	Session 1	Session 2	Realigning	Misaligned
Mean COV %	1.63	2.48	5.20	1.52
$ICC_{w/in}$	0.847	0.913	0.101	0.705

Table 7.2. *Mean CoV (%) and $ICC_{w/in}$ obtained for each of the sessions on the model eyes.*

Repeated measures ANOVA did not show significant differences between the values obtained in the different sessions (p=0.234).

7.4.II. Human eyes

Mean values and SD of retinal stray light (Log(s)) obtained with the C-Quant and objective scatter (Max_SD) obtained with the HS analyzer are shown in table 7.3.

	Log(s)		Max_SD	
Eye	**Mean**	**SD**	**Mean**	**SD**
1	1.15	0.13	115.0	91.0
2	0.7	0.02	138.3	12.5
3	1.04	0.03	126.0	0.0
4	0.79	0.06	132.0	7.5
5	0.76	0.08	140.3	20.1
6	1.16	0.05	28.6	3.8
7	1.13	0.05	121.5	0.7
8	0.81	0.01	42.3	21.4
9	1.01	0.01	135.0	10.15
10	0.85	0.09	63.3	22.4

Table 7.3. *Mean and SD of the subjective and objective measures of scatter obtained on each eye of the human eye sample.*

Correlation analysis did not show significant correlations between the subjective and objective measures of scatter (Pearson's correlation coefficient = -0.209, p=0.563).
Mean CoR of scatter in the human sample was 13.6%.

Patterns in which there were defects and omissions, such as those due to the upper eyelid or eyelashes (figure 7.4), caused some spots in the HS pattern to be altered and therefore affected the software analysis. These were considered severe when the HS patterns were not circular due to the presence of shadows affecting the pattern. HS patterns were then given a quality score out of 10 based on defects and omissions, with

10 being a complete image. Images with scores below 7 were excluded, and after removal from the sample (4 eyes), the mean CoR is reduced to 6.2%.

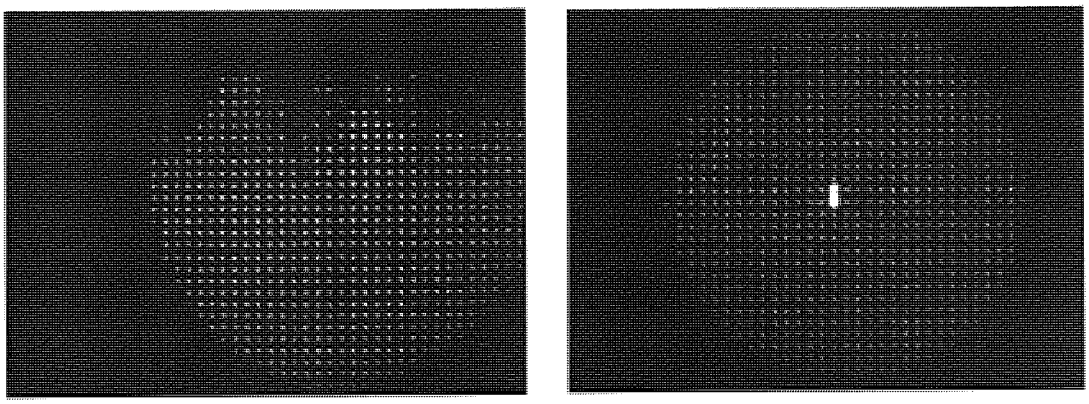

Figure 7.4. *Examples of an altered HS pattern (left) and an optimum HS (right) for HS analysis.*

Correlation analysis of the resultant sample (n=6 eyes) without the altered HS patterns showed a marked improvement in agreement between methods to 69.1% (Pearson's correlation coefficient = -0.831, p=0.040), (Figure 7.5).

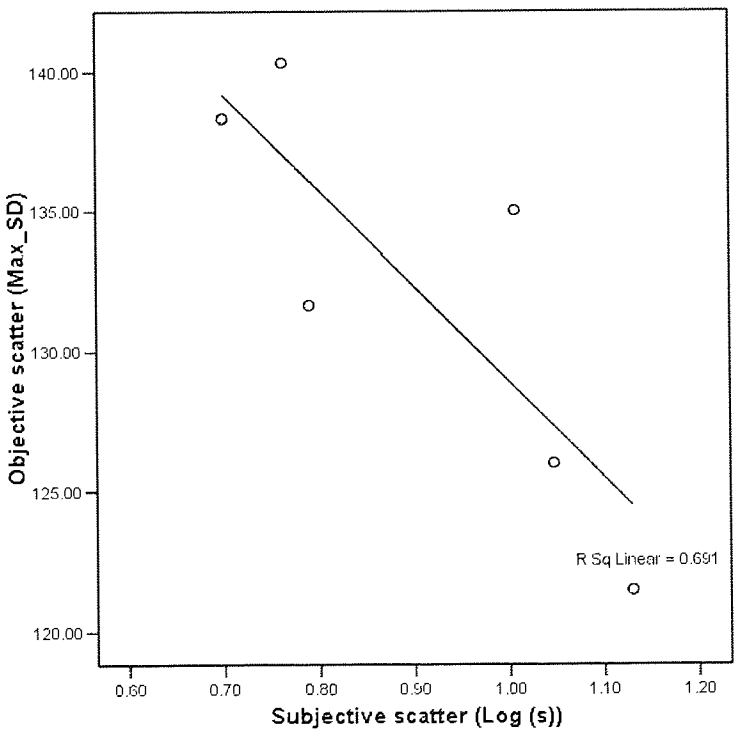

Figure 7.5. *Correlation plot of subjective and objective measures of scatter on 6 human eyes.*

7.5. DISCUSSION

This study shows that using a bespoke image analysis software system in conjunction with a commercially-available wavefront analyse reproducible objective measures of intraocular light scatter can be achieved; these are robust to factors such as refocusing and realignment and a good correlation with subjective light scatter responses can be achieved, although some data were rejected because of faulty degraded HS patterns.

7.5.I. Model Eye Study

Little has been reported on the reliability of objective methods for the measurement of scatter in model eyes, most likely since there is little immediate clinical relevance other than the need to validate and assess new technologies, but also because of the limited availability of optical surfaces with known amounts of scatter plus the lack of objective methods for determining scatter from a clinical point of view. However, Bueno et al (Bueno, Berrio, and Artal, 2003) reported good reliability of their aberro-polariscope in simultaneously determining wavefront aberrations and scatter on ceramic plates on which different amounts of scatter were induced by applying a voltage (see Chapter 1 for more detail). The results shown in this study demonstrate that the methodology for extracting forward scatter objectively from HS patterns is as repeatable and reproducible as found for model eyes. Also, it could be seen that realignment of the instrument and misalignment of the model eye with respect to the instrument axis does not significantly affect the scatter values obtained from the HS patterns.

There are, however, several aspects that need to be considered with regard to the repeatability and reproducibility values obtained on these model eyes. The characteristics of the components used in the model eyes meant that the HS pattern images were considerably saturated (figure 7.6).

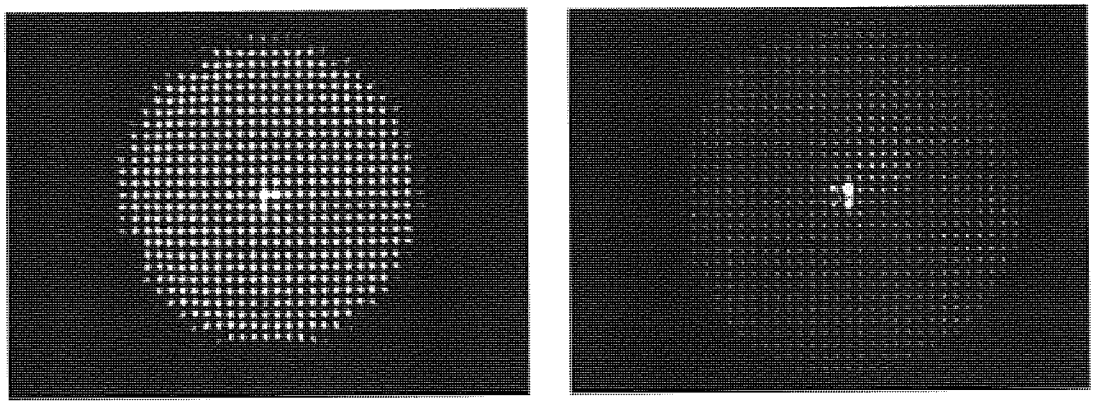

Figure 7.6.- *HS pattern from one of the model eyes used (left) and one of the human eyes examined (right). Note the difference in the exposure of the image. Although both patterns are for different pupil sizes,note that for a given area analyzed, objective measures of scatter using this method are not affected by pupil size (Donnelly and Applegate, 2005).*

Donnelly and Applegate established a criterion to determine the overexposure of HS images (Donnelly and Applegate, 2005). By plotting histograms of pixel intensity they determined the appearance of a third peak of bright pixels near 255 intensity exceeding the 2nd peak (figure 7.7). This third peak is only present in saturated images.

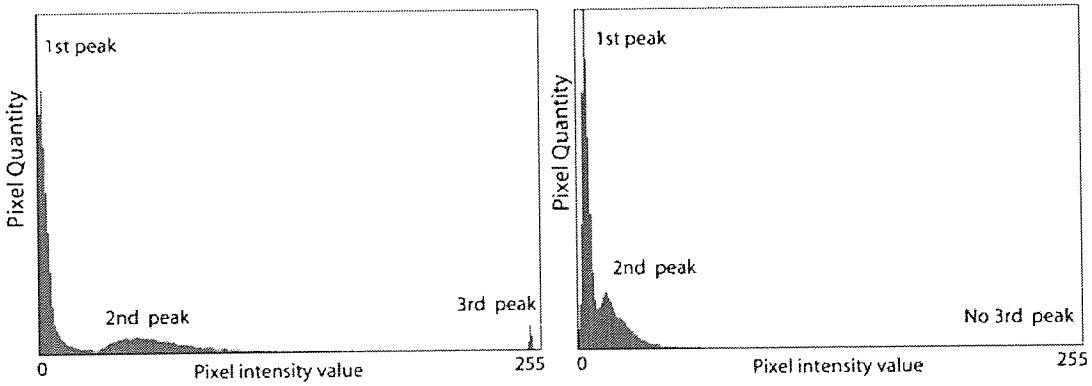

Figure 7.7. *HS image histograms corresponding to a saturated (left) and a non-saturated (right) HS pattern. With saturation, there is a 3rd peak in quantity of bright pixels exceeding the 2nd peak (graphs obtained from Donnelly and Applegate(Donnelly and Applegate, 2005))*

As pointed out by Donnelly and Applegate (Donnelly and Applegate, 2005), and seen in figure 7.6, overexposed images artificially widen the PSF size, affecting therefore the

ability of the image analysis to detect scatter values. This overexposure does not have an effect on wave front sensing. Consequently, the results obtained for intrasession, intersession and effect of realignment and misalignment cannot be fully assessed. Because the aims to use a currently marketed WA to extract scatter values, the exposure of the HS images cannot be controlled by the observer, and therefore further research with a WA optimized for exposure control is needed. HS wavefront sensing is somewhat insensitive to image overexposure whilst very sensitive to underexposure. This is translated into HS patterns being typically overexposed (Donnelly and Applegate, 2005). If the image exposure is optimized, by controlling exposure of the image capture system or by image processing, determination of intraocular scatter would be also be optimized without affecting wavefront analysis. Image processing to optimize image exposure before scatter analysis is an aim for future studies using the software facility presented here.

7.5.II. Human Eye Study

To date there are no published reports addressing both objective and subjective measures of intraocular scatter. Previous studies determining objectively the amount of forward scatter found a correlation between the amount of objective scatter measures and ageing (Shahidi and Yang, 2004), agreeing with previous studies using subjective measures of retinal stray light (Ijspeert et al., 1990; van den Berg, 1995). The methodology used by Shahidi for determining scatter objectively, as described in Chapter 1, has also been applied to diseased eyes (Shahidi et al., 2005).

The importance of the Hartmann-Shack patterns being complete and not degraded by the eyelid or eyelashes is of particular relevance in human studies where there is a wide variety of lid apertures, lash lengths, pupil sizes and other potentially confounding factors. Acquiring multiple images for analysis should help to reduce these effects and it is noteworthy that removal of images with such defects reduced the CoV from 21% to 6% and increased the correlation between subjective and objective scatter values to 69%.

It must be noted however that the differences between objective and subjective methods of scatter measurement are not all attributable to methodology. Objective determination of intraocular scatter is measured under low light conditions in order to achieve a pupil size as large as possible whereas the subjective determination of forward scatter with the compensation comparison method uses a glare source which induces pupil miosis. This difference alone could explain part of the discrepancy between methods since the scatter values obtained objectively are determined for full normal pupil size. Further, subjective stray light measures include the ability of the subject to detect and respond to the stimuli thus introducing a neural component that is absent in the objective method. These differences between the methods provide scope for future novel research work on the subjective implications of optical defects.

This study has shown that it is possible to determine the intraocular forward light scatter in humans *in vivo* using HS patterns. Further, the results obtained in a small healthy human population correlate well with the retinal stray light values obtained with a validated stray light meter. Areas for future work will include evaluation on a larger scale of patient populations who present with a range of diseases in order to establish which diseases might gain clinical benefit. Also of interest is the relationship of intraocular light scatter to visual perception and quality-of-life indexes. Further software development will include automated assessment of image quality such that unsuitable images (e.g. those that are over- or under-exposed, or those with other image artefacts such as eye lid or lash interference) can be automatically detected and excluded. In addition the software tool developed and used in the present study determines scatter for full normal pupil sizes only and future implementations that allow the examiner to choose the pupil area to be analyzed are now being considered. For a given area analyzed, objective measures of scatter using this method has been shown not to be affected by pupil size (Donnelly and Applegate, 2005).

In the next chapter the above methodology will be applied to pseudophakic patients having different types of intraocular implants. With the increasing number of intraocular lens designs in use measures of light scatter will be directly relevant to the efficacy of clinical outcomes, quality-of-life and potential medicolegal scenarios.

CHAPTER 8. OBJECTIVE AND SUBJECTIVE ASSESSMENT OF INTRAOCULAR SCATTER IN EYES WITH MONOFOCAL AND MULTIFOCAL INTRAOCULAR LENSES (IOLS)

8.1. ABSTRACT

Purpose: To determine the differences in assessment of objective and subjective intraocular light scatter in patients with monofocal and multifocal IOLs.

Methods: Residual mean spherical equivalent (MSE) refractive error, contrast sensitivity (CS:9% Bailey-Lovie), subjective retinal stray light and objective scatter were measured in 64 eyes of 40 pseudophakic patients: Group 1 (mean age 71.81±9.20years) treated with monofocal IOLs (n=15 ThinOptix, ThinOptx Inc, n=17 AcriSmart 48S, AcriTec); Group 2 (mean age 65.52±11.97years) treated with multifocal IOLs (n=10 Acrysof ReSTOR, Alcon; n=22 ReZoom, AMO). All investigations were conducted using natural pupil and between 6 months and 1 year after implantation. Equality of variances was tested by Levene's test. ANOVA was used to establish differences between groups; Pearson's analysis assessed the relationship of subjective and objective scatter measures to all other parameters.

Results: Only age was significantly different between groups (mean difference ± CI: 6.292 ± 5.754 years). There were no significant differences in pupil size, contrast sensitivity and MSE between the groups (mean difference ± CI = -0.20 ± 0.22 mm; p=0.383; 0.08 ± 0.08 LogMAR units, p=0.063 and -0.15 ± 0.56 D, 0.601; respectively). Significant trends were found between the retinal stray light values and age (Pearson's coefficient: 0.339; p=0.010), contrast sensitivity (Pearson's coefficient: 0.327; p=0.008), and pupil size (Pearson's coefficient: -0.282; p=0.024) for the whole sample. There was no significant effect of the type of IOL in the retinal stray light values obtained with the C-Quant stray light meter ($F_{1,54} = 3.00$, $p = 0.089$). Mean COV for the objective measures of scatter was 10.1%. No relationship was found between the objective scatter values and age, contrast sensitivity, pupil size or residual MSE for the

whole sample. No significant differences in the objective measures of scatter between the monofocal and the multifocal IOL groups ($F_{1,62}$=0.394) were found. Objective scatter values were significantly correlated with pupil size in the multifocal IOL group (Pearson's coefficient: 0.388; p=0.028). No significant relationship was found between the two methods of determining intraocular light scatter (Pearson's coefficient: 0.134; p=0.290). Multivariate analysis of variance did not show an effect of the type of lens in the values of scatter obtained ($F_{6,118}$=1.183, p=0.320). Independent analysis of each of the scatter variables, using a Bonferroni adjusted alpha level of 0.025, showed that there was no effect of the type of lens on the measures obtained both subjectively ($F_{3,60}$=2.278, p=0.089) and objectively ($F_{3,60}$=96.455, p=0.789).

Conclusions: Patients fitted with monofocal and multifocal IOLs following cataract surgery exhibit similar degrees of perceived (subjective) or actual (objective) light scatter. There is no apparent correlation between subjective and objective light scatter which may suggest that the method devised for the objective determination of intraocular scatter from HS patterns is unreliable..

8.2. INTRODUCTION

Advances in intraocular lens (IOL) design have improved considerably the visual outcomes of cataract surgery. Multifocal IOLs attempt to provide the patient with distance and near vision by increasing the depth-of-field, showing improved optical quality (Javitt and Steinert, 2000) and near vision (Steinert et al., 1992) which further improves with time (Montes-Mico and Alio, 2003). Multifocal IOLs are designed to take advantage of the brain's natural ability to adapt to near and far vision, as the different optical elements of the lens can be used as required, depending on the distance of fixation. For example, when viewing a distant object, a sharp retinal image is provided by those parts of the lens within the pupillary area which have the distance correction and a somewhat blurred image by the other parts of the lens, these images being superimposed on the retina. The unwanted effect of the light in the out-of-focus image is to reduce the contrast of the in-focus image (Artal et al., 1995; Montes-Mico et al., 2004; Navarro et al., 1993).

Much research has been carried out to improve this potential reduction in contrast acuity, for example by directing different amounts of the refracted-diffracted light on the different foci (Jacobi et al., 1999; Ravalico et al., 1998) or by directing different amounts of light to the different foci depending on pupil diameter (Hayashi et al., 2001; Montes-Mico et al., 2004). Despite this, reduced image contrast and unwanted visual phenomena, including glare and halos, have been associated with multifocal IOL performance(Javitt and Steinert, 2000; Kohnen et al., 2006; Lindstrom, 1993; Montes-Mico et al., 2004; Pieh et al., 2001; Pieh, Weghaupt, and Skorpik, 1998; Schmitz et al., 2000; Steinert et al., 1999). Up to now, no information regarding retinal stray light in multifocal IOL patients has been reported as it is a likely source of unwanted visual phenomena associated with these lens designs. Indeed the optical design of multifocal IOLs provides worse optical quality than with monofocal IOLs (Holladay et al., 1990), being highly dependent on pupil size to achieve the desired level of performance (Kawamorita and Uozato, 2005). Therefore, it is expected that some scatter created by multifocal designs would affect the visual performance of patients implanted with these IOLs.

The aims of the study are:

- To evaluate the retinal stray light perceived by patients implanted with multifocal IOLs and compare it with that perceived by patients implanted with monofocal IOLs.
- To determine objectively the intraocular light scatter in patients fitted with monofocal and multifocal IOLs.
- To establish the relationship, if any, between clinically-derived objective and subjective light scatter in patients treated with monofocal and multifocal IOLs.

8.3. MATERIAL AND METHODS

8.3.I. Sample details

Sixty four eyes from 40 pseudophakic patients (25 women, 15 men) were recruited consecutively to the study according to strict inclusion criteria: no ocular disease or post-operative complications; time after surgery between 6 months and 1 year.

The sample was divided into two groups: 1. Those treated with a monofocal lens (mean age 72.65±8.82 years), and 2. Those treated with a multifocal IOL (mean age 65.61±11.60 years). Patients in the monofocal group were implanted by microincision surgery with either the ThinOptx (ThinOptx Inc, 15 eyes) or the Acri.Smart 48S (Acri.Tec, 17 eyes) IOLs. Patients in the multifocal group where implanted with either the diffractive ReSTOR (Alcon Inc., 10 eyes) or the refractive ReZoom (Advanced Medical Optics, 22 eyes) IOLs.

The ThinOptx is a posterior chamber IOL of a hydrophilic acrylic material. The central thickness of the optic is from 350 μm to 450 μm; for a 20.00 D IOL, the central thickness is 450 μm. The lens has a meniscus-shape format. The posterior surface of the lens has a central clear portion (3 mm) which is surrounded by a series of concentric, planar, annular rings of increasing diameter.

The Acri.Smart 48S is a 1 piece foldable acrylic IOL with hydrophobic surfaces and water content of 25% when fully hydrated. It has an optic diameter of 5.5 mm, a spherical design, and an overall size of 11.0 mm. The haptic and optic portions have square truncated edges. The available powers range from plano to +32.0 D. The lens is made from AcriLyc material, a copolymer of hydroxyethylmethacrylate and ethoxymethacrylate and incorporates an ultraviolet absorber. The central thickness of a 23.00 D IOL is 700 μm.

The AcrySof ReSTOR multifocal is an apodized diffractive IOL. The optic consists of a 3.6 mm apodized diffractive region and within this region is a +4.00 D addition that equates to a +3.20 D addition at the spectacle plane. When light passes through the

central portion of the IOL's apodized optic the diffractive steps create light waves that are focused at both a near and a distant point. While the retina is receiving both the near and distance images it is the direction of the patient's attention that determines which image the brain perceives. Surrounding this diffractive area is a refractive area with a distance focal point. With increases in pupil size in low-light conditions, more light energy is sent to the distance focal point.

The ReZoom multifocal IOL is a five-zone, three-piece (hydrophobic acrylic with PMMA haptics) multifocal IOL with an add power of +3.50D at IOL plane (around +2.8D at corneal plane). The five zones correspond to alternating distance-near dominant zones that provide distance and near vision in a range of pupil sizes.

All surgical procedures were performed by the same surgeon (JA). Mean residual spherical equivalent for the monofocal group was -0.99 ± 1.03 D and for the multifocal group was -0.84 ± 1.20 D. Patients were not dilated for any of the procedures.

Table 8.1 shows the descriptive statistics the sample analysed split into two groups depending on the type of lens (monofocal and multifocal). All the values measured were very similar for both monofocal and multifocal eyes.

		MONOFOCAL (n=32)	MULTIFOCAL (n=32)
MSE (D)	Min	-3.64	-5.00
	Max	0.84	0.48
	Mean	-0.99	-0.84
	SD	1.03	1.20
PUPIL SIZE (mm)	Min	2.67	2.45
	Max	5.70	6.00
	Mean	4.59	4.79
	SD	0.84	0.94
AGE (years)	Min	58	45
	Max	86	84
	Mean	71.81	65.52
	SD	9.20	11.97
CONTRAST SENS. (LogMAR)	Min	0.20	0.14
	Max	1.00	1.00
	Mean	0.51	0.43
	SD	0.18	0.16
STRAYLIGHT (Log(s))	Min	0.80	0.75
	Max	1.68	1.72
	Mean	1.24	1.14
	SD	0.24	0.19
SCATTER (Max_SD)	Min	104.00	93.00
	Max	179.00	167.99
	Mean	138.54	135.02
	SD	16.27	16.48

Table 8.1.- *Descriptive statistics for both populations studied.*

Table 8.2 shows the descriptive statistics of the sample divided by IOL lens into four groups (two monofocal and two multifocal). This division will be used for some of the analysis.

		ThinOptx (n=15)	48 S (n=17)	ReZoom (n=10)	ReSTOR (n=22)
MSE (D)	Min	-2.31	-3.64	-3.23	-5.00
	Max	0.15	0.84	-0.44	0.48
	Mean	-0.90	-1.08	-1.49	-0.55
	SD	0.78	1.23	0.75	1.26
PUPIL SIZE (mm)	Min	3.63	2.67	3.80	2.45
	Max	5.70	5.23	6.00	5.78
	Mean	4.95	4.27	5.18	4.60
	SD	0.58	0.91	0.78	0.97
AGE (years)	Min	58	58	56	45
	Max	86	86	80	84
	Mean	71.9	71.7	67.2	64.7
	SD	8.6	10.3	10.9	12.6
CONTRAST SENS. (LogMAR)	Min	0.20	0.26	0.14	0.20
	Max	0.78	1.00	0.70	1.00
	Mean	0.46	0.55	0.45	0.42
	SD	0.16	0.18	0.16	0.17
STRAYLIGHT (Log(s))	Min	0.80	0.85	0.93	0.75
	Max	1.53	1.68	1.72	1.52
	Mean	1.19	1.29	1.20	1.11
	SD	0.22	0.26	0.22	0.17
SCATTER (Max_SD)	Min	104.0	114.0	113.0	93.0
	Max	161.3	179.0	168.0	158.0
	Mean	137.1	139.8	136.5	134.3
	SD	16.9	16.1	16.0	17.0

Table 8.2. *Descriptive statistics for the sample divided by lens implanted.*

8.3.II. Ethical approval

Procedures were approved by the Ethics Committee of VISSUM/Instituto Oftalmologico de Alicante, where the study took place. Informed consent was obtained from all patients after explanation of procedures. All the procedures follow the tenets of the Declaration of Helsinki.

8.3.III. Measurement of contrast sensitivity

Contrast sensitivity was measured uncorrected using the Low contrast (9%) Bailey-Lovie chart for distance under mesopic conditions (0.75 cd/m^2). Mesopic low contrast visual acuity has been shown to correlate well with optical quality measures (Pesudovs et al., 2004) and better than mesopic high contrast or photopic high and low contrast, and therefore was the test of choice for the study. The test was performed for distance (6m), monocular and uncorrected. All the patients had the surgery between 6 and 12 months prior to the measurements, therefore the contrast sensitivity is likely to be at an optimum level according to previous reports (Montes-Mico and Alio, 2003).

8.3.IV. Subjective measurement of retinal stray light

Stray light measurements were made using the C-Quant stray light meter. The system and procedures have been described and evaluated elsewhere (Coppens et al., 2006; Franssen, Coppens, and van den Berg, 2006). Briefly, the system uses what is called as "Compensation Comparison" method, which emerges as a modification of the original "Direct Compensation" method in order to make it more suitable for clinical use on a large scale. The method consists of a series of concentric rings. The smallest ring in divided into two halves and represents the test field. The patient is asked to look at the test field while a concentric ring flickers with varying intensity and frequency; this concentric ring represents the stray light source. The flickering in the stray light source induces a certain amount of perceived flickering in the test field. The patient is asked to compare both halves of the test field, one of which has some counterphase flickering added, and indicate which side flickers strongest by pressing a button. The distribution

of right and wrong answers is used to define a psychometric function from which the stray light value is obtained.

Evaluation of the technique has been shown to be very repeatable and reliable (Coppens et al., 2006; Franssen, Coppens, and van den Berg, 2006) with typical SDs around 0.07 log units(Franssen, Coppens, and van den Berg, 2006) and following the results reported in chapter 6 a mean of 3 repeated measures is suggested as the optimum for reliability of the values obtained.

8.3.V. Objective measurement of intraocular scatter

Objective assessments of intraocular light scatter were derived using the methodology described in chapter 7, based on work previously published by Donnelly and collaborators (Donnelly et al., 2004) using an analysis of Hartmann-Shack patterns in order to extract forward light scatter values from the centroids. The metric used is the maximum standard deviation (Max_SD) (see Chapter 6 for a full description of the methodology). Due to the results obtained in the validation study reported in chapter 6 where 40% of the HS patterns had to be removed from the sample due to problem with the image analysis and poor reliability of the results obtained, a minimum of two valid HS patterns were obtained for each patient and, therefore, none of the subjects examined had to be excluded.

8.3.VI. Data analysis

Independent samples t-test (SPSS v.12.0.1; SPSS Inc.) were used to compare the values obtained between the two samples. Pearson's correlation coefficients were used as a measure of correlation after Levene's test for equality of variances. Multivariate ANOVA was used to determine the impact of the type of IOL on the subjective and objective values of scatter obtained.

8.4. RESULTS

Equality of variances was tested by Levene's test. Only age was significantly different between groups, monofocal and multifocal IOL (mean difference ± CI: 6.292 ± 5.754 years). There were no significant differences in pupil size, contrast sensitivity and MSE between the groups (mean difference ± CI = -0.20 ± 0.22 mm; p=0.383; 0.08 ± 0.08 LogMAR units, p=0.063 and -0.15 ± 0.56 D, 0.601; respectively).

Correlation analysis showed a significant negative trend between contrast sensitivity and MSE (Pearson's correlation coefficient: -0.316; p=0.011) (figure 8.1).

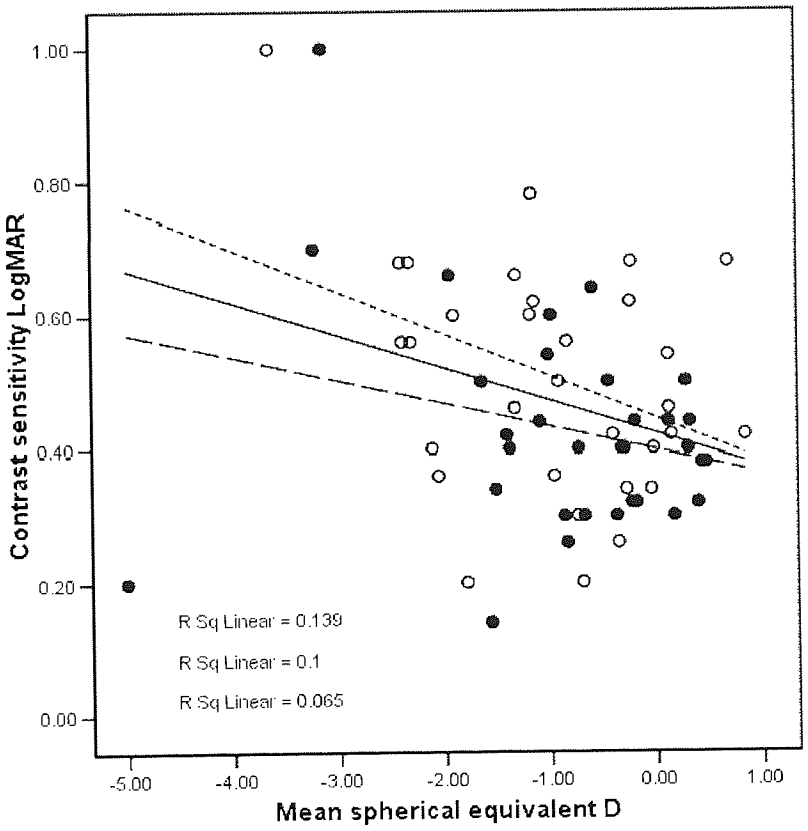

Figure 8.1.- *Correlation plot of contrast sensitivity values against residual MSE. Empty bins and the dotted line represent data for monofocal IOLs and full bins and dashed line data for multifocal IOLs.*

8.4.I. Subjective measurement of retinal straylight

Mean COV of the retinal stray light values obtained for the whole sample was 4.6%. Significant trends were found between the retinal stray light values and age (Pearson's coefficient: 0.339; p=0.010), contrast sensitivity (Pearson's coefficient: 0.327; p=0.008) (figure 8.2), and pupil size (Pearson's coefficient: -0.282; p=0.024) for the whole sample.

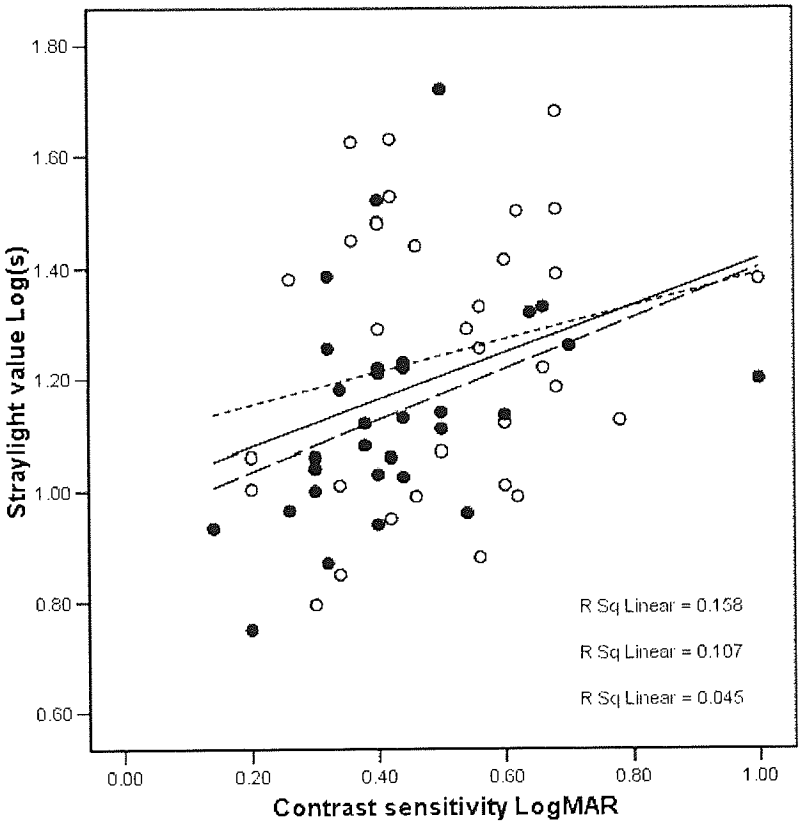

Figure 8.2.- *Correlation plot of retinal stray light values against contrast sensitivity LogMAR values for both types of patients: those with monofocal IOLs (empty bins, dotted line) and those with multifocal IOLs (full bins, dashed line)*

Figure 8.3. shows the relationship between stray light values obtained and subjects age for both types of IOL (monofocal and multifocal). Analysis of covariance (ANCOVA) showed that there was no significant effect of the type of IOL on the retinal stray light values obtained with the C-Quant stray light meter ($F_{1,54} = 3.00$, $p = 0.089$). Adjusted

mean scores suggest that although not significantly different, stray light values in the monofocal group were slightly higher than with the multifocal group.

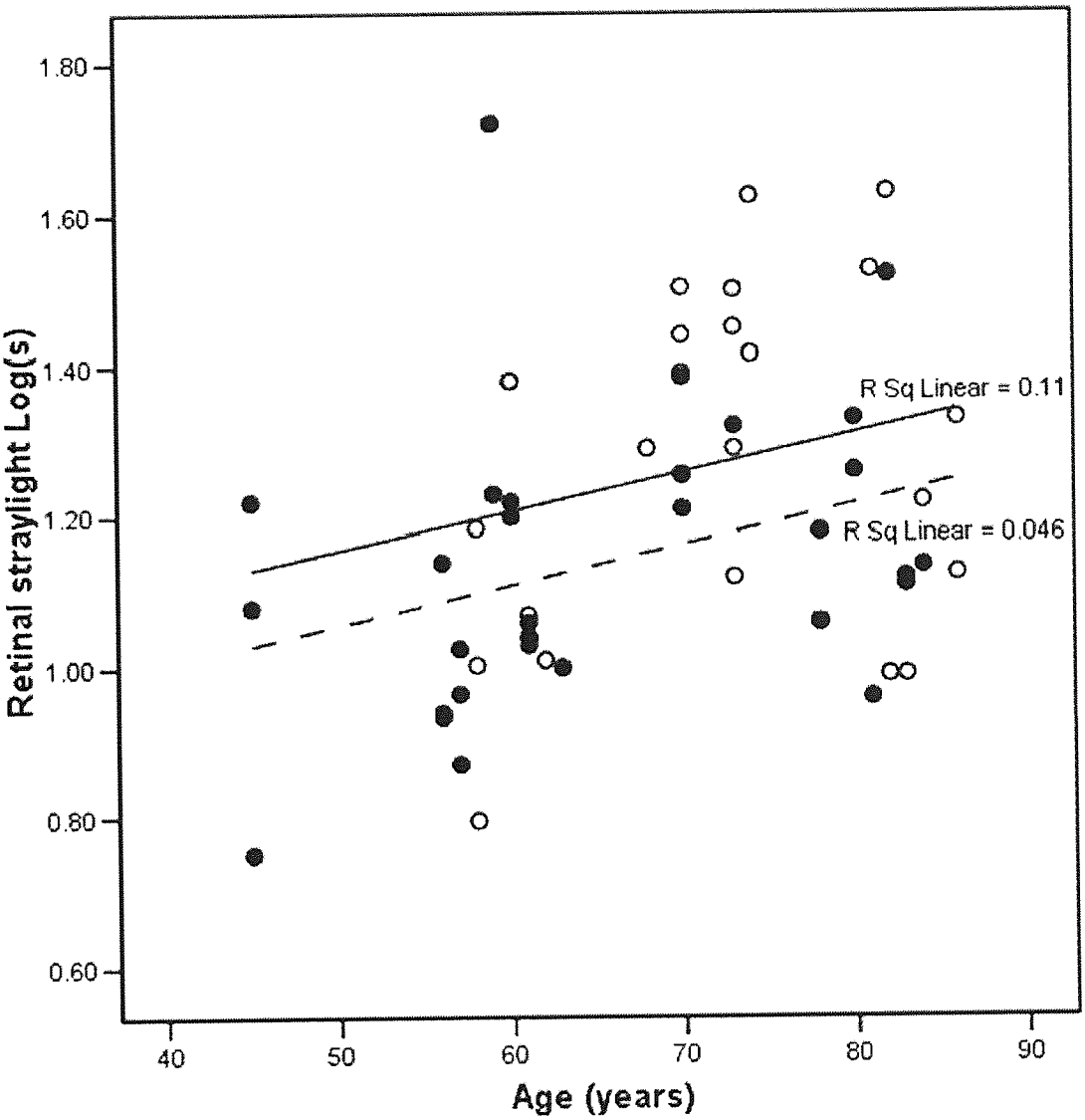

Figure 8.3. *Retinal stray light values and regression lines obtained in those subjects with monofcal (empty bins, solid line) and multifocal IOLs (full bins, dashed line).*

For the eyes with a monofocal IOL, stray light values were significantly correlated with pupil size (Pearson's coefficient: -0.377; p=0.033). For the eyes with a multifocal IOL this correlation was not significant (Pearson's coefficient:-0.145; p=0.427) although a significant correlation was found between stray light values and contrast sensitivity (Pearson's coefficient: 0.397; p=0.024) it was not significant for the monofocal group (Pearson's coefficient: 0.211; p=0.246).

Performing the analysis by specific type of IOL (ThinOptx, 48S, Rexoom or ReSTOR) an ANCOVA controlling for age differences showed no significant differences in retinal stray light ($F_{3,52}$=2.50, p=0.069). Adjusted mean scores suggest that although differences were not significant, ordered from lowest to highest stray light scores, the least stray light was perceived by patients with ReSTOR, followed by ThinOptx, Rezoom and 48S (figure 8.4).

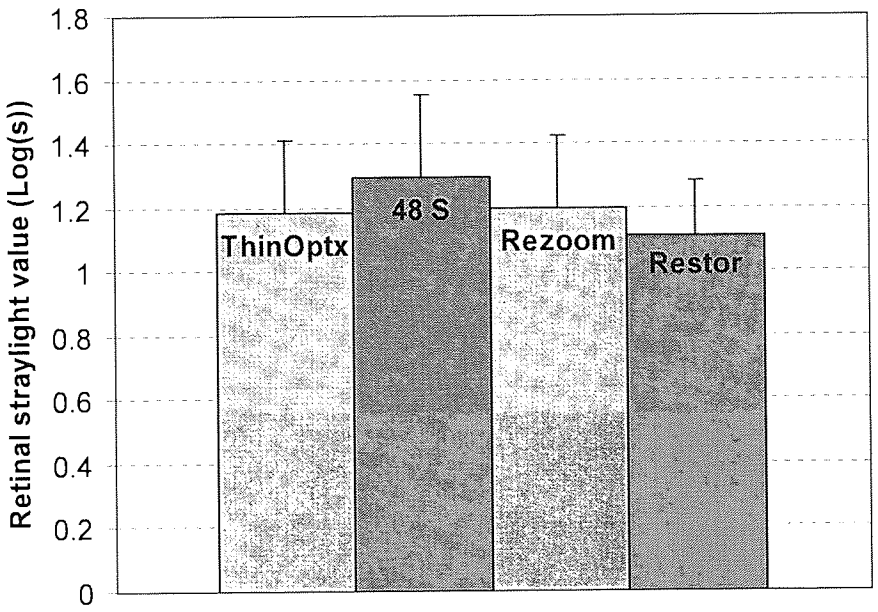

Figure 8.4. *Histogram representing the mean (error bars represent 1SD) of the retinal straylight values (Log(s)) for each of the IOL groups. There were no significant differences between groups.*

8.4.II. Objective measurement of intraocular scatter

Mean CoV for the objective measures of scatter was 10.1%.

No relationship was found between the objective scatter values and age, contrast sensitivity, pupil size or residual MSE for the whole sample.

Univariate analysis of variance (ANOVA) showed no statistically significant differences in the objective measures of scatter between the monofocal and the multifocal IOL groups ($F_{1,62}$=0.394) (see Appendix I for tables).

For the monofocal IOL group, objective scatter values were not significantly correlated with any of the parameters measured. However, objective scatter values were significantly correlated with pupil size in the multifocal IOL group (Pearson's coefficient: 0.388; p=0.028).

Univariate ANOVA for the specific type of lens (ThinOptx, 48S, Rezoom, ReSTOR) did not show significant differences between the objective scores obtained with any type of IOL.(F3,60=0.350, p=0.789). Adjusted mean scores suggest slightly lower scatter i.e. higher Max_SD values) in the subjects implanted with the 48S IOL and slightly higher scatter values in those implanted with the ReSTOR (figure 8.5).

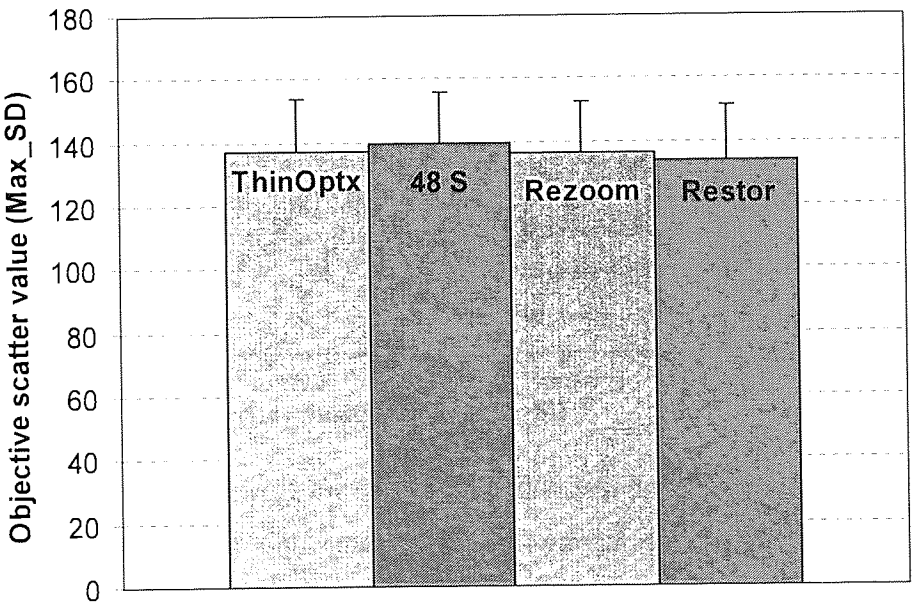

Figure. 8.5. *Histogram representing the mean (error bars represent 1SD) of the objective scatter value (Max_SD) for each of the IOL groups.*

7.4.III. Objective Vs. Subjective measurement of intraocular scatter

No significant relationship was found between the two methods of determining intraocular light scatter for the whole sample (Pearson's coefficient: 0.134; p=0.290) (figure 8.6). In addition, neither was significant for each of the groups when treated separately (Pearson coefficient: 0.069, p=0.707 for the monofocal group; and 0.171, p=0.350 for the multifocal group).

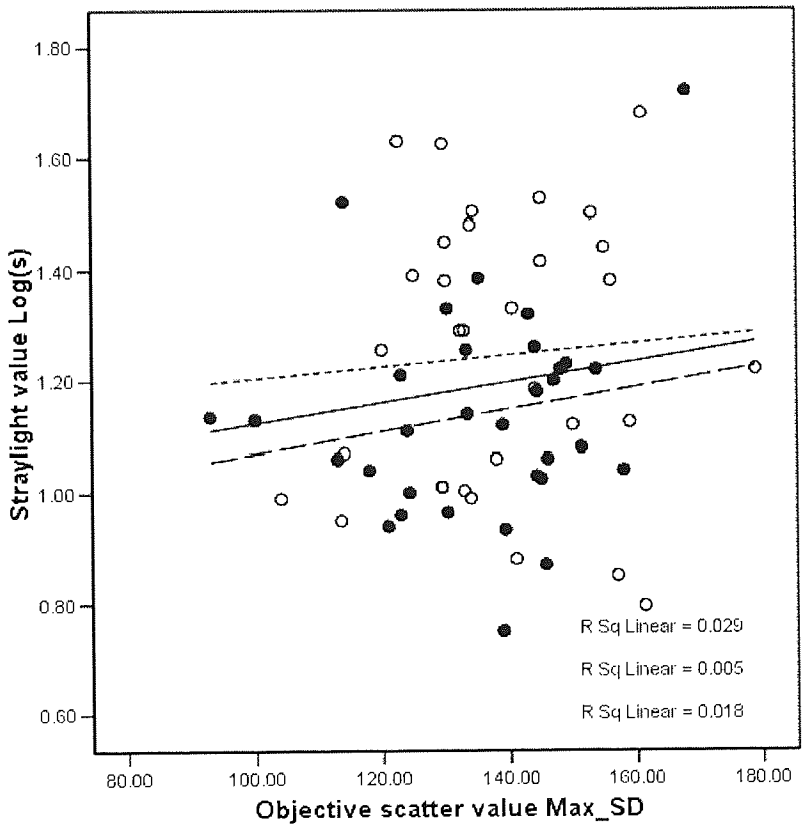

Figure 8.6. *Scatterplot showing the relationship between both the subjective (Stray light value) and objective (Max_SD) methods of determination of intraocular scatter. The solid line represents the regression line for the whole sample. Empty bins and dotted line represent monofocal IOLs, full bins and dashed line represent multifocal IOLs.*

Multivariate analysis of variance did not show a significant effect of the type of lens on the values of scatter obtained ($F_{6,118}$=1.183, p=0.320, Wilk's Lambda=0.890, partial Eta squared=0.057). Independent analysis of each of the scatter variables, using a Bonferroni adjusted alpha level of 0.025, showed that there was no effect of the type of lens on the measures obtained both subjectively ($F_{3,60}$=2.278, p=0.089) and objectively ($F_{3,60}$=96.455, p=0.789).

8.5. DISCUSSION

The results obtained in this study do not show significant differences in objective or subjective measures of intraocular scatter between subjects implanted with multifocal and monofocal IOLs. Furthermore, a relationship between subjective and objective measurement of scatter could not be demonstrated.

Measurement of retinal stray light with the direct compensation method has been shown to be a useful method of determining a measure of forward intraocular scatter in cataract (de Waard et al., 1992; Meacock et al., 2003), corneal dystrophies(van den Berg, Hwan, and Delleman, 1993) retinal disease(Alexander, Fishman, and Derlacki, 1996; Grover et al., 1998; Grover et al., 2002) as well as the effects of ocular lubricants(Veraart and van den Berg, 1992), laser refractive therapy(Harrison et al., 1995; Veraart et al., 1993; Veraart et al., 1995) and radial keratotomy(Veraart et al., 1992).

In a previous study, Alió et al. reported an excellent retinal image quality following implantation of both the monofocal lenses used in the present study (Alio et al., 2005b). Outcomes of Acri.Smart 48S IOL have also been reported as safe and predictable (Alio et al., 2005a).

Previous studies comparing visual outcomes between monofocal and multifocal diffractive IOLs found no significant difference in distance high contrast visual acuity. Montés-Micó and Alió reported an increase in contrast sensitivity with time after implantation of multifocal IOLs that stabilized at 3 to 6 months post-operatively (Montes-Mico and Alio, 2003). They also found lower contrast sensitivity for the eyes with multifocal IOLs compared to those with monofocal IOLs at 1 month post-

operation. However at three months post-operation the reduction was only significant for high spatial frequencies. Contrast sensitivity at low spatial frequencies (i.e.1.5 and 3 cpd) has been shown to be affected primarily by light scatter, whereas contrast sensitivity at higher spatial frequencies is degraded by optical blur (i.e. defocus and optical aberrations)(Montes-Mico and Charman, 2001). The results of the present study showed no significant differences between monofocal and multifocal contrast sensitivity (mean difference=0.08±0.08 logMAR units, p=0.063) and the existing differences should be attributed more to the slight difference in age rather than to the IOL type which might explain why the multifocal values were lower, contrary to what has been previously reported.

Theoretical predictions suggest that multifocal IOLs would induce more scatter than monofocal IOLs(Holladay et al., 1990). In a previous study, Dick et al. found no differences in contrast sensitivity between monofocal and multifocal IOL patients but found that halo size was bigger for patients over 70 years old in the multifocal group(Dick et al., 1999) concluding that not only IOL design, but also age and corneal surface quality have an important role in determining scatter values.

The results obtained in the present study show that the type of intraocular lens accounts for only 5% of the variance in intraocular scatter values obtained with these methods, agreeing with the results reported by Dick (Dick et al., 1999). There are no significant differences between the retinal stray light values as perceived by patients with monofocal and multifocal IOLs. Objective measurements of intraocular scatter with the HS analyzer also failed to show significant differences between monofocal and multifocal IOLs. This result was unexpected since although a good and similar response in the perceived straylight values might have been expected, the objective measurement of scatter should be different between the groups due to the monofocal and multifocal design of the lenses. This suggests that the methodology developed for the objective determination of intraocular light scatter from HS patterns obtained from commercial wavefront analysers is not reliable and must be improved further.

All the measurements of scatter were taken through natural pupils in order to test the correlation between subjective and objective measures of scatter and also to assess the

role of pupil size, i.e., correlation between pupil size and scatter. Pupil size has been found to correlate significantly with the values of perceived retinal stray light for the whole sample. Subjective measurement of stray light using the C-Quant is performed under photopic conditions; therefore, the significance of the relationship of the values obtained with the subject's pupil size is not immediately clear. Pupil size did correlate significantly with perceived retinal stray light values when eyes with monofocal IOL were analyzed separately and it also correlated significantly with the Max_SD values of objective forward scatter when the multifocal IOL group was analyzed separately. As expected, those eyes exhibiting higher values of scatter had the smaller pupil sizes, suggesting that pupil plays an important role in optimizing the quality of the retinal image under conditions of diminished optical quality. Further studies evaluating objectively the amount of scatter controlling for pupil size would be desirable.

It was also surprising to find that the multifocal IOLs used were not significantly different in terms of both objective and subjective scatter values. The fact that no differences were found in the perceived stray light values implies that the retinal process of adaptation may have an effect on the perception of the effects of scatter. Further research to investigate this hypothesis is, therefore, of interest.

The results reported here suggest that the differences found between both methods of scatter determination could occur for several reasons:

1. The methodology used to determine objectively the amount of intraocular scatter is not sensitive enough for the fine detection of variations in scatter. Donnelly et al. first used this methodology and concluded that up to 51% of the variance in visual acuity can be accounted for by combining backscatter and forward scatter metrics. However, they also state that the forward scatter metrics contribute approximately the same as backscatter metrics for predicting the variance in visual acuity in patients over 60 years old, whereas for younger patients back scatter metrics are dominant for explaining the variance (Donnelly et al., 2004). This metric was also found to be well correlated to cataract severity (Donnelly and Applegate, 2005). The HS sensor used by them was custom designed, whereas a commercial WA was used in the present study. The limitations of camera resolution and lack of control of

exposure times contribute to the limitations of the application developed. Applying the methodology used here after improvements in the software tool to control for image exposure is an interesting field for future study.

2. As mentioned earlier, subjective measures of scatter were determined under photopic conditions whereas the objective measures of scatter where determined under mesopic conditions and analyzing full pupil area. This means that in some subjects pupillary mydriasis meant that a larger peripheral area was included into the HS patterns and hence more scatter could be induced due to transition zones within the IOL (figure 8.7). A further improvement being considered in the software tool is the capability of analyzing a certain pupil area, user-defined and independent of pupil size. Since the amount of scatter measured objectively using this technique for a certain area within the pupil is not dependent of the full pupil size(Donnelly and Applegate, 2005) this would be a useful feature to apply in all further work.

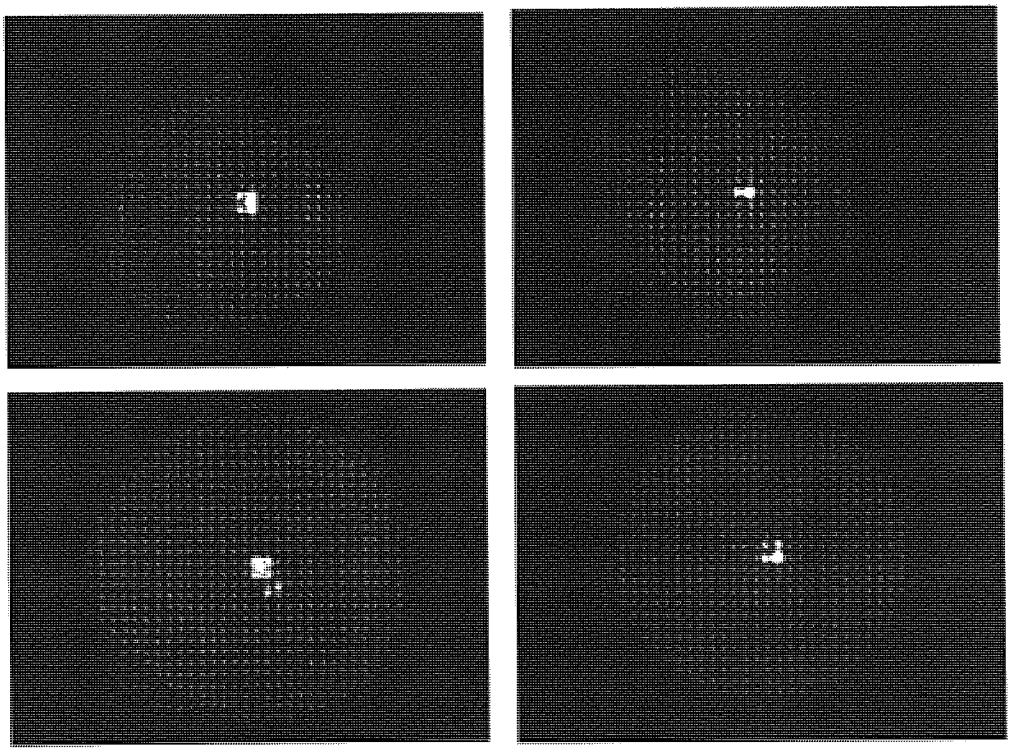

Figure 8.7. *Examples of HS patterns obtained in subjects with pupil sizes greater than 5mm under scotopic conditions. Note the transition zones visible in ThinOptx (upper*

left), 48S (upper right) and Rezoom (lower left). ReSTOR (lower right) does not have transition zones due to its diffractive design.

Despite the limitations of the methodology used here, as discussed in chapter 6, the mean COV of the scatter readings was acceptable. The results obtained in the validation study reported in chapter 7, where 40% of the HS patterns had to be removed from the sample due to the problem with image analysis and poor reliability of the results obtained, were taken into account here and, out of the three HS patterns obtained for each subject, a minimum of two were considered valid for analysis and, therefore, none of the subjects examined had to be excluded. The results reported in this study suggest the possibility of using HS analysis for the determination of scatter with commercial systems. Improvements such as control of exposure and/or optimization of the image for analysis, as well as better resolution of the cameras would be, however, desirable to obtain a reliable instrument for the simultaneous acquisition of wavefront aberrations and intraocular scatter.

8.6. CONCLUSIONS

There are several conclusions that can be reached from the results obtained in this study:

- The perceived effect of intraocular scatter induced by the design of the multifocal IOLs seems to be negligible given the similar response obtained from both groups to retinal stray light.

- Pupil plays a crucial role in optimizing the quality of the retinal image by decreasing its size in eyes with relatively worse optical quality for the same illumination levels.

- For patients with intraocular lenses, the methodology developed to determine objectively the value of intraocular scatter does not correlate well with the perceived retinal stray light. Whereas this would be expected to some extent, the results might suggest that the methodology is not sensitive enough to detect subclinical differences in intraocular scatter. Further studies controlling for the exposure of the HS image should improve the reliability of the outcomes, as reported by Donnelly and Applegate (Donnelly and Applegate, 2005).

- The results reported here provide a wide range of opportunities for the study of intraocular scatter in the human eye and associated aspects of visual performance.

CHAPTER 9. CONCLUSIONS

The research presented in this thesis examined the validity, optimisation and potential applications of clinically derived measures of higher order aberrations and subjective and objective light scatter in the human eye *in vivo* and their impact on retinal image quality.

9.1. Conclusions and applications

The proposed scheme of investigations for this thesis as described in the research rationale (chapter 2), identified two key areas of study as being of importance in defining retinal image quality: wavefront aberrations and intraocular scatter. This is far from an exhaustive list, there being many more fundamental aspects of ocular anatomy, physiology and pathology that will define retinal image quality, however exploration into these two areas of investigation perhaps marks a new era in ophthalmic investigation and management, and even in terms of patient expectation.

The past decade has seen an exponential growth in surgical intervention of eyes previously considered healthy, normal or even untreatable, that is to say, eyes with a refractive defect that are otherwise completely normal. Historically, in a discipline that reserved intervention largely for patients with deteriorating, damaged or threatened vision and visual acuity, patient and practitioner expectations were tempered by the need to preserve or restore vision. With refractive surgery now one of the world's leading choices for elective surgery, the need for highly accurate treatments with near perfect results in demanding patients, has paved the way for a host of new diagnostic technologies to improve the treatment modalities and interpretation of outcomes. Such technologies have applications in a host of other diseases or treatments, from uveitis to contact lens wear. Of these relatively new clinical tools, wavefront aberrometry, though still not well understood in clinical settings, has received much attention, while intraocular light scatter is less well explored and offers great potential importance in

understanding outcomes. The validation, optimisation and applications of these two investigative techniques has been the subject of this work.

9.1.I. Wavefront aberrations

1. Clinical wavefront analysers provide data that is very repeatable and reproducible. Despite this repeatability, the variability of the results is influenced by the operation of the instrument by the observer, which in this case increased by a factor of 3, although repeatability remains excellent. These findings were consistent with those of a previous study which demonstrated good repeatability, low variability and measures that were robust to axial and lateral misalignments (Cheng, Himebaugh et al. 2003). A particular feature of the methodology was to assess the impact of the type of operator errors that might be induced during normal clinical evaluation, that is, the clinician performing a normal realignment between measurements (combination of small axial and lateral misalignments), and with a small fixation error from the patient (angular misalignment of six degrees of the model eye). It is of interest that there is a substantial increase in the variability of measures acquired during the session in which the system was realigned after each measurement. This increase accounts for small differences in lateral and axial misalignments that occur between the measurements and are highly dependent on how capable the observer is in finding the correct focusing plane. The mean standard deviation did not vary widely with increasing numbers of readings in model eyes, suggesting that the reported variation in repeated measures associated with data from human eyes (Davies, Diaz-Santana et al. 2003), is most likely associated with a physiological variation in human WFEs over time. It is possible that any such variability is related to the ocular pulse, and pulse synchronisation of data acquisition may need to be considered to improve clinical wavefront measures in future iterations of the technology.

2. Angular misalignment does, however, influence the final readings significantly, mainly for the off-axis aberration, pointing out the importance of ensuring a proper fixation from the patient. The results show that, perhaps expectedly, the vertical component of coma were significantly affected by misalignment suggesting that they may be more sensitive to misalignment in the clinical setting. The extent of any

error will of course depend on the degree to which an eye is aberrated, and importantly, since the model eye utilised a spherical model for the cornea, it is possible that the aspheric nature of the human eye will result in further errors in a human system. Therefore, variations in horizontal coma and spherical aberrations may also be expected when measuring a misaligned human eye with respect to the values obtained when aligned. This should be a subject for future study.

3. Use of clinical wavefront analyzers without a cholinergic agent to control pupil size and accommodation means that clinicians must be extra-careful since instrument myopia may occur. On average, the amount of instrument myopia was found to be around 0.30 D, but it could reach much higher values. This phenomenon is more likely to occur as the baseline level of myopia of the patient decreases. The impact of instrument myopia on the final aberration readings may be significant even for intermediate levels of accommodation.

4. Wavefront analysis provided different patterns for Asian and Caucasian subjects, suggesting that ethnic differences may be present and, in fact, these differences may play a role in the prevalence of refractive error among ethnic groups. Spherical aberration was significantly higher on Caucasian eyes compared to Asian.

9.1.II. Intraocular scatter

The advent of refractive surgery procedures and the increasing range of applications of retinal image quality assessment have increased substantially the interest on methods for determining clinically parameters to describe it. Up to now, there were no clinical methods for determine objectively the amount of intraocular scatter. There are a wide range of so called glare testers, and now clinical straylightmeters provide a measure of the response to intraocular scatter (reviewed in chapter 1). Successful approaches have been made to obtaining objective measures of scatter with customized devices in laboratory and clinical settings(Donnelly, Pesudovs et al. 2004; Shahidi, Yang et al. 2005)

As a result of the different studies described, the following conclusions can be reached:

5. Measurement of retinal straylight using the C-Quant straylightmeter has been shown to be reliable previously in the literature. In this thesis, the response curve to repeated measurements of retinal straylight has been shown, concluding that there is a curve that increases the variability of the results as the number of repeated measures increased. A balance between the number of measurements and the reliability of the subjective response from the subject (due to tireness from the test) must be met and, therefore, 2-3 measurements are suggested as the optimum num\ber to maximize the reliability.

6. The application of this methodology to the study of the effect of tint on spectral lenses for contrast enhancement reveals that the subjective response with the tinted contact lenses on gives higher straylight values than that from a clear lens of the same parameters. The difference was not significant for the amber tinted lens, but it reached significance for the grey/green lens.

7. Based on previous studies from Donelly et al, a software tool was developed to apply the methodology to images obtained from a commercial clinical WA in order to extract objective values of intraocular scatter. Repeatability of the measurements on model eyes was very high, as well as reproducibility. The influence of operator realignment and angular misalignment was minimal. The images obtained from the model eyes were overexposed and, therefore, the results obtained must be interpreted with caution. Repeatability on human eyes was very high too, COV lower than 10%, and however the system needs complete HS patterns for analysis (no shadows from eyelashes or eyelids...). On a small sample of healthy human eyes, the objective scatter values correlated very well with subjective scatter values.

8. Applying the methodology described in 6 and 7 to monofocal and multifocal IOLs, it could be seen that the subjective values of retinal straylight obtained from both groups were not significantly different. The reasons for this lack of correlation would be:

- Adaptation to blur for the patients, so that the response is similar regardless the type of IOL design implanted, whereas different designs imply different light scatter. Theory says that multifocal IOLs should give more scattered light.

- Aging implies changes not only in the optical path, but also in the neural path, therefore it should be expected that subjective and objective measures of scatter differ more as age increases.

This thesis has shown that the performance of wavefront analysers can be improved and that clinical HS devices have a great potential of providing much more information from the same amount of data they already obtain. Further, using a HS wavefront analyzer it has been shown that there are ethnic differences in the wavefront aberration patterns of young adults, and that, in pseudophakic older subjects, subjective and objective measures of scatter do not seem to be related possibly due to a neural factor.

9.2. Future research

Future work currently being carried out includes:

- A long-term study evaluating retinal image quality, visual performance, macroscopic and microscopic structural changes and quality of life measures following laser refractive surgery.

- Objective and subjective measures of intraocular scatter applying the methodologies described here, as well as wavefront aberrations taking into account the findings reported here will be obtained and followed during a 6 years post-surgery period.

- Further studies on the differences in aberrometric patterns between ethnic groups over much larger samples and involving more than two ethnic groups. These studies would be of major interest if developed alongside epidemiological studies on the onset and progression of refractive defects.

- The objective methodology for the determination of intraocular scatter evaluated here will also be further researched in order to optimise the results obtained, first by improving and standardizing the image analyzed, and then by improving the software tool for image analysis and by applying the methodology to reference systems of known optical properties. Evaluation in larger scale patient populations across a range of diseases in order to establish those diseases in which such measures provide clinical value, and the relationship of intraocular light scatter to visual perception and quality of life. Further work to develop the software approach will include automated image quality assessments such that unsuitable images (eg those that are over or under exposed, or those with other image artefacts such as from eye lid or lash interference) can be automatically detected and excluded. Also, the software tool developed and used in the present study determines scatter for full pupil size only, and future implementations where the examiner may choose the pupil area to be analysed are now being considered.

- After further evaluations of the determination of intraocular scatter objectively, this will be assessed on a numerous range of types of refractive correction, from contact lenses to surgical procedures, and compared to the visual outcomes and straylight perception. Further research on the hypothesis of retinal adaptation to increased scatter values with certain correction types will also be pursued.

REFERENCES

Aghaian, E., Choe, J. E., Lin, S., and Stamper, R. L. (2004). Central corneal thickness of Caucasians, Chinese, Hispanics, Filipinos, African Americans, and Japanese in a glaucoma clinic. *Ophthalmology* **111**(12), 2211-9.

Alexander, K. R., Fishman, G. A., and Derlacki, D. J. (1996). Intraocular light scatter in patients with retinitis pigmentosa. *Vision Res* **36**(22), 3703-9.

Alio, J. L., Rodriguez-Prats, J. L., Vianello, A., and Galal, A. (2005a). Visual outcome of microincision cataract surgery with implantation of an Acri.Smart lens. *J Cataract Refract Surg* **31**(8), 1549-56.

Alio, J. L., Schimchak, P., Montes-Mico, R., and Galal, A. (2005b). Retinal image quality after microincision intraocular lens implantation. *J Cataract Refract Surg* **31**(8), 1557-60.

Applegate, R. A., and Howland, H. C. (1997). Refractive surgery, optical aberrations, and visual performance. *J Refract Surg* **13**(3), 295-9.

Applegate, R. A., Ballentine, C., Gross, H., Sarver, E. J., and Sarver, C. A. (2003a). Visual acuity as a function of Zernike mode and level of root mean square error. *Optom Vis Sci* **80**(2), 97-105.

Applegate, R. A., Marsack, J. D., Ramos, R., and Sarver, E. J. (2003b). Interaction between aberrations to improve or reduce visual performance. *J Cataract Refract Surg* **29**(8), 1487-95.

Applegate, R. A., Sarver, E. J., and Khemsara, V. (2002). Are all aberrations equal? *J Refract Surg* **18**(5), S556-62.

Arbelaez, M. C. (2001). Super vision: dream or reality. *J Refract Surg* **17**(2 Suppl), S211-8.

Argento, C., Cosentino, M. J., Tytiun, A., Rapetti, G., and Zarate, J. (2001). Corneal ectasia after laser in situ keratomileusis. *J Cataract Refract Surg* **27**(9), 1440-8.

Artal, P., Fernandez, E. J., and Manzanera, S. (2002). Are optical aberrations during accommodation a significant problem for refractive surgery? *J Refract Surg* **18**(5), S563-6.

Artal, P., Guirao, A., Berrio, E., and Williams, D. R. (2001). Compensation of corneal aberrations by the internal optics in the human eye. *J Vis* **1**(1), 1-8.

Artal, P., Marcos, S., Navarro, R., Miranda, I., and Ferro, M. (1995). Through focus image quality of eyes implanted with monofocal and multifocal intraocular lenses. *Optical Eng* **34**, 772-9.

Artal, P., Santamaria, J., and Bescos, J. (1988a). Phase-transfer function of the human eye and its influence on point-spread function and wave aberration. *J Opt Soc Am A* **5**(10), 1791-5.

Artal, P., Santamaria, J., and Bescos, J. (1988b). Retrieval of wave aberration of human eyes from actual point-spread-function data. *J Opt Soc Am A* **5**(8), 1201-6.

Aslam, T. M., and Patton, N. (2004). Methods of assessment of patients for Nd:YAG laser capsulotomy that correlate with final visual improvement. *BMC Ophthalmol* **4**, 13.

Atchison, D. A. (2003). Comparison of peripheral refractions determined by different instruments. *Optom Vis Sci* **80**(9), 655-60.

Atchison, D. A. (2004). Recent advances in representation of monochromatic aberrations of human eyes. *Clin Exp Optom* **87**(3), 138-48.

Atchison, D. A., Collins, M. J., Wildsoet, C. F., Christensen, J., and Waterworth, M. D. (1995). Measurement of monochromatic ocular aberrations of human eyes as a function of accommodation by the Howland aberroscope technique. *Vision Res* **35**(3), 313-23.

Babizhayev, M. A. (2003). Glare disability and driving safety. *Ophthalmic Res* **35**(1), 19-25.

Babizhayev, M. A., Deyev, A. I., Yermakova, V. N., Davydova, N. G., Kurysheva, N. I., Doroshenko, V. S., and Zhukotskii, A. V. (2003). Image analysis and glare sensitivity in human age-related cataracts. *Clin Exp Optom* **86**(3), 157-72.

Barry, J. C., Dunne, M., and Kirschkamp, T. (2001). Phakometric measurement of ocular surface radius of curvature and alignment: evaluation of method with physical model eyes. *Ophthalmic Physiol Opt* **21**(6), 450-60.

Bartmann, M., and Schaeffel, F. (1994). A simple mechanism for emmetropization without cues from accommodation or colour. *Vision Res* **34**(7), 873-6.

Bencic, G., Zoric-Geber, M., Saric, D., Corak, M., and Mandic, Z. (2005). Clinical importance of the lens opacities classification system III (LOCS III) in phacoemulsification. *Coll Antropol* **29**(Suppl 1), 91-94.

Bettelheim, F. A., and Ali, S. (1985). Light scattering of normal human lens. III. Relationship between forward and back scatter of whole excised lenses. *Exp Eye Res* **41**(1), 1-9.

Bland, J. M., and Altman, D. G. (1986). Statistical methods for assessing agreement between two methods of clinical measurement. *Lancet* **1**(8476), 307-10.

Bohren, C. (1995). Scattering by particles. 2nd ed. *In* "Handbook of Optics" (O. S. o. America, ed.), pp. 6-19. McGraw-Hill, New York.

Brunette, I., Bueno, J. M., Parent, M., Hamam, H., and Simonet, P. (2003). Monochromatic aberrations as a function of age, from childhood to advanced age. *Invest Ophthalmol Vis Sci* **44**(12), 5438-46.

Buehren, T., and Collins, M. J. (2005). Accommodation stimulus-response function and retinal image quality. *Vision Res* **46**, 1633-45.

Bueno, J. M., Berrio, E., and Artal, P. (2003). Aberro-polariscope for the human eye. *Opt Lett* **28**(14), 1209-11.

Bueno, J. M., Berrio, E., Ozolinsh, M., and Artal, P. (2004). Degree of polarization as an objective method of estimating scattering. *J Opt Soc Am A Opt Image Sci Vis* **21**(7), 1316-21.

Bullimore, M. A., Fusaro, R. E., and Adams, C. W. (1998). The repeatability of automated and clinician refraction. *Optom Vis Sci* **75**(8), 617-22.

Burns, S. A. (2000). The spatially resolved refractometer. *J Refract Surg* **16**(5), S566-9.

Buscemi, P. (2004). Retinoscope double pass aberrometry: principles and application of the Nidek OPD-Scan. *In* "Wavefront customized visual correction: the quest for super vision II" (A. R. Krueger RR, MacRae SM, ed.), pp. 149-153. Slack Incorporated, Thorofare.

Calver, R. I., Cox, M. J., and Elliott, D. B. (1999). Effect of aging on the monochromatic aberrations of the human eye. *J Opt Soc Am A Opt Image Sci Vis* **16**(9), 2069-78.

Campbell, F. W., and Green, D. G. (1965). Optical and retinal factors affecting visual resolution. *J Physiol* **181**(3), 576-93.

Carkeet, A., Luo, H. D., Tong, L., Saw, S. M., and Tan, D. T. (2002). Refractive error and monochromatic aberrations in Singaporean children. *Vision Res* **42**(14), 1809-24.

Carkeet, A., Velaedan, S., Tan, Y. K., Lee, D. Y., and Tan, D. T. (2003). Higher order ocular aberrations after cycloplegic and non-cycloplegic pupil dilation. *J Refract Surg* **19**(3), 316-22.

Carney, L. G., Mainstone, J. C., and Henderson, B. A. (1997). Corneal topography and myopia. A cross-sectional study. *Invest Ophthalmol Vis Sci* **38**(2), 311-20.

Casprini, F., Balestrazzi, A., Tosi, G. M., Miracco, F., Martone, G., Cevenini, G., and Caporossi, A. (2005). Glare disability and spherical aberration with five foldable intraocular lenses: a prospective randomized study. *Acta Ophthalmol Scand* **83**(1), 20-5.

Cervino, A., Hosking, S. L., Rai, G. K., Naroo, S. A., Gilmartin, B. (2006). Wavefront analyzers induce instrument myopia. *J Refract Surg* **22**(8), 795-803.

Cervino, A., McDonald, M. B., and Klyce, S. D. (2002). Shack-Hartmann Pattern as an Aid in the Diagnosis and Evaluation of Dry Eye: A Retrospective Study. *Invest. Ophthalmol. Vis. Sci.* **43**(12), 2029

Chalita, M. R., Chavala, S., Xu, M., and Krueger, R. R. (2004). Wavefront analysis in post-LASIK eyes and its correlation with visual symptoms, refraction, and topography. *Ophthalmology* **111**(3), 447-53.

Charman, W. N. (1991). Wavefront aberration of the eye: a review. *Optom Vis Sci* **68**(8), 574-83.

Charman, W. N. (2005). Aberrations and myopia. *Ophthalmic Physiol Opt* **25**(4), 285-301.

Charman, W. N., and Jennings, J. A. (1976). Objective measurements of the longitudinal chromatic aberration of the human eye. *Vision Res* **16**(9), 999-1005.

Chat, S. W., and Edwards, M. H. (2001). Clinical evaluation of the Shin-Nippon SRW-5000 autorefractor in children. *Ophthalmic Physiol Opt* **21**(2), 87-100.

Chateau, N., Blanchard, A., and Baude, D. (1998). Influence of myopia and aging on the optimal spherical aberration of soft contact lenses. *J Opt Soc Am A Opt Image Sci Vis* **15**(9), 2589-96.

Chen, L., Singer, B., Guirao, A., Porter, J., and Williams, D. R. (2005). Image metrics for predicting subjective image quality. *Optom Vis Sci* **82**(5), 358-69.

Cheng, H., Barnett, J. K., Vilupuru, A. S., Marsack, J. D., Kasthurirangan, S., Applegate, R. A., and Roorda, A. (2004a). A population study on changes in wave aberrations with accommodation. *J Vis* **4**(4), 272-80.

Cheng, X., Bradley, A., Hong, X., and Thibos, L. N. (2003). Relationship between refractive error and monochromatic aberrations of the eye. *Optom Vis Sci* **80**(1), 43-9.

Cheng, X., Himebaugh, N. L., Kollbaum, P. S., Thibos, L. N., and Bradley, A. (2003). Validation of a clinical Shack-Hartmann aberrometer. *Optom Vis Sci* **80**(8), 587-95.

Cheng, X., Himebaugh, N. L., Kollbaum, P. S., Thibos, L. N., and Bradley, A. (2004b). Test-retest reliability of clinical Shack-Hartmann measurements. *Invest Ophthalmol Vis Sci* **45**(1), 351-60.

Chylack, L. T., Jr., Wolfe, J. K., Singer, D. M., Leske, M. C., Bullimore, M. A., Bailey, I. L., Friend, J., McCarthy, D., and Wu, S. Y. (1993). The Lens Opacities Classification System III. The Longitudinal Study of Cataract Study Group. *Arch Ophthalmol* **111**, 831-836.

CIE. (2004). Colorimetry. *CIE Publication* 15.

Collins, M. J., Wildsoet, C. F., and Atchison, D. A. (1995). Monochromatic aberrations and myopia. *Vision Res* **35**(9), 1157-63.

Connors, R., 3rd, Boseman, P., 3rd, and Olson, R. J. (2002). Accuracy and reproducibility of biometry using partial coherence interferometry. *J Cataract Refract Surg* **28**(2), 235-8.

Coppens, J. E., Franssen, L., and van den Berg, T. J. (2006). Wavelength dependence of intraocular straylight. *Exp Eye Res* **82**(4), 688-92.

Coppens, J. E., Franssen, L., van Rijn, L. J., and van den Berg, T. J. (2006). Reliability of the compensation comparison stray-light measurement method. *J Biomed Opt* **11**(3), 34027.

Cox, M. J., Atchison, D. A., and Scott, D. H. (2003). Scatter and its implications for the measurement of optical image quality in human eyes. *Optom Vis Sci* **80**(1), 58-68.

Davies, N., Diaz-Santana, L., and Lara-Saucedo, D. (2003). Repeatability of ocular wavefront measurement. *Optom Vis Sci* **80**(2), 142-50.

de Brabander, J., Chateau, N., Marin, G., Lopez-Gil, N., Van Der Worp, E., and Benito, A. (2003). Simulated optical performance of custom wavefront soft contact lenses for keratoconus. *Optom Vis Sci* **80**(9), 637-43.

de Waard, P. W., JK, I. J., van den Berg, T. J., and de Jong, P. T. (1992). Intraocular light scattering in age-related cataracts. *Invest Ophthalmol Vis Sci* **33**(3), 618-25.

de Wit, G., Franssen, L., Coppens, J.E., van den Berg, T.J.T.P. (2006). Straylight contribution of cataracts and its simulation. *J Cataract Refract Surg* In press.

Dick, H. B., Krummenauer, F., Schwenn, O., Krist, R., and Pfeiffer, N. (1999). Objective and subjective evaluation of photic phenomena after monofocal and multifocal intraocular lens implantation. *Ophthalmology* **106**(10), 1878-86.

Dietze, H. H., and Cox, M. J. (2003). On- and off-eye spherical aberration of soft contact lenses and consequent changes of effective lens power. *Optom Vis Sci* **80**(2), 126-34.

Donnelly, W. J., 3rd, and Applegate, R. A. (2005). Influence of exposure time and pupil size on a Shack-Hartmann metric of forward scatter. *J Refract Surg* **21**(5), S547-51.

Donnelly, W. J., 3rd, Pesudovs, K., Marsack, J. D., Sarver, E. J., and Applegate, R. A. (2004). Quantifying scatter in Shack-Hartmann images to evaluate nuclear cataract. *J Refract Surg* **20**(5), S515-22.

Dorronsoro, C., Barbero, S., Llorente, L., and Marcos, S. (2003). On-eye measurement of optical performance of rigid gas permeable contact lenses based on ocular and corneal aberrometry. *Optom Vis Sci* **80**(2), 115-25.

Dunne, M. C., Davies, L. N., Mallen, E. A., Kirschkamp, T., and Barry, J. C. (2005). Non-invasive phakometric measurement of corneal and crystalline lens alignment in human eyes. *Ophthalmic Physiol Opt* **25**(2), 143-52.

Elliott, D. B., and Bullimore, M. A. (1993). Assessing the reliability, discriminative ability, and validity of disability glare tests. *Invest Ophthalmol Vis Sci* **34**(1), 108-19.

Elliott, D. B., Fonn, D., Flanagan, J., and Doughty, M. (1993). Relative sensitivity of clinical tests to hydrophilic lens-induced corneal thickness changes. *Optom Vis Sci* **70**(12), 1044-8.

Elliott, D. B., Mitchell, S., and Whitaker, D. (1991). Factors affecting light scatter in contact lens wearers. *Optom Vis Sci* **68**(8), 629-33.

Endl, M. J., Martinez, C. E., Klyce, S. D., McDonald, M. B., Coorpender, S. J., Applegate, R. A., and Howland, H. C. (2001). Effect of larger ablation zone and transition zone on corneal optical aberrations after photorefractive keratectomy. *Arch Ophthalmol* **119**(8), 1159-64.

Fan-Paul, N. I., Li, J., Miller, J. S., and Florakis, G. J. (2002). Night vision disturbances after corneal refractive surgery. *Surv Ophthalmol* **47**(6), 533-46.

Fernandez, E. J., and Artal, P. (2005). Study on the effects of monochromatic aberrations in the accommodation response by using adaptive optics. *J Opt Soc Am A Opt Image Sci Vis* **22**(9), 1732-8.

Fraenkel, G., Comaish, F., Lawless, M. A., Kelly, M. R., Dunn, S. M., Byth, K., Webber, S. K., Sutton, G. L., and Rogers, C. M. (2004). Development of a questionnaire to assess subjective vision score in myopes seeking refractive surgery. *J Refract Surg* **20**(1), 10-9.

Franssen, L., Coppens, J. E., and van den Berg, T. J. (2006). Compensation comparison method for assessment of retinal straylight. *Invest Ophthalmol Vis Sci* **47**(2), 768-76.

Freeman, G., and Pesudovs, K. (2005). The impact of cataract severity on measurement acquisition with the IOLMaster. *Acta Ophthalmologica Scandinavica* **83**(4), 439-442.

Fujikado, T., Kuroda, T., Maeda, N., Ninomiya, S., Goto, H., Tano, Y., Oshika, T., Hirohara, Y., and Mihashi, T. (2004). Light scattering and optical aberrations as objective parameters to predict visual deterioration in eyes with cataracts. *J Cataract Refract Surg* **30**(6), 1198-208.

Gilmartin, B., Amer, A. C., and Ingleby, S. (1995). Reversal of tropicamide mydriasis with single instillations of pilocarpine can induce substantial pseudo-myopia in young adults. *Ophthalmic Physiol Opt* **15**(5), 475-9.

Gilmartin, B., and Hogan, R. E. (1985). The magnitude of longitudinal chromatic aberration of the human eye between 458 and 633 nm. *Vision Res* **25**(11), 1747-53.

Gimbel, H. V., and Stoll, S. B. (2001). Photorefractive keratectomy with customized segmental ablation to correct irregular astigmatism after laser in situ keratomileusis. *J Refract Surg* **17**(2 Suppl), S229-32.

Gimbel, H. V., Sofinski, S. J., Mahler, O. S., van Westenbrugge, J. A., Ferensowicz, M. I., and Triebwasser, R. W. (2003). Wavefront-guided multipoint (segmental) custom ablation enhancement using the Nidek NAVEX platform. *J Refract Surg* **19**(2 Suppl), S209-16.

Gobin, L. (2002). Reproducibility of the IOLMaster. *J Cataract Refract Surg* **28**(7), 1087-8.

Grover, S., Alexander, K. R., Choi, D. M., and Fishman, G. A. (1998). Intraocular light scatter in patients with choroideremia. *Ophthalmology* **105**(9), 1641-5.

Grover, S., Alexander, K. R., Fishman, G. A., and Ryan, J. (2002). Comparison of intraocular light scatter in carriers of choroideremia and X-linked retinitis pigmentosa. *Ophthalmology* **109**(1), 159-63.

Guirao, A., Redondo, M., Geraghty, E., Piers, P., Norrby, S., and Artal, P. (2002). Corneal optical aberrations and retinal image quality in patients in whom monofocal intraocular lenses were implanted. *Arch Ophthalmol* **120**(9), 1143-51.

Gwiazda, J., Marsh-Tootle, W. L., Hyman, L., Hussein, M., and Norton, T. T. (2002). Baseline refractive and ocular component measures of children enrolled in the correction of myopia evaluation trial (COMET). *Invest Ophthalmol Vis Sci* **43**(2), 314-21.

Gwiazda, J., Thorn, F., Bauer, J., and Held, R. (1993). Myopic children show insufficient accommodative response to blur. *Invest Ophthalmol Vis Sci* **34**(3), 690-4.

Hament, W. J., Nabar, V. A., and Nuijts, R. M. (2002). Repeatability and validity of Zywave aberrometer measurements. *J Cataract Refract Surg* **28**(12), 2135-41.

Hanna, C. L., Roberts, R. T., Hwang, S. J., and Wilhelmus, K. R. (2004). Pachymetry of donor corneas: effect of ethnicity and gender on central corneal thickness. *Cornea* **23**(7), 701-3.

Harris, M. G., Haririfar, M., and Hirano, K. Y. (1999). Transmittance of tinted and UV-blocking disposable contact lenses. *Optom Vis Sci* **76**(3), 177-80.

Harris, W. F. (2001). Clinical measurement, artifact, and data analysis in dioptric power space. *Optom Vis Sci* **78**(11), 839-45.

Harrison, J. M., Tennant, T. B., Gwin, M. C., Applegate, R. A., Tennant, J. L., van den Berg, T. J., and Lohmann, C. P. (1995). Forward light scatter at one month after photorefractive keratectomy. *J Refract Surg* **11**(2), 83-8.

Hayashi, K., and Hayashi, H. (2006). Visual function in patients with yellow tinted intraocular lenses compared with vision in patients with non-tinted intraocular lenses. *Br J Ophthalmol* **90**(8), 1019-23.

Hayashi, K., Hayashi, H., Nakao, F., and Hayashi, F. (2001). Correlation between pupillary size and intraocular lens decentration and visual acuity of a zonal-progressive multifocal lens and a monofocal lens. *Ophthalmology* **108**(11), 2011-7.

Hazel, C. A., Cox, M. J., and Strang, N. C. (2003). Wavefront aberration and its relationship to the accommodative stimulus-response function in myopic subjects. *Optom Vis Sci* **80**(2), 151-8.

He, J. C., Burns, S. A., and Marcos, S. (2000). Monochromatic aberrations in the accommodated human eye. *Vision Res* **40**(1), 41-8.

He, J. C., Gwiazda, J., Thorn, F., Held, R., and Huang, W. (2003). Change in corneal shape and corneal wave-front aberrations with accommodation. *J Vis* **3**(7), 456-63.

He, J. C., Gwiazda, J., Thorn, F., Held, R., and Vera-Diaz, F. A. (2005). The association of wavefront aberration and accommodative lag in myopes. *Vision Res* **45**(3), 285-90.

He, J. C., Marcos, S., Webb, R. H., and Burns, S. A. (1998). Measurement of the wave-front aberration of the eye by a fast psychophysical procedure. *J Opt Soc Am A Opt Image Sci Vis* **15**(9), 2449-56.

He, J. C., Sun, P., Held, R., Thorn, F., Sun, X., and Gwiazda, J. E. (2002). Wavefront aberrations in eyes of emmetropic and moderately myopic school children and young adults. *Vision Res* **42**(8), 1063-70.

Hennelly, M. L., Barbur, J. L., Edgar, D. F., and Woodward, E. G. (1998). The effect of age on the light scattering characteristics of the eye. *Ophthalmic Physiol Opt* **18**(2), 197-203.

Hersh, P. S., Fry, K., and Blaker, J. W. (2003). Spherical aberration after laser in situ keratomileusis and photorefractive keratectomy. Clinical results and theoretical models of etiology. *J Cataract Refract Surg* **29**(11), 2096-104.

Hieda, O., and Kinoshita, S. (2003). Measuring of ocular wavefront aberration in large pupils using OPD-scan. *Semin Ophthalmol* **18**(1), 35-40.

Holladay, J. T., Piers, P. A., Koranyi, G., van der Mooren, M., and Norrby, N. E. (2002). A new intraocular lens design to reduce spherical aberration of pseudophakic eyes. *J Refract Surg* **18**(6), 683-91.

Holladay, J. T., Van Dijk, H., Lang, A., Portney, V., Willis, T. R., Sun, R., and Oksman, H. C. (1990). Optical performance of multifocal intraocular lenses. *J Cataract Refract Surg* **16**(4), 413-22.

Hong, X., Himebaugh, N., and Thibos, L. N. (2001). On-eye evaluation of optical performance of rigid and soft contact lenses. *Optom Vis Sci* **78**(12), 872-80.

Hong, X., Thibos, L. N., Bradley, A., Woods, R. L., and Applegate, R. A. (2003). Comparison of monochromatic ocular aberrations measured with an objective cross-cylinder aberroscope and a Shack-Hartmann aberrometer. *Optom Vis Sci* **80**(1), 15-25.

Horn, F. K., Junemann, A. G., and Korth, M. (2001). Two methods of lens opacity measurements in glaucomas. *Doc Ophthalmol* **103**(2), 105-17.

Horner, D. G., Soni, P. S., Vyas, N., and Himebaugh, N. L. (2000). Longitudinal changes in corneal asphericity in myopia. *Optom Vis Sci* 77(4), 198-203.

Howarth, P. A., and Bradley, A. (1986). The longitudinal chromatic aberration of the human eye, and its correction. *Vision Res* **26**(2), 361-6.

Howland, B., and Howland, H. C. (1976). Subjective measurement of high-order aberrations of the eye. *Science* **193**(4253), 580-2.

Howland, H. C. (2000). The history and methods of ophthalmic wavefront sensing. *J Refract Surg* **16**(5), S552-3.

Howland, H. C., and Howland, B. (1977). A subjective method for the measurement of monochromatic aberrations of the eye. *J Opt Soc Am* **67**(11), 1508-18.

Huang, B., Mirza, M. A., Qazi, M. A., and Pepose, J. S. (2004). The effect of punctal occlusion on wavefront aberrations in dry eye patients after laser in situ keratomileusis. *Am J Ophthalmol* **137**(1), 52-61.

Huang, D., and Arif, M. (2002). Spot size and quality of scanning laser correction of higher-order wavefront aberrations. *J Cataract Refract Surg* **28**(3), 407-16.

Hyman, L., Gwiazda, J., Hussein, M., Norton, T. T., Wang, Y., Marsh-Tootle, W., and Everett, D. (2005). Relationship of age, sex, and ethnicity with myopia progression and axial elongation in the correction of myopia evaluation trial. *Arch Ophthalmol* **123**(7), 977-87.

Iglesias, I., Berrio, E., and Artal, P. (1998). Estimates of the ocular wave aberration from pairs of double-pass retinal images. *J Opt Soc Am A Opt Image Sci Vis* **15**(9), 2466-76.

Ijspeert, J., de Waard, P. W., van den Berg, T. J., and de Jong, P. T. (1990). The intraocular straylight function in 129 healthy volunteers; dependence on angle, age and pigmentation. *Vision Res* **30**(5), 699-707.

Jacobi, F. K., Kammann, J., Jacobi, K. W., Grosskopf, U., and Walden, K. (1999). Bilateral implantation of asymmetrical diffractive multifocal intraocular lenses. *Arch Ophthalmol* **117**(1), 17-23.

Javitt, J. C., and Steinert, R. F. (2000). Cataract extraction with multifocal intraocular lens implantation: a multinational clinical trial evaluating clinical, functional, and quality-of-life outcomes. *Ophthalmology* **107**(11), 2040-8.

Jorge, J., Queiros, A., Almeida, J. B., and Parafita, M. A. (2005a). Retinoscopy/autorefraction: which is the best starting point for a noncycloplegic refraction? *Optom Vis Sci* **82**(1), 64-8.

Jorge, J., Queiros, A., Gonzalez-Meijome, J., Fernandes, P., Almeida, J. B., and Parafita, M. A. (2005b). The influence of cycloplegia in objective refraction. *Ophthalmic Physiol Opt* **25**(4), 340-5.

Joslin, C. E., Wu, S. M., McMahon, T. T., and Shahidi, M. (2003). Higher-order wavefront aberrations in corneal refractive therapy. *Optom Vis Sci* **80**(12), 805-11.

Kaemmerer, M., Mrochen, M., Mierdel, P., Krinke, H. E., and Seiler, T. (2000). Clinical experience with the Tscherning aberrometer. *J Refract Surg* **16**(5), S584-7.

Kanjani, N., Jacob, S., Agarwal, A., Agarwal, S., Agarwal, T., Doshi, A., and Doshi, S. (2004). Wavefront- and topography-guided ablation in myopic eyes using Zyoptix. *J Cataract Refract Surg* **30**(2), 398-402.

Kawamorita, T., and Uozato, H. (2005). Modulation transfer function and pupil size in multifocal and monofocal intraocular lenses in vitro. *J Cataract Refract Surg* **31**(12), 2379-85.

Kelly, J. E., Mihashi, T., and Howland, H. C. (2004). Compensation of corneal horizontal/vertical astigmatism, lateral coma, and spherical aberration by internal optics of the eye. *J Vis* **4**(4), 262-71.

Kirschkamp, T., Jockel, M., Wahlisch, G., and Barry, J. C. (1998). [Construction of a model eye for simulation of Purkinje reflections for determining the radii of curvature and the position of the crystalline lens]. *Biomed Tech (Berl)* **43**(11), 318-25.

Kohnen, T., Allen, D., Boureau, C., Dublineau, P., Hartmann, C., Mehdorn, E., Rozot, P., and Tassinari, G. (2006). European multicenter study of the AcrySof ReSTOR apodized diffractive intraocular lens. *Ophthalmology* **113**(4), 584 e1.

Kuroda, T., Fujikado, T., Maeda, N., Oshika, T., Hirohara, Y., and Mihashi, T. (2002a). Wavefront analysis in eyes with nuclear or cortical cataract. *Am J Ophthalmol* **134**(1), 1-9.

Kuroda, T., Fujikado, T., Maeda, N., Oshika, T., Hirohara, Y., and Mihashi, T. (2002b). Wavefront analysis of higher-order aberrations in patients with cataract. *J Cataract Refract Surg* **28**(3), 438-44.

Kuroda, T., Fujikado, T., Ninomiya, S., Maeda, N., Hirohara, Y., and Mihashi, T. (2002c). Effect of aging on ocular light scatter and higher order aberrations. *J Refract Surg* **18**(5), S598-602.

Lam, A. K., Chan, R., and Chiu, R. (2004). Effect of posture and artificial tears on corneal power measurements with a handheld automated keratometer. *J Cataract Refract Surg* **30**(3), 645-52.

Lam, A. K., Chan, R., and Pang, P. C. (2001). The repeatability and accuracy of axial length and anterior chamber depth measurements from the IOLMaster. *Ophthalmic Physiol Opt* **21**(6), 477-83.

Levy, Y., Segal, O., Avni, I., and Zadok, D. (2005). Ocular higher-order aberrations in eyes with supernormal vision. *Am J Ophthalmol* **139**(2), 225-8.

Liang, C. L., Juo, S. H., and Chang, C. J. (2005). Comparison of higher-order wavefront aberrations with 3 aberrometers. *J Cataract Refract Surg* **31**(11), 2153-6.

Liang, J., and Williams, D. R. (1997). Aberrations and retinal image quality of the normal human eye. *J Opt Soc Am A Opt Image Sci Vis* **14**(11), 2873-83.

Liang, J., Grimm, B., Goelz, S., and Bille, J. F. (1994). Objective measurement of wave aberrations of the human eye with the use of a Hartmann-Shack wave-front sensor. *J Opt Soc Am A Opt Image Sci Vis* **11**(7), 1949-57.

Lichter, H., Staver, P. R., Thompson, K., and Garcia, J. (2002). InterWave aberrometry for custom ablation. *Int Ophthalmol Clin* **42**(4), 41-54.

Lindstrom, R. L. (1993). Food and Drug Administration study update. One-year results from 671 patients with the 3M multifocal intraocular lens. *Ophthalmology* **100**(1), 91-7.

Llorente, L., Barbero, S., Merayo, J., and Marcos, S. (2004). Total and corneal optical aberrations induced by laser in situ keratomileusis for hyperopia. *J Refract Surg* **20**(3), 203-16.

Logan, N. S., Davies, L. N., Mallen, E. A., and Gilmartin, B. (2005). Ametropia and ocular biometry in a U.K. university student population. *Optom Vis Sci* **82**(4), 261-6.

Lopez-Gil, N., Castejon-Mochon, J. F., Benito, A., Marin, J. M., Lo-a-Foe, G., Marin, G., Fermigier, B., Renard, D., Joyeux, D., Chateau, N., and Artal, P. (2002). Aberration generation by contact lenses with aspheric and asymmetric surfaces. *J Refract Surg* **18**(5), S603-9.

Lu, F., Mao, X., Qu, J., Xu, D., and He, J. C. (2003). Monochromatic wavefront aberrations in the human eye with contact lenses. *Optom Vis Sci* **80**(2), 135-41.

Ma, L., Atchison, D. A., and Charman, W. N. (2005). Off-axis refraction and aberrations following conventional laser in situ keratomileusis. *J Cataract Refract Surg* **31**(3), 489-98.

MacRae, S., and Fujieda, M. (2000). Slit skiascopic-guided ablation using the Nidek laser. *J Refract Surg* **16**(5), S576-80.

Maeda, N., Fujikado, T., Kuroda, T., Mihashi, T., Hirohara, Y., Nishida, K., Watanabe, H., and Tano, Y. (2002). Wavefront aberrations measured with Hartmann-Shack sensor in patients with keratoconus. *Ophthalmology* **109**(11), 1996-2003.

Mainstone, J. C., Carney, L. G., Anderson, C. R., Clem, P. M., Stephensen, A. L., and Wilson, M. D. (1998). Corneal shape in hyperopia. *Clin Exp Optom* **81**(3), 131-137.

Mallen, E. A., Wolffsohn, J. S., Gilmartin, B., and Tsujimura, S. (2001). Clinical evaluation of the Shin-Nippon SRW-5000 autorefractor in adults. *Ophthalmic Physiol Opt* **21**(2), 101-7.

Marcos, S. (2001). Aberrations and visual performance following standard laser vision correction. *J Refract Surg* **17**(5), S596-601.

Marcos, S. (2002). Are changes in ocular aberrations with age a significant problem for refractive surgery? *J Refract Surg* **18**(5), S572-8.

Marcos, S., and Burns, S. A. (2000). On the symmetry between eyes of wavefront aberration and cone directionality. *Vision Res* **40**(18), 2437-47.

Marcos, S., Barbero, S., and Llorente, L. (2002). The Sources Of Optical Aberrations In Myopic Eyes. *Invest. Ophthalmol. Vis. Sci.* **43**(12), 1510

.

Marcos, S., Barbero, S., Llorente, L., and Merayo-Lloves, J. (2001a). Optical response to LASIK surgery for myopia from total and corneal aberration measurements. *Invest Ophthalmol Vis Sci* **42**(13), 3349-56.

Marcos, S., Burns, S. A., Moreno-Barriusop, E., and Navarro, R. (1999). A new approach to the study of ocular chromatic aberrations. *Vision Res* **39**(26), 4309-23.

Marcos, S., Burns, S. A., Prieto, P. M., Navarro, R., and Baraibar, B. (2001b). Investigating sources of variability of monochromatic and transverse chromatic aberrations across eyes. *Vision Res* **41**(28), 3861-71.

Martin, J. A., and Roorda, A. (2003). Predicting and assessing visual performance with multizone bifocal contact lenses. *Optom Vis Sci* **80**(12), 812-9.

Martinez, C. E., Applegate, R. A., Klyce, S. D., McDonald, M. B., Medina, J. P., and Howland, H. C. (1998). Effect of pupillary dilation on corneal optical aberrations after photorefractive keratectomy. *Arch Ophthalmol* **116**(8), 1053-62.

Mastropasqua, L., Toto, L., Zuppardi, E., Nubile, M., Carpineto, P., Di Nicola, M., and Ballone, E. (2006). Zyoptix wavefront-guided versus standard photorefractive keratectomy (PRK) in low and moderate myopia: randomized controlled 6-month study. *Eur J Ophthalmol* **16**(2), 219-28.

McLellan, J. S., Marcos, S., and Burns, S. A. (2001). Age-related changes in monochromatic wave aberrations of the human eye. *Invest Ophthalmol Vis Sci* **42**(6), 1390-5.

Meacock, W. R., Spalton, D. J., Boyce, J., and Marshall, J. (2003). The effect of posterior capsule opacification on visual function. *Invest Ophthalmol Vis Sci* **44**(11), 4665-9.

Mester, U., Dillinger, P., and Anterist, N. (2003). Impact of a modified optic design on visual function: clinical comparative study. *J Cataract Refract Surg* **29**(4), 652-60.

Mierdel, P., Kaemmerer, M., Mrochen, M., Krinke, H. E., and Seiler, T. (2001). Ocular optical aberrometer for clinical use. *J Biomed Opt* **6**(2), 200-4.

Mierdel, P., Krinke, H. E., Wiegand, W., Kaemmerer, M., and Seiler, T. (1997). [Measuring device for determining monochromatic aberration of the human eye]. *Ophthalmologe* **94**(6), 441-5.

Miller, J. M., Anwaruddin, R., Straub, J., and Schwiegerling, J. (2002). Higher order aberrations in normal, dilated, intraocular lens, and laser in situ keratomileusis corneas. *J Refract Surg* **18**(5), S579-83.

Mirshahi, A., Buhren, J., Gerhardt, D., and Kohnen, T. (2003). In vivo and in vitro repeatability of Hartmann-Shack aberrometry. *J Cataract Refract Surg* **29**(12), 2295-301.

Molebny, V. V., Panagopoulou, S. I., Molebny, S. V., Wakil, Y. S., and Pallikaris, I. G. (2000). Principles of ray tracing aberrometry. *J Refract Surg* **16**(5), S572-5.

Montes-Mico, R., Alio, J. L., and Charman, W. N. (2005). Dynamic changes in the tear film in dry eyes. *Invest Ophthalmol Vis Sci* **46**(5), 1615-9.

Montes-Mico, R., Alio, J. L., Munoz, G., and Charman, W. N. (2004). Temporal changes in optical quality of air-tear film interface at anterior cornea after blink. *Invest Ophthalmol Vis Sci* **45**(6), 1752-7.

Montes-Mico, R., and Alio, J. L. (2003). Distance and near contrast sensitivity function after multifocal intraocular lens implantation. *J Cataract Refract Surg* **29**(4), 703-11.

Montes-Mico, R., and Charman, W. N. (2001). Choice of spatial frequency for contrast sensitivity evaluation after corneal refractive surgery. *J Refract Surg* **17**(6), 646-51.

Montes-Mico, R., Caliz, A., and Alio, J. L. (2004a). Changes in ocular aberrations after instillation of artificial tears in dry-eye patients. *J Cataract Refract Surg* **30**(8), 1649-52.

Montes-Mico, R., Caliz, A., and Alio, J. L. (2004b). Wavefront analysis of higher order aberrations in dry eye patients. *J Refract Surg* **20**(3), 243-7.

Montes-Mico, R., Espana, E., Bueno, I., Charman, W. N., and Menezo, J. L. (2004). Visual performance with multifocal intraocular lenses: mesopic contrast sensitivity under distance and near conditions. *Ophthalmology* **111**(1), 85-96.

Moreno-Barriuso, E., and Navarro, R. (2000). Laser Ray Tracing versus Hartmann-Shack sensor for measuring optical aberrations in the human eye. *J Opt Soc Am A Opt Image Sci Vis* **17**(6), 974-85.

Moreno-Barriuso, E., Lloves, J. M., Marcos, S., Navarro, R., Llorente, L., and Barbero, S. (2001a). Ocular aberrations before and after myopic corneal refractive surgery: LASIK-induced changes measured with laser ray tracing. *Invest Ophthalmol Vis Sci* **42**(6), 1396-403.

Moreno-Barriuso, E., Marcos, S., Navarro, R., and Burns, S. A. (2001b). Comparing laser ray tracing, the spatially resolved refractometer, and the Hartmann-Shack sensor to measure the ocular wave aberration. *Optom Vis Sci* **78**(3), 152-6.

Mrochen, M., Kaemmerer, M., and Seiler, T. (2000). Wavefront-guided laser in situ keratomileusis: early results in three eyes. *J Refract Surg* **16**(2), 116-21.

Mrochen, M., Kaemmerer, M., and Seiler, T. (2001). Clinical results of wavefront-guided laser in situ keratomileusis 3 months after surgery. *J Cataract Refract Surg* **27**(2), 201-7.

Mrochen, M., Kaemmerer, M., Mierdel, P., Krinke, H. E., and Seiler, T. (2000). Principles of Tscherning aberrometry. *J Refract Surg* **16**(5), S570-1.

Mutti, D. O., Jones, L. A., Moeschberger, M. L., and Zadnik, K. (2000). AC/A ratio, age, and refractive error in children. *Invest Ophthalmol Vis Sci* **41**(9), 2469-78.

Nakamura, K., Bissen-Miyajima, H., Toda, I., Hori, Y., and Tsubota, K. (2001). Effect of laser in situ keratomileusis correction on contrast visual acuity. *J Cataract Refract Surg* **27**(3), 357-61.

Nakano, K., Portellinha, W., Oliveira, M., Alvarenga, L., Nakano, C., and Nakano, E. (2003). Refractive outcome of Nidek OPD-scan customized ablations. *J Refract Surg* **19**(2 Suppl), S221-2.

Navarro, R., and Losada, M. A. (1997). Aberrations and relative efficiency of light pencils in the living human eye. *Optom Vis Sci* **74**(7), 540-7.

Navarro, R., Ferro, M., Artal, P., and Miranda, I. (1993). Modulation transfer functions of eyes implanted with intraocular lenses. *Appl Opt* **32**(31), 6359-67.

Ninomiya, S., Fujikado, T., Kuroda, T., Maeda, N., Tano, Y., Hirohara, Y., and Mihashi, T. (2003). Wavefront analysis in eyes with accommodative spasm. *Am J Ophthalmol* **136**(6), 1161-3.

Ninomiya, S., Fujikado, T., Kuroda, T., Maeda, N., Tano, Y., Oshika, T., Hirohara, Y., and Mihashi, T. (2002). Changes of ocular aberration with accommodation. *Am J Ophthalmol* **134**(6), 924-6.

O'Donnell, C., and Wolffsohn, J. S. (2004). Grading of corneal transparency. *Cont Lens Anterior Eye* **27**(4), 161-70.

Oliver, K. M., Hemenger, R. P., Corbett, M. C., O'Brart, D. P., Verma, S., Marshall, J., and Tomlinson, A. (1997). Corneal optical aberrations induced by photorefractive keratectomy. *J Refract Surg* **13**(3), 246-54.

Oshika, T., Miyata, K., Tokunaga, T., Samejima, T., Amano, S., Tanaka, S., Hirohara, Y., Mihashi, T., Maeda, N., and Fujikado, T. (2002). Higher order wavefront aberrations of cornea and magnitude of refractive correction in laser in situ keratomileusis. *Ophthalmology* **109**(6), 1154-8.

Pallikaris, I. G., Panagopoulou, S. I., and Molebny, V. V. (2000). Clinical experience with the Tracey technology wavefront device. *J Refract Surg* **16**(5), S588-91.

Pallikaris, L. G., Panagopoulou, S. I., Siganos, C. S., and Molebny, V. V. (2001). Objective measurement of wavefront aberrations with and without accommodation. *J Refract Surg* **17**(5), S602-7.

Paquin, M. P., Hamam, H., and Simonet, P. (2002). Objective measurement of optical aberrations in myopic eyes. *Optom Vis Sci* **79**(5), 285-91.

Patel, S. V., McLaren, J. W., Hodge, D. O., and Bourne, W. M. (2002). Confocal microscopy in vivo in corneas of long-term contact lens wearers. *Invest Ophthalmol Vis Sci* **43**(4), 995-1003.

Patel, S., Fakhry, M., and Alio, J. L. (2002). Objective assessment of aberrations induced by multifocal contact lenses in vivo. *CLAO J* **28**(4), 196-201.

Pesudovs, K., Marsack, J. D., Donnelly, W. J., 3rd, Thibos, L. N., and Applegate, R. A. (2004). Measuring visual acuity--mesopic or photopic conditions, and high or low contrast letters? *J Refract Surg* **20**(5), S508-14.

Pieh, S., Lackner, B., Hanselmayer, G., Zohrer, R., Sticker, M., Weghaupt, H., Fercher, A., and Skorpik, C. (2001). Halo size under distance and near conditions in refractive multifocal intraocular lenses. *Br J Ophthalmol* **85**(7), 816-21.

Pieh, S., Weghaupt, H., and Skorpik, C. (1998). Contrast sensitivity and glare disability with diffractive and refractive multifocal intraocular lenses. *J Cataract Refract Surg* **24**(5), 659-62.

Plainis, S., and Murray, I. J. (2002). Reaction times as an index of visual conspicuity when driving at night. *Ophthalmic Physiol Opt* **22**(5), 409-15.

Plainis, S., Ginis, H. S., and Pallikaris, A. (2005). The effect of ocular aberrations on steady-state errors of accommodative response. *Journal of Vision* **5**(5), 466-477.

Platt, B. C., and Shack, R. (2001). History and principles of Shack-Hartmann wavefront sensing. *J Refract Surg* **17**(5), S573-7.

Porter, J., Guirao, A., Cox, I. G., and Williams, D. R. (2001). Monochromatic aberrations of the human eye in a large population. *J Opt Soc Am A Opt Image Sci Vis* **18**(8), 1793-803.

Potgieter, F. J., Roberts, C., Cox, I. G., Mahmoud, A. M., Herderick, E. E., Roetz, M., and Steenkamp, W. (2005). Prediction of flap response. *J Cataract Refract Surg* **31**(1), 106-14.

Prieto, P. M., Vargas-Martin, F., Goelz, S., and Artal, P. (2000). Analysis of the performance of the Hartmann-Shack sensor in the human eye. *J Opt Soc Am A Opt Image Sci Vis* **17**(8), 1388-98.

Puell, M. C., Palomo, C., Sanchez-Ramos, C., and Villena, C. (2004). Mesopic contrast sensitivity in the presence or absence of glare in a large driver population. *Graefes Arch Clin Exp Ophthalmol* **242**(9), 755-61.

Randleman, J. B., Thompson, K. P., and Staver, P. R. (2004). Wavefront aberrations from corneal ectasia after laser in situ keratomileusis demonstrated by InterWave aberrometry. *J Refract Surg* **20**(2), 170-5.

Ravalico, G., Parentin, F., Sirotti, P., and Baccara, F. (1998). Analysis of light energy distribution by multifocal intraocular lenses through an experimental optical model. *J Cataract Refract Surg* **24**(5), 647-52.

Riley, A. F., Grupcheva, C. N., Malik, T. Y., Craig, J. P., and McGhee, C. N. (2001). The Auckland Cataract Study: demographic, corneal topographic and ocular biometric parameters. *Clin Experiment Ophthalmol* **29**(6), 381-6.

Rodriguez, P., Navarro, R., Gonzalez, L., and Hernandez, J. L. (2004). Accuracy and reproducibility of Zywave, Tracey, and experimental aberrometers. *J Refract Surg* **20**(6), 810-7.

Rodriguez-Galietero, A., Montes-Mico, R., Munoz, G., and Albarran-Diego, C. (2005a). Blue-light filtering intraocular lens in patients with diabetes: contrast sensitivity and chromatic discrimination. *J Cataract Refract Surg* **31**(11), 2088-92.

Rodriguez-Galietero, A., Montes-Mico, R., Munoz, G., and Albarran-Diego, C. (2005b). Comparison of contrast sensitivity and color discrimination after clear and yellow intraocular lens implantation. *J Cataract Refract Surg* **31**(9), 1736-40.

Roorda, A. (2000). Adaptive optics ophthalmoscopy. *J Refract Surg* **16**(5), S602-7.

Rosenfield, M., and Abraham-Cohen, J. A. (1999). Blur sensitivity in myopes. *Optom Vis Sci* **76**(5), 303-7.

Rosenfield, M., and Gilmartin, B. (1988). Disparity-induced accommodation in late-onset myopia. *Ophthalmic Physiol Opt* **8**(3), 353-5.

Russell, G. E., Stulting, R. D., and Thompson, K. P. (2003). Postoperative LASIK visual aberrations and treatment with InterWave-guided multipass, multistage correction. *Optom Vis Sci* **80**(2), 93-6.

Rynders, M. C., Navarro, R., and Losada, M. A. (1998). Objective measurement of the off-axis longitudinal chromatic aberration in the human eye. *Vision Res* **38**(4), 513-22.

Rynders, M., Lidkea, B., Chisholm, W., and Thibos, L. N. (1995). Statistical distribution of foveal transverse chromatic aberration, pupil centration, and angle psi in a population of young adult eyes. *J Opt Soc Am A Opt Image Sci Vis* **12**(10), 2348-57.

Sacu, S., Menapace, R., and Findl, O. (2006). Effect of optic material and haptic design on anterior capsule opacification and capsulorrhexis contraction. *Am J Ophthalmol* **141**(3), 488-493.

Salmon, T. O., and van de Pol, C. (2005). Evaluation of a clinical aberrometer for lower-order accuracy and repeatability, higher-order repeatability, and instrument myopia. *Optometry* **76**(8), 461-72.

Salmon, T. O., Thibos, L. N., and Bradley, A. (1998). Comparison of the eye's wave-front aberration measured psychophysically and with the Shack-Hartmann wave-front sensor. *J Opt Soc Am A Opt Image Sci Vis* **15**(9), 2457-65.

Salmon, T. O., West, R. W., Gasser, W., and Kenmore, T. (2003). Measurement of refractive errors in young myopes using the COAS Shack-Hartmann aberrometer. *Optom Vis Sci* **80**(1), 6-14.

Santodomingo-Rubido, J., Mallen, E. A., Gilmartin, B., and Wolffsohn, J. S. (2002). A new non-contact optical device for ocular biometry. *Br J Ophthalmol* **86**(4), 458-62.

Sarkisian, K. A., and Petrov, A. A. (2002). Clinical experience with the customized low spherical aberration ablation profile for myopia. *J Refract Surg* **18**(3 Suppl), S352-6.

Saw, S. M., Tong, L., Chua, W. H., Chia, K. S., Koh, D., Tan, D. T., and Katz, J. (2005). Incidence and progression of myopia in Singaporean school children. *Invest Ophthalmol Vis Sci* **46**(1), 51-7.

Scheimpflug, T. (1906). Der Photospektograph und seine Anwendung. *Photographische Korrespondez* **43**.

Schmitz, S., Dick, H. B., Krummenauer, F., Schwenn, O., and Krist, R. (2000). Contrast sensitivity and glare disability by halogen light after monofocal and multifocal lens implantation. *Br J Ophthalmol* **84**(10), 1109-12.

Schwiegerling, J. (2000). Theoretical limits to visual performance. *Surv Ophthalmol* **45**(2), 139-46.

Seidemann, A., and Schaeffel, F. (2002). Effects of longitudinal chromatic aberration on accommodation and emmetropization. *Vision Res* **42**(21), 2409-17.

Seiler, T., Holschbach, A., Derse, M., Jean, B., and Genth, U. (1994). Complications of myopic photorefractive keratectomy with the excimer laser. *Ophthalmology* **101**(1), 153-60.

Seo, K. Y., Lee, J. B., Kang, J. J., Lee, E. S., and Kim, E. K. (2004). Comparison of higher-order aberrations after LASEK with a 6.0 mm ablation zone and a 6.5 mm ablation zone with blend zone. *J Cataract Refract Surg* **30**(3), 653-7.

Shade, O. H. (1956). Optical and photoelectric analog of the eye. *J Opt Soc Am* **46**, 721-739.

Shah, S., Naroo, S., Hosking, S., Gherghel, D., Mantry, S., Bannerjee, S., Pedwell, K., and Bains, H. S. (2003). Nidek OPD-scan analysis of normal, keratoconic, and penetrating keratoplasty eyes. *J Refract Surg* **19**(2 Suppl), S255-9.

Shahidi, M., and Yang, Y. (2004). Measurements of ocular aberrations and light scatter in healthy subjects. *Optom Vis Sci* **81**(11), 853-7.

Shahidi, M., Blair, N. P., Mori, M., and Zelkha, R. (2004). Optical section retinal imaging and wavefront sensing in diabetes. *Optom Vis Sci* **81**(10), 778-84.

Shahidi, M., Yang, Y., Rajagopalan, A. S., Alexander, K. R., Zelkha, R., and Fishman, G. A. (2005). A method for differentiating ocular higher-order aberrations from light scatter applied to retinitis pigmentosa. *Optom Vis Sci* **82**(11), 976-80.

Siik, S., Chylack, L. T., Jr., Friend, J., Wolfe, J., Teikari, J., Nieminen, H., and Airaksinen, P. J. (1999). Lens autofluorescence and light scatter in relation to the lens opacities classification system, LOCS III. *Acta Ophthalmol Scand* 77(5), 509-14.

Simonet, P., and Campbell, M. C. (1990). The optical transverse chromatic aberration on the fovea of the human eye. *Vision Res* **30**(2), 187-206.

Smirnov, M. S. (1961). Measurement of the wave aberration of the human eye. *Biofizika* **6**, 776-95.

Smith, E. L., 3rd, Hung, L. F., and Harwerth, R. S. (1994). Effects of optically induced blur on the refractive status of young monkeys. *Vision Res* **34**(3), 293-301.

Smith, G., Applegate, R. A., and Howland, H. C. (1996). The crossed-cylinder aberroscope: an alternative method of calculation of the aberrations. *Ophthalmic Physiol Opt* **16**(3), 222-9.

Smolek, M. K., and Klyce, S. D. (2003). Zernike polynomial fitting fails to represent all visually significant corneal aberrations. *Invest Ophthalmol Vis Sci* **44**(11), 4676-81.

Steen, R., Whitaker, D., Elliott, D. B., and Wild, J. M. (1993). Effect of filters on disability glare. *Ophthalmic Physiol Opt* **13**(4), 371-6.

Steinert, R. F., Aker, B. L., Trentacost, D. J., Smith, P. J., and Tarantino, N. (1999). A prospective comparative study of the AMO ARRAY zonal-progressive multifocal silicone intraocular lens and a monofocal intraocular lens. *Ophthalmology* **106**(7), 1243-55.

Steinert, R. F., Post, C. T., Jr., Brint, S. F., Fritch, C. D., Hall, D. L., Wilder, L. W., Fine, I. H., Lichtenstein, S. B., Masket, S., Casebeer, C., and et al. (1992). A prospective, randomized, double-masked comparison of a zonal-progressive multifocal intraocular lens and a monofocal intraocular lens. *Ophthalmology* **99**(6), 853-60; discussion 860-1.

Stifter, E., Sacu, S., Thaler, A., and Weghaupt, H. (2006). Contrast Acuity in Cataracts of Different Morphology and Association to Self-Reported Visual Function. *Invest. Ophthalmol. Vis. Sci.* **47**(12), 5412-5422.

Strang, N. C., Schmid, K. L., and Carney, L. G. (1998). Hyperopia is predominantly axial in nature. *Curr Eye Res* **17**(4), 380-3.

Swarbrick, H. A. (2004). Orthokeratology (corneal refractive therapy): what is it and how does it work? *Eye Contact Lens* **30**(4), 181-5; discussion 205-6.

Theeuwes, J., Alferdinck, J. W., and Perel, M. (2002). Relation between glare and driving performance. *Hum Factors* **44**(1), 95-107.

Thibos, L. N. (1987). Calculation of the influence of lateral chromatic aberration on image quality across the visual field. *J Opt Soc Am A* **4**(8), 1673-80.

Thibos, L. N. (2000). Principles of Hartmann-Shack aberrometry. *J Refract Surg* **16**(5), S563-5.

Thibos, L. N. (2001). Wavefront data reporting and terminology. *J Refract Surg* **17**(5), S578-83.

Thibos, L. N., and Hong, X. (1999). Clinical applications of the Shack-Hartmann aberrometer. *Optom Vis Sci* **76**(12), 817-25.

Thibos, L. N., Applegate, R. A., and Marcos, S. (2003). Aberrometry: the past, present, and future of optometry. *Optom Vis Sci* **80**(1), 1-2.

Thibos, L. N., Applegate, R. A., Schwiegerling, J. T., and Webb, R. (2002). Standards for reporting the optical aberrations of eyes. *J Refract Surg* **18**(5), S652-60.

Thibos, L. N., Bradley, A., and Zhang, X. X. (1991). Effect of ocular chromatic aberration on monocular visual performance. *Optom Vis Sci* **68**(8), 599-607.

Thibos, L. N., Bradley, A., Still, D. L., Zhang, X., and Howarth, P. A. (1990). Theory and measurement of ocular chromatic aberration. *Vision Res* **30**(1), 33-49.

Thibos, L. N., Hong, X., Bradley, A., and Applegate, R. A. (2004). Accuracy and precision of objective refraction from wavefront aberrations. *J Vis* **4**(4), 329-51.

Thibos, L. N., Wheeler, W., and Horner, D. (1997). Power vectors: an application of Fourier analysis to the description and statistical analysis of refractive error. *Optom Vis Sci* **74**(6), 367-75.

Thompson, K. P., Staver, P. R., Garcia, J. R., Burns, S. A., Webb, R. H., and Stulting, R. D. (2004). Using InterWave aberrometry to measure and improve the quality of vision in LASIK surgery. *Ophthalmology* **111**(7), 1368-79.

Twa, M. D., Roberts, C., Mahmoud, A. M., and Chang, J. S., Jr. (2005). Response of the posterior corneal surface to laser in situ keratomileusis for myopia. *J Cataract Refract Surg* **31**(1), 61-71.

van den Berg, T. J. (1986). Importance of pathological intraocular light scatter for visual disability. *Doc Ophthalmol* **61**(3-4), 327-33.

van den Berg, T. J. (1991). On the relation between glare and straylight. *Doc Ophthalmol* **78**(3-4), 177-81.

van den Berg, T. J. (1995). Analysis of intraocular straylight, especially in relation to age. *Optom Vis Sci* **72**(2), 52-9.

van den Berg, T. J. T. P., and van Rijn, L. J. (2005). Relevance of glare sensitivity and impairment of visual function among European drivers. *Final report EU project SUB-B27020B-E3-GLARE-2002-S07* 18091.

van den Berg, T. J. T. P., IJspeert, J. K. (1992). Clinical assessment of intraocular straylight. *Appl. Opt.* **31**, 3694-3696.

van den Berg, T. J., and Coppens, J. C. (1999). Conversion of lens slit lamp photographs into physical light-scattering units. *Invest Ophthalmol Vis Sci* **40**(9), 2151-7.

van den Berg, T. J., Hwan, B. S., and Delleman, J. W. (1993). The intraocular straylight function in some hereditary corneal dystrophies. *Doc Ophthalmol* **85**(1), 13-9.

van den Berg, T. J., JK, I. J., and de Waard, P. W. (1991). Dependence of intraocular straylight on pigmentation and light transmission through the ocular wall. *Vision Res* **31**(7-8), 1361-7.

van der Heijde, G. L., Weber, J., and Boukes, R. (1985). Effects of straylight on visual acuity in pseudophakia. *Doc Ophthalmol* **59**(1), 81-4.

van Rijn, L. J., Nischler, C., Gamer, D., Franssen, L., de Wit, G., Kaper, R., Vonhoff, D., Grabner, G., Wilhelm, H., Volker-Dieben, H. J., and van den Berg, T. J. (2005). Measurement of stray light and glare: comparison of Nyktotest, Mesotest, stray light meter, and computer implemented stray light meter. *Br J Ophthalmol* **89**(3), 345-51.

Veraart, H. G., and van den Berg, T. J. (1992). Ocular lubricants and intraocular stray light. *Doc Ophthalmol* **82**(1-2), 29-31.

Veraart, H. G., van den Berg, T. J., Hennekes, R., and Adank, A. M. (1993). Stray light in photorefractive keratectomy for myopia. *Bull Soc Belge Ophtalmol* **249**, 57-62.

Veraart, H. G., van den Berg, T. J., Hennekes, R., and Adank, A. M. (1995). Stray light in photorefractive keratectomy for myopia. *Doc Ophthalmol* **90**(1), 35-42.

Veraart, H. G., van den Berg, T. J., JK, I. J., and Cardozo, O. L. (1992). Stray light in radial keratotomy and the influence of pupil size and straylight angle. *Am J Ophthalmol* **114**(4), 424-8.

Vilarrodona, L., Barrett, G. D., and Johnson, B. (2004). High-order aberrations in pseudophakia with different intraocular lenses. *J Cataract Refract Surg* **30**(3), 571-5.

Villegas, E. A., and Artal, P. (2003). Spatially resolved wavefront aberrations of ophthalmic progressive-power lenses in normal viewing conditions. *Optom Vis Sci* **80**(2), 106-14.

Vilupuru, A. S., Roorda, A., and Glasser, A. (2004). Spatially variant changes in lens power during ocular accommodation in a rhesus monkey eye. *J Vis* **4**(4), 299-309.

Vogel, A., Dick, H. B., and Krummenauer, F. (2001). Reproducibility of optical biometry using partial coherence interferometry : intraobserver and interobserver reliability. *J Cataract Refract Surg* **27**(12), 1961-8.

Vos, J. J. (1984). Disability glare: a state of the art report. *Comm Int de l'Eclairage J* **3**(2), 39-53.

Walsh, G., and Charman, W. N. (1985). Measurement of the axial wavefront aberration of the human eye. *Ophthalmic Physiol Opt* **5**(1), 23-31.

Walsh, G., Charman, W. N., and Howland, H. C. (1984). Objective technique for the determination of monochromatic aberrations of the human eye. *J Opt Soc Am A* **1**(9), 987-92.

Wang, L., Misra, M., Pallikaris, I. G., and Koch, D. D. (2002). Comparison of a ray-tracing refractometer, autorefractor, and computerized videokeratography in measuring pseudophakic eyes. *J Cataract Refract Surg* **28**(2), 276-82.

Wang, L., Wang, N., and Koch, D. D. (2003). Evaluation of refractive error measurements of the Wavescan Wavefront system and the Tracey Wavefront aberrometer. *J Cataract Refract Surg* **29**(5), 970-9.

Webb, R. H., and Hughes, G. W. (1981). Scanning laser ophthalmoscope. *IEEE Trans Biomed Eng* **28**(7), 488-92.

Webb, R. H., Penney, C. M., Sobiech, J., Staver, P. R., and Burns, S. A. (2003). SSR (spatially resolved refractometer): a null-seeking aberrometer. *Appl Opt* **42**(4), 736-44.

West, C. G., Gildengorin, G., Haegerstrom-Portnoy, G., Lott, L. A., Schneck, M. E., and Brabyn, J. A. (2003). Vision and driving self-restriction in older adults. *J Am Geriatr Soc* **51**(10), 1348-55.

Westheimer, G. (1973). Fourier analysis of vision. *Invest Ophthalmol* **12**, 86-87.

Whitaker, D., Steen, R., and Elliott, D. B. (1993). Light scatter in the normal young, elderly, and cataractous eye demonstrates little wavelength dependency. *Optom Vis Sci* **70**(11), 963-8.

Wolffsohn, J. S., Gilmartin, B., Mallen, E. A., and Tsujimura, S. (2001). Continuous recording of accommodation and pupil size using the Shin-Nippon SRW-5000 autorefractor. *Ophthalmic Physiol Opt* **21**(2), 108-13.

Wolffsohn, J. S., O'Donnell, C., Charman, W. N., and Gilmartin, B. (2004). Simultaneous continuous recording of accommodation and pupil size using the modified Shin-Nippon SRW-5000 autorefractor. *Ophthalmic Physiol Opt* **24**(2), 142-7.

Zadnik, K., Mutti, D. O., Mitchell, G. L., Jones, L. A., Burr, D., and Moeschberger, M. L. (2004). Normal eye growth in emmetropic schoolchildren. *Optom Vis Sci* **81**(11), 819-28.

Zadok, D., Levy, Y., Segal, O., Barkana, Y., Morad, Y., and Avni, I. (2005). Ocular higher-order aberrations in myopia and skiascopic wavefront repeatability. *J Cataract Refract Surg* **31**(6), 1128-32.

Zernike, F. (1934). Diffraction theory of the cut procedure and its improved form, the phase contrast method. *Physica* **1**, 689-704.

APPENDIX I. ANALYSIS OF VARIANCE TABLES

CHAPTER 4. CHANGES IN ZERNIKE COEFFICIENTS WITH ACCOMMODATION TO REAL DISTANCE TARGETS

COEFFICIENT Z(3,-3)

factor1	Dependent Variable
1	Z3_3
2	Z3_3_3m
3	Z3_3_2m
4	Z3_3_1m
5	Z3_3_0.33m

Intra-subject effects

Source		Type III Sum of squares	df	Mean square	F	Sig.
factor1	Sphericity assumed	,003	4	,001	1,530	,203
	Greenhouse-Geisser	,003	3,103	,001	1,530	,217
	Huynh-Feldt	,003	3,875	,001	1,530	,205
	Lower limit	,003	1,000	,003	1,530	,233
Error(factor1)	Sphericity assumed	,033	68	,000		
	Greenhouse-Geisser	,033	52,750	,001		
	Huynh-Feldt	,033	65,877	,001		
	Lower limit	,033	17,000	,002		

Intra-subject contrasts

Source	factor1	Type III Sum of squares	df	Mean square	F	Sig.
factor1	Linear	,000	1	,000	,311	,584
	Cuadratic	,001	1	,001	2,445	,136
	Cubic	,001	1	,001	1,587	,225
	Order 4	,001	1	,001	3,210	,091
Error(factor1)	Linear	,010	17	,001		
	Cuadratic	,005	17	,000		
	Cubic	,013	17	,001		
	Order 4	,004	17	,000		

Estimated marginal means

Estimations

factor1	Mean	Typ Error	95%.Confidence Interval	
			Upper	Lower
1	-,071	,018	-,107	-,034
2	-,063	,019	-,102	-,024
3	-,077	,020	-,118	-,036
4	-,071	,016	-,106	-,037
5	-,061	,017	-,096	-,026

Comparaciones por pares

(I) factor1	(J) factor1	Mean diff (I-J)	Error df	Sig.	95 % confidence interval for the difference	
					Lower	Upper
1	2	-,008	,006	,250	-,021	,006
	3	,006	,007	,369	-,008	,021
	4	,001	,008	,922	-,016	,018
	5	-,009	,009	,291	-,027	,009
2	1	,008	,006	,250	-,006	,021
	3	,014(*)	,006	,038	,001	,027
	4	,008	,009	,364	-,011	,027
	5	-,002	,006	,758	-,014	,010
3	1	-,006	,007	,369	-,021	,008
	2	-,014(*)	,006	,038	-,027	-,001
	4	-,006	,007	,434	-,020	,009
	5	-,016(*)	,007	,035	-,030	-,001
4	1	-,001	,008	,922	-,018	,016
	2	-,008	,009	,364	-,027	,011
	3	,006	,007	,434	-,009	,020
	5	-,010	,009	,250	-,028	,008
5	1	,009	,009	,291	-,009	,027
	2	,002	,006	,758	-,010	,014
	3	,016(*)	,007	,035	,001	,030
	4	,010	,009	,250	-,008	,028

COEFFICIENT Z(3,-1)

factor1	Dependent Variable
1	Z3_1
2	Z3_1_3m
3	Z3_1_2m
4	Z3_1_1m
5	Z3_1_0.33m

Multivariate contrasts

Effect		Value	F	Hypothesis df	Error df	Sig.
factor1	Pillai's trace	,555	4,365	4,000	14,000	,017
	Wilks' lambda	,445	4,365	4,000	14,000	,017
	Hotelling's trace	1,247	4,365	4,000	14,000	,017
	Roy's largest root	1,247	4,365	4,000	14,000	,017

Mauchly sphericity test

Intra-subjects effects	Mauchly's W	approx Chi-square	df	Sig.	Epsilon		
					Greenhouse-Geisser	Huynh-Feldt	Lower limit
factor1	,057	44,062	9	,000	,447	,496	,250

Intrasubject effectsPruebas de efectos intra-sujetos.

Source		Type III Sum of squares	df	Mean square	F	Sig.
factor1	Sphericity assumed	,028	4	,007	6,011	,000
	Greenhouse-Geisser	,028	1,789	,016	6,011	,008
	Huynh-Feldt	,028	1,985	,014	6,011	,006
	Lower limit	,028	1,000	,028	6,011	,025
Error(factor1)	Sphericity assumed	,080	68	,001		
	Greenhouse-Geisser	,080	30,407	,003		
	Huynh-Feldt	,080	33,747	,002		
	Lower limit	,080	17,000	,005		

Intra-subjects contrasts

Source	factor1	Type III Sum of squares	df	Mean square	F	Sig.
factor1	Linear	,022	1	,022	13,325	,002
	Cuadratic	,003	1	,003	1,605	,222
	Cubic	,002	1	,002	1,947	,181
	Order 4	,001	1	,001	6,183	,024
Error(factor1)	Linear	,028	17	,002		
	Cuadratic	,027	17	,002		
	Cubic	,021	17	,001		
	Order 4	,003	17	,000		

Inter.-subjects effects

Transformed Variable: Average

Source	Type III Sum of squares	df	Mean square	F	Sig.
Intersection	,112	1	,112	3,290	,087
Error	,580	17	,034		

Estimated marginal means

Estimations

factor1	Mean	Error df	95% confidence interval	
			Lower	Upper
1	,017	,024	-,033	,067
2	,025	,020	-,018	,067
3	,035	,020	-,007	,076
4	,032	,021	-,012	,076
5	,068	,019	,028	,109

Parwise comparisons

(I) factor1	(J) factor1	Mean difference (I-J)	Typ Error	Sig.(a)	95 % confidence interval for the difference(a)	
					Lower	Upper
1	2	-,008	,007	,313	-,023	,008
	3	-,018	,008	,052	-,036	,000
	4	-,015(*)	,006	,028	-,029	-,002
	5	-,052(*)	,016	,005	-,085	-,018
2	1	,008	,007	,313	-,008	,023
	3	-,010(*)	,005	,049	-,020	-5,31E-005
	4	-,007	,008	,364	-,024	,009
	5	-,044(*)	,014	,007	-,074	-,014
3	1	,018	,008	,052	,000	,036
	2	,010(*)	,005	,049	5,31E-005	,020
	4	,003	,007	,721	-,012	,017
	5	-,034	,016	,053	-,068	,000
4	1	,015(*)	,006	,028	,002	,029
	2	,007	,008	,364	-,009	,024
	3	-,003	,007	,721	-,017	,012
	5	-,036(*)	,017	,042	-,071	-,001
5	1	,052(*)	,016	,005	,018	,085
	2	,044(*)	,014	,007	,014	,074
	3	,034	,016	,053	,000	,068
	4	,036(*)	,017	,042	,001	,071

Based on estimated marginal means.
* Mean difference is significant at the ,05 level.
a Adjust for multiple comparisons. Difference less significant (equivalent to lack of adjust).

Multivariate contrasts

	Value	F	Hypothesis df	Error df	Sig.
Pillai's trace	,555	4,365(a)	4,000	14,000	,017
Wilks' lambda	,445	4,365(a)	4,000	14,000	,017
Hotelling's trace	1,247	4,365(a)	4,000	14,000	,017
Roy's largest root	1,247	4,365(a)	4,000	14,000	,017

COEFFICIENT Z(3,1)

factor1	Dependent variable
1	Z31
2	Z31_3m
3	Z31_2m
4	Z31_1m
5	Z31_0.33m

Multivariate contrasts

Effect		Value	F	Hypothesis df	Error df	Sig
factor1	Pillai's trace	,709	8,508	4,000	14,000	,001
	Wilks' lambda	,291	8,508	4,000	14,000	,001
	Hotelling's trace	2,431	8,508	4,000	14,000	,001
	Roy's largest root	2,431	8,508	4,000	14,000	,001

Mauchly's sphericity test

Intra-subject effects	Mauchly's W	Approx.Chi-square	df	Sig	Epsilon		
					Greenhouse-Geisser	Huynh-Feldt	Lower limit
factor1	,039	50,007	9	,000	,430	,473	,250

Intra-subject effects.

Source		Type III Sum of squares	df	Mean square	F	Sig
factor1	Sphericity assumed	,073	4	,018	14,965	,000
	Greenhouse-Geisser	,073	1,719	,042	14,965	,000
	Huynh-Feldt	,073	1,894	,038	14,965	,000
	Lower limit	,073	1,000	,073	14,965	,001
Error(factor1)	Sphericity assumed	,083	68	,001		
	Greenhouse-Geisser	,083	29,218	,003		
	Huynh-Feldt	,083	32,191	,003		
	Lower limit	,083	17,000	,005		

Intra-subjects contrasts

Source	factor1	Type III Sum of squares	df	Mean square	F	Sig
factor1	Linear	,058	1	,058	21,216	,000
	Cuadratic	,013	1	,013	8,197	,011
	Cubic	4,92E-005	1	4,92E-005	,132	,721
	Order 4	,002	1	,002	8,660	,009
Error(factor1)	Linear	,047	17	,003		
	Cuadratic	,026	17	,002		
	Cubic	,006	17	,000		
	Order 4	,003	17	,000		

Inter-subjects effects

Transformed variable: Average

Source	Type III Sum of squares	df	Mean square	F	Sig
Intersection	,003	1	,003	,132	,721
Error	,340	17	,020		

Estimated marginal means

Estimations

factor1	Mean	Typ. Error	95% confidence interval	
			Lower	Upper
1	-,016	,017	-,051	,019
2	-,023	,017	-,059	,013
3	-,002	,016	-,035	,031
4	,011	,015	-,021	,042
5	,057	,018	,018	,096

Parwise comparisons

(I) factor1	(J) factor1	Mean differences (I-J)	Typ. Error	Sig(a)	95 % confidence interval for the difference(a)	
					Lower	Upper
1	2	,007	,007	,327	-,008	,023
	3	-,014	,008	,112	-,031	,004
	4	-,027(*)	,010	,021	-,049	-,005
	5	-,073(*)	,018	,001	-,110	-,036
2	1	-,007	,007	,327	-,023	,008
	3	-,021(*)	,004	,000	-,030	-,013
	4	-,034(*)	,006	,000	-,047	-,020
	5	-,081(*)	,017	,000	-,116	-,045
3	1	,014	,008	,112	-,004	,031
	2	,021(*)	,004	,000	,013	,030
	4	-,013(*)	,005	,026	-,024	-,002
	5	-,059(*)	,016	,002	-,092	-,026
4	1	,027(*)	,010	,021	,005	,049
	2	,034(*)	,006	,000	,020	,047
	3	,013(*)	,005	,026	,002	,024
	5	-,047(*)	,014	,004	-,077	-,017
5	1	,073(*)	,018	,001	,036	,110
	2	,081(*)	,017	,000	,045	,116
	3	,059(*)	,016	,002	,026	,092
	4	,047(*)	,014	,004	,017	,077

Based on estimated marginal means.
* Mean difference is significant at the ,05 level.
a Adjust for multiple comparisons. Difference less significant (equivalent to lack of adjust).

Multivariate contrasts

	Value	F	Hypothesis df	Error df	Sig.
Pillai's trace	,709	8,508	4,000	14,000	,001
Wilks' lambda	,291	8,508	4,000	14,000	,001
Hotelling's trace	2,431	8,508	4,000	14,000	,001
Roy's largest root	2,431	8,508	4,000	14,000	,001

COEFFICIENT Z(3,3)

factor1	Dependent variable
1	Z33
2	Z33_3m
3	Z33_2m
4	Z33_1m
5	Z33_0.33m

Multivariate contrasts

Effect		Value	F	Hypothesis df	Error df	Sig
factor1	Pillai's trace	,045	,164	4,000	14,000	,953
	Wilks' lambda	,955	,164	4,000	14,000	,953
	Hotelling's trace	,047	,164	4,000	14,000	,953
	Roy's largest root	,047	,164	4,000	14,000	,953

Mauchly's sphericity test

Intra-subject effect	Mauchly's W	Approx. Chi-square	df	Sig	Epsilon		
					Greenhouse-Geisser	Huynh-Feldt	Lower limit
factor1	,395	14,308	9	,114	,700	,852	,250

Intra-subject effects

Source		Type III Sum of squares	df	Mean square	F	Sig
factor1	Sphericity assumed	,000	4	6,79E-005	,193	,941
	Greenhouse-Geisser	,000	2,801	9,69E-005	,193	,889
	Huynh-Feldt	,000	3,410	7,96E-005	,193	,920
	Lower limit	,000	1,000	,000	,193	,666
Error(factor1)	Sphericity assumed	,024	68	,000		
	Greenhouse-Geisser	,024	47,616	,001		
	Huynh-Feldt	,024	57,967	,000		
	Lower limit	,024	17,000	,001		

Intra-subjects contrasts

Source	factor1	Type III Sum of squares	df	Mean square	F	Sig
factor1	Linear	1,96E-008	1	1,96E-008	,000	,995
	Cuadratic	2,34E-006	1	2,34E-006	,008	,931
	Cubic	,000	1	,000	,755	,397
	Order 4	1,81E-010	1	1,81E-010	,000	,999
Error(factor1)	Linear	,009	17	,001		
	Cuadratic	,005	17	,000		
	Cubic	,006	17	,000		
	Order 4	,003	17	,000		

Inter-subject effects

Transformed variable: Average

Source	Type III Sum of squares	df	Mean square	F	Sig
Intersection	,027	1	,027	3,728	,070
Error	,124	17	,007		

Estimated marginal means

Estimations

factor1	Mean	Typ Error	95% confidence interval	
			Lower	Upper
1	,019	,010	-,002	,039
2	,015	,011	-,009	,038
3	,017	,010	-,003	,037
4	,020	,010	-,001	,040
5	,016	,009	-,002	,034

Pairwise comparisons

(I) factor1	(J) factor1	Mean differences (I-J)	Typ. Error	Sig(a)	95 % confidence interval for the difference(a)	
					Lower	Upper
1	2	,004	,006	,504	-,008	,016
	3	,002	,006	,788	-,011	,014
	4	-,001	,005	,855	-,011	,009
	5	,002	,008	,764	-,015	,020
2	1	-,004	,006	,504	-,016	,008
	3	-,002	,005	,652	-,013	,008
	4	-,005	,006	,420	-,017	,008
	5	-,001	,008	,858	-,019	,016
3	1	-,002	,006	,788	-,014	,011
	2	,002	,005	,652	-,008	,013
	4	-,003	,004	,573	-,012	,007
	5	,001	,006	,882	-,011	,013
4	1	,001	,005	,855	-,009	,011
	2	,005	,006	,420	-,008	,017
	3	,003	,004	,573	-,007	,012
	5	,003	,007	,646	-,012	,019
5	1	-,002	,008	,764	-,020	,015
	2	,001	,008	,858	-,016	,019
	3	-,001	,006	,882	-,013	,011
	4	-,003	,007	,646	-,019	,012

Based on estimated marginal means.
a Adjust for multiple comparisons. Difference less significant (equivalent to lack of adjust).

Multivariate contrasts

	Value	F	Hypothesis df	Error df	Sig.
Pillai's trace	,045	,164	4,000	14,000	,953
Wilks' lambda	,955	,164	4,000	14,000	,953
Hotelling's trace	,047	,164	4,000	14,000	,953
Roy's largest root	,047	,164	4,000	14,000	,953

COEFFICIENT Z(4,-4)

factor1	Dependent variable
1	Z4_4
2	Z4_4_3m
3	Z4_4_2m
4	Z4_4_1m
5	Z4_4_0.33m

Multivariate contrasts

Effect		Value	F	Hypothesis df	Error df	Sig
factor1	Pillai's trace	,186	,799	4,000	14,000	,545
	Wilks' lambda	,814	,799	4,000	14,000	,545
	Hotelling's trace	,228	,799	4,000	14,000	,545
	Roy's largest root	,228	,799	4,000	14,000	,545

Mauchly's sphericity test

Intra-subject effects	Mauchly's W	Approx. Chi-square	df	Sig	Epsilon		
					Greenhouse-Geisser	Huynh-Feldt	Lower limit
factor1	,123	32,298	9	,000	,463	,517	,250

Intra-subjects effects

Source		Type III Sum of squares	df	Mean square	F	Sig
factor1	Sphericity assumed	,001	4	,000	2,022	,101
	Greenhouse-Geisser	,001	1,851	,001	2,022	,152
	Huynh-Feldt	,001	2,067	,001	2,022	,146
	Lower limit	,001	1,000	,001	2,022	,173
Error(factor1)	Sphericity assumed	,012	68	,000		
	Greenhouse-Geisser	,012	31,469	,000		
	Huynh-Feldt	,012	35,147	,000		
	Lower limit	,012	17,000	,001		

Intra-subjects contrasts

Source	factor1	Type III Sum of squares	df	Mean square	F	Sig
factor1	Linear	,001	1	,001	2,798	,113
	Cuadratic	4,90E-005	1	4,90E-005	,689	,418
	Cubic	1,06E-006	1	1,06E-006	,011	,917
	Order 4	9,92E-006	1	9,92E-006	,211	,652
Error(factor1)	Linear	,008	17	,000		
	Cuadratic	,001	17	7,11E-005		
	Cubic	,002	17	9,38E-005		
	Order 4	,001	17	4,71E-005		

Inter-subjects effects

Transformed variable: Average

Source	Type III Sum of squares	df	Mean square	F	Sig
Intersection	,004	1	,004	1,394	,254
Error	,044	17	,003		

Estimated marginal means

Estimations

factor1	Mean	Typ Error	95% confidence interval	
			Lower	Upper
1	,002	,008	-,015	,018
2	,004	,006	-,010	,017
3	,005	,006	-,007	,017
4	,009	,005	-,002	,019
5	,013	,005	,003	,023

Pairwise comparisons

(I) factor1	(J) factor1	Mean differences (I-J)	Typ Error	Sig(a)	95 % confidence interval for the differencesa(a)	
					Lower	Upper
1	2	-,002	,003	,556	-,009	,005
	3	-,003	,004	,417	-,012	,005
	4	-,007	,004	,122	-,017	,002
	5	-,011	,007	,131	-,026	,004
2	1	,002	,003	,556	-,005	,009
	3	-,001	,003	,661	-,007	,005
	4	-,005	,004	,203	-,013	,003
	5	-,009	,006	,142	-,021	,003
3	1	,003	,004	,417	-,005	,012
	2	,001	,003	,661	-,005	,007
	4	-,004	,003	,167	-,010	,002
	5	-,008	,004	,087	-,017	,001
4	1	,007	,004	,122	-,002	,017
	2	,005	,004	,203	-,003	,013
	3	,004	,003	,167	-,002	,010
	5	-,004	,004	,313	-,012	,004
5	1	,011	,007	,131	-,004	,026
	2	,009	,006	,142	-,003	,021
	3	,008	,004	,087	-,001	,017
	4	,004	,004	,313	-,004	,012

Based on estimated marginal means.
a Adjust for multiple comparisons. Difference less significant (equivalent to lack of adjust).

Multivariate contrasts

	Value	F	Hypothesis df	Error df	Sig
Pillai's trace	,186	,799	4,000	14,000	,545
Wilks' lambda	,814	,799	4,000	14,000	,545
Hotelling's trace	,228	,799	4,000	14,000	,545
Roy's largest root	,228	,799	4,000	14,000	,545

COEFFICIENT Z(4,-2)

factor1	Dependent variable
1	Z4_2
2	Z4_2_3m
3	Z4_2_2m
4	Z4_2_1m
5	Z4_2_0.33m

Multivariate contrasts

Effect		Value	F	Hypothesis df	Error df	Sig.
factor1	Pillai's trace	,214	,955	4,000	14,000	,462
	Wilks' lambda	,786	,955	4,000	14,000	,462
	Hotelling's trace	,273	,955	4,000	14,000	,462
	Roy's largest root	,273	,955	4,000	14,000	,462

Mauchly's sphericity test

Intra-subject effects	Mauchly's W	Approx Chi-square	df	Sig	Epsilon		
					Greenhouse-Geisser	Huynh-Feldt	Lower limit
factor1	,269	20,229	9	,017	,710	,867	,250

Intra-subjects effects

Source		Squares sum III	df	Cuadratic mean	F	Sig
factor1	Sphericity assumed	,001	4	,000	2,053	,097
	Greenhouse-Geisser	,001	2,838	,000	2,053	,122
	Huynh-Feldt	,001	3,466	,000	2,053	,108
	Lower limit	,001	1,000	,001	2,053	,170
Error(factor1)	Sphericity assumed	,008	68	,000		
	Greenhouse-Geisser	,008	48,248	,000		
	Huynh-Feldt	,008	58,923	,000		
	Lower limit	,008	17,000	,000		

Intra-subjects contrasts

Source	factor1	Type III Sum of squares	df	Mean square	F	Sig
factor1	Linear	,001	1	,001	3,511	,078
	Cuadratic	,000	1	,000	1,359	,260
	Cubic	1,83E-005	1	1,83E-005	,259	,618
	Order 4	8,11E-005	1	8,11E-005	1,424	,249
Error(factor1)	Linear	,003	17	,000		
	Cuadratic	,002	17	,000		
	Cubic	,001	17	7,08E-005		
	Order 4	,001	17	5,69E-005		

Inter-subjects effects

Transformed variable: Average

Source	Type III Sum of squares	df	Mean square	F	Sig
Intersection	1,28E-005	1	1,28E-005	,019	,893
Error	,012	17	,001		

Estimated marginal means

Estimations

factor1	Mean	Typ Error	95% confidence interval	
			Lower	Upper
1	-,001	,004	-,009	,006
2	-,004	,003	-,011	,003
3	,000	,003	-,006	,006
4	,001	,003	-,006	,008
5	,006	,004	-,003	,015

Pairwise comparisons

(I) factor1	(J) factor1	Mean differences (I-J)	Typ Error	Sig(a)	95 % confidence interval for the difference(a)	
					Lower	Upper
1	2	,003	,004	,447	-,005	,011
	3	-,001	,003	,676	-,007	,005
	4	-,002	,004	,616	-,010	,006
	5	-,007	,004	,116	-,015	,002
2	1	-,003	,004	,447	-,011	,005
	3	-,004	,003	,126	-,010	,001
	4	-,005	,003	,144	-,012	,002
	5	-,010	,005	,053	-,020	,000
3	1	,001	,003	,676	-,005	,007
	2	,004	,003	,126	-,001	,010
	4	-,001	,002	,687	-,005	,003
	5	-,006	,003	,109	-,013	,001
4	1	,002	,004	,616	-,006	,010
	2	,005	,003	,144	-,002	,012
	3	,001	,002	,687	-,003	,005
	5	-,005	,004	,211	-,013	,003
5	1	,007	,004	,116	-,002	,015
	2	,010	,005	,053	,000	,020
	3	,006	,003	,109	-,001	,013
	4	,005	,004	,211	-,003	,013

Based on estimated marginal means.
a Adjust for multiple comparisons. Difference less significant (equivalent to lack of adjust).

Multivariate contrasts

	Value	F	Hypothesis df	Error df	Sig
Pillai's trace	,214	,955	4,000	14,000	,462
Wilks' lambda	,786	,955	4,000	14,000	,462
Hotelling's trace	,273	,955	4,000	14,000	,462
Roy's largest root	,273	,955	4,000	14,000	,462

COEFFICIENT Z(4,0)

factor1	Dependent variable
1	Z40
2	Z40_3m
3	Z40_2m
4	Z40_1m
5	Z40_0.33m

Multivariate contrasts

Effect		Value	F	Hypothesis df	Error df	Sig
factor1	Pillai's trace	,908	34,449	4,000	14,000	,000
	Wilks' lambda	,092	34,449	4,000	14,000	,000
	Hotelling's trace	9,843	34,449	4,000	14,000	,000
	Roy's largest root	9,843	34,449	4,000	14,000	,000

Mauchly's sphericity test

Intra-subjects effects	Mauchly's W	Approx. Chi-square	df	Sig	Epsilon		
					Greenhouse-Geisser	Huynh-Feldt	Lower limit
factor1	,137	30,589	9	,000	,458	,510	,250

Intra-subjects effects

Source		Type III Sum of squares	df	Mean square	F	Sig
factor1	Sphericity assumed	,105	4	,026	78,532	,000
	Greenhouse-Geisser	,105	1,830	,057	78,532	,000
	Huynh-Feldt	,105	2,040	,051	78,532	,000
	Lower limit	,105	1,000	,105	78,532	,000
Error(factor1)	Sphericity assumed	,023	68	,000		
	Greenhouse-Geisser	,023	31,114	,001		
	Huynh-Feldt	,023	34,678	,001		
	Lower limit	,023	17,000	,001		

Intra-subjects contrasts

Source	factor1	Type III Sum of squares	df	Mean square	F	Sig
factor1	Linear	,068	1	,068	97,790	,000
	Cuadratic	,027	1	,027	140,885	,000
	Cubic	,010	1	,010	36,702	,000
	Order 4	2,11E-006	1	2,11E-006	,012	,915
Error(factor1)	Linear	,012	17	,001		
	Cuadratic	,003	17	,000		
	Cubic	,005	17	,000		
	Order 4	,003	17	,000		

Inter-subjects effects

Transformed variable: Average

Source	Type III Sum of squares	df	Mean square	F	Sig
Intersección	,088	1	,088	6,382	,022
Error	,233	17	,014		

Estimated marginal means

Estimations

factor1	Mean	Typ Error	95% confidence interval	
			Lower	Upper
1	,057	,014	,028	,085
2	,046	,012	,021	,072
3	,052	,013	,024	,080
4	,037	,013	,009	,064
5	-,036	,012	-,062	-,009

Pairwise comparisons

(I) factor1	(J) factor1	Mean difference (I-J)	Typ Error	Sig(a)	95 % confidence interval for the difference(a)	
					Lower	Upper
1	2	,011(*)	,004	,010	,003	,019
	3	,005	,005	,340	-,005	,015
	4	,020(*)	,004	,000	,012	,028
	5	,093(*)	,010	,000	,072	,113
2	1	-,011(*)	,004	,010	-,019	-,003
	3	-,006	,004	,160	-,015	,003
	4	,009(*)	,004	,024	,001	,018
	5	,082(*)	,008	,000	,065	,099
3	1	-,005	,005	,340	-,015	,005
	2	,006	,004	,160	-,003	,015
	4	,015(*)	,004	,002	,006	,025
	5	,088(*)	,007	,000	,073	,103
4	1	-,020(*)	,004	,000	-,028	-,012
	2	-,009(*)	,004	,024	-,018	-,001
	3	-,015(*)	,004	,002	-,025	-,006
	5	,072(*)	,008	,000	,056	,089
5	1	-,093(*)	,010	,000	-,113	-,072
	2	-,082(*)	,008	,000	-,099	-,065
	3	-,088(*)	,007	,000	-,103	-,073
	4	-,072(*)	,008	,000	-,089	-,056

Based on estimated marginal means.
* Mean difference is significant at the ,05 level.
a Adjust for multiple comparisons. Difference less significant (equivalent to lack of adjust).

Multivariate contrasts

	Value	F	Hypothesis df	Error df	Sig
Pillai's trace	,908	34,449	4,000	14,000	,000
Wilks' lambda	,092	34,449	4,000	14,000	,000
Hotelling's trace	9,843	34,449	4,000	14,000	,000
Roy's largest root	9,843	34,449	4,000	14,000	,000

COEFFICIENT Z(4,2)

factor1	Dependent variable
1	Z42
2	Z42_3m
3	Z42_2m
4	Z42_1m
5	Z42_0.33m

Multivariate contrasts

Effect		Value	F	Hypothesis df	Error df	Sig
factor1	Pillai's trace	,568	4,604	4,000	14,000	,014
	Wilks' lambda	,432	4,604	4,000	14,000	,014
	Hotelling's trace	1,315	4,604	4,000	14,000	,014
	Roy's largest root	1,315	4,604	4,000	14,000	,014

Prueba de esfericidad de Mauchly's sphericity test

Intra-subject effects	Mauchly's W	Approx Chi-square	df	Sig	Epsilon		
					Greenhouse-Geisser	Huynh-Feldt	Lower limit
factor1	,374	15,170	9	,088	,678	,819	,250

Intra-subjects effects

Source		Type III Sum of squares	df	Mean square	F	Sig
factor1	Sphericity assumed	,004	4	,001	4,587	,002
	Greenhouse-Geisser	,004	2,712	,002	4,587	,009
	Huynh-Feldt	,004	3,277	,001	4,587	,005
	Lower limit	,004	1,000	,004	4,587	,047
Error(factor1)	Sphericity assumed	,016	68	,000		
	Greenhouse-Geisser	,016	46,105	,000		
	Huynh-Feldt	,016	55,704	,000		
	Lower limit	,016	17,000	,001		

Intra-subjects contrasts

Source	factor1	Type III Sum of squares	df	Mean square	F	Sig
factor1	Linear	,001	1	,001	3,074	,098
	Cuadratic	,000	1	,000	1,301	,270
	Cubic	,003	1	,003	8,195	,011
	Order 4	,000	1	,000	1,210	,287
Error(factor1)	Linear	,004	17	,000		
	Cuadratic	,002	17	,000		
	Cubic	,007	17	,000		
	Order 4	,003	17	,000		

Inter-subjects effectsPruebas de los efectos inter-sujetos

Transformed variable: Average

Source	Type III Sum of squares	df	Mean square	F	Sig
Intersection	,016	1	,016	2,602	,125
Error	,105	17	,006		

Estimated marginal means

Estimations

factor1	Mean	Typ Error	95% confidence interval	
			Lower	Upper
1	-,012	,010	-,033	,008
2	-,002	,008	-,019	,016
3	-,018	,010	-,039	,004
4	-,023	,010	-,043	-,003
5	-,012	,006	-,025	,001

Pairwise comparisons

(I) factor1	(J) factor1	Diferencia entre medias (I-J)	Error típ.	Sig(a)	Intervalo de confianza al 95 % para la diferencia(a)	
					Límite inferior	Límite superior
1	2	-,010(*)	,005	,049	-,020	-6,27E-005
	3	,005	,004	,181	-,003	,013
	4	,011(*)	,003	,002	,005	,017
	5	,000	,007	,968	-,014	,014
2	1	,010(*)	,005	,049	6,27E-005	,020
	3	,016(*)	,005	,006	,005	,026
	4	,021(*)	,005	,001	,010	,033
	5	,010	,005	,073	-,001	,021
3	1	-,005	,004	,181	-,013	,003
	2	-,016(*)	,005	,006	-,026	-,005
	4	,006	,004	,225	-,004	,015
	5	-,006	,006	,346	-,018	,007
4	1	-,011(*)	,003	,002	-,017	-,005
	2	-,021(*)	,005	,001	-,033	-,010
	3	-,006	,004	,225	-,015	,004
	5	-,011	,007	,108	-,025	,003
5	1	,000	,007	,968	-,014	,014
	2	-,010	,005	,073	-,021	,001
	3	,006	,006	,346	-,007	,018
	4	,011	,007	,108	-,003	,025

Based on estimated marginal means.
* Mean difference is significant at the ,05 level.
a Adjust for multiple comparisons. Difference less significant (equivalent to lack of adjust).

Multivariate contrasts

	Value	F	Hypothesis df	Error df	Sig.
Pillai's trace	,568	4,604	4,000	14,000	,014
Wilks' lambda	,432	4,604	4,000	14,000	,014
Hotelling's trace	1,315	4,604	4,000	14,000	,014
Roy's largest root	1,315	4,604	4,000	14,000	,014

COEFFICIENT Z(4,4)

factor1	Dependent variable
1	Z44
2	Z44_3m
3	Z44_2m
4	Z44_1m
5	Z44_0.33m

Multivariate contrasts

Efecto		Value	F	Hypothesis df	Error df	Sig.
factor1	Pillai's trace	,297	1,482	4,000	14,000	,260
	Wilks' lambda	,703	1,482	4,000	14,000	,260
	Hotelling's trace	,423	1,482	4,000	14,000	,260
	Roy's largest root	,423	1,482	4,000	14,000	,260

Mauchly's sphericity test

Inter-subject effects	Mauchly's W	Approx Chi-square	df	Sig	Epsilon		
					Greenhouse-Geisser	Huynh-Feldt	Lower limit
factor1	,625	7,258	9	,612	,850	1,000	,250

Intra-subjects effects.

Source		Type III Sum of squares	df	Mean square	F	Sig
factor1	Sphericity assumed	,002	4	,001	2,041	,098
	Greenhouse-Geisser	,002	3,399	,001	2,041	,111
	Huynh-Feldt	,002	4,000	,001	2,041	,098
	Lower limit	,002	1,000	,002	2,041	,171
Error(factor1)	Sphericity assumed	,017	68	,000		
	Greenhouse-Geisser	,017	57,786	,000		
	Huynh-Feldt	,017	68,000	,000		
	Lower limit	,017	17,000	,001		

Intra-subjects contrasts

Source	factor1	Type III Sum of squares	df	Mean square	F	Sig
factor1	Linear	,001	1	,001	3,565	,076
	Cuadratic	,000	1	,000	2,335	,145
	Cubic	,000	1	,000	1,553	,230
	Order 4	,000	1	,000	,472	,502
Error(factor1)	Linear	,005	17	,000		
	Cuadratic	,003	17	,000		
	Cubic	,003	17	,000		
	Order 4	,005	17	,000		

Inter.-subjects effects

Transformed variable: Average

Fuente	Type III Sum of squares	df	Mean square	F	Sig
Intersección	,013	1	,013	5,431	,032
Error	,041	17	,002		

Estimated marginal means

Estimations

factor1	Mean	Typ Error	95%.Confidence Interval	
			Upper	Lower
1	,016	,007	,000	,032
2	,012	,006	-,001	,025
3	,017	,007	,003	,031
4	,012	,005	,001	,023
5	,003	,005	-,007	,014

Pairwise comparisons

(I) factor1	(J) factor1	Mean difference (I-J)	Typ Error	Sig(a)	95 % confidence interval for the difference	
					Lower	Upper
1	2	,004	,003	,269	-,003	,011
	3	-,001	,005	,887	-,012	,011
	4	,004	,005	,493	-,007	,015
	5	,013(*)	,005	,030	,001	,024
2	1	-,004	,003	,269	-,011	,003
	3	-,005	,006	,431	-,017	,008
	4	,000	,005	,960	-,012	,011
	5	,009	,005	,092	-,002	,019
3	1	,001	,005	,887	-,011	,012
	2	,005	,006	,431	-,008	,017
	4	,004	,006	,449	-,008	,017
	5	,013(*)	,006	,039	,001	,026
4	1	-,004	,005	,493	-,015	,007
	2	,000	,005	,960	-,011	,012
	3	-,004	,006	,449	-,017	,008
	5	,009	,005	,081	-,001	,019
5	1	-,013(*)	,005	,030	-,024	-,001
	2	-,009	,005	,092	-,019	,002
	3	-,013(*)	,006	,039	-,026	-,001
	4	-,009	,005	,081	-,019	,001

Based on estimated marginal means.
* Mean difference is significant at the ,05 level.
a Adjust for multiple comparisons. Difference less significant (equivalent to lack of adjust).

Multivariate contrasts

	Value	F	Hypothesis df	Error df	Sig.
Pillai's trace	,297	1,482	4,000	14,000	,260
Wilks' lambda	,703	1,482	4,000	14,000	,260
Hotelling's trace	,423	1,482	4,000	14,000	,260
Roy's largest root	,423	1,482	4,000	14,000	,260

CHAPTER 5. SPHERICAL ABERRATION AND ETHNICITY

Univariate Analysis of Variance

Between-Subjects Factors

		N
Ethnicity	1	44
	2	30

Descriptive Statistics

Dependent Variable: mn_Z40

Ethnicity	Mean	Std. Deviation	N
1	.01967	.042524	44
2	.05297	.060846	30
Total	.03317	.052981	74

Levene's Test of Equality of Error Variances(a)

Dependent Variable: mn_Z40

F	df1	df2	Sig.
2.617	1	72	.110

Tests of Between-Subjects Effects

Dependent Variable: mn_Z40

Source	Type III Sum of Squares	df	Mean Square	F	Sig.
Corrected Model	.030(a)	2	.015	6.164	.003
Intercept	.014	1	.014	5.799	.019
Axial_length	.011	1	.011	4.282	.042
Ethnicity	.017	1	.017	7.059	.010
Error	.175	71	.002		
Total	.286	74			
Corrected Total	.205	73			

a R Squared = .148 (Adjusted R Squared = .124)

Estimated Marginal Means

Ethnicity

Dependent Variable: mn_Z40

Ethnicity	Mean	Std. Error	95% Confidence Interval	
			Lower Bound	Upper Bound
1	.020(a)	.007	.006	.035
2	.052(a)	.009	.034	.070

a Covariates appearing in the model are evaluated at the following values: Axial_length = 24.1391.

CHAPTER 6. INTRASESSION AND INTERSESSION VARIANCE IN RETINAL STRAYLIGHT MEASUREMENT

INTRASESSION ANOVA

General linear model

Intra-subjects factors

factor1	Dependent variable
1	Log1
2	Log2
3	Log3
4	Log4
5	Log5
6	Log6
7	Log7
8	Log8
9	Log9
10	Log10

Multivariate contrasts

Efecto		Value	F	Hypothesis df	Error df	Sig.
factor1	Pillai's trace	,710	1,632	9,000	6,000	,284
	Wilks' lambda	,290	1,632	9,000	6,000	,284
	Hotelling's trace	2,449	1,632	9,000	6,000	,284
	Roy's largest root	2,449	1,632	9,000	6,000	,284

Mauchly's sphericity test

Intra-subject effects	Mauchly's W	Approx Chi-square	df	Sig	Epsilon		
					Greenhouse-Geisser	Huynh-Feldt	Lower limit
factor1	,000	108,679	44	,000	,455	,667	,111

Intra-subjects effects

Source		Type III Sum of squares	df	Mean square	F	Sig
factor1	Sphericity assumed	,400	9	,044	1,257	,267
	Greenhouse-Geisser	,400	4,097	,098	1,257	,297
	Huynh-Feldt	,400	6,004	,067	1,257	,286
	Lower limit	,400	1,000	,400	1,257	,281
Error(factor1)	Sphericity assumed	4,458	126	,035		
	Greenhouse-Geisser	4,458	57,361	,078		
	Huynh-Feldt	4,458	84,059	,053		
	Lower limit	4,458	14,000	,318		

Intra-subjects contrasts

Fuente	factor1	Type III Sum of squares	df	Mean square	F	Sig
factor1	Linear	,122	1	,122	5,792	,030
	Cuadratic	,027	1	,027	,443	,517
	Cubic	,007	1	,007	,374	,551
	Order 4	,006	1	,006	,223	,644
	Order 5	,017	1	,017	,713	,413
	Order 6	,011	1	,011	,494	,494
	Order 7	,000	1	,000	,020	,888
	Order 8	,115	1	,115	4,265	,058
	Order 9	,093	1	,093	1,026	,328
Error(factor1)	Linear	,295	14	,021		
	Cuadratic	,861	14	,061		
	Cubic	,278	14	,020		
	Order 4	,386	14	,028		
	Order 5	,342	14	,024		
	Order 6	,324	14	,023		
	Order 7	,324	14	,023		
	Order 8	,376	14	,027		
	Order 9	1,271	14	,091		

Inter.-subjects effects

Transformed variable: Average

Source	Type III Sum of squares	df	Mean square	F	Sig
Intersection	141,368	1	141,368	769,839	,000
Error	2,571	14	,184		

INTERSESSION ANOVA

General linear model

Intra-subjects factors

factor1	Dependent variable
1	LOG1
2	LOG2
3	LOG3
4	LOG4
5	LOG5

Multivariate contrasts

Effect		Value	F	Hypothesis df	Error df	Sig.
factor1	Pillai's trace	,724	,656(a)	4,000	1,000	,715
	Wilks' lambda	,276	,656(a)	4,000	1,000	,715
	Hotelling's trace	2,624	,656(a)	4,000	1,000	,715
	Roy's largest root	2,624	,656(a)	4,000	1,000	,715

Mauchly's sphericity test

Intra-subject effects	Mauchly's W	Approx Chi-square	df	Sig	Epsilon		
					Greenhouse-Geisser	Huynh-Feldt	Lower limit
factor1	,065	6,616	9	,755	,648	1,000	,250

Intra-subjects effects

Source		Type III Sum of squares	df	Mean square	F	Sig
factor1	Sphericity assumed	,026	4	,007	2,456	,088
	Greenhouse-Geisser	,026	2,591	,010	2,456	,126
	Huynh-Feldt	,026	4,000	,007	2,456	,088
	Lower limit	,026	1,000	,026	2,456	,192
Error(factor1)	Sphericity assumed	,043	16	,003		
	Greenhouse-Geisser	,043	10,363	,004		
	Huynh-Feldt	,043	16,000	,003		
	Lower limit	,043	4,000	,011		

Intra-subjects contrasts

Source	factor1	Type III Sum of squares	df	Mean square	F	Sig
factor1	Linear	,020	1	,020	4,157	,111
	Cuadratic	,002	1	,002	1,561	,280
	Cubic	,001	1	,001	,223	,662
	Order 4	,003	1	,003	1,654	,268
Error(factor1)	Linear	,019	4	,005		
	Cuadratic	,006	4	,001		
	Cubic	,009	4	,002		
	Order 4	,008	4	,002		

Inter.-subjects effects

Transformed variable: Average

Source	Type III Sum of squares	df	Mean square	F	Sig
Intersection	18,530	1	18,530	628,221	,000
Error	,118	4	,029		

CHAPTER 7. REPEATED MEASURES ANOVA FOR THE OBJECTIVE METHOD OF DETERMINATION OF INTRAOCULAR SCATTER ON MODEL EYES. EFFECT OF REALIGNMENT AND MISALIGNMENT.

General linear model

Intra-subject effects

factor1	Dependent variable
1	SESSION1
2	SESSION2
3	REFOCUSING
4	MISALIGNED

Multivariate contrasts

Efecto		Value	F	Hypothesis df	Error df	Sig.
factor1	Pillai's trace	,715	2,504	3,000	3,000	,235
	Wilks' lambda	,285	2,504	3,000	3,000	,235
	Hotelling's trace	2,504	2,504	3,000	3,000	,235
	Roy's largest root	2,504	2,504	3,000	3,000	,235

Mauchly's sphericity test

Intra-subject effects	Mauchly's W	Approx Chi-square	df	Sig	Epsilon		
					Greenhouse-Geisser	Huynh-Feldt	Lower limit
factor1	,086	9,118	5	,115	,455	,569	,333

Intra-subject effects

Source		Type III Sum of squares	df	Mean square	F	Sig
factor1	Sphericity assumed	106,632	3	35,544	1,770	,196
	Greenhouse-Geisser	106,632	1,366	78,043	1,770	,234
	Huynh-Feldt	106,632	1,706	62,516	1,770	,227
	Lower limit	106,632	1,000	106,632	1,770	,241
Error(factor1)	Sphericity assumed	301,281	15	20,085		
	Greenhouse-Geisser	301,281	6,832	44,101		
	Huynh-Feldt	301,281	8,528	35,327		
	Lower limit	301,281	5,000	60,256		

Intra-subject contrasts

Source	factor1	Type III Sum of squares	df	Mean square	F	Sig
factor1	Linear	98,140	1	98,140	3,044	,142
	Cuadratic	7,983	1	7,983	,370	,570
	Cubic	,509	1	,509	,079	,790
	Order 4	161,221	5	32,244		
Error(factor1)	Linear	107,931	5	21,586		
	Cuadratic	32,130	5	6,426		

Inter.-subject effects

Transformed variable: Average

Source	Type III Sum of squares	df	Mean square	F	Sig
Intersection	130918,697	1	130918,697	3796,300	,000
Error	172,429	5	34,486		

Estimated marginal means

Estimations

factor1	Mean	Typ Error	95%.confidence interval	
			Lower	Upper
1	77,212	3,269	68,808	85,617
2	73,990	1,403	70,384	77,596
3	72,572	1,474	68,783	76,360
4	71,656	,980	69,136	74,176

Pairwise comparisons

(I) factor1	(J) factor1	Mean difference (I-J)	Typ Error	Sig(a)	95 % confidence interval for the difference(a)	
					Límite inferior	Límite superior
1	2	3,223	2,611	,272	-3,489	9,934
	3	4,641	4,021	,301	-5,696	14,977
	4	5,556	2,869	,111	-1,818	12,931
2	1	-3,223	2,611	,272	-9,934	3,489
	3	1,418	2,159	,540	-4,131	6,967
	4	2,334	1,504	,182	-1,534	6,201
3	1	-4,641	4,021	,301	-14,977	5,696
	2	-1,418	2,159	,540	-6,967	4,131
	4	,916	1,426	,549	-2,749	4,580
4	1	-5,556	2,869	,111	-12,931	1,818
	2	-2,334	1,504	,182	-6,201	1,534
	3	-,916	1,426	,549	-4,580	2,749

Based on estimated marginal means.
a Adjust for multiple comparisons. Difference less significant (equivalent to lack of adjust).

Contrastes multivariados

	Value	F	Hypothesis df	Error df	Sig.
Pillai's trace	,715	2,504	3,000	3,000	,235
Wilks' lambda	,285	2,504	3,000	3,000	,235
Hotelling's trace	2,504	2,504	3,000	3,000	,235
Roy's largest root	2,504	2,504	3,000	3,000	,235

CHAPTER 8. MULTIVARIATE ANALYSIS OF VARIANCE TO DETERMINE THE EFFECT OF IOL TYPE ON INTRAOCULAR SCATTER MEASUREMENTS.

General Linear Model

Between-Subjects Factors

		N
Lens	1	15
	2	17
	3	10
	4	22

Descriptive Statistics

	Lens	Mean	Std. Deviation	N
Log_s	1	1.1870	.22528	15
	2	1.2952	.26207	17
	3	1.2003	.22465	10
	4	1.1107	.17070	22
	Total	1.1916	.22549	64
Max_SD	1	137.1063	16.85997	15
	2	139.7984	16.15066	17
	3	136.5440	15.97232	10
	4	134.3275	17.02678	22
	Total	136.7783	16.34288	64

Box's Test of Equality of Covariance Matrices

Box's M	10.141
F	1.051
df1	9
df2	14232.238
Sig.	.396

Multivariate Tests

Effect		Value	F	Hypothesis df	Error df	Sig.	Partial Eta Squared
Intercept	Pillai's trace	.989	2611.864(a)	2.000	59.000	.000	.989
	Wilks' lambda	.011	2611.864(a)	2.000	59.000	.000	.989
	Hotelling's trace	88.538	2611.864(a)	2.000	59.000	.000	.989
	Roy's largest root	88.538	2611.864(a)	2.000	59.000	.000	.989
Lens	Pillai's trace	.110	1.167	6.000	120.000	.328	.055
	Wilks' lambda	.890	1.183(a)	6.000	118.000	.320	.057
	Hotelling's trace	.124	1.198	6.000	116.000	.313	.058
	Roy's largest root	.124	2.471(b)	3.000	60.000	.070	.110

Levene's Test of Equality of Error Variances

	F	df1	df2	Sig.
Log_s	2.006	3	60	.123
Max_SD	.077	3	60	.972

Tests of Between-Subjects Effects

Source	Dependent Variable	Type III Sum of Squares	df	Mean Square	F	Sig.	Partial Eta Squared
Corrected Model	Log_s	.328(a)	3	.109	2.278	.089	.102
	Max_SD	289.364(b)	3	96.455	.350	.789	.017
Intercept	Log_s	84.795	1	84.795	1769.286	.000	.967
	Max_SD	1107453.991	1	1107453.991	4018.024	.000	.985
Lens	Log_s	.328	3	.109	2.278	.089	.102
	Max_SD	289.364	3	96.455	.350	.789	.017
Error	Log_s	2.876	60	.048			
	Max_SD	16537.292	60	275.622			
Total	Log_s	94.076	64				
	Max_SD	1214158.609	64				
Corrected Total	Log_s	3.203	63				
	Max_SD	16826.657	63				

a R Squared = .102 (Adjusted R Squared = .057)
b R Squared = .017 (Adjusted R Squared = -.032)

APPENDIX II. PUBLICATIONS AS A RESULT OF THIS THESIS

A.1. Publications to refereed journals

The following contributions of this research have been published in different peer-reviewed journals:

- Cervino A, Hosking SL, Sammi GK, Naroo SA, Gilmartin B. Wavefront analyzers induce instrument myopia. *J Refract Surg.* 2006; 22: 795-803

- Cervino A, Hosking SL, Dunne MCM. Operator-induced errors in Hartmann-Shack wavefront sensing: A model eye study. *J Cataract Refract Surg.* 2007; 33: 115-121

- Cervino A, Hosking SL, Montes-Mico R, Bates K. Ocular wavefront analyzers. A review. *J Refract Surg.* 2007; Accepted

A.2. Conference abstracts published

The following abstracts have been published in peer-reviewed journals:

- A. Cervino, SL Hosking, SA Naroo, MCM Dunne (2004). Repeatability of the Complete Ophthalmic Analysis System (COAS) on determining higher order aberrations on model eyes. *Ophthalmic Physiol Opt* **24**, 148-57

- A Cervino, SL Hosking, SA Naroo, B Gilmartin (2005). *Determination of refractive error with wavefront analyzers. Ophthalmic Physiol Opt* **25**, *464-75*

Wavefront Analyzers Induce Instrument Myopia

Alejandro Cervino, OD(EC), MCOptom; Sarah L. Hosking, BSc(Hon), PhD, MCOptom, FAAO, DBO; Gurjeet K. Rai, BSc(Hon), MCOptom; Shezhad A. Naroo, BSc(Hon), MSc, PhD, MCOptom, FIACLE; Bernard Gilmartin, BSc(Hon), PhD, FCOptom, FAAO

ABSTRACT

PURPOSE: To assess the accuracy of three wavefront analyzers versus a validated binocular open-view autorefractor in determining refractive error in non-cycloplegic eyes.

METHODS: Eighty eyes were examined using the SRW-5000 open-view infrared autorefractor and, in randomized sequence, three wavefront analyzers: 1) OPD-Scan (NIDEK, Gamagori, Japan), 2) WASCA (Zeiss/Meditec, Jena, Germany), and 3) Allegretto (WaveLight Laser Technologies AG, Erlangen, Germany). Subjects were healthy adults (19 men and 21 women; mean age: 20.8±2.5 years). Refractive errors ranged from +1.5 to −9.75 diopters (D) (mean: +1.83±2.74 D) with up to 1.75 D cylinder (mean: 0.58±0.53 D). Three readings were collected per instrument by one examiner without anticholinergic agents. Refraction values were decomposed into vector components for analysis, resulting in mean spherical equivalent refraction (M) and J_0 and J_{45} being vectors of cylindrical power at 0° and 45°, respectively.

RESULTS: Positive correlation was observed between wavefront analyzers and the SRW-5000 for spherical equivalent refraction (OPD-Scan, r=0.959, $P<.001$; WASCA, r=0.981, $P<.001$; Allegretto, r=0.942, $P<.001$). Mean differences and limits of agreement showed more negative spherical equivalent refraction with wavefront analyzers (OPD-Scan, 0.406±0.768 D [range: 0.235 to 0.580 D] [$P<.001$]; WASCA, 0.511±0.550 D [range: 0.390 to 0.634 D] [$P<.001$]; and Allegretto, 0.434±0.904 D [range: 0.233 to 0.635 D] [$P<.001$]). A second analysis eliminating outliers showed the same trend but lower differences: OPD-Scan (n=75), 0.24±0.41 D (range: 0.15 to 0.34 D) ($P<.001$); WASCA (n=78), 0.46±0.47 D (range: 0.36 to 0.57 D) ($P<.001$); and Allegretto (n=77), 0.30±0.62 D (range: 0.16 to 0.44 D) ($P<.001$). No statistically significant differences were noted for J_0 and J_{45}.

CONCLUSIONS: Wavefront analyzer refraction resulted in 0.30 D more myopia compared to SRW-5000 refraction in eyes without cycloplegia. This is the result of the accommodation excess attributable to instrument myopia. For the relatively low degrees of astigmatism in this study (≤2.0 D), good agreement was noted between wavefront analyzers and the SRW-5000. [*J Refract Surg.* 2006;22:795-803.]

Ocular wavefront analysis systems are widely considered state-of-the-art autorefractors, which go beyond the assessment of spherocylindrical error.[1-3] Although autorefraction per se is commonly used as a starting point for subjective refraction, or for refractive screening purposes,[4,5] wavefront analyzers may be used to establish higher and lower order aberrations prior to refractive surgical techniques, and appropriate interpretation of their output is therefore critical to a successful surgical outcome.

In customized refractive surgery procedures, greater accuracy of wavefront analysis preoperatively should translate into better results of the surgery itself, as well as the assessment of these results in subsequent follow-up. This is particularly important when measuring the aberrations of the eye in normal viewing conditions. Currently, the assessment of wavefront aberrations with clinical wavefront analyzers is commonly performed after instillation of dilating drops to ensure a pupil size sufficient to facilitate collection of wavefront readings. Pharmacologically induced dilation of the pupil prior to wavefront aberration assessment is currently a subject of debate, as it would offer an aberration profile that is less relevant to the natural pupil view normally experienced by the patient.[6] A balance exists between the need for a sufficiently large pupil to provide reliable aberrometry data and the desire to establish the impact of aberrations as they affect the patient in the natural viewing state. It therefore follows that the acquisition of clinically relevant, stable refractive/aberrometry data without the use of dilating agents would provide an ideal baseline for treatment.

From the School of Life and Health Sciences, Aston University, United Kingdom (Cervino, Hosking, Rai, Naroo, Gilmartin); and the School of Optics and Optometry, Universidad de Santiago de Compostela, Spain (Cervino).

The authors have no proprietary or financial interest in the materials presented herein.

Correspondence: Sarah L. Hosking, Aston Academy of Life Sciences, School of Life and Health Sciences, Aston University, B4 7ET Birmingham, United Kingdom. Tel: 44 121 204 3800; Fax: 44 121 333 4220; E-mail: S.L.Hosking@aston.ac.uk

Received: October 20, 2005

Accepted: March 9, 2006

Posted online: July 15, 2006

Shack-Hartmann sensors exhibit good agreement with open field autorefractors, both centrally and peripherally in cycloplegic eyes.[7] Because cycloplegic refraction invariably differs from manifest refraction, it follows that the corresponding wavefront error will differ from that found in the non-cycloplegic state due to the effect on the tone of the ciliary muscle. Pupil dilation with anticholinergic agents typically has a modest effect in reducing distance refraction, particularly in adults; however, it can reduce the range of near accommodation by up to 6.0 diopters (D), which in turn reduces the impact of instrument myopia.[8] Instrument myopia is attributed to a relatively low level surfeit of accommodation, and variations in accommodation have been widely reported to induce variations in higher order aberrations.[9-11] Therefore, when patients are not dilated pharmacologically, it is imperative to know that excessive instrument myopia is not being induced.

The OPD-Scan/ARK-10000 (NIDEK, Gamagori, Japan) is a device that determines wavefront aberration using the principle of dynamic skiascopy. With this device, an infrared slit scans across the pupil and measures the time difference of the light reflected by the retina between the center and several photodetectors on each side from the center.[2,12] The slit rotates through 180°, covering all 360° semi-meridians. The system then generates autorefraction data as well as wavefront aberrations from the difference in refractive power across the pupil area. Little has been reported on the performance of clinical devices using this principle, showing poor repeatability for higher order aberration values in non-cycloplegic eyes[13] and close agreement with Shack-Hartmann wavefront sensors in determining root-mean-square (RMS) values in model eyes and human eyes with induced mydriasis[14]; however, it has been successfully coupled to laser systems for customized refractive surgery procedures[15-19] and for the assessment of the optical quality of pathological and postoperative eyes.[20]

The Wavefront Analysis Supported Customized Ablation system (WASCA; Zeiss/Meditec, Jena, Germany) is a Shack-Hartmann wavefront analyzer. Most current clinical wavefront analyzers use this principle. If a wavefront is divided spatially, then each subdivision can be approximated to a tilted flat wave. The reconstruction of the tilts of every division will result in an approximation to the original wavefront,[21] a process that forms the basis of all Shack-Hartmann wavefront analyzers. The sensor used by the WASCA gives highly accurate and reproducible measures of both low and higher order aberrations up to the fourth order in human and model eyes[22] with low variability.[23]

The Allegretto Wave analyzer (WaveLight Laser Technologies AG, Erlangen, Germany), developed by Mierdel et al,[24,25] is an objective version of the Tscherning aberroscope. This method uses a dot pattern mask, which allows several laser rays from the original beam to be projected on the retina. Five to ten frames of the image formed on the retina are first captured and defined through a small aperture and then deformed to greater and lesser extents depending on the aberrations produced by the eye.[26,27] The deviation of each retinal spot from its equivalent in the ideal reference image is measured and processed to give local slopes and, therefore, the corresponding wavefront aberrations. Good reproducibility has been demonstrated for this technique for measures of spherocylindrical refraction and total RMS values for higher order aberrations in human eyes.[26]

All three wavefront analyzers use a closed field internal fixation target, imaged at infinity to minimize accommodation during measurements. In the OPD, the internal target consists of a road receding into the distance. In contrast, a high contrast circular web-like grid and an orange light emitting diode with a central star are the fixation targets for the WASCA and Allegretto, respectively.

Closed field autorefractors are sometimes considered less suitable as a starting point for subjective refraction than other procedures, such as retinoscopy.[28,29] The Shin-Nippon SRW-5000, also marketed as Grand Seiko WV500 (Shin-Nippon Ltd, Tokyo, Japan), is an infrared, open-view, objective autorefractor. Its open-view arrangement allows an unimpeded 63.4° horizontal (33.7° either side of fixation) by 31.5° vertical (14.8° above fixation and 16.7° below fixation) binocular view and thus minimizes instrument myopia. It has been shown to compare favorably with subjective refraction, being reliable in both adults (mean difference for the spherical equivalent refraction 0.16±0.44 D)[30] and children (mean difference for the spherical equivalent refraction 0.24±0.34 D [cycloplegic]),[31] and can be converted to measure continuously the accommodative response with high precision.[32,33] For these reasons it will be used in this report as the gold standard against which to assess the performance of the OPD-Scan, WASCA, and Allegretto in the determination of spherocylindrical refractive error without cycloplegia.

The clinical application of wavefront analysis is generally to measure ocular aberrations with the eye in its natural state, often in the pre- and postoperative setting. The efficacy of the closed field targets used in wavefront analyzers to relax a patient's accommodation during the measurement process in eyes without cycloplegia is unknown. By comparison to a validated objective

TABLE 1

Descriptive Statistics for the Different Components of the Power Vectors Corresponding to the Measurements Obtained With the SRW-5000 and Three Wavefront Analyzers

Instrument	Power Vector	Minimum (D)	Maximum (D)	Mean (D)	SD (D)
SRW-5000	M	−9.88	2.19	−2.1158	2.6923
	J_0	−0.82	0.80	−0.0080	0.2440
	J_{45}	−1.77	1.04	0.0008	0.3120
OPD-Scan/ARK10000	M	−9.88	1.75	−2.5219	2.5864
	J_0	−1.31	0.37	−0.0478	0.2540
	J_{45}	−0.45	1.54	0.0471	0.2479
WASCA	M	−9.44	1.28	−2.6270	2.4739
	J_0	−0.60	1.05	−0.0220	0.1904
	J_{45}	−0.28	0.71	0.0156	0.1329
Allegretto	M	−9.00	2.58	−2.5501	2.4583
	J_0	−1.48	0.47	−0.0612	0.2894
	J_{45}	−7.49	0.81	−0.0745	0.8724

SD = standard deviation, M = mean spherical equivalent of the refraction, J_0 = Jackson cross cylinder at 0°, J_{45} = Jackson cross cylinder at 45°

refractive technique, this study aims to show whether wavefront analyzer readings taken with physiological mydriasis only is a safe method by which to perform wavefront analysis. The performance of the OPD-Scan, WASCA, and Allegretto wavefront analyzers as clinical autorefractors for the determination of non-cycloplegic refractive error is examined in a group of young adults.

PATIENTS AND METHODS

The refractive errors of 80 eyes of 40 young adults (19 men and 21 women; mean age 20.8±2.5 years) with refractive errors ranging from +1.5 to −9.75 D sphere (mean: −1.83±2.74 D) and up to 1.75 D cylinder (mean: 0.58±0.53 D) were examined with the SRW-5000 autorefractor, OPD-Scan, WASCA, and Allegretto wavefront analyzers under similar low illumination conditions. Initially, right and left eyes were plotted separately (as Bland-Altman difference versus mean plots), but because no differences were found, both eyes were included in the analysis.

This study was approved by the University Ethical Committee of Aston University. All procedures follow the agreement of the Declaration of Helsinki. Measurements were performed after informed consent was obtained from all volunteers.

The examinations were performed by a single examiner (A.C.). Three readings of spherocylindrical refractive error were obtained for the central 5 mm from each of the wavefront analyzers.

Refraction data in conventional clinical notation present a problem for analysis and comparison due to the variance in astigmatic power and axis and consequently need to be transformed to dioptric power space for ready comparison.[34,35] For this reason, data were converted into power vector representation as a spherical component M, equal to the mean spherical equivalent of the refraction (sphere+½ cylinder) and a cylindrical component being represented by a Jackson cross cylinder at 0°, with a power J_0 (½ cylinder×cos(2axis)), and a Jackson cross cylinder at 45°, with power J_{45} (½ cylinder×sin(2axis)).[36]

Wavefront and refraction data were obtained for the central 5 mm with all three wavefront analyzers, as it would be the closest diameter to the 3 mm analyzed by the SRW-5000 but still offering clinically useful wavefront aberration data.

The bias was assessed statistically (SPSS 12.0; SPSS Inc, Chicago, Ill) as the mean of the differences compared to zero. The hypothesis of zero bias was assessed by two-tailed paired *t* tests with the Bonferroni adjustment for repeated comparisons, so that $P<.012$ was the criterion for statistical significance.

Plots of difference against mean were used to represent the agreement between methods.[37]

RESULTS

The descriptive statistics for the vectorial components M, J_0, and J_{45} given by the four instruments, as

TABLE 2

Mean Difference, Significance Level, and 95% Limits of Agreement Between the SRW-5000 and Wavefront Analyzers for the Components M, J_0, and J_{45}

					Limits of Agreement (D)	
Instrument	Vector	Mean (D)	SD (D)	*P* Value	Mean −1.96*SD	Mean +1.96*SD
OPD-Scan	M	0.41	0.77	.000	0.23	0.58
	J_0	0.04	0.38	.358	−0.05	0.13
	J_{45}	−0.05	0.48	.388	−0.15	0.06
WASCA	M	0.51	0.55	.000	0.39	0.63
	J_0	−0.10	0.28	.747	−0.07	0.05
	J_{45}	−0.01	0.37	.723	−0.10	0.07
Allegretto	M	0.43	0.90	.000	0.23	0.63
	J_0	0.053	0.40	.240	−0.04	0.14
	J_{45}	0.07	0.98	.495	−0.14	0.29

SD = standard deviation, M = mean spherical equivalent of the refraction, J_0 = Jackson cross cylinder at 0°, J_{45} = Jackson cross cylinder at 45°

shown in Table 1, indicate slightly higher negative values for the three wavefront analyzers for the M, J_0, and J_{45} components compared to the autorefractor.

Good correlation between the readings obtained for the spherical equivalent M with the three wavefront analyzers and the autorefractor was evident (Pearson's correlation coefficients were 0.959, 0.981, and 0.942 for the OPD-Scan, WASCA, and Allegretto, respectively). However, as shown in Table 2, the mean differences, level of significance, and limits of agreement for the three components yield, for each of the wavefront analyzers, more negative power for the M component: OPD-Scan, 0.41±0.79 D (range: 0.23 to 0.58 D), $P<.001$; WASCA, 0.51±0.55 D (range: 0.39 to 0.63 D), $P<.001$; and Allegretto, 0.43±0.77 D (range: 0.23 to 0.63 D), $P<.001$; however, no statistically significant differences were noted for the astigmatic components J_0 and J_{45} (−0.01±0.29, $P=.832$ and −0.03±0.32, $P=.474$, respectively) for OPD-Scan, WASCA, and Allegretto.

Bland-Altman dispersion plots show that each of the three wavefront analyzers induce approximately 0.50 D more myopia than the SRW-5000 ($P<.001$) and a positive bias towards smaller refractive errors, showing less differences between the wavefront analyzers and the SRW-5000 for more myopic eyes. The WASCA shows the smallest confidence intervals and fewer outliers, whereas the OPD-Scan shows the lowest mean difference compared to the SRW-5000 (Figs 1-3).

When the outliers observed in Figures 1-3 are removed, stating a criteria of differences ≤2.0 D, and a new analysis is done (Table 3), the mean differences and confidence intervals for the M component are reduced to: OPD-Scan (n=75), 0.24±0.41 D (range: 0.15 to 0.34 D) ($P<.001$); WASCA (n=78), 0.46±0.47 D (range: 0.36 to 0.57 D) ($P<.001$); and Allegretto (n=77), 0.30±0.62 D (range: 0.16 to 0.44 D) ($P<.001$), although the same trend can be observed in the corresponding Bland-Altman dispersion plots (Figs 4-6).

The astigmatic components J_0 and J_{45} show mean differences close to zero, which are not statistically significant, compared to the SRW-5000. Confidence intervals are smaller for the WASCA and OPD-Scan, and considerably wider for the Allegretto (Fig 7).

DISCUSSION

The results of this study show statistically significant differences between the wavefront analyzers and the SRW-5000 autorefractor for the spherical component M of the power vector. Specifically, the mean value of M is approximately 0.30 D more myopic when measured using wavefront analyzer technology. We suggest that this finding is the result, at least in part, of instrument myopia induced using these technologies. This finding is consistent with the differences obtained by Jorge et al[29] in comparing closed-field autorefraction, retinoscopy, and subjective refraction, also in eyes without cycloplegia. Retinoscopy was found to be a better starting point for subjective refraction than close-field autorefraction as the latter was approximately 0.50 D more myopic, possibly due to instrument myopia. In a study comparing refractions in young myopic eyes with and without cycloplegia as measured using the Complete Ophthalmic Analysis System (COAS) aberrometer (a Shack-Hartmann aberrometer with the same

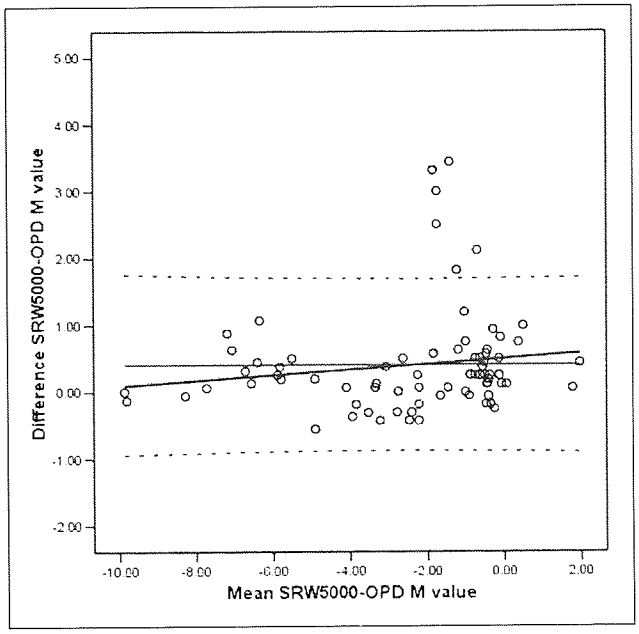

Figure 1. Bland-Altman plot for differences against mean (and 95% confidence intervals) and regression line between the SRW-5000 and the OPD-Scan for the spherical component M in diopters.

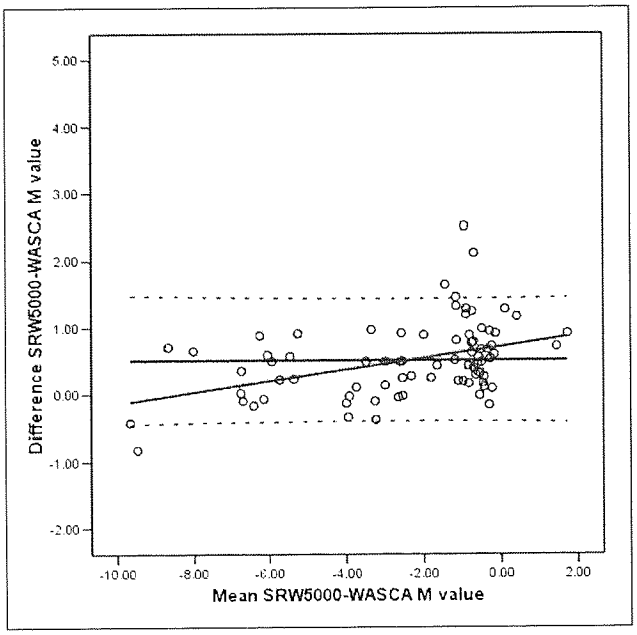

Figure 2. Bland-Altman plot for differences against mean (and 95% confidence intervals) and regression line between the SRW-5000 and the WASCA for the spherical component M in diopters.

sensor as the WASCA), the NIDEK ARK-2000 autorefractor, and subjective refraction, the wavefront analyzer and autorefractor each showed a vector error of 0.3 to 0.4 D without cycloplegia; under cycloplegia, the vector error for the COAS remained unchanged.[1] The lower values of instrument myopia found in this study could possibly be due to the range of refractive errors sampled, as the authors suggest in a more recent study with results in close agreement with those reported here.[38] Zadok et al[13] reported low repeatability for the OPD-Scan in non-cycloplegic eyes, and suggest disruptions in the tear film and accommodative microfluctuations as a possible cause.

The confidence intervals from the Bland-Altman plots indicate the variability of the data with respect to the SRW-5000, such that a narrow interval indicates better agreement. The confidence intervals in this sample were ±0.171 for OPD-Scan, ±0.201 for Allegretto, and ±0.121 for WASCA, suggesting that the agreement was slightly better for WASCA and slightly worse for Allegretto. After removing the outliers from the analysis and plots, the confidence intervals were ±0.096 for OPD-Scan, ±0.140 for Allegretto, and ±0.106 for WASCA, making it slightly better for OPD-Scan and slightly worse for Allegretto.

Compared to the SRW-5000 there was a trend for the myopic overcorrection measured using the wavefront analyzers to be greater in low degrees of myopia or hypermetropia, as demonstrated by the positive regression line on each graph. This regression line was shallow for the OPD-Scan, suggesting only a mild effect of absolute power, whereas the Allegretto exhibited a steeper regression line indicating that the effect

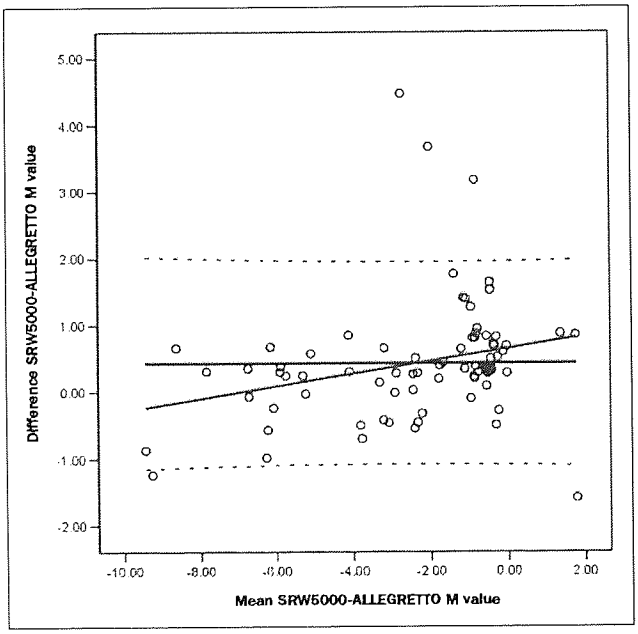

Figure 3. Bland-Altman plot for differences against mean (and 95% confidence intervals) and regression line between the SRW-5000 and the Allegretto for the spherical component M in diopters.

TABLE 3

Mean Difference, Significance Level, and 95% Limits of Agreement Between the SRW-5000 and Wavefront Analyzers for the M Component After Removing Outliers

					Limits of Agreement (D)	
Instrument	**N**	**Mean**	**SD**	***P* Value**	**Mean −1.96*SD**	**Mean +1.96*SD**
OPD-Scan	75	0.240	0.41	.000	0.15	0.34
WASCA	78	0.046	0.47	.000	0.36	0.57
Allegretto	77	0.300	0.62	.000	0.16	0.44

SD = standard deviation

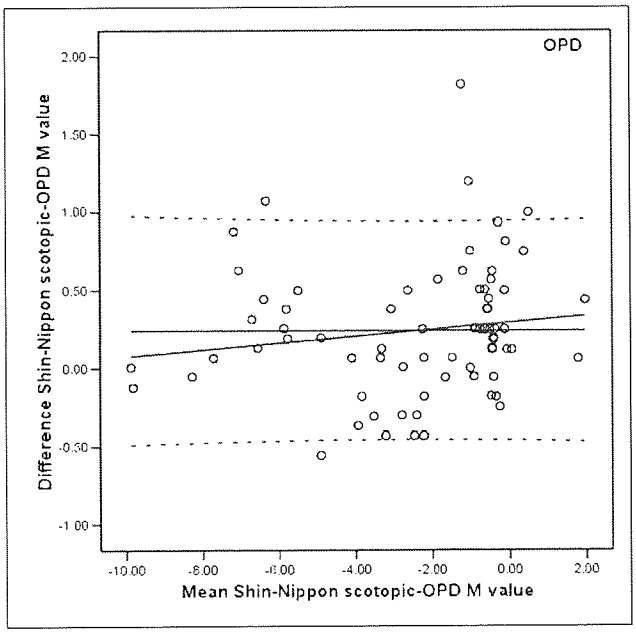

Figure 4. Bland-Altman plot for differences against mean (and 95% confidence intervals) and regression line between the SRW-5000 and the OPD-Scan for the spherical component M in diopters after removing the outliers.

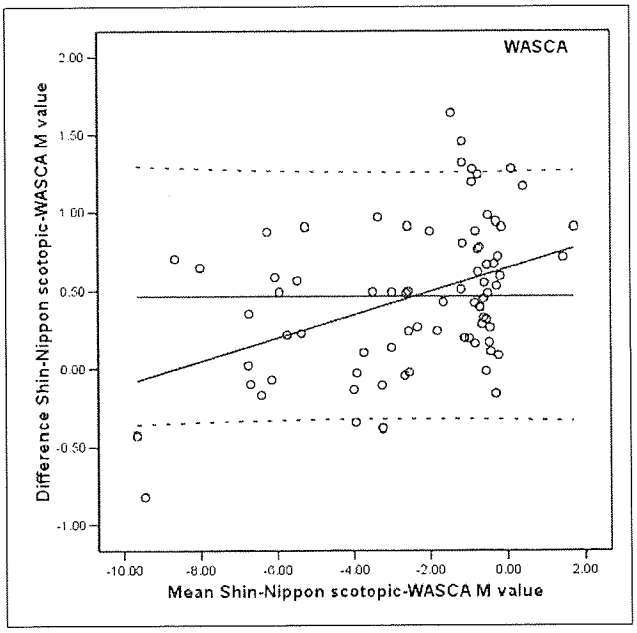

Figure 5. Bland-Altman plot for differences against mean (and 95% confidence intervals) and regression line between the SRW-5000 and the WASCA for the spherical component M in diopters after removing the outliers.

was greater with this device. In addition, careful inspection of the Bland-Altman plots shows a number of data points falling outside of the limits of agreement. This suggests that in each case, some patients differ in measurement from the SRW-5000 by an amount that is outside the normal variability of the device. Typically, these outliers arise when the actual refraction is <-2.00 D, and the wavefront analyzer errors in these cases can be as high as -3.50 D (OPD-Scan) or even -4.50 D (Allegretto). It is important to note that comparison of the data shows that the outliers obtained in the three data sets can be attributed to both eyes of the same few patients in each case, suggesting that this is a finding that arises in certain patients and will affect all devices to some lesser or greater extent. These outliers account for the positive regression line and suggest that the interpretation of myopia <-2.00 D when measured with all three devices, but particularly with the OPD-Scan and Allegretto devices, can not be relied upon on a case-wise basis when cycloplegia is not used.

Differences in the cylindrical components were not statistically significant. This suggests that for the mild to moderate degrees of astigmatism exhibited within the study sample all three methods provided reliable cylindrical data. Conclusions should not be drawn regarding the determination of astigmatism of values greater than those included in this study.

Overall, the three wavefront analyzers demonstrate similar behaviors regarding accuracy and repeatability of measurement although particular differences arose in relation to the effects of absolute refraction, limits of agreement, and the presence of outliers. The different fixation targets used by the three devices may play some role in causing these differences. For example, the OPD-Scan uses a natural scene similar to that used in closed-field autorefractors, whereas the WASCA uses a high contrast web-like pattern and the Allegretto uses an orange light emitting diode with a central star pattern. Equally, the differences in the wavelengths used by the different fixation targets may result in a different response by the accommodation system due to the presence of chromatic aberration.[39] The relatively narrower limits of agreement and more moderate outliers observed in the WASCA device would suggest that, if the target is a factor, it may have the better target for the purpose, particularly in eyes with lower degrees of myopia.

It is possible that the mathematical derivations of refractive error impact the agreement with the autorefractor findings. For small pupil sizes, second order coefficients may be sufficient for calculating the spherocylindrical refraction. However, as the pupil size increases, higher order aberrations (mainly spherical aberration) also increase their contribution to these refraction values and should therefore be considered in the calculation.[40] In this study, natural pupils were examined with all instruments using similar illumination levels, and the wavefront and refraction data were obtained for the central 5 mm with all three wavefront analyzers, as it would be the closest diameter to the 3 mm analyzed by the SRW-5000 but still offering clinically useful wavefront aberrations data.

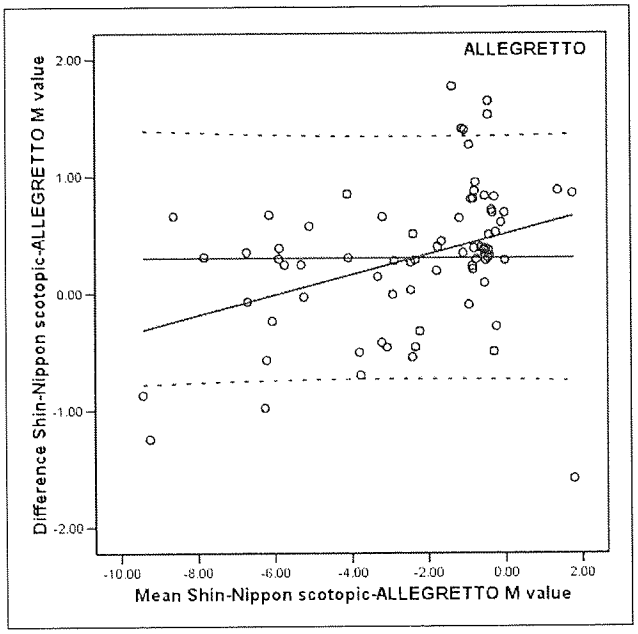

Figure 6. Bland-Altman plot for differences against mean (and 95% confidence intervals) and regression line between the SRW-5000 and the Allegretto for the spherical component M in diopters after removing the outliers.

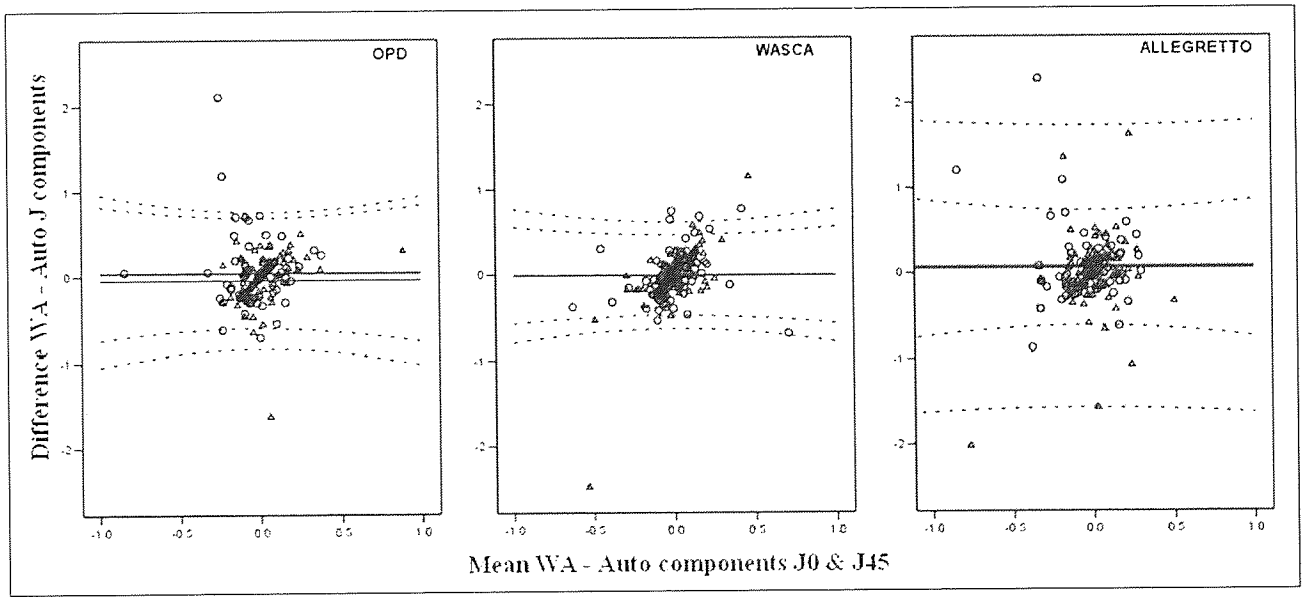

Figure 7. Bland-Altman plots for differences against mean (and 95% confidence intervals) between the SRW-5000 and the three wavefront analyzers for the astigmatic components J_0 (o) and J_{45} (Δ) in diopters.

All values of refraction were obtained from the default settings of the wavefront analyzers. According to the manufacturers, both the OPD-Scan and Allegretto provide an integral "best fit" refraction, which includes higher order aberrations. The WASCA, however, gives the default refraction values from the low order aberrations only, having been found to give better repeatability,[38] with the option of using a Seidel sphere fit that includes spherical aberration in the computation.

In this respect, the acquisition protocols were consistent, suggesting that the contribution of spherical aberration to the incident image would be similar for the three devices; any variability would therefore be due to differences in the optical setup and image analysis.

The determination of mean spherical power obtained with the three clinical wavefront analyzers used in this study, without the instillation of anticholinergic drops, resulted in a myopic overestimation of approximately 0.30 D, which varied to some extent with the degree of myopia (being less with higher degrees of myopia), and in some individuals was seen to be excessive. The relatively frequent finding of outliers in the data suggest that on a case-wise basis preoperative data must be interpreted with caution if optimal postoperative results are to be achieved. With respect to wavefront aberrations per se, it has previously been shown that myopic shifts associated with relatively small amounts of excess accommodation have little impact on the RMS value[9,11]; however, the implications for those patients exhibiting large amounts of over-accommodation (>3.00 D) may be profound.

REFERENCES

1. Salmon TO, West RW, Gasser W, Kenmore T. Measurement of refractive errors in young myopes using the COAS Shack-Hartmann aberrometer. *Optom Vis Sci.* 2003;80:6-14.
2. MacRae S, Fujieda M. Slit skiascopic-guided ablation using the Nidek laser. *J Refract Surg.* 2000;16:S576-S580.
3. Atchison DA. Recent advances in measurement of monochromatic aberrations of human eyes. *Clin Exp Optom.* 2005;88:5-27.
4. Saw SM, Tong L, Chua WH, Chua WH, Koh D, Tan DT, Katz J. Incidence and progression of myopia in Singaporean school children. *Invest Ophthalmol Vis Sci.* 2005;46:51-57.
5. Zadnik K, Mutti DO, Mitchell GL, Jones LA, Burr D, Moeschberger ML. Normal eye growth in emmetropic schoolchildren. *Optom Vis Sci.* 2004;81:819-828.
6. Carkeet A, Velaedan S, Tan YK, Lee DY, Tan DT. Higher order aberrations alter cycloplegic and non-cycloplegic pupil dilation. *J Refract Surg.* 2003;19:316-322.
7. Atchison DA. Comparison of peripheral refractions determined by different instruments. *Optom Vis Sci.* 2003;80:655-660.
8. Gilmartin B, Amer AC, Ingleby S. Reversal of tropicamide mydriasis with single instillations of pilocarpine can induce substantial pseudo-myopia in young adults. *Ophthalmic Physiol Opt.* 1995;15:475-479.
9. He JC, Burns SA, Marcos S. Monochromatic aberrations in the accommodated human eye. *Vision Res.* 2000;40:41-48.
10. Pallikaris LG, Panagopoulou SI, Siganos CS, Molebny VV. Objective measurement of wavefront aberrations with and without accommodation. *J Refract Surg.* 2001;17:S602-S607.
11. Cheng H, Barnett JK, Vilupuru AS, Marsack JD, Kasthurirangan S, Applegate RA, Roorda A. A population study on changes in wave aberrations with accommodation. *J Vis.* 2004;4:272-280.
12. Buscemi PM. Retinoscopic double pass aberrometry: principles and application of the Nidek OPD-scan. In: Krueger RR, Applegate RA, McRae SM, eds. *Wavefront Customized Visual Correction: The Quest for Super Vision II.* Thorofare, NJ: SLACK Inc; 2004:149-160.
13. Zadok D, Levy Y, Segal O, Barkana Y, Morad Y, Avni I. Ocular higher-order aberrations in myopia and skiascopic wavefront repeatability. *J Cataract Refract Surg.* 2005;31:1128-1132.
14. Hieda O, Kinoshita S. Measuring of ocular wavefront aberration in large pupils using OPD-scan. *Semin Ophthalmol.* 2003;18:35-40.
15. Arbelaez MC. Super vision: dream or reality. *J Refract Surg.* 2001;17:S211-S218.
16. Gimbel HV, Stoll SB. Photorefractive keratectomy with customized segmental ablation to correct irregular astigmatism after laser in situ keratomileusis. *J Refract Surg.* 2001;17:S229-S232.
17. Sarkisian KA, Petrov AA. Clinical experience with the customized low spherical aberration ablation profile for myopia. *J Refract Surg.* 2002;18:S352-S356.
18. Gimbel HV, Sofinski SJ, Mahler OS, van Westenbrugge JA, Ferensowicz MI, Triebwasser RW. Wavefront-guided multipoint (segmental) custom ablation enhancement using the Nidek NAVEX platform. *J Refract Surg.* 2003;19:S209-S216.
19. Nakano K, Portellinha W, Oliveira M, Alvarenga L, Nakano C, Nakano E. Refractive outcome of Nidek OPD-scan customized ablations. *J Refract Surg.* 2003;19:S221-S222.
20. Shah S, Naroo S, Hosking S, Gherghel D, Mantry S, Bannerjee S, Pedwell K, Bains HS. Nidek OPD-scan analysis of normal, keratoconic, and penetrating keratoplasty eyes. *J Refract Surg.* 2003;19:S255-S259.
21. Thibos LN. Principles of Hartmann-Shack aberrometry. *J Refract Surg.* 2000;16:S563-S565.
22. Cheng X, Himebaugh NL, Kollbaum PS, Thibos LN, Bradley A. Validation of a clinical Shack-Hartmann aberrometer. *Optom Vis Sci.* 2003;80:587-595.
23. Cheng X, Himehaugh NL, Kollbaum PS, Thihos LN, Bradley A. Test-retest reliability of clinical Shack-Hartmann measurements. *Invest Ophthalmol Vis Sci.* 2004;45:351-360.
24. Mierdel P, Krinke HE, Wiegand W, Kaemmerer M, Seiler T. Measuring device for determining monochromatic aberration of the human eye [German]. *Ophthalmologe.* 1997;94:441-445.
25. Mierdel P, Kaemmerer M, Mrochen M, Krinke HE, Seiler T. Ocular optical aberrometer for clinical use. *J Biomed Opt.* 2001;6:200-204.
26. Mrochen M, Kaemmerer M, Mierdel P, Krinke HE, Seiler T. Principles of Tscherning aberrometry. *J Refract Surg.* 2000;16:S570-S571.
27. Kaemmerer M, Mrochen M, Mierdel P, Krinke HE, Seiler T. Clinical experience with the Tscherning aberrometer. *J Refract Surg.* 2000;16:S584-S587.
28. Jorge J, Queiros A, Gonzalez-Meijome J, Fernandes P, Almeida JB, Parafita MA. The influence of cycloplegia in objective refraction. *Ophthalmic Physiol Opt.* 2005;25:340-345.
29. Jorge J, Queiros A, Almeida JB, Parafita MA Retinoscopy/

autorefraction: which is the best starting point for a noncycloplegic refraction? *Optom Vis Sci.* 2005;82:64-68.

30. Mallen EA, Wolffsohn JS, Gilmartin B, Tsujimura S. Clinical evaluation of the Shin-Nippon SRW-5000 autorefractor in adults. *Ophthalmic Physiol Opt.* 2001;21:101-107.
31. Chat SW, Edwards MH. Clinical evaluation of the Shin-Nippon SRW-5000 autorefractor in children. *Ophthalmic Physiol Opt.* 2001;21:87-100.
32. Wolffsohn JS, Gilmartin B, Mallen EA, Tsujimura S. Continuous recording of accommodation and pupil size using the Shin-Nippon SRW-5000 autorefractor. *Ophthalmic Physiol Opt.* 2001;21:108-113.
33. Wolffsohn JS, O'Donnell C, Charman WN, Gilmartin B. Simultaneous continuous recording of accommodation and pupil size using the modified Shin-Nippon SRW-5000 autorefractor. *Ophthalmic Physiol Opt.* 2004;24:142-147.
34. Bullimore MA, Fusaro RE, Adams CW. The repeatability of automated and clinician refraction. *Optom Vis Sci.* 1998;75:617-622.
35. Harris WF. Clinical measurement, artifact, and data analysis in dioptric power space. *Optom Vis Sci.* 2001;78:839-845.
36. Thibos LN, Wheeler W, Horner D. Power vectors: an application of Fourier analysis to the description and statistical analysis of refractive error. *Optom Vis Sci.* 1997;74:367-375.
37. Bland JM, Altman DG. Statistical methods for assessing agreement between two methods of clinical measurement. *Lancet.* 1986;1:307-310.
38. Salmon TO, van de Pol C. Evaluation of a clinical aberrometer for lower-order accuracy and repeatability, higher-order repeatability, and instrument myopia. *Optometry.* 2005;76:461-472.
39. Seidemann A, Schaeffel F. Effects of longitudinal chromatic aberration on accommodation and emmetropization. *Vision Res.* 2002;42:2409-2417.
40. Thibos LN, Hong X, Bradley A, Applegate RA. Accuracy and precision of objective refraction from wavefront aberrations. *J Vis.* 2004;4:329-351.

LABORATORY SCIENCE

Operator-induced errors in Hartmann-Shack wavefront sensing: Model eye study

Alejandro Cervino, OD(EC), MCOptom, Sarah L. Hosking, PhD, MCOptom, FAAO, DBO, Mark C.M. Dunne, PhD, MCOptom

PURPOSE: To evaluate the effects of instrument realignment and angular misalignment during the clinical determination of wavefront aberrations by simulation in model eyes.

SETTING: Aston Academy of Life Sciences, Aston University, Birmingham, United Kingdom.

METHODS: Six model eyes were examined with wavefront-aberration-supported cornea ablation (WASCA) (Carl Zeiss Meditec) in 4 sessions of 10 measurements each: sessions 1 and 2, consecutive repeated measures without realignment; session 3, realignment of the instrument between readings; session 4, measurements without realignment but with the model eye shifted 6 degrees angularly. Intersession repeatability and the effects of realignment and misalignment were obtained by comparing the measurements in the various sessions for coma, spherical aberration, and higher-order aberrations (HOAs).

RESULTS: The mean differences between the 2 sessions without realignment of the instrument were 0.020 μm ± 0.076 (SD) for Z_3^{-1} ($P = .551$), 0.009 ± 0.139 μm for Z_3^1 ($P = .877$), 0.004 ± 0.037 μm for Z_4^0 ($P = .820$), and 0.005 ± 0.01 μm for HO root mean square (RMS) ($P = .301$). Differences between the nonrealigned and realigned instruments were −0.017 ± 0.026 μm for Z_3^{-1} ($P = .159$), 0.009 ± 0.028 μm for Z_3^1 ($P = .475$), 0.007 ± 0.014 μm for Z_4^0 ($P = .296$), and 0.002 ± 0.007 μm for HO RMS ($P = 0.529$; differences between centered and misaligned instruments were −0.355 ± 0.149 μm for Z_3^{-1} ($P = .002$), 0.007 ± 0.034 μm for Z_3^1 ($P = .620$), −0.005 ± 0.081 μm for Z_4^0 ($P = .885$), and 0.012 ± 0.020 μm for HO RMS ($P = .195$). Realignment increased the standard deviation by a factor of 3 compared with the first session without realignment.

CONCLUSIONS: Repeatability of the WASCA was excellent in all situations tested. Realignment substantially increased the variance of the measurements. Angular misalignment can result in significant errors, particularly in the determination of coma. These findings are important when assessing highly aberrated eyes during follow-up or before surgery.

J Cataract Refract Surg 2007; 33:115–121 © 2007 ASCRS and ESCRS

Over the past decade, an increasing number of clinical devices for measuring the ocular aberration of the human eye have been developed; these are based on well-known principles that have been extensively tested in laboratory environments.[1–6] Several studies evaluate the performance of these clinical wavefront analyzers in the determination of low[7–9] and higher-order aberrations (HOAs).[5,10–12] They all agree on the capabilities of wavefront analysis systems to determine low-order aberrations with high accuracy, although the studies yield discrepant conclusions for the determination of HOAs with different instruments.

When a clinical examination is performed with any instrument, several sources of error must be accounted for before the data are interpreted. Currently, there are several instruments that automatically capture data only when the system is properly aligned (eg, corneal topography analyzers such as the Medmont or wavefront analyzers such as the Nidek OPD-Scan). However, most systems require observer judgment of the best alignment position followed by image capture. This alignment is therefore strongly dependent on the skills of the practitioner to judge the optimum position, as well as on the patient to hold a proper fixation.

0886-3350/07/$-see front matter
doi:10.1016/j.jcrs.2006.09.025

Table 1. Parameters of the elements used in the model eyes studied.

Parameter	Eye 1	Eye 2	Eye 3	Eye 4	Eye 5	Eye 6
Anterior corneal radius	8.84 ± 0.02	8.84 ± 0.02	8.84 ± 0.02	7.83 ± 0.02	7.83 ± 0.02	7.83 ± 0.02
Corneal thickness	0.80 ± 0.002	0.80 ± 0.002	0.80 ± 0.002	0.8 ± 0.002	0.80 ± 0.002	0.80 ± 0.002
Posterior corneal radius	8.45 ± 0.01	8.45 ± 0.01	8.45 ± 0.01	7.44 ± 0.01	7.44 ± 0.01	7.44 ± 0.01
Anterior chamber	3.67 ± 0.003	4.18 ± 0.003	5.19 ± 0.003	3.67 ± 0.003	4.18 ± 0.003	5.19 ± 0.003
Anterior lens radius	13.60 ± 0.02	13.60 ± 0.02	13.60 ± 0.02	13.60 ± 0.02	13.6 ± 0.02	13.6 ± 0.02
Lens thickness	3.50 ± 0.01	3.50 ± 0.01	3.50 ± 0.01	3.50 ± 0.01	3.50 ± 0.01	3.50 ± 0.01
Posterior lens radius	8.32 ± 0.01	8.32 ± 0.01	8.32 ± 0.01	8.32 ± 0.01	8.32 ± 0.01	8.32 ± 0.01
Posterior chamber	20.52 ± 0.18	20.52 ± 0.18	20.52 ± 0.18	20.52 ± 0.18	20.52 ± 0.18	20.52 ± 0.18

All values are mean ± SD (mm).

Davies et al.[13] assessed the repeatability of Shack-Hartmann wavefront sensing in 9 human eyes using pupil centration and a dental bite bar. They showed that repeated measurement of ocular wavefront led to significant differences in the Zernike coefficient values obtained as a result of small misalignment errors, short-term variation of aberration, and drifts in the equipment position. In the present study, model eyes removed physiological short-term variations in wavefront aberration associated with human eyes and also enabled quantification of the degree of misalignment and its impact on the values obtained.

When wavefront analysis is performed in clinical settings, it is advisable to take several readings, as with many other clinical instruments, due to the temporal variations of wavefront error,[14] small errors in the measurement due to the instrument, as well as small axial and lateral misalignments due to the manipulation of the instrument during the focusing procedure.[11,13] When doing this, the ability of the observer to choose the right moment to take the reading may be crucial for the reliability of the values obtained. In the same way, small shifts in the fixation of the patient may affect the final readings. This is especially important when high values of aberration are to be quantified and/or treated; for example, when a customized ablation is considered.

Cheng et al.[11] report different aspects of the performance of the Complete Ophthalmic Analysis System (COAS, Wavefront Sciences Ltd.) for determining low-order aberrations and HOAs in human and model eyes. They also show that measurements with the COAS tolerate axial and lateral misalignments within a range greater than that in which the system appears aligned to the clinician. The sensor has been shown to be highly accurate and repeatable, with very low variability, and strong to lateral and axial misalignment. The WASCA is essentially the same wavefront sensor as the COAS, so the results obtained by Cheng et al. could be extrapolated to this system.

This study evaluated the effect of small lateral or axial misalignments, such as those incurred when relocating the optimum z-wise alignment before the data capture, or small angular (x, y) misalignments, such as those due to positioning of the patient, on the intrasession and intersession repeatability of measurements. To negate the inherent variability associated with the human eye, a model eye system was used for all experimental measures.

MATERIAL AND METHODS

Model Eye

The sample comprised an artificial eye with a set of removable elements of known parameters (Table 1). Six of the possible resulting eyes from the combination of these elements were used in this study. This eye comprises a brass body with 4 segments on which the optical components are mounted (Figure 1). It has been described[15] and has been widely used in research studies, such as the simulation of Purkinje reflections for determining radii of curvature and position of the crystalline lens[15] and phacometric measurement of ocular surface radius of curvature and alignment.[16,17] The model eyes were chosen to have relatively high values of coma and spherical aberration (Table 2). Note that the model eyes did not permit the study of instrument accuracy since the removable elements fit so that coupling the parts prior to measurement can be varied; equally, once the model eye was set up for each set of experiments, it was not moved between measurements or between sessions.

Wavefront Analyzer

The WASCA wavefront analyzer is based on the Shack-Hartmann principle, which is the most widely used technique for

Accepted for publication September 27, 2006.

From the School of Life and Health Sciences (Cervino, Hosking, Dunne), Aston University, United Kingdom, and the School of Optics and Optometry (Cervino), Universidad de Santiago de Compostela, Spain.

No author has a proprietary or financial interest in any material or method mentioned.

Corresponding author: Dr. Sarah L. Hosking, School of Life & Health Sciences, Aston University, Aston Triangle, Birmingham B4 7ET, United Kingdom. E-mail: s.l.hosking@aston.ac.uk.

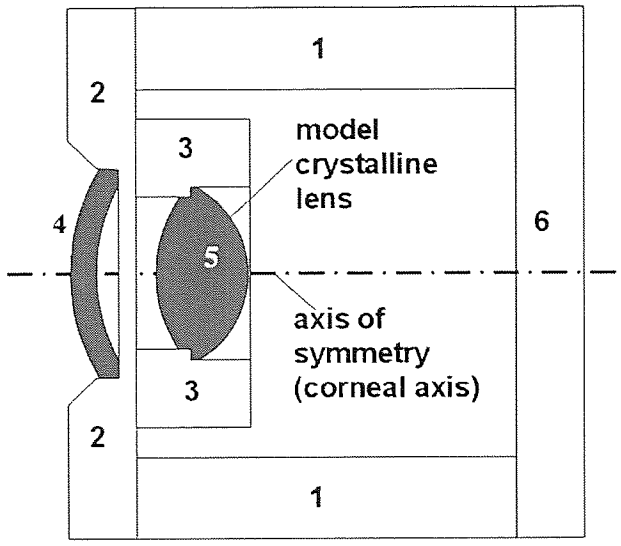

Figure 1. Cross-section of brass segments of the elements used: 1 = outer casing; 2 = anterior segment mounting designed to hold model cornea; 3 = interior segment mounting designed to hold model crystalline lens; 4 = model corneas; 5 = model crystalline lens; 6 = posterior cap of the outer casing (redrawn with permission from Barry et al.[17]).

determining the ocular wavefront aberration in clinical settings and has been well described for ocular applications.[3,18,19] It measures the profile of the light wavefront reflected from the retina after it passes through the eye's optical media. The WASCA uses a source diode, emitting at a wavelength of 850 nm, and a 44 × 33 lenslet array that measures the tilt of the wavefront over several pupil locations. It can be used to determine aberrations to the 5th order.

The model eye was coupled to the wavefront analyzer to take all the measurements.

Experimental Design

Ten consecutive measurements of the model eyes were made in each of 2 sessions. The system was not realigned between the measurements. Ten additional measurements were taken after an angular misalignment of 6 degrees between the model eye and the instrument was induced, and 10 more were made after the system was realigned before each measurement (joystick displacement in the *x-y-z* directions out of focus after each reading).

The data were obtained and analyzed as Zernike coefficients, complying with the standards recommended by the Optical Society of America.[20] Due to the physical limitations of the model eye, data were obtained and analyzed for a 5.0 mm pupil. Analysis was done on primary coma and spherical aberration coefficients, the main off-axis and axial wavefront errors and, therefore, the most compromising for visual performance, as well as for HO root mean square (RMS).

Intrasession repeatability was assessed by determination of the intraclass correlation coefficient, a reliability coefficient calculated from variance estimates obtained through an analysis of variance (ANOVA)[21] and by the graphic representation of the variations of the standard deviation with the number of measurements analyzed.

Intersession variation, differences with realignment, and the effect of angular misalignment were assessed by the Pearson correlation coefficient, paired *t* tests, and Bland-Altman plots of difference against mean. Bonferroni adjustment for repeated measures was applied, resulting in $P \leq 012$ for statistical significance.

Repeated-measures ANOVA was also applied to test the effect of each situation on each of the eyes.

RESULTS

The mean values of the spherocylindrical error and the Zernike coefficients for primary coma (Z_3^{-1}, Z_3^1), primary spherical aberration (Z_4^0), and HO RMS for each of the model eyes as measured in the first session are shown in Table 2.

Intrasession Repeatability

Intrasession correlations coefficients were used to determine the intrasession repeatability for all data sets and are shown in Table 3.

Figure 2 shows the plots of the mean standard deviations obtained in each experimental sessions for the 3rd-order aberrations and HOA. The plots show that the standard deviation of 2 readings does not differ significantly from that of 10 readings.

Table 2. Mean value of spherocylindrical refractive error, axis, and the Zernike coefficients for coma, spherical aberration, and HO RMS measured by the WASCA in each of the model eyes.

Measurement	Eye 1	Eye 2	Eye 3	Eye 4	Eye 5	Eye 6
Sphere (D)	−10.07 ± 0.00	−9.39 ± 0.00	−7.45 ± 0.01	−5.74 ± 0.00	−4.86 ± 0.00	−3.16 ± 0.01
Cylinder (D)	−0.30 ± 0.00	−0.15 ± 0.00	−0.23 ± 0.00	−0.46 ± 0.00	−0.43 ± 0.00	−0.43 ± 0.01
Axis (degrees)	85.0 ± 0.0	17.3 ± 0.5	61.1 ± 0.3	94.0 ± 0.0	150.4 ± 0.0	135.9 ± 0.3
Z_3^{-1}	−0.464 ± 0.003	−0.182 ± 0.009	−0.553 ± 0.008	−0.170 ± 0.004	0.018 ± 0.004	0.008 ± 0.008
Z_3^1	−0.141 ± 0.012	0.216 ± 0.009	0.441 ± 0.013	0.170 ± 0.008	0.138 ± 0.005	0.241 ± 0.003
Z_4^0	−0.760 ± 0.004	−0.838 ± 0.008	−0.719 ± 0.006	−0.644 ± 0.002	−0.641 ± 0.002	−0.628 ± 0.004
HO RMS (μm)	0.382 ± 0.004	0.383 ± 0.005	0.414 ± 0.007	0.308 ± 0.010	0.290 ± 0.000	0.290 ± 0.005

HO RMS = higher-order root mean square

Table 3. Intraclass correlation coefficients for the measurements of HOAs in each session.

HOA	Session 1	Session 2	Refocusing	Misaligned
Z_3^{-1}	0.999	1.000	0.991	0.998
Z_3^{1}	0.997	0.992	0.970	0.996
Z_4^{0}	0.999	1.000	0.971	1.000
HO RMS	0.989	1.000	0.981	0.992

HOA = higher-order aberration; HO RMS = higher-order root mean square

Intersession Repeatability

Bland-Altman plots of mean difference against mean for the Zernike coefficients obtained for the eye models between all sessions are displayed in Figures 3 to 6. From the Bland-Altman plots (Figure 3), the coefficients of repeatability are plotted and the confidence intervals can be compared. The agreement between realigning and non-realigning was generally very good; the angular misalignment had a greater effect. In each case, there was a slightly greater confidence interval than expected for the 2 sessions in which there was no realignment, which appear to result from 2 outlier data points. It is possible that these arise due to a shift in the positioning of the model eye components during data acquisition, although great care was taken not to alter the model eye setup during the data collection process.

As shown in Table 4, 2-tailed paired *t* tests demonstrated that with the exception of HO RMS, there were no statistically significant differences between the first 2 sessions, with high correlation between the values obtained. For HO RMS, there was a significant difference between values at the first 2 sessions ($P = .002$); however, the measures were highly correlated.

Realignment

No statistically significant differences were found between the values obtained with realignment and those without realignment; there was a high correlation between the values. Only the differences between the values of Z_3^{-1} were statistically significantly different, but the mean difference was low (0.017 ± 0.033 μm) and there was a statistically significant high positive correlation (Table 4).

Angular Misalignment

Angular misalignment of the model eyes induced statistically significant differences in the values obtained for Z_3^{-1} and HO RMS, although the values correlated well. The mean differences for Z_3^{-1} were high (Table 4).

DISCUSSION

This study confirmed the WASCA to be a highly repeatable instrument for measuring the Zernike coefficients studied. Further, intrasession repeatability did not decrease when the model eye was angularly misaligned with the instrument axis. These findings were consistent with those of a previous study[11] that demonstrated good repeatability, low variability (standard deviations less than 1% of the mean value without realignment and less than 10% with realignment), and measures that were robust to axial and lateral misalignments. The study did demonstrate that in highly aberrated eyes, angular misalignment results in a significant change in the degree of coma.

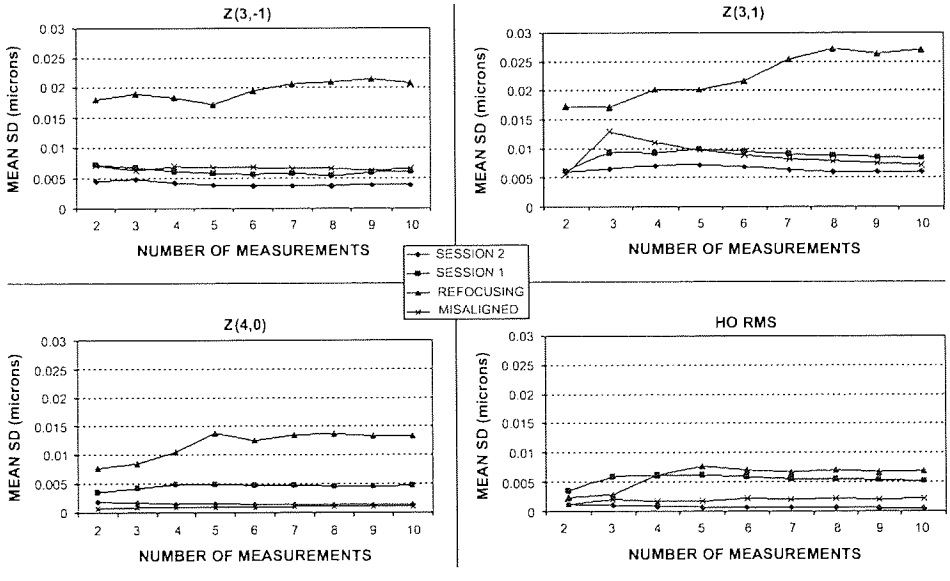

Figure 2. Plots of mean standard deviation against the number of measurements for all Zernike coefficients measured.

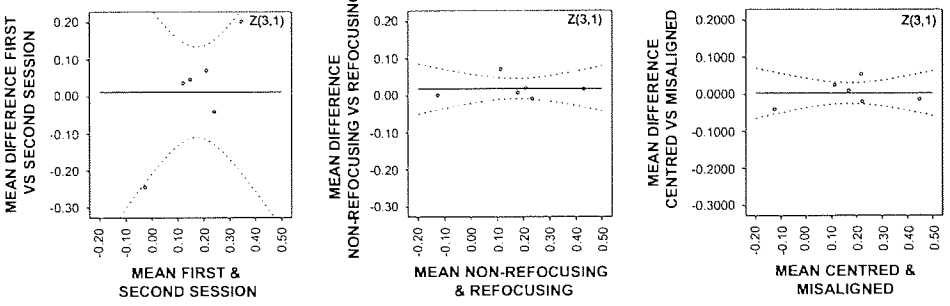

Figure 3. Bland-Altman plots of difference versus mean of the values obtained for the Zernike coefficient Z_3^1 in all the conditions measured. All the values are in microns.

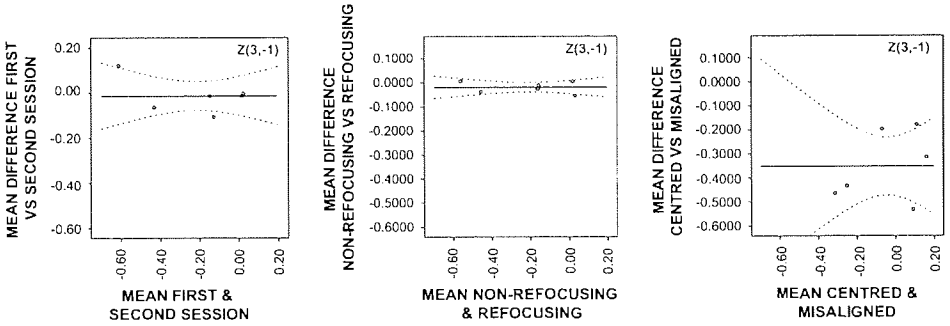

Figure 4. Bland-Altman plots of difference versus mean of the values obtained for the Zernike coefficient Z_3^{-1} in all the conditions measured. All the values are in microns.

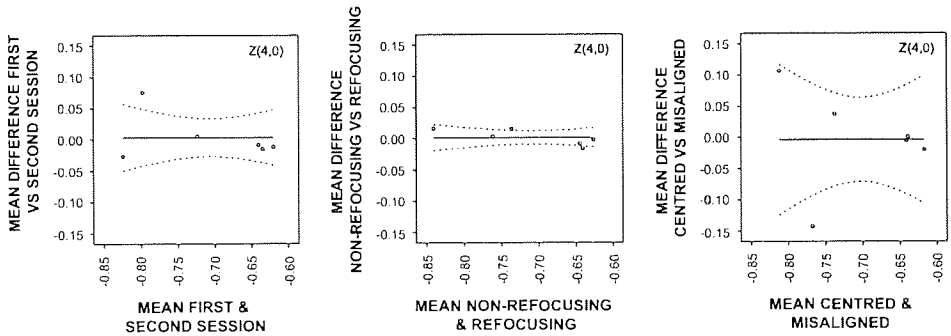

Figure 5. Bland-Altman plots of difference versus mean of the values obtained for the Zernike coefficient Z_4^0 in all the conditions measured. All the values are in microns.

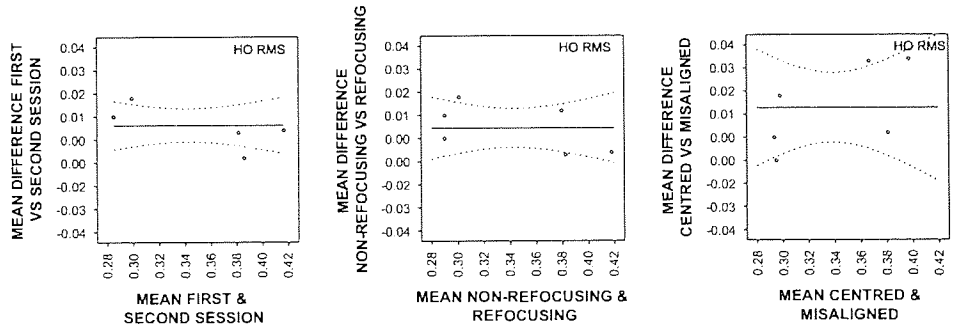

Figure 6. Bland-Altman plots of difference versus mean of the values obtained for different values of HO RMS obtained in all the conditions measured. All the values are in microns.

Table 4. Results of the 2-tailed paired *t* tests comparing the results obtained in the 4 sessions. For each comparison, the mean difference between the 2 sessions, along with the corresponding SD and *P* value, and the Pearson correlation coefficient, along with its corresponding *P* value, are shown.

	Session 1 Versus Session 2 No Realignment				No Realignment Versus Realignment				Centered Versus Misaligned No Realignment			
HOA	Mean ± SD	*P* Value	Pearson	*P* Value	Mean ± SD	*P* Value	Pearson	*P* Value	Mean ± SD	*P* Value	Pearson	*P* Value
Z_3^{-1}	−0.014 ± 0.070	.119	0.967	<.001	−0.017 ± 0.033	<.001	0.991	<.001	−0.355 ± 0.137	<.001	0.778	<.001
Z_3^{1}	0.009 ± 0.128	.579	0.761	<.001	0.009 ± 0.038	.072	0.977	<.001	0.007 ± 0.035	.109	0.979	<.001
Z_4^{0}	0.004 ± 0.034	.417	0.927	<.001	0.007 ± 0.021	.015	0.966	<.001	−0.005 ± 0.074	.603	0.605	<.001
HO RMS	0.005 ± 0.011	.002	0.989	<.001	0.002 ± 0.012	.193	0.977	<.001	0.012 ± 0.019	<.001	0.938	<.001

HOA = higher-order aberration; HO RMS = higher-order root mean square

A particular feature of the methodology in this study was to assess the impact of the type of operator errors that might be induced during normal clinical evaluation; that is, the clinician performing a normal realignment between measurements (combination of small axial and lateral misalignments) and a small fixation error from the patient (angular misalignment of 6 degrees of the model eye). There was a substantial increase in the variability of measures acquired during the session in which the system was realigned after each measurement. This increase accounts for small differences in lateral and axial misalignments that occur between the measurements and are highly dependent on the observer's ability to find the right focusing place. The reference for focusing of the COAS/WASCA consists of 6 light circles that the observer has to focus and center on the cornea. The observer's perception of these lights as focused will depend on factors such as the patient's corneal curvature, the observer's refractive error, and the depth of focus, resulting in a range of conditions during which a particular observer may see the reference as equally focused. These clinically important factors should be taken into consideration, especially if monitoring or treating patients is based on a single data measurement.

As shown in Figure 2, the mean standard deviation did not vary widely with increasing numbers of readings in the model eyes, suggesting that the reported variation in repeated measures associated with data from human eyes[13] is probably associated with a physiological variation in human wavefront errors.[14] It is possible that any such variability is related to the ocular pulse, and pulse synchronization of data acquisition may have to be considered to improve clinical wavefront measures in future iterations of the technology.

A further aim of this study was to assess the impact that angular misalignment, as would occur when the patient is not fixating properly, would have in the determination of the wavefront aberration pattern. The results show, perhaps as expected, that the vertical component of coma was significantly affected by misalignment, suggesting that it may be more sensitive to misalignment in the clinical setting. The extent of any error will depend on the degree to which an eye is aberrated. Since the model eye used a spherical model for the cornea, the aspheric nature of the human eye will possibly result in further errors in a human system. Therefore, variations in horizontal coma and spherical aberrations can also be expected when measuring a misaligned human eye with respect to the values obtained when aligned. This is a subject for future study.

In summary, this study reaffirms previous findings that the WASCA is a highly repeatable instrument for the measurement of ocular wavefront aberrations both intersession and intrasession. However, the study also shows that manipulation of the instrument during the realignment process between measurements increases the variance of the values and is probably dependent on the clinician's skills to realign the system; repeated measures such as those acquired in the follow-up of patients should be measured and interpreted with caution. Nonetheless, the repeatability after realignment is still high. Angular misalignment of the eye during the image acquisition leads to significant differences in the values of coma obtained, mainly its vertical component. It is likely that the impact of this on the aspheric human cornea may be greater. These findings are of particular importance in the assessment of highly aberrated eyes, which are perhaps those most likely to benefit from customized ablation procedures.[22] Careful repositioning of the instrument and alignment of the patient will therefore provide the best data for treatment or follow-up. Automated acquisition protocols with pulse synchronization may enhance the accuracy and repeatability of measurements in the future.

REFERENCES

1. Salmon TO, Thibos LN, Bradley A. Comparison of the eye's wave-front aberration measured psychophysically and with the Shack-Hartmann wave-front sensor. J Opt Soc Am A Opt Image Sci Vis 1998; 15: 2457–2465

2. Walsh G, Charman WN, Howland HC. Objective technique for the determination of monochromatic aberrations of the human eye. J Opt Soc Am A 1984; 1:987–992
3. Liang J, Grimm B, Goelz S, Bille JF. Objective measurement of wave aberrations of the human eye with the use of a Hartmann-Shack wave-front sensor. J Opt Soc Am A Opt Image Sci Vis 1994; 11:1949–1957
4. Moreno-Barriuso E, Marcos S, Navarro R, Burns SA. Comparing laser ray tracing, the spatially resolved refractometer, and the Hartmann-Shack sensor to measure the ocular wave aberration. Optom Vis Sci 2001; 78:152–156
5. Rodríguez P, Navarro R, González L, Hernández JL. Accuracy and reproducibility of Zywave, Tracey, and experimental aberrometers. J Refract Surg 2004; 20:810–817
6. He JC, Marcos S, Webb RH, Burns SA. Measurement of the wave-front aberration of the eye by a fast psychophysical procedure. J Opt Soc Am A Opt Image Sci Vis 1998; 15:2449–2456
7. Salmon TO, West RW, Gasser W, Kenmore T. Measurement of refractive errors in young myopes using the COAS Shack-Hartmann aberrometer. Optom Vis Sci 2003; 80:6–14
8. Wang L, Wang N, Koch DD. Evaluation of refractive error measurements of the WaveScan WaveFront system and the Tracey wavefront aberrometer. J Cataract Refract Surg 2003; 29:970–979
9. Hament WJ, Nabar VA, Nuijts RMMA. Repeatability and validity of Zywave aberrometer measurements. J Cataract Refract Surg 2002; 28:2135–2141
10. Mirshahi A, Bühren J, Gerhardt D, Kohnen T. In vivo and in vitro repeatability of Hartmann-Shack aberrometry. J Cataract Refract Surg 2003; 29:2295–2301
11. Cheng X, Himebaugh NL, Kollbaum PS, et al. Validation of a clinical Shack-Hartmann aberrometer. Optom Vis Sci 2003; 80: 587–595
12. Zadok D, Levy Y, Segal O, et al. Ocular higher-order aberrations in myopia and skiascopic wavefront repeatability. J Cataract Refract Surg 2005; 31:1128–1132
13. Davies N, Diaz-Santana L, Lara-Saucedo D. Repeatability of ocular wavefront measurement. Optom Vis Sci 2003; 80:142–150
14. Cheng X, Himebaugh NL, Kollbaum PS, et al. Test-retest reliability of clinical Shack-Hartmann measurements. Invest Ophthalmol Vis Sci 2004; 45:351–360
15. Kirschkamp T, Jöckel M, Wählisch G, Barry JC. Konstruktion eines Modellauges zur Simulation von Purkinje-Spiegelbildern für die Bestimmung der Krummungsradien und der Lage der Augenlinse. Biomed Tech (Berl) 1998; 43:318–325
16. Dunne MCM, Davies LN, Mallen EAH, et al. Non-invasive phakometric measurement of corneal and crystalline lens alignment in human eyes. Ophthalmic Physiol Opt 2005; 25:143–152
17. Barry J-C, Dunne M, Kirschkamp T. Phakometric measurement of ocular surface radius of curvature and alignment: evaluation of method with physical model eyes. Ophthalmic Physiol Opt 2001; 21:450–460
18. Thibos LN, Hong X. Clinical applications of the Shack-Hartmann aberrometer. Optom Vis Sci 1999; 76:817–825
19. Thibos LN. Principles of Hartmann-Shack aberrometry. J Refract Surg 2000; 16:S563–S565
20. Thibos LN, Applegate RA, Schwiegerling JT, Webb R. Standards for reporting the optical aberrations of eyes; VSIA Standards Taskforce Members. J Refract Surg 2002; 18:S652–S660
21. Lam AKC, Chan R, Chiu R. Effect of posture and artificial tears on corneal power measurements with a handheld automated keratometer. J Cataract Refract Surg 2004; 30:645–652
22. Mastropasqua L, Toto L, Zuppardi E, et al. Zyoptix wavefront-guided versus standard photorefractive keratectomy (PRK) in low and moderate myopia: randomized controlled 6-month study. Eur J Ophthalmol 2006; 16:219–228

REVIEW ARTICLE

Clinical Ocular Wavefront Analyzers

Alejandro Cerviño, OD(EC), MCOptom; Sarah L. Hosking, BSc(Hns), PhD, MCOptom, FAAO, DBO; Roberto Montes-Mico, OD, MPhil, PhD; Keith Bates, MA, FRCS, FRCOphth

ABSTRACT

PURPOSE: To provide a summary of the methods utilized by clinical wavefront analyzers and their historical, current, and future applications.

METHODS: Review of the literature and author's experience with the various devices.

RESULTS: A wide range of clinical wavefront aberrometers, which use different principles, are available to clinicians and researchers.

CONCLUSIONS: Applications of wavefront analyzers in vision sciences range from assessment of refractive error, refractive surgery planning, evaluation of outcomes, optimization of contact lenses and IOL designs, evaluation of pathology relating to optical performance of the eye, and evaluation of accommodation alterations. [*J Refract Surg.* 2007;xx:xxx-xxx.]

The purpose of vision is to extract information from the physical environment by means of the light emitted, reflected, or transmitted by objects or surfaces. To obtain useful information, the visual system must classify and interpret the changes that occur in the visual image. The visual system is limited in its resolution by numerous physical and physiological factors, making it an imperfect optical system; the extent of these optical limitations varies greatly in the normal population.

The optical quality of the retinal image is limited by wavefront aberrations (chromatic and achromatic), diffraction, and scatter. Visual perception and interpretation of the retinal image is then further constrained by the anatomy of the visual system, from receptor cell density in the retina, through all of the neural connections of the visual pathway and brain.

The blur process in the formation of optical images is described mathematically with a simple equation if the system is isoplanatic (ie, its point spread function is independent):

$$i(x', y') = o(x, y) \times p(x', y')$$

ie, the image i is equal to the convolution of the object o, with the image being formed at the point p. Convolution is effectively the mathematical equivalent to blurring, so that the image would be more or less blurred depending on the image of a point p (point spread function [PSF]) being more or less extensive. The mathematical determination of convolution is complicated, but can be more easily estab-

From the School of Life and Health Sciences, Aston University, United Kingdom (Cerviño, Hosking, Botes); E.U. Óptica y Optometría, Universidad de Santiago de Compostela, Spain (Cerviño); Universidad de Valencia, Spain (Montes-Mico); and Taunton and Somerset NHS Trust, Taunton, United Kingdom (Bates).

The authors have no proprietary or financial interest in the materials presented herein.

Correspondence: Sarah L. Hosking, BSc(Hns), PhD, MCOptom, FAAO, DBO, School of Life and Health Sciences, Aston University, Aston Triangle, Birmingham B4 7ET, United Kingdom. Tel: 44 121 204 3800; Fax: 44 121 333 4220; E-mail: S.L.Hosking@aston.ac.uk

Received: March 29, 2006

Accepted: October 16, 2006

lished in the spatial frequency domain by Fourier analysis.

Two major developments have increased interest in visual optics: refractive surgery and the application of adaptive optics to the eye. The advances in surgical techniques for correcting the optics of the eye have renewed interest in developing accurate, reproducible techniques for measuring the wavefront aberrations of the human eye, as well as for studying changes in the optics of the eye under different conditions, such as those associated with aging, accommodation, or pathology. The human eye presents an array of different aberrations,[1-9] with high variability between individuals and eyes.[10] Over the past few years, several devices have been designed to measure these aberrations in clinical settings, using different principles and aiming to make it part of everyday clinical practice.

Wavefront aberrations can be defined as any deviation from the wavefront that would be expected through a perfect optical system in which a wavefront emerging from a point in the object plane converges on a single point in the image plane. They are a result of the lack of homogeneity of the ocular media as well as local irregularities of the optical surfaces.

This article reviews the current commercially available systems for the clinical determination of optical aberrations of the eye, their advantages and disadvantages, and their applications both clinically and in vision science.

ABERROMETRY PRINCIPLES

Some of the instruments used for the determination of ocular wavefront aberrations analyze an image on the retina, whereas others place a source of light on the retina and analyze the wavefront as it leaves the eye.

Almost all methods used for the clinical determination of wavefront aberrations of the eye are based on ray tracing and the reconstruction of the original wavefront from local slopes.[11] The aberrations are derived for various points in the pupil and, typically using least squares, are converted into wave aberration functions. Interferometric methods have the additional difficulty associated with stability and for this reason they are not used for the clinical measurement of ocular aberration.

Early aberrometry techniques were subjective, requiring the individual to report his or her observations and included 1) the Tscherning aberroscope,[11] 2) Howland's cross-cylinder technique,[1,12] and 3) the spatially resolved refractometer[13,14]—all of which are widely described and used for research purposes.[10,14-23] These technologies have been superseded by objective methods, and the different principles used currently are described below.

TSCHERNING'S ABERROSCOPE

Tscherning's principle was first introduced at the end of the 19th century with what is known as Tscherning's aberroscope. A grid in the pupil plane was shadowed with a +5.00-diopter (D) lens on the patient's retina while fixating a distant point; the aberrations were then inferred from the distortion of the grid.[11,12,24] This aberroscope set the basis for some modern objective aberrometers currently used in practice.

CROSS-CYLINDER TECHNIQUE

Bradford Howland developed this technique in 1960 initially for testing the quality of camera lenses.[11] It is a modification of Tscherning's aberroscope, having several advantages such as a sharper grid, which clearly indicates a zero defocus point. A cross cylinder of ±5.00 D was used to shadow a grid on the retina. It was first used to subjectively determine the wavefront aberrations of the human eye[1,25] but was modified to an objective version in 1984[2] using a second ophthalmoscopic channel to capture the retinal image. The improved reconstruction algorithms provided more reliable results,[26] although the variability between eyes was found to be slightly worse than with other objective techniques.[27]

SPATIALLY RESOLVED REFRACTOMETER

The spatially resolved refractometer, based on Scheiner's principle described by Smirnov,[28] allows a psychophysical measurement of ocular wavefront aberrations. The principle is simple—a reference centered aperture and a peripheral subaperture allow two parallel laser beams to pass through the ocular media and be projected on the patient's retina. Depending on the aberration at the point measured, the retinal spots will be separated. Changing the angle of the peripheral illumination source brings the retinal spots together. By measuring the angle needed to obtain a single retinal spot, the aberration components relative to that pupil location can be calculated. By sampling a number of points, the wavefront can be reconstructed (Fig 1). The results obtained with this subjective technique have been reported to be similar to those obtained with other objective methods.[29]

Currently, the InterWave scanner (InView, Atlanta, Ga) is the only clinical wavefront sensor using this principle. It requires the patient to perform the alignment of the two points in the presence of local aberrations using a joystick. Although it was originally intended as a psychophysical task, requiring input from the patient, an objective version has also been described.[30] It has been successfully used in combination with surgical lasers to correct spherical aberration and to detect corneal ectasia.[31-34]

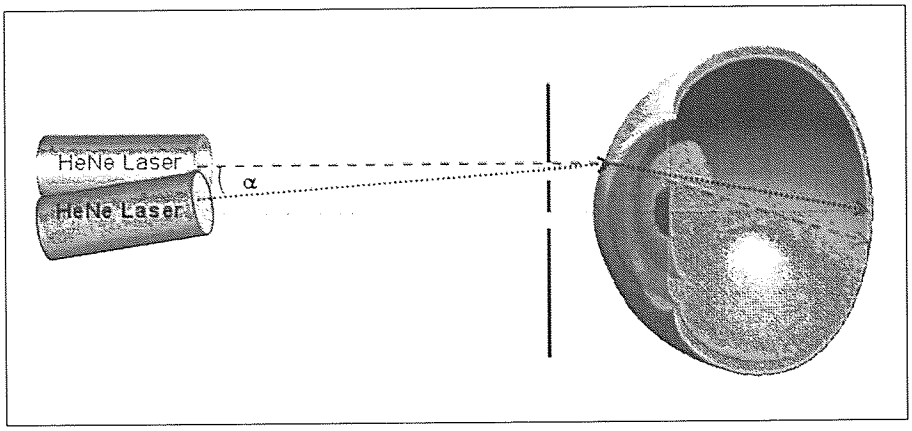

Figure 1. Diagram representing the basic functioning of the principle used by the spatially resolved refractometer.

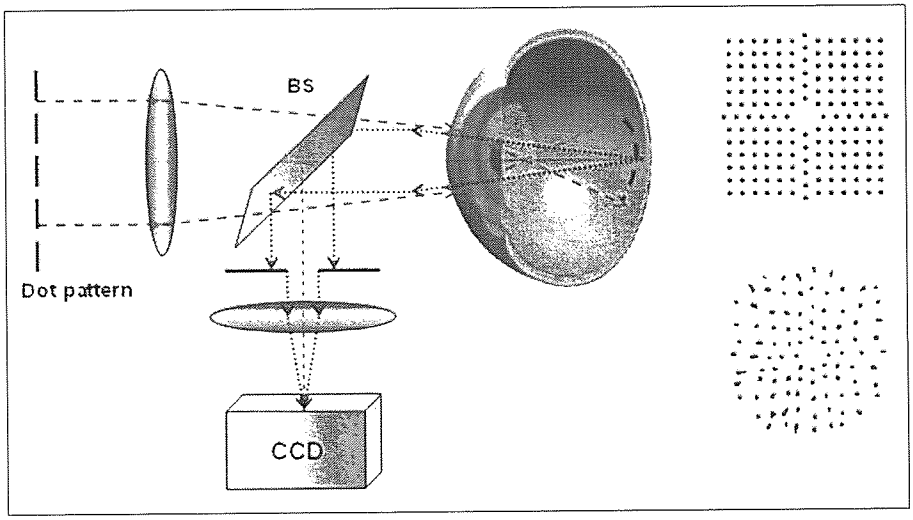

Figure 2. Left) Diagram representing the basic functioning of aberrometers using Tscherning's principle. **Upper right)** Example of a reference grid and **lower right)** distorted grid on an aberrated eye.

This principle also set the basis for the ray-tracing objective aberrometers described later in this review.

OBJECTIVE METHODS

The objective methods used currently in clinical practice and resulting from the original techniques include those based on Tscherning's principle, laser ray tracing, Hartmann-Shack, and skiascopy.

Several classifications have been suggested to group these systems according to the different principles they use, either by the direction of the light analyzed (ingoing or outgoing) or the way in which data from the different locations are collected (sequential or simultaneous). In this review, methods will be grouped depending on whether they analyze the light going into the patient's eye (ingoing), ie, the retinal image, or the light coming out of the patient's eye (outgoing).

The Table provides a summary of the sensor characteristics currently used in the different commercially available clinical wavefront analyzers.

INGOING SYSTEMS

The systems classified into this group measure wavefront data based on retinal imaging, ie, the system measures the position of the laser beam projections on the patient's retina, analyzes a retinal spot distribution, and calculates the wavefront.

Tscherning Principle Systems. Based on Tscherning's aberroscope, the current clinical devices using this principle use a dot pattern mask, which allows several laser rays from the original beam to reach the eye and be projected on the retina and analyzed on a subjective basis. Five to ten frames of the image formed in the retina are captured and defined through a small aperture and will be more or less deformed depending on the aberrations produced by the examined eye[24,35] (Fig 2).

The deviation of each retinal spot from its equivalent in the ideal reference image is measured and processed to give the local slopes and, therefore, the wavefront aberrations. Provided aberrations are not very high, it will be clear which image point coincides with which

TABLE

Technical specifications of Currently Available Clinical Aberrometers*

	Wavescan	Zywave	COAS	LADARWave
Manufacturer	VISX	Bausch & Lomb	Wavefront Sciences	Alcon Lab Inc
Principle used	HS	HS	HS	HS
Pupil diameter (mm)				
Minimum	5-6	2.5, 6 for Zemike	N/A	2.5
Maximum	N/A	8.5	9.0	10.0
Dynamic Range (D)	+6.00 to −8.00	+6.00 to −12.00	+7.00 to −15.00	+15.00 to −15.00 +8.00 to −14.00
Cylinder (D)		≤5.00	≤5.00	≤8.00
Sampling points	240	80	1452	204-213 (>190 over a 7-mm pupil)
Fogging	Auto	Auto	1.50 D, fixed	Auto
Capture time (ms)	N/A	≤1000	13	N/A
Repeatability (full pupil size) (D)	N/A	±0.25 SE† ±0.29 sphere ±0.29 cylinder[50]*	±0.10† ±0.24 w/o cyclo ±0.12 w/ cyclo[51]	N/A
Accuracy (D) (sphere, cylinder, axis)	±0.13 SE ±0.51 sphere ±0.34 cylinder[41]	N/A	±0.15(−14.00 to +6.00, ±3.00 cylinder); ±0.50 (−15.00 to +7.00, ±5.00 cylinder)†	N/A
Chart type	N/A	Scenery	Circular grid	N/A
Laser wavelength (nm)	785	785	830	820
HOA	Up to 6th order	Up to 5th order	Up to 10th order	Up to 8th order
Corneal aberrations	No	No	No	No

HS = Hartmann−Shack, N/A = not available, SE = spherical equivalent, HOA = high order aberrations
**Results obtained under cyclopegia.*
†Company data.
Note. The sources of this data were published papers (as stated within the table) and manufacturers.

pupil position. The method has shown good reproducibility for spherocylindrical refraction and total root-mean-square values for higher order aberrations on human eyes.[24]

WaveLight Laser Technologie AG (Erlangen, Germany) is, to our knowledge, the only manufacturer of sensors using this principle for clinical purposes. It was developed by Mierdel et al[7,36] and is successfully used for performing customized ablations.[37,38]

Ray Tracing. From a technical perspective, this technique falls between the spatially resolved refractometer and Tscherning methods, whereby the laser beam is projected onto the eye's retina, parallel to the visual axis, at several points on the eye's entrance (Fig 3).

In contrast to the Tscherning devices in which, as mentioned earlier, a grid is projected on the retina providing simultaneous distortion on every point, in ray-tracing techniques, a laser beam is projected each time, making a rapid scan over several points, providing a corresponding projection on the patient's retina. With the data acquired, a complete pattern is obtained in just a few milliseconds; the system generates maps showing the behavior of the visual system. Unlike the spatially resolved refractometer method in which the retinal spot is displaced towards the reference by modifying the entrance angle, the distance to the retinal reference position, or ideal spot location, is measured and used to compute the aberration.[39]

In laboratory settings, this method showed results in good agreement with other techniques such as the Hartmann-Shack or spatially resolved refractometer,[29] and proved to be reliable in the evaluation of changes in ocular wavefront due to surgery.[40]

The main advantage is that the sequential projection

Irx3	KR–9000 PW	OPD–Scan	Allegretto	Tracey
Imagine Eyes	Topcon	NIDEK	WaveLight	Tracey Technologies
HS	HS	Dynamic skiascopy	Tscheming	Ray tracing
2	4 (4th order) 6 (6th order)	2.6	N/A	N/A
7.2	N/A	6.0	8.0	8.0
+20.00 to −15.00	+15.00 to −15.00	+22.00 to −20.00	+6.00 to −12.00[24]	+15.00 to −15.00
≤10.00	≤7.00	≤12.00	≤4.00	N/A
230 μm spatial resolution†	85	1440	168	64 95 optionally
Auto, user-controlled	N/A	Auto	User defined	N/A
33	N/A	≤400	≤40[24]	<50
±0.003 sphere ±0.003 cylinder (model eye)†	N/A	N/A	N/A	±0.10†
N/A	N/A	±0.50 (>10.00)† ±0.25 (0 to ±10.00)†	N/A	±0.10†, ±0.59 SE ±0.64 sphere ±0.38 cylinder[41]
User defined: optotypes, custom images, etc	N/A	Scenery	Star in yellow circle	Red cross
780 (830 optional)	840	808	660	650
Up to 12th order	Up to 6th order	Up to 8th order	Up to 6th order	Up to 6th order
No	No	Yes	No	No

of the laser beam avoids the possibility of overlapping image points as seen in some devices. This would also facilitate the measurement of relatively high aberrations with a higher level of confidence than seen in other devices.

Tracey Technologies Inc (Houston, Tex) is, to our knowledge, the only manufacturer of sensors using this principle for clinical purposes. This system has shown a good performance for spherocylindrical determination, in close match with clinical Hartmann-Shack sensors.[41] In studies with earlier versions of the Tracey device, it was found to provide accurate,[42] highly reproducible[39,42,43] measurements. The same was found with the later version.[41] It has a multiple acquisition mode that allows a rapid screening of changes such as those occurring during accommodation.[44]

OUTGOING SYSTEMS

Hartmann-Shack Method. This is the most popular technology for wavefront analysis. In 1900, Hartmann designed a disc, based on one used earlier by Scheiner, in which he drilled several holes. He used it for measuring the optical quality of lenses by ray tracing the light rays that emerged from it. Some time later, Shack included microlenses in the holes. From that moment, the technique was known as the Hartmann-Shack (or Shack-Hartmann) method.[45] It has been widely used in the past for astronomical observation, and approximately 10 years ago Liang first successfully applied this technology to the human eye.[4]

If a wavefront is divided spatially, each subdivision can be approximated to a tilted perfect wave (flat). The reconstruction of the tilts of every division will result in an approximation to the original wavefront.[46] Hart-

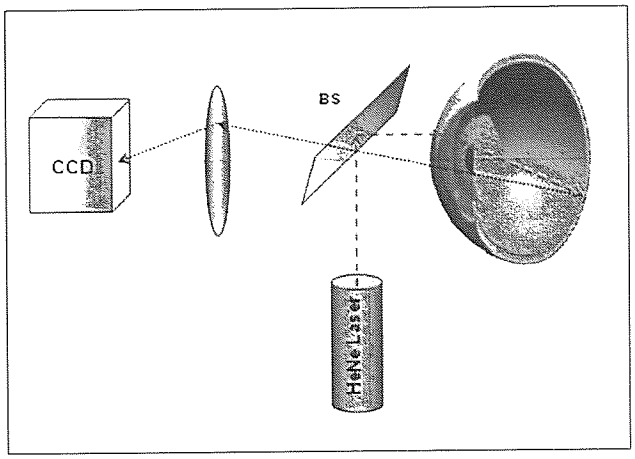

Figure 3. Diagram representing the basic functioning of aberrometers using laser ray tracing.

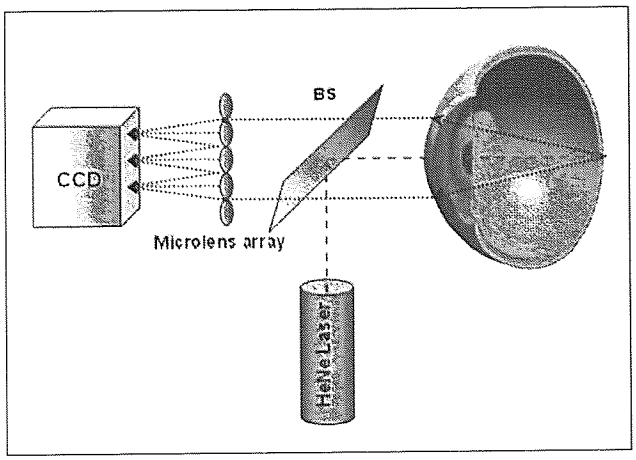

Figure 4. Diagram representing the basic functioning of aberrometers using the Hartmann-Shack principle.

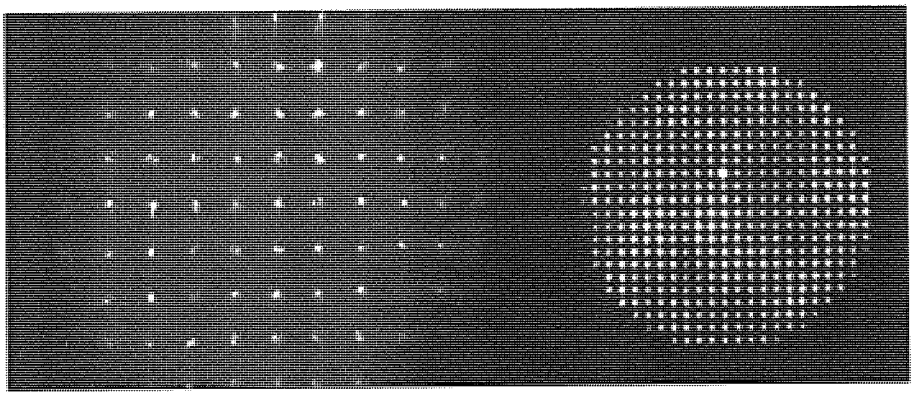

Figure 5. Hartmann-Shack pattern obtained from two different commercially available clinical sensors. Note the differences in spatial resolution.

mann-Shack–based wavefront analyzers rely on this principle. The sensor comprises a lenslet array, necessary for wavefront decomposition and focusing of the secondary wavefronts from each subaperture, and a detector (Fig 4).

The main difference between the various commercial sensors using the Hartmann-Shack principle is spatial resolution, which is limited by the microlens size and number, as well as by the number of modes used to fit the wavefront[47] (Fig 5). From a manufacturing perspective, it is difficult to obtain a balance between the need for a large number of lenslets within the array to provide adequate resolution and the high cost of production of microlenses for such a technique. These factors should be considered when selecting a technique for clinical application.

Hartmann-Shack–based aberrometers are the most commonly used in clinical settings and the most prevalent in research literature. In laboratory settings, the performance of Hartmann-Shack sensors has been found to be better in the discrimination of wavefront error between eyes than the objective cross-cylinder technique,[27] and to be in good agreement with Smirnov's psychophysical test,[48] laser ray tracing,[29,49] and spatially resolved refractometers.[29] Also, studies report good repeatability[5,48] and accuracy[5] of Hartmann-Shack measures.

Relatively few studies have reported the performance of clinical Hartmann-Shack devices, which analyze mostly low order aberrations. Reliability of Hartmann-Shack–based wavefront sensors in the determination of refractive error has been proved to be highly accurate and reproducible[41] and similar to or better than autorefractors,[50,51] although the possibility of inducing instrument myopia in non-cyclopleged eyes must be considered.[52] In relation to higher order aberrations, clinical Hartmann-Shack sensors also show low variability.[53] Nevertheless, these results cannot be applied to all commercially available Hartmann-Shack devices, as differences between various clinical sensors in the determination of higher order wavefront aberrations occur and are due mainly to differences in the spatial resolution and reconstruction algorithms of the numerous systems. The Zywave (Bausch & Lomb, Roch-

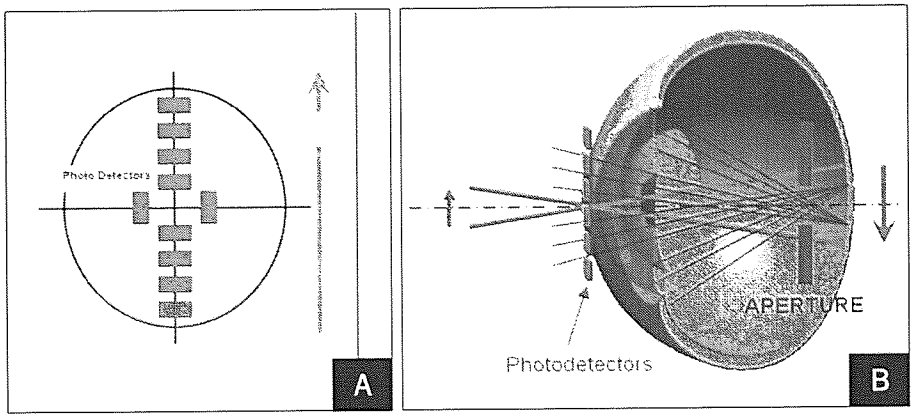

Figure 6. A) Diagram of the skiascopy-based wavefront sensor and **B)** how it functions. The photodetectors are conjugated with the comea, and the aperture is conjugate with the retina in emmetropia, and in front or behind it in myopia and hyperopia, respectively. Diagrams adapted from Buscemi.[58]

ester, NY), for instance, has shown poor repeatability for the determination of higher order aberrations, even for low degrees of aberration,[54] suggesting the need for multiple acquisitions of measurements to provide more reliable results. However, in a different study on a small sample, results have been found to be equivalent to those given by ray-tracing and an experimental spatially resolved refractometer system.[55] In the evaluation of devices using a model eye, the performance of just one commercially available Hartmann-Shack clinical aberrometer, the COAS (Wavefront Sciences, Albuquerque, NM [also commercialized as WASCA]), was found to provide highly accurate and reproducible measures of higher order aberrations.[56]

Current manufacturers of sensors using this principle for clinical purposes are Bausch & Lomb, Wavefront Sciences Inc (Albuquerque, NM), Topcon Ltd (Tokyo, Japan), VISX Inc (Irvine, Calif), Imagine Eyes Ltd (Orsay, France), and Alcon Laboratories Inc (Ft Worth, Tex). Differences between these commercially available sensors can be seen in the Table.

Skiascopy Methods. These technologies use the principle of dynamic skiascopy and could be considered as an objective variant of spatially resolved refractometers. An infrared slit scans through the pupil measuring the time difference, as opposed to position difference, of the light reflected by the retina between the center and several photodetectors on each side.[57] It rotates through 180°, generating autorefraction data, as well as calculating wavefront aberration from the difference of refractive power between areas within the pupil area[58] (Fig 6). Therefore, it measures directly in diopters, although wavefront data can be reported as either diopters or microns. This system measures longitudinal aberration, as opposed to the other systems that compute aberration from local slopes (ie, transversal aberration).

Little has been reported on the performance of clinical devices using this principle, although it has been successfully used in combination with laser systems for customized refractive surgery procedures[59-63] and the assessment of the optical quality of pathological and postoperative eyes.[64]

NIDEK Co Ltd (Gamagori, Japan) is currently the only manufacturer of this type of wavefront sensor for clinical purposes—the Optical Path Difference (OPD) Scan. This system is also the only one that obtains data within the same examination for corneal topography, enabling the assessment not only of whole eye aberrations but also anterior corneal and internal aberrations.

"Talbot Effect" Method. Although not widely reported, the "Talbot effect" can be used in the calculation of customized spectacle, contact, and intraocular lenses. The Z-View Aberrometer (Ophthonix, San Diego, Calif) is the only commercial aberrometer using this principle. The effect is observed when certain periodic intensity modulation patterns fall on the optical pupil. These pattern images reappear along a propagation path called "Talbot planes." In a way, this is a form of "self-imaging" of the pupil, with the resulting modulated pattern being recorded by a detector or series of detectors in the Talbot planes. If the patient's vision contains wavefront aberrations, the resulting modulation pattern is distorted relative to the input periodic modulation source.

The aberrometer offers a significantly higher level of resolution than, for instance, Hartmann-Shack–based systems; whereas Hartmann-Shack–based systems measure between 40 and 3500 points across a 7-mm pupil, the Z-View measures almost an order of magnitude more, 21,000 points across a 7-mm pupil.

ADVANTAGES AND INCONVENIENCES

Sequential acquisition of wavefront aberrations (as used by spatially resolved refractometry, laser ray tracing, dynamic skiascopy) has the advantage of avoiding the possibility of "overlapping" or "cross-over" phe-

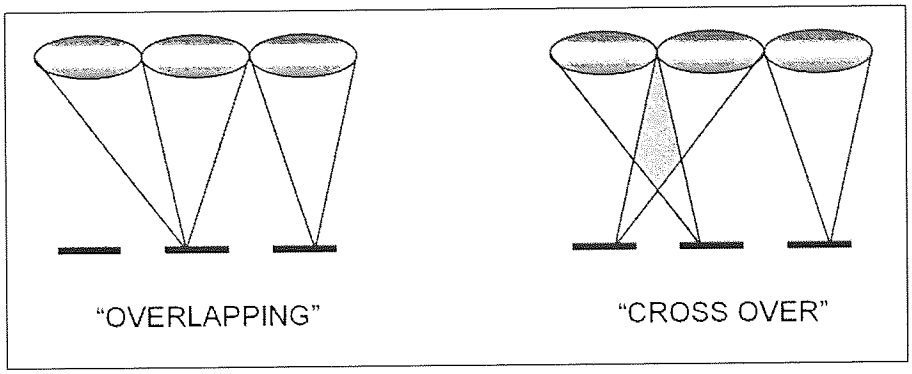

Figure 7. Scheme representing two main disadvantages of simultaneous measurement of wavefront error in highly aberrated eyes.

nomena (Fig 7), one of the main drawbacks of simultaneous acquisition measurement (Hartmann-Shack, Tscherning), altering the readings particularly in highly aberrated eyes. These refer to the possibility that, in the case of large distortions of the wavefront, focus points might overlap or cross-over to noncorresponding detectors, resulting in underestimated readings. In this sense, these devices are particularly useful when examining highly aberrated or optically altered eyes such as those with keratoconus, surgical complications, or other pathology.

On the other hand, simultaneous acquisition measurements allow higher reliability in assessing wavefront error even during short acquisition periods and enable continuous readings over short periods of time. This fact also makes them stronger against temporal factors affecting wavefront measurement, such as fluctuations in accommodation or micromovements of the eye.[49]

Ingoing methods measure the retinal image (ie, first-pass aberrations), which is more direct and not affected by any bias induced in outgoing methods, which require a double-pass through the optical system. However, Moreno-Barriuso and Navarro[49] found the same results for ingoing and outgoing light analysis, confirming the reversibility of light and the equivalence of both types of methods.

Simultaneous acquisition methods are limited by the spatial resolution arising from the distribution of the microlenses (Hartmann-Shack) or the mask configuration (Tscherning), making it difficult to adjust the sampling pattern. In sequential acquisition methods, such as laser ray tracing, the sampling pattern can be easily modified, whereas skiascopy-based techniques achieve the highest spatial resolution of all systems (Table).

It is important to point out that this review is concerned with comparisons only of the technologies and their modus operandi.

THE ROLE OF THE PUPIL

Because local aberrations are commonly measured at the pupil plane, and the Zernike description depends on the pupil area analyzed, the pupil area is of major importance when using a device for measuring wavefront error.

With increasing pupil sizes, the resolution of the retinal image may be altered less by diffraction and more by aberrations in the optical system. Campbell and Green[65] first quantified the impact of aberration with pupil size. For high magnitudes of spherical aberration, the refraction will be highly dependent on the pupil size, although subjective refraction does not seem to change much with varying pupil sizes,[5] presumably because subjective refraction is always dependent on a foveal result.

Light forming the image fills the exit pupil. Because the exit pupil is the image of the aperture (ie, the iris) as seen from the image space of the optical system of the eye, all of the effects of aberrations in the resulting image are contained in the distribution within the pupil. Therefore, it is a good place to define, characterize, and measure the effects on the light forming the image. Once the light distribution on the exit pupil of the system is known, the impulse response or PSF can be calculated.

Nevertheless, because the representation of the wave aberration using Zernike coefficients is relative to the pupil size, it changes when pupil size changes. This needs to be taken into account especially when measurements are compared. All of the clinical devices reported herein use Zernike coefficients to establish wavefront aberration data.

CLINICAL APPLICATIONS OF WAVEFRONT ANALYSIS

Clinical applications of wavefront aberration analysis can be grouped into two main fields: 1) imaging of the internal structures of the eye and 2) analysis and correction of the visual performance.

The difference is based on the direction of the light analyzed. For imaging internal structures, the light entering the eye needs to be compensated, whereas for visual performance the outgoing light needs to be measured.

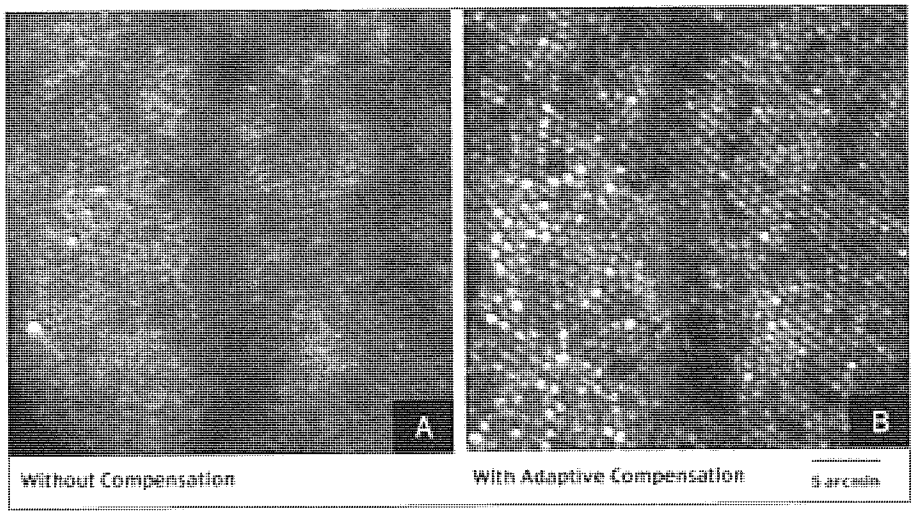

Figure 8. A) Scheme of the Adaptive Optics Laser Scanning Ophthalmoscope (AOLSO), and **B)** the improvement obtained in resolving the image of the retinal mosaic. Images courtesy of Austin Roorda.

Imaging of the Internal Structures of the Eye

This first group comprises all optical improvements in terms of lens design, system filtering, and computation to achieve better results when observing the inner structures of the eye.

Following the invention of the laser-scanning ophthalmoscope,[66] adaptive optics have been combined to provide real-time wavefront aberration correction and incredible resolution for retinal imaging[67] (Fig 8). The wavefront analysis systems provide the information needed to make the observation system perfect for the imaging of an individual eye. The aberrometers have been described essentially as modified fundus cameras, which take multiple pictures of a single spot of light on the retina.[68]

The improved systems for noninvasive imaging of the internal structures of the eye have a direct and important clinical relevance in the early detection of pathological and progressive conditions. The assessment of leukocyte velocity,[69] foveal dimensions and state,[70] and photoreceptors evaluation,[71] among others, can now be performed in real time and noninvasively, and alterations in the retina can be detected earlier.

Analysis and Correction of Visual Performance

This second group comprises all of the techniques developed to study and improve the visual performance of the human eye from the optical side. For this purpose, "aberrometry emerges as the essential clinical instrument for planning sophisticated optical treatments and measuring optical outcome."[72]

Refractive Surgery. The main force behind the rapid developments in ocular wavefront sensing over the past 10 years is the advancement of refractive surgery. An increase in high order aberration, particularly spherical aberration, has been widely reported following traditional refractive surgery procedures (ie, those without wavefront guidance).[21,40,73,74] Under normal photopic viewing conditions these do not substantially affect the visual performance of the eye; however, during scotopic viewing conditions their effects manifest as reduced low contrast performance and have particular implications regarding night-time driving.[73,75,76]

This increase in higher order aberrations is due largely to the reshaping of the anterior corneal surface,[21,77-80] and to a lesser extent changes in the posterior surface,[81] which typically arise following high magnitude correction, resulting in a considerably thinner stromal bed, but may also occur as a result of flap creation and replacement[82] or laser spot size.[83]

The increases in high order aberrations are known to be responsible for complaints of glare, halo, and night vision disturbances frequently reported by traditional refractive surgery patients.[84-86]

Customized excimer laser ablation procedures use the same technique as those without wavefront guidance except for the pattern of laser ablation itself. This pattern is calculated from the wavefront error measured with the wavefront analyzers on a case-wise basis. The algorithms used to perform customized ablations are continuously monitored and improved to obtain the best outcomes; the aims are to avoid any increase in aberrations after surgery and to reduce higher than normal preoperative aberration values to a more normal level.

The direct benefits of customized ablation arise therefore from the reduction in high order aberrations and may result in increased contrast sensitivity and visual performance, mainly under scotopic conditions.[87] Several technical factors interact to dictate the quality of this outcome, including the optical quality and performance of the wavefront analyzer, the precision of

the laser ablation, surgical planning in terms of deciding the extent of any correction, and the optimal size of the ablation zone.[88-90]

Spectacle Lenses. The advent of wavefront-guided refractive surgery has revealed new possibilities for the correction of higher order aberrations. It is, therefore, not surprising that this technology is now being applied to spectacles. The first wavefront-guided spectacles, iZon Wavefront-Guided Eye Glasses (Ophthonix Inc), are currently still undergoing clinical studies; however, Ophthonix Inc recently launched their iZon spectacle lens. The iZon lenses are made using a three-step process, which integrates three proprietary technologies. First, the Ophthonix Z-View Aberrometer (described above) captures a patient's unique wavefront measurement. Second, the information is converted into a prescription. Finally, the prescription is transferred using an ultraviolet (UV) laser to an epoxy polymer sandwiched between two optical surfaces. In the last step, the UV laser alters the refractive index of the epoxy polymer on a point-by-point basis to generate the desired refractive profile. The iZon lens uses 1.6 index cover plates, which cure seamlessly with the epoxy polymer in between. The resulting lenses receive a premium antireflective coating. Currently, the iZon lens is available in single vision only, although there are plans to extend the technology to progressive addition lenses, sunglasses, and other spectacle lens types.

Fully correcting a large degree of higher order aberrations also requires exact vertex distance, pantoscopic tilt, and facial wrap—not something easily maintained as the position of spectacles on the face cannot be ensured.

Contact Lenses. In theory, contact lenses could offer the benefits of correcting high order aberrations in the same way they are successfully used for correcting low order aberrations. The customized design of the surfaces would allow the modification of the direction of light through every point of the contact lens optical zone so that the combination with the eye's optical characteristics would, theoretically, produce an aberration-free system.

Contact lenses have many advantages over surgery, particularly in relation to reversibility, and also by permitting changes to the correction of aberrations associated with aging and other physiological factors[91,92] or following other ocular surgeries, progression of ectasia, or other anterior eye pathology.[93]

As for the postoperative outcomes following traditional refractive surgery, both rigid gas permeable and soft contact lenses seem to produce an increase in high order aberrations,[94] although these tend to be relatively predictable, depending on the parameters of the contact lens.[95-99] It has been shown that improvements can be achieved when the lens design is modified to compensate for the wavefront aberration, particularly in relation to spherical aberration. The possibility of predicting and correcting aberrations to improve visual performance can be of greater value in some special contact lens fits.[100] Nevertheless, the rotation of the lens on the eye reduces the predictability of this aberration correction.[95] As these customized contact lenses seek to correct lower and higher order aberrations, the translational and rotational movements of the lens will need to be more accurate and predictable. Once this is effectively achieved, wavefront analysis will be used to extend the visual benefits of contact lens wear.

Optical Connection Inc (San Jose, Calif) works with Ophthonix Inc to create the customized iZon by Definition wavefront-guided contact lenses. The patient is fitted with a single-use trial contact lens. After the lens settles on the eye, a wavefront analysis is performed. The wavefront data are captured as a string of Zernike coefficients. From that data, the required wavefront correction can be determined, including the lower order aberrations of sphere and cylinder and higher order aberrations, such as coma, trefoil, and spherical aberration. The wavefront analysis also captures the error that is induced by a contact lens placed on the eye. The system measures lens decentration and rotation on the eye. This information, along with the Zernike data, is used to generate a lens power profile that will correct the error.

Special mention should be made to orthokeratology, a technique of long-standing that has recently received renewed attention by some enthusiasts. The basis of the technique is the remodeling of the corneal topography by specially fitted contact lenses in an attempt to reduce myopia.[101] The method, although controversial, benefits from the present greater understanding of corneal biomechanics and the wider range of techniques available to assess and monitor corneal changes, and an extended range of contact lens materials and designs. It has been reported that patients exhibit an increase in high order aberrations similar to that obtained after refractive surgery.[102]

Ocular Pathology. Aside from all of the benefits previously mentioned regarding adaptive optics in imaging intraocular structures, wavefront analysis may aid the diagnosis and evaluation of ocular anomalies in other ways. Numerous pathologies produce changes in the wavefront aberrations of the eye, so the ability to measure the wavefront pattern of the pathological eye may allow an objective assessment of the optical, and therefore visual, consequences of pathology.[64] In

particular, anterior pole pathologies, such as those coincident with morphometric alterations of the cornea, produce a noticeable increase in the high order aberrations, worsening the visual function and limiting the options for correction.[64,103] Pathology of the crystalline lens may result in increased high order aberrations, and it has been reported that cataracts increase wavefront aberration coefficients, but the polarity has been shown to be negative in nuclear cataract and positive in cortical cataract, demonstrating the potential benefit of wavefront analysis for characterizing eyes with lens pathology.[104,105]

A further application of wavefront aberration analysis systems is in the evaluation of the tear film. It is known that the tear film plays an important role in smoothing the anterior corneal surface, therefore any disruption to the tear film will affect the optical quality of the system. Thibos and Hong[68] demonstrated that tear film stability is an important factor in successfully imaging intraocular structures, whereas Montes-Mico et al[106] showed that wavefront aberrations increase to cause perceptible degradation of the retinal image after extended interblink intervals (approximately 4 seconds). It has therefore been suggested that assessment of the tear film provides a further potential application of Hartmann-Shack aberrometers[107-109] as well as in monitoring the effects of treatment,[108,110,111] not withstanding the additional complication that the tear film provides when assessing aberrations in preoperative refractive surgery cases.

Intraocular Lens Selection and Design. It has been reported that the implantation of intraocular lenses (IOLs) can produce more high order aberrations than LASIK by increasing spherical aberration in particular.[112] In contrast, clear lensectomy reduces aberrations in hypermetropic patients compared to those treated with LASIK.[80]

Factors such as lens material, curvature, and thickness all impact the wavefront pattern in various ways, and all parameters need to be considered when deciding the potential impact of lens design on high order aberrations. Acrylic materials seem to produce more aberrations than silicone or polymethylmethacarylate,[113] although the reason has not yet been clarified but involves changes in the refraction index of the lens.

The direct benefits of wavefront analysis in terms of IOL design and indeed surgical technique are easily understandable. Lens designs have advanced considerably in the past few years, with resulting improvement in the optical performance of the most recent IOLs. Designing a more prolate anterior surface, for instance, significantly reduces the spherical aberration,[114-116] with particular benefits to patients with large pupil sizes.

A recent study[117] concluded that the benefit of correcting spherical aberration in a pseudophakic eye is limited by various factors including the need to wear spectacles, age-related miosis, tilt and decentration of the IOL, as well as small contributions of spherical aberration and inter-patient variability.

Evaluation of Accommodation. The accommodative response of the eye results in changes to the lens shape, thickness, and location and substantially affects the wavefront aberration pattern. Most eyes suffer from positive spherical aberration when unaccommodated, with a trend toward negative spherical aberration on accommodation.[16,118-120]

These changes in high order aberrations are of importance when a customized correction is being considered, as such correction would only be effective for one state of accommodation.[121] However, recent reports suggest a high level of predictability for changes in spherical aberration, and the typical eye would benefit from correcting aberrations at distance for any accommodative state.[118]

Wavefront analysis may also be potentially useful for the assessment of accommodation anomalies, such as accommodative spasm,[122] as the optical behavior in terms of high order aberrations seems to be different, showing an increase in high order aberrations in these cases but with different polarity than observed during normal accommodative processes.

SUMMARY

A wide range of clinical wavefront aberrometers are now available for clinicians and researchers. They use different principles to measure the optical quality of the eye, each having their own benefits according to the purpose for which they are used. Many of these have already been studied in detail, and great potential for future applications exists in the different fields of clinical vision sciences. Applications in vision sciences range from assessment of refractive error, refractive surgery planning or evaluation of outcomes, optimization of designs for contact lenses or IOLs to evaluation of the impact of pathology in the optical performance of the eye or evaluation of accommodation alterations, aside from all of the applications yet to be discovered.

The proven neural adaptation to wavefront aberrations,[123] should be taken into account when a correction of "optical defects" is considered.

REFERENCES

1. Howland HC, Howland B. A subjective method for the measurement of monochromatic aberrations of the eye. *J Opt Soc Am.* 1977;67:1508-1518.
2. Walsh G, Charman WN, Howland HC. Objective technique for

the determination of monochromatic aberrations of the human eye. *J Opt Soc Am A.* 1984;1:987-992.

3. Artal P, Santamaria J, Bescos J. Retrieval of wave aberration of human eyes from actual point-spread-function data. *J Opt Soc Am A.* 1988;5:1201-1206.
4. Liang J, Grimm B, Goelz S, Bille JF. Objective measurement of wave aberrations of the human eye with the use of a Hartmann-Shack wave-front sensor. *J Opt Soc Am A Opt Image Sci Vis.* 1994;11:1949-1957.
5. Liang J, Williams DR. Aberrations and retinal image quality of the normal human eye. *J Opt Soc Am A Opt Image Sci Vis.* 1997;14:2873-2883.
6. Navarro R, Losada MA. Aberrations and relative efficiency of light pencils in the living human eye. *Optom Vis Sci.* 1997;74:540-547.
7. Mierdel P, Krinke HE, Wiegand W, Kaemmerer M, Seiler T. Measuring device for determining monochromatic aberration of the human eye [German]. *Ophthalmologe.* 1997;94:441-445.
8. Iglesias I, Berrio E, Artal P. Estimates of the ocular wave aberration from pairs of double-pass retinal images. *J Opt Soc Am A Opt Image Sci Vis.* 1998;15:2466-2476.
9. He JC, Marcos S, Webb RH, Burns SA. Measurement of the wave-front aberration of the eye by a fast psychophysical procedure. *J Opt Soc Am A Opt Image Sci Vis.* 1998;15:2449-2456.
10. Marcos S, Burns SA, Prieto PM, Navarro R, Baraibar B. Investigating sources of variability of monochromatic and transverse chromatic aberrations across eyes. *Vision Res.* 2001;41:3861-3871.
11. Howland HC. The history and methods of ophthalmic wavefront sensing. *J Refract Surg.* 2000;16:S552-S553.
12. Atchison DA, Collins MJ, Wildsoet CF, Christensen J, Waterworth MD. Measurement of monochromatic ocular aberrations of human eyes as a function of accommodation by the Howland aberroscope technique. *Vision Res.* 1995;35:313-323.
13. Burns SA. The spatially resolved refractometer. *J Refract Surg.* 2000;16:S566-S569.
14. Marcos S, Burns SA, Moreno-Barriusop E, Navarro R. A new approach to the study of ocular chromatic aberrations. *Vision Res.* 1999;39:4309-4323.
15. Collins MJ, Wildsoet CF, Atchison DA. Monochromatic aberrations and myopia. *Vision Res.* 1995;35:1157-1163.
16. He JC, Burns SA, Marcos S. Monochromatic aberrations in the accommodated human eye. *Vision Res.* 2000;40:41-48.
17. Marcos S, Burns SA. On the symmetry between eyes of wavefront aberration and cone directionality. *Vision Res.* 2000;40:2437-2447.
18. McLellan JS, Marcos S, Burns SA. Age-related changes in monochromatic wave aberrations of the human eye. *Invest Ophthalmol Vis Sci.* 2001;42:1390-1395.
19. Villegas EA, Artal P. Spatially resolved wavefront aberrations of ophthalmic progressive-power lenses in normal viewing conditions. *Optom Vis Sci.* 2003;80:106-114.
20. Marcos S. Are changes in ocular aberrations with age a significant problem for refractive surgery? *J Refract Surg.* 2002;18:S572-S578.
21. Marcos S, Barbero S, Llorente L, Merayo-Lloves J. Optical response to LASIK surgery for myopia from total and corneal aberration measurements. *Invest Ophthalmol Vis Sci.* 2001;42:3349-3356.
22. Walsh G, Charman WN. Measurement of the axial wavefront aberration of the human eye. *Ophthalmic Physiol Opt.* 1985;5:23-31.
23. Calver RI, Cox MJ, Elliott DB. Effect of aging on the monochromatic aberrations of the human eye. *J Opt Soc Am A Opt Image Sci Vis.* 1999;16:2069-2078.
24. Mrochen M, Kaemmerer M, Mierdel P, Krinke HE, Seiler T. Principles of Tscherning aberrometry. *J Refract Surg.* 2000;16:S570-S571.
25. Howland B, Howland HC. Subjective measurement of high-order aberrations of the eye. *Science.* 1976;193:580-582.
26. Smith G, Applegate RA, Howland HC. The crossed-cylinder aberroscope: an alternative method of calculation of the aberrations. *Ophthalmic Physiol Opt.* 1996;16:222-229.
27. Hong X, Thibos LN, Bradley A, Woods RL, Applegate RA. Comparison of monochromatic ocular aberrations measured with an objective cross-cylinder aberroscope and a Shack-Hartmann aberrometer. *Optom Vis Sci.* 2003;80:15-25.
28. Smirnov MS. Measurement of the wave aberration of the human eye [Russian]. *Biofizika.* 1961;6:776-795.
29. Moreno-Barriuso E, Marcos S, Navarro R, Burns SA. Comparing laser ray tracing, the spatially resolved refractometer, and the Hartmann-Shack sensor to measure the ocular wave aberration. *Optom Vis Sci.* 2001;78:152-156.
30. Webb RH, Penney CM, Sobiech J, Staver PR, Burns SA. SSR (spatially resolved refractometer): a null-seeking aberrometer. *Appl Opt.* 2003;42:736-744.
31. Licbter H, Staver PR, Thompson K, Garcia J. InterWave aberrometry for custom ablation. *Int Ophthalmol Clin.* 2002;42:41-54.
32. Randleman JB, Thompson KP, Staver PR. Wavefront aberrations from corneal ectasia after laser in situ keratomileusis demonstrated by InterWave aberrometry. *J Refract Surg.* 2004;20:170-175.
33. Russell GE, Stulting RD, Thompson KP. Postoperative LASIK visnal aberrations and treatment with InterWave-guided multipass, multistage correction. *Optom Vis Sci.* 2003;80:93-96.
34. Thompson KP, Staver PR, Garcia JR, Burns SA, Webb RH, Stulting RD. Using InterWave aberrometry to measure and improve the quality of vision in LASIK surgery. *Ophthalmology.* 2004;111:1368-1379.
35. Kaemmerer M, Mrochen M, Mierdel P, Krinke HE, Seiler T. Clinical experience with the Tscherning aberrometer. *J Refract Surg.* 2000;16:S584-S587.
36. Mierdel P, Kaemmerer M, Mrochen M, Krinke HE, Seiler T. Ocular optical aberrometer for clinical use. *J Biomed Opt.* 2001;6:200-204.
37. Mrochen M, Kaemmerer M, Seiler T. Clinical results of wavefront-guided laser in situ keratomileusis 3 months after surgery. *J Cataract Refract Surg.* 2001;27:201-207.
38. Mrochen M, Kaemmerer M, Seiler T. Wavefront-guided laser in situ keratomileusis: early results in three eyes. *J Refract Surg.* 2000;16:116-121.
39. Molebny VV, Panagopoulou SI, Molebny SV, Wakil YS, Pallikaris IG. Principles of ray tracing aberrometry. *J Refract Surg.* 2000;16:S572-S575.
40. Moreno-Barriuso E, Lloves JM, Marcos S, Navarro R, Llorente L, Barbero S. Ocular aberrations before and after myopic corneal refractive surgery: LASIK-induced changes measured with laser ray tracing. *Invest Ophthalmol Vis Sci.* 2001;42:1396-1403.
41. Wang L, Wang N, Koch DD. Evaluation of refractive error measurements of the Wavescan Wavefront system and the Tracey Wavefront aberrometer. *J Cataract Refract Surg.* 2003;29:970-979.
42. Wang L, Misra M, Pallikaris IG, Koch DD. Comparison of a ray-tracing refractometer, autorefractor, and computerized videokeratography in measuring pseudophakic eyes. *J Cataract Refract Surg.* 2002;28:276-282.
43. Pallikaris IG, Panagopoulou SI, Molebny VV. Clinical experience with the Tracey technology wavefront device. *J Refract Surg.* 2000;16:S588-S591.

44. Pallikaris LG, Panagopoulou SI, Siganos CS, Molebny VV. Objective measurement of wavefront aberrations with and without accommodation. *J Refract Surg.* 2001;17:S602-S607.
45. Platt BC, Shack R. History and principles of Shack-Hartmann wavefront sensing. *J Refract Surg.* 2001;17:S573-S577.
46. Thibos LN. Principles of Hartmann-Shack aberrometry. *J Refract Surg.* 2000;16:S563-S565.
47. Prieto PM, Vargas-Martin F, Goelz S, Artal P. Analysis of the performance of the Hartmann-Shack sensor in the human eye. *J Opt Soc Am A Opt Image Sci Vis.* 2000;17:1388-1398.
48. Salmon TO, Thibos LN, Bradley A. Comparison of the eye's wave-front aberration measured psychophysically and with the Shack-Hartmann wave-front sensor. *J Opt Soc Am A Opt Image Sci Vis.* 1998;15:2457-2465.
49. Moreno-Barriuso E, Navarro R. Laser Ray Tracing versus Hartmann-Sback sensor for measuring optical aberrations in the human eye. *J Opt Soc Am A Opt Image Sci Vis.* 2000;17:974-985.
50. Hament WJ, Nabar VA, Nuijts RM. Repeatability and validity of Zywave aberrometer measurements. *J Cataract Refract Surg.* 2002;28:2135-2141.
51. Salmon TO, West RW, Gasser W, Kenmore T. Measurement of refractive errors in young myopes using the COAS Shack-Hartmann aberrometer. *Optom Vis Sci.* 2003;80:6-14.
52. Cervino A, Hosking, SL, Rai GK, Naroo SA, Gilmartin B. Wavefront analyzers induce instrument myopia. *J Refract Surg.* 2006;22:795-803.
53. Cheng X, Himebaugh NL, Kollbaum PS, Thibos LN, Bradley A. Test-retest reliability of clinical Shack-Hartmann measurements. *Invest Ophthalmol Vis Sci.* 2004;45:351-360.
54. Mirshahi A, Buhren J, Gerhardt D, Kohnen T. In vivo and in vitro repeatability of Hartmann-Shack aberrometry. *J Cataract Refract Surg.* 2003;29:2295-2301.
55. Rodriguez P, Navarro R, Gonzalez L, Hernandez JL. Accuracy and reproducibility of Zywave, Tracey and experimental aberrometers. *J Refract Surg.* 2004;20:810-817.
56. Cheng X, Himebaugh NL, Kollbaum PS, Thibos LN, Bradley A. Validation of a clinical Shack-Hartmann aberrometer. *Optom Vis Sci.* 2003;80:587-595.
57. MacRae S, Fujieda M. Slit skiascopic-guided ablation using the Nidek laser. *J Refract Surg.* 2000;16:S576-S580.
58. Buscemi P. Retinoscope double pass aberrometry: principles and application of the Nidek OPD-Scan. In: Krueger RR, Applegate RA, MacRae SM, eds. *Wavefront Customized Visual Correction: The Quest for Super Vision II.* Thorofare, NJ: SLACK Incorporated; 2004:149-153.
59. Arbelaez MC. Super vision: dream or reality. *J Refract Surg.* 2001;17:S211-S218.
60. Gimbel HV, Stoll SB. Photorefractive keratectomy with customized segmental ablation to correct irregular astigmatism after laser in situ keratomileusis. *J Refract Surg.* 2001;17:S229-S232.
61. Sarkisian KA, Petrov AA. Clinical experience with the customized low spherical aberration ablation profile for myopia. *J Refract Surg.* 2002;18:S352-S356.
62. Gimbel HV, Sofinski SJ, Mahler OS, van Westenbrugge JA, Ferensowicz MI, Triebwasser RW. Wavefront-guided multipoint (segmental) custom ablation enhancement using the Nidek NAVEX platform. *J Refract Surg.* 2003;19:S209-S216.
63. Nakano K, Portellinha W, Oliveira M, Alvarenga L, Nakano C, Nakano E. Refractive outcome of Nidek OPD-scan customized ablations. *J Refract Surg.* 2003;19:S221-S222.
64. Shah S, Naroo S, Hosking S, Gherghel D, Mantry S, Bannerjee S, Pedwell K, Bains HS. Nidek OPD-scan analysis of normal, keratoconic, and penetrating keratoplasty eyes. *J Refract Surg.* 2003;19:S255-S259.
65. Campbell FW, Green DG. Optical and retinal factors affecting visual resolution. *J Physiol.* 1965;181:576-593.
66. Webb RH, Hughes GW. Scanning laser ophthalmoscope. *IEEE Trans Biomed Eng.* 1981;28:488-492.
67. Roorda A. Adaptive optics ophthalmoscopy. *J Refract Surg.* 2000;16:S602-S607.
68. Thibos LN, Hong X. Clinical applications of the Shack-Hartmann aberrometer. *Optom Vis Sci.* 1999;76:817-825.
69. Martin JA, Roorda A. Direct and noninvasive assessment of parafoveal capillary leukocyte velocity. *Ophthalmology.* 2005;112:2219-2224.
70. Van A, Roorda A. The radius of curvature of the foveal pit. *Invest Ophthalmol Vis Sci.* 2003;44:663.
71. Wolfing JI, Chung M, Carroll J, Roorda A, Poonja S, Vilupuru AS, Williams DR. High resolution imaging of cone-rod dystrophy with adaptive optics. *Invest Ophthalmol Vis Sci.* 2005;46:2567.
72. Thibos LN, Applegate RA, Marcos S. Aberrometry: the past, present, and future of optometry. *Optom Vis Sci.* 2003;80:1-2.
73. Marcos S. Aberrations and visual performance following standard laser vision correction. *J Refract Surg.* 2001;17:S596-S601.
74. Oliver KM, Hemenger RP, Corbett MC, O'Brart DP, Verma S, Marshall J, Tomlinson A. Corneal optical aberrations induced by photorefractive keratectomy. *J Refract Surg.* 1997;13:246-254.
75. Applegate RA, Howland HC. Refractive surgery, optical aberrations, and visual performance. *J Refract Surg.* 1997;13:295-299.
76. Nakamura K, Bissen-Miyajima H, Toda I, Hori Y, Tsubota K. Effect of laser in situ keratomileusis correction on contrast visual acuity. *J Cataract Refract Surg.* 2001;27:357-361.
77. Llorente L, Barbero S, Merayo J, Marcos S. Total and corneal optical aberrations induced by laser in situ keratomileusis for hyperopia. *J Refract Surg.* 2004;20:203-216.
78. Hersh PS, Fry K, Blaker JW. Spherical aberration after laser in situ keratomileusis and photorefractive keratectomy. Clinical results and theoretical models of etiology. *J Cataract Refract Surg.* 2003;29:2096-2104.
79. Oshika T, Miyata K, Tokunaga T, Samejima T, Amano S, Tanaka S, Hirohara Y, Mihashi T, Maeda N, Fujikado T. Higher order wavefront aberrations of cornea and magnitude of refractive correction in laser in situ keratomileusis. *Ophthalmology.* 2002;109:1154-1158.
80. Ma L, Atchison DA, Charman WN. Off-axis refraction and aberrations following couventional laser in situ keratomileusis. *J Cataract Refract Surg.* 2005;31:489-498.
81. Twa MD, Roberts C, Mahmoud AM, Chang JS Jr. Response of the posterior corneal surface to laser in situ keratomileusis for myopia. *J Cataract Refract Surg.* 2005;31:61-71.
82. Potgieter FJ, Roberts C, Cox IG, Mahmoud AM, Herderick EE, Roetz M, Steenkamp W. Prediction of flap response. *J Cataract Refract Surg.* 2005;31:106-114.
83. Huang D, Arif M. Spot size and quality of scanning laser correction of higher-order wavefront aberrations. *J Cataract Refract Surg.* 2002;28:407-416.
84. Seiler T, Holschbach A, Derse M, Jean B, Genth U. Complications of myopic photorefractive keratectomy with the excimer laser. *Ophthalmology.* 1994;101:153-160.
85. Martinez CE, Applegate RA, Klyce SD, McDonald MB, Medina JP, Howland HC. Effect of pupillary dilation on corneal optical aberrations after photorefractive keratectomy. *Arch Ophthalmol.* 1998;116:1053-1062.

86. Chalita MR, Chavala S, Xu M, Krueger RR. Wavefront analysis in post-LASIK eyes and its correlation with visual symptoms, refraction, and topography. *Ophthalmology.* 2004;111:447-453.
87. Kanjani N, Jacob S, Agarwal A, Agarwal A, Agarwal S, Agarwal T, Doshi A, Doshi S. Wavefront- and topography-guided ablation in myopic eyes using Zyoptix. *J Cataract Refract Surg.* 2004;30:398-402.
88. Seo KY, Lee JB, Kang JJ, Lee ES, Kim EK. Comparison of higher-order aberrations after LASEK with a 6.0 mm ablation zone and a 6.5 mm ablation zone with blend zone. *J Cataract Refract Surg.* 2004;30:653-657.
89. Endl MJ, Martinez CE, Klyce SD, McDonald MB, Coorpender SJ, Applegate RA, Howland HC. Effect of larger ablation zone and transition zone on corneal optical aberrations after photorefractive keratectomy. *Arch Ophthalmol.* 2001;119:1159-1164.
90. Argento C, Cosentino MJ, Tytiun A, Rapetti G, Zarate J. Corneal ectasia after laser in situ keratomileusis. *J Cataract Refract Surg.* 2001;27:1440-1448.
91. Kuroda T, Fujikado T, Ninomiya S, alameda N, Hirohara Y, Mihashi T. Effect of aging on ocular light scatter and higher order aberrations. *J Refract Surg.* 2002;18:S598-S602.
92. Chateau N, Blanchard A, Baude D. Influence of myopia and aging on the optimal spherical aberration of soft contact lenses. *J Opt Soc Am A Opt Image Sci Vis.* 1998;15:2589-2596.
93. de Brabander J, Chateau N, Marin G, Lopez-Gil N, Van der Worp E, Benito A. Simulated optical performance of custom wavefront soft contact lenses for keratoconus. *Optom Vis Sci.* 2003;80:637-643.
94. Lu F, Mao X, Qu J, Xu D, He JC. Monochromatic wavefront aberrations in the human eye with contact lenses. *Optom Vis Sci.* 2003;80:135-141.
95. Lopez-Gil N, Castejon-Mochon JF, Benito A, Marin JM, Lo-a-Foe G, Marin G, Fermigier B, Renard D, Joyeux D, Chateau N, Artal P. Aberration generation by contact lenses with aspheric and asymmetric surfaces. *J Refract Surg.* 2002;18:S603-S609.
96. Patel S, Fakhry M, Alio JL. Objective assessment of aberrations induced by multifocal contact lenses in vivo. *CLAO J.* 2002;28:196-201.
97. Hong X, Himebaugh N, Thibos LN. On-eye evaluation of optical performance of rigid and soft contact lenses. *Optom Vis Sci.* 2001;78:872-880.
98. Dorronsoro C, Barbero S, Llorente L, Marcos S. On-eye measurement of optical performance of rigid gas permeable contact lenses based on ocular and corneal aberrometry. *Optom Vis Sci.* 2003;80:115-125.
99. Dietze HH, Cox MJ. On- and off-eye spherical aberration of soft contact lenses and consequent changes of effective lens power. *Optom Vis Sci.* 2003;80:126-134.
100. Martin JA, Roorda A. Predicting and assessing visual performance with multizone bifocal contact lenses. *Optom Vis Sci.* 2003;80:812-819.
101. Swarbrick HA. Orthokeratology (corneal refractive therapy): what is it and how does it work? *Eye Contact Lens.* 2004;30:181-185.
102. Joslin CE, Wu SM, McMahon TT, Shahidi M. Higher-order wavefront aberrations in corneal refractive therapy. *Optom Vis Sci.* 2003;80:805-811.
103. Maeda N, Fujikado T, Kuroda T, Mihashi T, Hirohara Y, Nishida K, Watanabe H, Tano Y. Wavefront aberrations measured with Hartmann-Shack sensor in patients with keratoconus. *Ophthalmology.* 2002;109:1996-2003.
104. Kuroda T, Fujikado T, Maeda N, Oshika T, Hirohara Y, Mihashi T. Wavefront analysis in eyes with nuclear or cortical cataract. *Am J Ophthalmol.* 2002;134:1-9.
105. Kuroda T, Fujikado T, Maeda N, Oshika T, Hirohara Y, Mihashi T. Wavefront analysis of higher-order aberrations in patients with cataract. *J Cataract Refract Surg.* 2002;28:438-444.
106. Montes-Mico R, Alio JL, Munoz G, Charman WN. Temporal changes in optical quality of air-tear film interface at anterior cornea after blink. *Invest Ophthalmol Vis Sci.* 2004;45:1752-1757.
107. Giraldez Fernandez MJ, Yebra-Pimentel E, Parafita M, et al. Comparison of keratometric values of healthy eyes measured by Javal keratometer, Nidek autokeratometer, and corneal analysis system (EyeSys). *ICLC.* 2000;27:33-40.
108. Montes-Mico R, Alio JL, Charman WN. Dynamic changes in the tear film in dry eyes. *Invest Ophthalmol Vis Sci.* 2005;46:1615-1619.
109. Montes-Mico R, Caliz A, Alio JL. Wavefront analysis of higher order aberrations in dry eye patients. *J Refract Surg.* 2004;20:243-247.
110. Montes-Mico R, Caliz A, Alio JL. Changes in ocular aberrations after instillation of artificial tears in dry-eye patients. *J Cataract Refract Surg.* 2004;30:1649-1652.
111. Huang B, Mirza MA, Qazi MA, Pepose JS. The effect of punctal occlusion on wavefront aberrations in dry eye patients after laser in situ keratomileusis. *Am J Ophthalmol.* 2004;137:52-61.
112. Miller JM, Anwaruddin R, Straub J, Schwiegerling J. Higher order aberrations in normal, dilated, intraocular lens, and laser in situ keratomileusis corneas. *J Refract Surg.* 2002;18:S579-S583.
113. Vilarrodona L, Barrett GD, Johnson B. High-order aberrations in pseudophakia with different intraocular lenses. *J Cataract Refract Surg.* 2004;30:571-575.
114. Casprini F, Balestrazzi A, Tosi GM, Miracco F, Martone G, Cevenini G, Caporossi A. Glare disability and spherical aberration with five foldable intraocular lenses: a prospective randomized study. *Acta Ophthalmol Scand.* 2005;83:20-25.
115. Mester U, Dillinger P, Anterist N. Impact of a modified optic design on visual function: clinical comparative study. *J Cataract Refract Surg.* 2003;29:652-660.
116. Holladay JT, Piers PA, Koranyi G, van der Mooren M, Norrby NE. A new intraocular lens design to reduce spherical aberration of pseudophakic eyes. *J Refract Surg.* 2002;18:683-691.
117. Dietze HH, Cox MJ. Limitations of correcting spherical aberration with aspheric intraocular lenses. *J Refract Surg.* 2005;21:S541-S546.
118. Cheng H, Barnett JK, Vilupuru AS, Marsack JD, Kasthurirangun S, Applegate RA, Roorda A. A population study on changes in wave aberrations with accommodation. *J Vis.* 2004;4:272-280.
119. Artal P, Fernandez EJ, Manzanera S. Are optical aberrations during accommodation a significant problem for refractive surgery? *J Refract Surg.* 2002;18:S563-S566.
120. Hazel CA, Cox MJ, Strang NC. Wavefront aberration and its relationship to the accommodative stimulus-response function in myopic subjects. *Optom Vis Sci.* 2003;80:151-158.
121. Ninomiya S, Fujikado T, Kuroda T, Maeda N, Tano Y, Oshika T, Hirohara Y, Mihashi T. Changes of ocular aberration with accommodation. *Am J Ophthalmol.* 2002;134:924-926.
122. Ninomiya S, Fujikado T, Kuroda T, Maeda N, Tano Y, Hirohara Y, Mihashi T. Wavefront analysis in eyes with accommodative spasm. *Am J Ophthalmol.* 2003;136:1161-1163.
123. Artal P, Chen L, Fernández EJ, Singer B, Manzanera S, Williams DR. Neural compensation for the eye's optical aberrations. *J Vis.* 2004;4:281-287.

AUTHOR QUERIES

Pg 2, right column, second paragraph: "It was first used to subjectively determine the wavefront aberrations of the human eye[1,25] and had its first objective version in 1984[2] using a second ophthalmoscopic channel to capture the retinal image." was changed to "It was first used to subjectively determine the wavefront aberrations of the human eye[1,25] but was modified to an objective version in 1984[2] using a second ophthalmoscopic channel to capture the retinal image." Please okay as edited.

Pg 2, right column, third paragraph: "Based on Scheiner's principle described by Smirnov,[28] the spatially resolved refractometer allows a psychophysical measurement of ocular wavefront aberrations." was changed to "The spatially resolved refractometer, based on Scheiner's principle described by Smirnov,[28] allows a psychophysical measurement of ocular wavefront aberrations." Please okay as edited.

Regarding the following statements, please identify the specific model names.

In studies with **earlier versions** of the Tracey device, it was found to provide accurate,[42] highly reproducible[39,42,43] measurements. The same was found with the **later version**.[41]

Pg 6, right column: "Relatively few studies have reported the performance of clinical Hartmann-Shack devices, and **most are directed towards the performance** of low order aberrations." was changed to "Relatively few studies have reported the performance of clinical Hartmann-Shack devices, which analyze mostly low order aberrations." Please okay as edited.

Pg 10, left column, please confirm correctness of terminology "...to progressive **addition** lenses...."

Pg 10, leflt column "Fully correcting a large degree of higher order aberrations also requires exact vertex distance, pantoscopic tilt, and facial wrap—not something easily maintained if the spectacles **lose adjustment**." was changed to "Fully correcting a large degree of higher order aberrations also requires exact vertex distance, pantoscopic tilt, and facial wrap—not something easily maintained as the position of spectacles on the face cannot be ensured." Please okay as edited.

Please specify the clinical sensors in Figure 5.

In the legend for Figure 6, please replace the word "conjugate" with a more appropriate and familiar term.

Please provide the manufacturer (and its location) of the Adaptive Optics Laser Scanning Ophthalmoscope (AOLSO).

Please okay Abstract as edited.

Please provide all author names for reference 107. Please spell out journal name.

Ophthal. Physiol. Opt. 2004 **24:** 148–157

BCOVS 2003 Abstracts

British Congress of Optometry and Vision Science (BCOVS) meeting held at Aston University, Birmingham, UK 18th December 2003

Paediatric visual electrophysiology

D. Thompson

Visual Electrophysiology Unit, Great Ormond Street Hospital for Children, London WC1N 3JH, UK

Some of the main uses of visual electrophysiology in paediatric practice are to determine why an infant is not fixing or following, or why they have unusual eye movements or nystagmus. The electroretinogram and visual evoked potential (VEP) tests can be adapted so that they may be carried out in the same session in alert infants and children without restraint or sedation. If used together they will distinguish Leber's amaurosis, cone dysfunction, congenital stationary night blindness, optic nerve hypoplasia, or chiasmal anomalies (e.g. albinism or achiasmia), as causes of nystagmus. In textbooks these clinical entities are often depicted as obvious, but fundi may appear normal, and the clinical signs can be subtle. For example, albinism may be clinically overlooked, but identified by the transoccipital asymmetry of monocular VEPs, which reflects the chiasmal misrouting of too many fibres to the contralateral hemisphere.

A number of patients demonstrating crossed transoccipital VEP asymmetry have shown discrepancies and variations in phenotype/gentotype characteristics. These provide interesting clues about chiasmal axonal guidance, macula development and its relationship to the development of vision and nystagmus. For example, a boy who underwent an electrodiagnostic assessment to estimate his vision level, when behavioural assessment was not possible, was co-incidentally noted to have a VEP-crossed asymmetry typical of albinism. Clinically his fundi were normal with good macula differentiation and he did not have nystagmus. This VEP observation was discrepant until his continued lack of developmental progress prompted further investigation including DNA analysis, and he was found to have Angelman's syndrome. This is caused by a loss of imprinted gene expression on chromosome 15q11-13. When the maternal chromosome is missing, Angelman's syndrome manifests, and if the paternal contribution is missing, Prader Willi syndrome results. The most common deletion of this part of the chromosome includes the P gene within the fracture sites (pink-eyed dilution gene homologue in mice) or OCA2 gene. In this patient, the lack of one P gene appeared sufficient to alter axonal pathfinding at the chiasm, but caused minimal ocular effect. Indeed a review of all patients demonstrating a crossed asymmetry ($n \approx 114$), showed around 11 patients who did not demonstrate clinical nystagmus and seven patients who had apparently well-defined maculae.

The lack of nystagmus is interesting. Nystagmus has been attributed to the lack of macula differentiation in albinism that would be expected to underlie poor visual acuity: although this has been termed foveal hypoplasia, optical coherence tomography sections suggest that this is a misnomer as the retinal thickness is fairly constant over this region. Yet some interesting discrepancies have arisen in our cobort of patients, where better vision has developed in the sibling manifesting nystagmus rather than in the sibling with no nystagmus. We are continuing multi-disciplinary investigations of the ocular manifestations and factors that may, cumulatively, tip the balance towards ocular motor instabilities and chiasmal misrouting.

Variant Creutzfeldt–Jakob disease and the eye

R. A. Armstrong

Vision Sciences, Aston University, Birmingham B4 7ET, UK

Purpose: Variant Creutzfeldt–Jakob disease (vCJD) was first described in the UK in 1996 and is one of a group of diseases, the transmissible spongiform encephalopathies (TSEs), which affect both animals and humans. This review discusses vCJD in the context of other TSEs, considers the controversial 'prion' hypothesis as to the cause of the disease, the ocular features of vCJD, and the possible transmission of the disease via optometric devices.

Methods: Pathological studies were carried out on 11 vCJD patients, including two cases that were the basis of the original description of the disease. Thin sections (7 μm) of frontal, parietal, occipital and temporal cortex and cerebellum were stained with haematoxylin and eosin and with various antibodies (12F10, 3F4) raised against prion protein (PrP).

Results: The TSEs include scrapie in sheep (first described in 1772), bovine spongiform encephalopathy (BSE) in cows (described in 1986) and CJD, Gerstman–Straussler–Scheinker syndrome (GSS) and fatal familial insomnia (FFI) in humans. CJD is the most important form of TSE in humans and was first described by Creutzfeldt and Jakob in 1921. Variant CJD has several features that differ from the classical forms of the disease including early age of onset, longer duration of disease, psychiatric presentation (e.g. depression), and extensive florid plaque development in the brain. Examination of affected brain tissue suggests these diseases are due to the acquisition and deposition of PrP in the brain. There are two forms of PrP, viz. a normal cellular form (PrPc), which has a normal function in the brain, and the 'scrapie' form (PrPSc) that causes disease. PrPc is believed to comprise four α-helices with virtually no β-sheets. PrPSc displays an identical primary structure to PrPc but differs in secondary and tertiary structures comprising a four-stranded β-sheet configuration covered on one face by two α-helices. The presence of β-sheets enables PrPSc to assemble into the insoluble fibrils that accumulate in the brain as prion deposits. The 'prion hypothesis' states that the development of PrP deposits in the brain is 'seeded' by PrPSc that acts as an auto-catalyst converting normal PrPc to PrPSc. Once the process is initiated, it may proceed at an exponential rate within the brain, the PrPSc deposits growing with time. It can be shown that if the deposits do grow with time according to this hypothesis, the size distribution of PrP deposits in brain sections should be log-normal. In many areas of the cerebral cortex, the size distributions of the deposits fit this model quite closely. Variant CJD patients may exhibit a range of ocular symptoms; the most commonly reported being diplopia, supranuclear palsies, complex visual disturbances, and hallucinations (*Table 1*). Some patients with sporadic CJD

Table 1. Ocular features of variant Creutzfeldt–Jakob disease (vCJD) (Lueck, 2000)

Feature	Occurrence
Blurred vision	Approx. 9% at presentation
Homonymous defects	In 7% of sporadic cases (vCJD?)
Diplopia	Commonly reported
Supranuclear palsies	30% of cases of vCJD
Nystagmus	Common in iatrogenic CJD
Saccadic/smooth pursuit movements	Rare
Complex visual disturbances	Depth perception impaired, agnosis, dyslexia, optic ataxia
Visual hallucinations	Common in vCJD (10–50%)
Cortical blindness	25–50% of cases

(sCJD) may exhibit homonymous visual field defects at presentation but the occurrence of this symptom in vCJD is uncertain. Saccadic and smooth pursuit movements appear to be more rarely affected in vCJD. The primary visual cortex (V1) is one of the areas of the cerebral cortex most significantly affected by the pathological changes with a bimodal distribution (laminae II/III and V/VI) of the vacuolation while PrP deposits are distributed largely in laminae II/III. Variant CJD could be transmitted by a variety of methods including corneal transplant, the use of depth electrodes in the brain, neurosurgery, via growth hormone extracts, and by blood transfusion. Whether PrPSc can be transmitted by blood transfusion has been of considerable concern. Most aspects of the pathology of vCJD, including the vacuolation and diffuse PrP deposits, do not show a distribution in the brain consistent with blood spread. By contrast, the florid PrP deposits are clustered around cerebral blood vessels but this appears to be due to the leaking of 'chaperone' molecules from the blood vessels enhancing the condensation of PrP. The agent causing vCJD does appear to accumulate in lymphoid tissue such as the spleen and tonsils. Hence, sheep can be infected by scrapie by mouth, the agent replicating in lymphoid tissue, before entering the brain through the spinal cord. The cornea also has lymphoid tissue in the form of corneal dendritic cells that are important in the regulation of the immune response in the anterior segment of the eye. The presence of these cells in the cornea has raised the possibility of transmission between patients via optical devices.

Conclusions: The size distribution of PrP deposits in the brain is consistent with their growth in brain tissue as predicted by the 'prion' hypothesis. The processing of visual information in laminae II/III and V/VI of V1 is likely to be significantly affected in vCJD thereby influencing the information passed to visual association areas and to subcortical areas. The distribution of the pathology in the brain in vCJD is not consistent with spread of prions in the bloodstream. Although transmission via optical devices is theoretically possible it remains highly improbable.

Reference

Lueck, C. (2000) Ocular features of CJD. *Optician* **220**, 23–27.

Visual impairment, age, IQ and driving

C. Dickinson, M. Mahmud and W. Holmes
Department of Optometry and Neuroscience, UMIST, PO Box 88, Manchester M60 1QD, UK

The link between good vision and driving performance is very controversial, with surprisingly little evidence of its existence. Some individuals have therefore argued that they could still drive safely despite their visual impairment.

The useful field of view (UFOV) – an indirect measurement of the area of the visual field from which information can be simultaneously processed – has been found to predict the risk of having a traffic accident better than do standard clinical tests of visual acuity, visual field or contrast sensitivity (Owsley, 1993). The UFOV was therefore used as a measure of the driving performance of young and old normal subjects with simulated visual impairment, in the form of reduced visual acuity and reduced contrast sensitivity. Both increased age and impaired vision were found to significantly affect the UFOV, especially on the test for selective attention, suggesting that both factors increase the risk of driving accidents. There was no interaction between impairment and age, however, older individuals did not appear to be disproportionately affected by equivalent levels of impairment. Nonetheless, the same level of accident risk is associated with a better level of acuity in older compared with younger individuals.

Although the mean performance of older subjects was worse than that of younger subjects, there were individual exceptions. What might be the basis of these individual differences? Earlier studies on reading performance (Dickinson and Rabbitt, 1991) suggested that IQ might be an important factor, as this is a measure of the processing speed of the individual. Further experiments were carried out to measure the UFOV of young normal subjects with simulated visual impairment, to investigate any link to their IQ. A modest correlation was found between IQ and selective attention, although it only accounted for approximately 14% of the variance.

These studies have provided further evidence that effective performance of a complex visual task such as driving is not predictable from simple clinical measures of vision. The complete range of factors which influence performance still remains to be discovered.

References

Dickinson, C. M. and Rabbitt, P. M. A. (1991) Simulated visual impairment: effects on text comprehension and reading speed. *Clin. Vis. Sci.* **6**, 301–308.

Owsley, C. (1993) Vision and driving in the elderly. *Optom. Vis. Sci.* **71**, 727–735.

Anisometropia: a cross-sectional study in 87892 subjects

Xuejiao Qin[a] *and J. A. Guggenheim*[b]
[a]Department of Ophthalmology, Qilu Hospital of Shandong University, China
[b]School of Optometry and Vision Sciences, Cardiff University, Cardiff CF10 3NB, UK

Purpose: To explore associations of anisometropia with sex and age, the potential for bias in such analyses, and indirectly, emmetropisation.

Method: Anisometropia was classified as a ≥1.00 D difference in mean spherical equivalent power (MSE) or, for separate analyses, as a ≥1.00 D difference in spherical power (SPH). Anisometropes were categorised into three severity groups: (a) ≥1.00 D and <2.00 D, (b) ≥2.00 D and <3.00 D, (c) ≥3.00 D, and into 10-year interval age groups. Myopes were classified as subjects with a least minus meridian power of ≥−0.25 D in both eyes and hyperopes as those with a most minus meridian power of ≥+0.25 D in both eyes. Non-parametric statistical analysis was implemented using Statistica software.

Results: The overall prevalence of anisometropia (by MSE) was 14.5%. The prevalence was higher in myopes than hyperopes (15.3% vs 13.0%, $p < 0.0001$) and in females than males (14.8% vs 14.0%, $p = 0.002$), when not corrected for bias. Prevalence varied significantly with age ($p < 0.0001$). However, only the difference between the age groups 21–30 and 31–40 years was convincing in not being subject to strong bias. Multiple regression analysis showed that age has opposite effects in anisomyopes (positive slope) and anisohyperopes (negative slope), while there was no significant effect of sex. The frequency distribution of MSE in the right eyes of non-anisometropes and in the less ametropic eyes of anisometropes differed significantly for each age group.

Conclusions: The analysis of anisometropia is hampered by statistical bias, because of the nature of its definition. Our results were not consistent with the hypothesis that the less ametropic eyes of anisometropes emmetropise exactly like the eyes of non-anisometropes.

Acknowledgements

We thank John Welsby (Conlons Opticians) and Robert Ward (Relcon Software) for their invaluable assistance.

Bifocals improve accommodative accuracy for children with Down's syndrome

R. E. Stewart, J. M. Woodhouse and L. D. Trojanowska
School of Optometry and Vision Sciences, Cardiff University, Cardiff CF10 3NB, UK

Purpose: Inaccurate accommodation is a characteristic of most (70–80%) children with Down's syndrome. We conducted a controlled trial to investigate the feasibility of bifocal spectacles in addressing the defect.

Methods: Two groups of 17 children with Down's syndrome (aged 5–11 years) were matched for age, cognitive ability, type of school

placement, refractive error type, and current spectacle wear. The treatment group was prescribed bifocals (+2.50 D addition, D28 seg) while the control group was prescribed new single-vision spectacles (if required). Both groups wore their new glasses for school and were followed over a 20-week period.

Results: At the outset of the study, there was no significant difference in the Accommodative Error Index (AEI, the averaged accommodative error over three testing distances) between the two groups (3.45 D for the bifocal group and 3.37 D for the control group). Once bifocal wear commenced, accommodation was significantly more accurate for the bifocal group, with their AEI through the bifocal seg (0.64 D at the final visit) lying within the normal range. Unexpectedly, the bifocal group also had better accommodative accuracy through the distance part of the lens (AEI 1.67 D). AEI for the control group remained 2.92 D at the final visit. Near acuity was also better for the bifocal group, although this did not reach significance. Compliance was good in both groups, and four children preferred to wear their bifocals at home as well as at school. Anecdotal reports from teachers suggested that concentration and writing skills improved with bifocals. A high-fitting height for the bifocal seg (at pupil centre) was crucial for successful wear.

Conclusions: Accommodation should be measured routinely in children with Down's syndrome and bifocals considered for those who have poor accommodative accuracy.

Development of a critical flicker/fusion frequency test for potential vision testing in media opacities

M. Vianya-Estopà,[a] *W. A. Douthwaite,*[a] *K. Pesudovs,*[a] *B. A. Noble*[b] *and D. B. Elliott*[a]

[a]Department of Optometry, University of Bradford, Bradford BD7 1DP, UK

[b]Department of Ophthalmology, Leeds General Infirmary, Clarendon Wing, Belmont Grove, Leeds LS2 9NS, UK

Purpose: To determine whether critical flicker fusion (CFF) thresholds fulfil the criteria for a potential vision test (PVT) by being unaffected by media opacity yet affected by retinal disease, and to determine the optimal target size for such a test.

Methods: CFF thresholds for three different stimulus sizes (0.5, 1.0 and 1.5 degrees) were measured in 72 subjects (mean age 78.43 ± 7.07 years), with 31 subjects having media opacity, 21 having macular disease and 20 pseudophakes.

Results: There were no statistically significant differences between CFF values from the media opacity and the pseudophake groups for any target size (ANOVA). However, CFF values were significantly lower in patients with macular disease for all target sizes ($p < 0.05$). Analysis of a subset of six media opacity and seven macular disease subjects, with visual acuity of 6/60 (1.0 logMAR equivalent) or worse, showed that the media opacity group still had CFF values similar to the pseudophake group and had significantly higher CFF than the macular disease group. A receiver-operating characteristic curve (ROC) showed that the 1.5-degree target size best discriminated between macular disease and media opacities.

Conclusions: CFF testing is shown to fulfil the requirements for a PVT and may prove to be particularly useful in patients with dense media opacity.

Cortical colour mechanisms revealed by visual masking

S. R. Abdelaal, D. McKeefry, B. T. Barrett and P. V. McGraw

Department of Optometry, University of Bradford, Bradford BD7 1DP, UK

Purpose: Post-receptoral chromatic processing can be modelled either in terms of a discrete number of cardinal mechanisms in conjunction with a luminance mechanism, or as higher-order chromatic mechanisms tuned to many different directions in colour space. We explore these competing hypotheses using a masking effect known to be cortical in origin.

Methods: The stimulus arrangements consisted of a central target bar, masked by presentation of adjacent bars, with no spatial or temporal overlap. In each trial, the target was preceded and followed by the masking stimuli. This sequence of mask–target–mask appeared on one side of fixation, while a reference bar, against which contrast of the target bar was judged, appeared on the opposite side. The reference and target appeared randomly on either side of fixation. We manipulated the chromatic and luminance content in MBDKL colour space, of both target and mask stimuli. The perceived contrast of the target was taken as a measure of masking strength.

Results: The pattern of masking was always highly selective. Maximum effects were obtained when the target and mask were identical in terms of their chromatic and/or luminance contrast composition. When target and mask differed in their chromatic or luminance content, the magnitude of masking was reduced. In the case of opponent-colour stimuli, the masking effect was negligible. Furthermore, the pattern of results obtained was the same irrespective of whether the target and mask were located along cardinal or non-cardinal axes.

Conclusions: The patterns of masking effects do not conform to a colour-opponency model of chromatic processing. Instead, the results support the existence of multiple chromatic mechanisms tuned to non-cardinal directions in colour space.

Glucose transport kinetics in the bovine ciliary epithelium*

C. Y. Chan,[a,b] *J. A. Guggenheim*[a] *and C. H. To*[b]

[a]School of Optometry and Vision Sciences, Cardiff University CF10 3NB, UK

[b]Department of Optometry and Radiography, The Hong Kong Polytechnic University

Purpose: Diabetic patients are more prone to develop cataract than non-diabetic patients. Researchers have proposed that hyperglycaemia of the crystalline lens is the major risk factor in diabetic cataract. This study aims to characterise the mechanism of glucose transport into the aqueous humour. This knowledge may be important in developing strategies to control lens' glycemic level and prevent cataract development in diabetic patients.

Methods: Fresh bovine ciliary epithelium (CE) was isolated and sandwiched in a modified Ussing-type chamber. Glucose fluxes across the CE were studied by radioactive isotopes, 3-O-methyl-D-[^{14}C]-glucose (MDG) and L-[^{3}H]-glucose (LG), in the presence of different inhibitors (phloretin, cytochalasin-B, phlorizin and ouabain). In addition, the effect on glucose flux of glucose concentrations of 7.5, 15, 30, 45 and 60 mM at the stromal side (with osmolarity at the aqueous side balanced using sorbitol) were investigated. The Michaelis constant (K_m) and maximal velocity (V_{max}) of glucose transport in bovine CE were estimated from plots of glucose flux from stroma (S) to aqueous (A), against stromal glucose concentration.

Results: There was no significant net glucose flux across the bovine CE for either LG or MDG ($p > 0.05$, $n = 10$). The LG flux was 26 ± 2 nmol h^{-1} cm^{-2} in both the stroma-to-aqueous and aqueous-to-stroma directions. MDG flux was 196 ± 15 nmol h^{-1} cm^{-2} (S → A) and 190 ± 5 nmol h^{-1} cm^{-2} (A → S). Bilateral addition of phloretin, cytochalasin-B and phlorizin significantly reduced the MDG (but not LG) flux by 59% ($p < 0.001$, $n = 11$), 80% ($p < 0.001$, $n = 9$) and 22% ($P < 0.001$, $n = 8$) respectively. No significant reduction was found in glucose flux after the addition of ouabain. The glucose transport was saturable, with a K_m of 5.27 mM and a V_{max} of 350 nmol h^{-1} cm^{-2}.

Conclusion: Glucose transport across the bovine CE is passive, stereospecific and saturable. Facilitative glucose transport is the major mode of glucose transport mechanism in the bovine CE.

Acknowledgements

This study is supported by HKPolyU grant (8-ZF84).

*Winner of the Cambridge Research Systems Sponsored Paper Prize.

Heritability of refractive error within a multi-generational pedigree

R. C. Creer,[a] *A. Murphy,*[b] *R. Pong-Wong,*[c] *C. S. Haley*[c] *and J. A. Guggenheim*[a]

[a]School of Optometry & Vision Sciences, Cardiff University, Cardiff CF10 3NB, UK

[b]Jones & Murphy Optometrists, Carmarthen SA31 3AD, UK

[c]Roslin Institute, Edinburgh EH25 9PS, UK

Purpose: The 'Family Study of Myopia' is a project aiming to discover genetic loci causing high myopia. As part of this investigation, the 'heritability' of refractive error was estimated for a large multi-generational pedigree. Heritability indicates the proportion of the variance of a trait which is due to genetic factors within a specific population. A heritability of 1 suggests that a trait is determined wholly by genetic factors, whilst a heritability of 0 suggests that it is determined by wholly environmental factors.

Methods: Members of the family were recruited by the use of postal questionnaires. The optometrists of consenting subjects were contacted to obtain spectacle prescriptions and additional information regarding ocular and systemic conditions (with the aim of excluding syndromic or secondary causes of refractive error). The spherical refraction of the right eye in the least minus meridian was analysed as the quantitative trait of interest. Heritability was calculated by (1) parent–offspring regression, (2) a polygenic variance components analysis (SOLAR) and (3) a Monte Carlo Markov chain (Gibbs sampling) method.

Results: The pedigree can be traced over seven generations. Of the 192 subjects in three generations still living, 109 have agreed to participate so far, and refractive details have been obtained for 96. The heritability of refractive error calculated by (1) parent–offspring regression was 0.56 and 0.52 (S.E. = 0.42 and 0.23), (2) SOLAR was 0.58 and 0.67 (S.E. = 0.23 and 0.20) and (3) MCMC was 0.59 and 0.68 (S.E. = 0.20 and 0.17) for models where non-spectacle wearers were classified as unknown or emmetropic, respectively.

Conclusions: The consistently high heritability values for refractive error suggest that the prospects for mapping refractive error susceptibility loci in this family are good.

Acknowledgements

This research is funded by grants from the College of Optometrists and the Sir Jules Thorn Charitable Trust (03SC/07A). Thanks also to the family involved in the study.

Contrast sensitivity in external noise with defocus in myopes: optical or neural?

H. Radhakrishnan, S. Pardhan, R. I. Calver and D. J. O'Leary

Department of Optometry and Ophthalmic Dispensing, Anglia Polytechnic University, Cambridge CB1 1PT, UK

Purpose: Our previous studies have shown an asymmetrical loss in contrast sensitivity with positive and negative lenses at low-medium spatial frequencies in myopes compared with non-myopes. Contrast thresholds were measured in four levels of externally added visual noise for four different levels of positive and negative defocus. The contrast detection in noise function allows a given loss in visual sensitivity to be attributed to two components, sampling efficiency and equivalent noise. Previous work has shown that sampling efficiency gives an indication of the neural effects, and equivalent noise represents the optical factors.

Methods: Contrast detection in noise functions were measured in three myopic and three non-myopic subjects for gratings of 3 and 16 c/deg. Measurements were obtained under cycloplegia with 0 D, ±0.50 D and ±1.00 D defocusing lenses.

Results: Myopes were found to have lower equivalent noise with negative defocus when compared with positive defocus ($p = 0.048$) for gratings of 3 c/deg, indicating an optical cause for the previously observed asymmetry in contrast sensitivity in myopes. We also then calculated the modulation transfer functions from the third order spherical aberration to ascertain whether this observed optical effect can be predicted from the aberration data. The predicted contrast sensitivity results agreed with the measured contrast sensitivity (one way intra-class correlation, $p = 0.00001$).

Conclusions: Optical factors contribute significantly to the differences in contrast sensitivity with defocus between myopes and non-myopes for gratings of 3 c/deg.

Heart rate variability, silent myocardial ischaemia, and 24-h blood pressure in primary open-angle glaucoma patients

D. Gherghel and S. Hosking

Neurosciences Research Institute, Aston University, Birmingham B4 7ET, UK

Purpose: To compare heart rate variability (HRV) parameters, circadian changes of systemic blood pressure (BP) and frequency of silent cardiac ischaemia in patients with primary open-angle glaucoma (POAG) and normal subjects.

Methods: Both 24-h ambulatory BP monitoring and HRV measurements were performed in 19 subjects with POAG and in 17 age-matched controls using the CardioTens-01 (Meditech Ltd, Hungary) which simultaneously records a continuous electrocardiogram (ECG) and intermittent non-invasive BP measurements at 30-min intervals, with extra measurements triggered by detection of a horizontal or down-sloping ST depression (as a measure of a silent cardiac ischaemic event).

Results: No significant differences in diurnal or nocturnal BP and HRV parameters were found between the groups ($p > 0.05$). Significant ST-segment depression (> 1 mm amplitude and > 60 s duration) was demonstrated in 14 (74%) glaucoma patients and in 10 (59%) controls. Eighty-six per cent of the glaucoma patients and 18% of the controls exhibited ST-segment depressions with a peak in the early morning hours. For the glaucoma patients showing an ischaemic event, in 50% of cases the ST-segment depressions occurred during episodes of significant increase in BP (10.89 ± 12.28 mmHg), 33% during episodes of BP drops (−26.76 ± 17.71 mmHg) and 17% occurred without any changes in BP. There was no pattern of BP-related ischaemic events in controls.

Conclusions: POAG patients have a high risk for nocturnal ischaemic events during episodes of abnormal systemic blood pressure.

Changes in quality of life after LASIK for myopia

E. Garamendi,[a] *K. Pesudovs,*[b] *and D. B. Elliott*[a]

[a]Department of Optometry, University of Bradford, Richmond Road, Bradford BD7 1DP, UK

[b]UH College of Optometry, 505 J Davis Armistead Bldg, 77204-2020, Houston, TX, USA

Purpose: The purpose of the study was to compare the quality of life (QoL) of pre-presbyopic myopic subjects before and after LASIK refractive surgery.

Methods: Sixty-six subjects (mean age ± 1 SD: 30.3 ± 4.6; range 21–39 years) completed the validated Quality of Life Impact of Refractive Correction (QIRC) questionnaire before and at least 3 months (4.25 ± 1.5 months) after LASIK refractive surgery for myopia. QIRC consists of 20 questions associated with refractive correction-related quality of life with a five-category response scale. Scale responses were assigned weightings from Rasch analysis of 312 subjects (spectacles or contact lens wearers or post-refractive surgery subjects) from the original validation study. This created true linear measurement from categorical data. Higher QIRC scores represent better QoL. Subjects were also asked if their QoL had improved after surgery.

Results: Pre-operative mean spherical refractive error was −3.36 ± 1.86 DS and −3.34 ± 1.74 DS in the right and left eyes

respectively. Mean ± 1 SD QIRC scores improved after LASIK from 40.09 ± 4.33 to 52.09 ± 6.02 ($F_{1,130} = 172.65$, $p < 0.0001$). The majority of the individual questions also showed significantly improved scores. Subjects who 'strongly agreed' (53.96 ± 4.91) or 'agreed' (51.78 ± 6.19) that their QoL had improved after surgery had significantly higher ($F_{1,60} = 11.24$, $p < 0.01$) QIRC scores than those who 'neither agreed nor disagreed' (44.36 ± 4.97) or 'strongly disagreed' (42.82, $n = 1$). Three subjects (4.5%) had lower QIRC scores post-operatively.

Conclusion: Large improvements in self-reported QoL were found after LASIK surgery for myopia in the majority of pre-presbyopic subjects although a small number of subjects (4.5%) had a decreased QoL score. Pre-operative LASIK subjects had lower self-reported QoL than previously reported data from contact lens wearers (46.7 ± 5.5) and spectacle wearers (44.1 ± 5.9) from an optometric practice population.

The menstrual cycle and susceptibility to visual discomfort

S. A. Clemes and P. A. Howarth

Visual Ergonomics Research Group, Department of Human Sciences, Loughborough University, Leicestershire LE11 3TU, UK

Purpose: We have previously found changes in the amount of visual discomfort reported over the menstrual cycle when naturally cycling females wore a head-mounted display (HMD) to view a nauseogenic virtual reality (VR) racing game. Visual discomfort increased during the second week of the cycle and this mirrored the changes in motion sickness-like symptoms that are associated with the use of this equipment. The purpose of the current research was to determine whether visual discomfort in other situations is influenced by the menstrual cycle. There were two parts to this research. The first was a laboratory based study in which visual discomfort was induced by prolonged accommodative effort, and the second was a field-based study which examined reports of visual discomfort from individuals conducting intensive VDU work at four telephone call centres in the UK.

Methods: Part 1: 12 naturally cycling female volunteers attended the laboratory on days 5, 12, 19 and 26 of their menstrual cycle. Menstrual cycle phase was confirmed by the analysis of salivary oestradiol and progesterone levels. Participants wore −2.00 DS lenses in a trial frame, or clipped over their normal correction, whilst playing the PC game Solitaire displayed on a VDU, for a maximum of 30 min. A visual symptoms questionnaire was completed prior to and following the visual task. Part 2: Call centre workers were given an initial health screening, irrespective of their age or gender. This enabled them to be categorised into one of four groups: (*i*) an experimental group (naturally cycling females, $n = 59$), (*ii*) oral contraceptive users ($n = 38$), (*iii*) postmenopausal females ($n = 21$), and (*iv*) men ($n = 26$). Visual discomfort was measured using a visual symptoms questionnaire completed at the beginning and end of the shift, twice a week for 5 weeks.

Results: Visual discomfort did not vary significantly over the menstrual cycle in either part of this investigation. In the field study, the amount of visual discomfort reported by the experimental group did not differ significantly on any occasion from that reported by any of the control groups.

Conclusions: The results of both parts of this investigation indicate that the previously seen changes in visual discomfort over the menstrual cycle were not a consequence of performing an intensive visual task. We suggest that the vection of the VR game produced different amounts of nausea at different stages of the menstrual cycle, and this led to general overall changes in bodily comfort. The reported change in visual discomfort is a consequence of these general changes rather than having a specific ocular origin as might otherwise have been supposed.

The changing workload of an eye unit in East Africa

P. J. Murphy,[a] *C. A. MacLeod*[b] *and D. Yorston*[c]

[a]School of Optometry and Vision Sciences, Cardiff University, Cardiff CF10 3NB, UK

[b]Private Practice, Inverness, UK

[c]Department of Epidemiology and International Eye Health, Institute of Ophthalmology, London EC1V 9EL, UK

Purpose: To assess the incidence of ocular disease, treatment adopted and visual status of patients attending the Kikuyu Eye Unit, Kenya.

Method: The clinical records of 444 patients (62% male, 38% female), attending the outpatients clinic over a 9-day period, were reviewed and the following details recorded: gender, age, visual acuity, ocular disease and treatment prescribed. Data were analysed to assess the prevalence of abnormal unilateral and bilateral ocular conditions, according to gender and age, and their effect on visual acuity. Many patients were diagnosed as suffering from more than one condition, but to provide the widest analysis, all conditions were included in the investigation.

Results: A total of 369 cases having unilateral conditions were diagnosed: cataract and pseudophakia ($n = 103$, 27.9%), trauma ($n = 99$, 26.8%); 189 (51.2%) patients were treated non-surgically, and 63 (17%) surgically. In 247 cases, bilateral conditions were diagnosed: glaucoma ($n = 32$, 13%), diabetic retinopathy ($n = 31$, 12.5%), uncorrected refractive error ($n = 24$, 9.7%); 147 (59.5%) patients were treated non-surgically, and 12 (4.8%) surgically. No cases having xerophthalmia, trachoma or onchocerciasis were identified. Visual status: 142 (34.7%) patients had normal visual acuity (6/4–6/18), 55 (13.4%) unilateral low vision (6/24–6/60), 76 (18.6%) bilateral low vision, 106 (25.9%) unilateral blind (<6/60) and 30 (7.3%) bilateral blind; 48 had undetermined visual acuity. Of the total, 103 subjects were children (≤ 15 years): 44 (53.6%) had unilateral ocular trauma; 50 (34%) had bilateral conjunctival and nine (18%) bilateral corneal conditions.

Conclusions: (1) The majority of conditions presenting at this Eye Unit are treated by non-surgical intervention, indicating that many could be seen by Ophthalmic Medical Assistants; (2) 10% of patients were given refractive error correction, indicating the need for trained refractionists; (3) xerophthalmia, trachoma and onchocerciasis were not major ocular health problems; (4) the very high levels of visual impairment emphasise the need to educate patients to seek early treatment.

Real-time pupillary monitoring in children

M. O. Roberts,[a] *J. S. Wolffsohn,*[b] *A. C. Liasis,*[c] *J. Veness*[a] *and D. A. Thompson*[c]

[a]Biomedical Engineering, Great Ormond Street Hospital for Children, London WC1N 3JH, UK

[b]Neurosciences Research Institute, Aston University, Birmingham B4 7ET, UK

[c]Visual Electrophysiology Unit, Great Ormond Street Hospital for Children, London WC1N 3JH, UK

Purpose: Paediatric visual electrodiagnostic techniques can provide objective information about the function of the retina, and the visual pathway to the cortex, simultaneously. One technical challenge is to determine the dynamic retinal illuminance of a natural pupil when recording electroretinograms (ERGs). Another is determining when and where a child is fixating a visual evoked potential (VEP) stimulus.

Methods: These problems are being addressed by the development of a system that is capable of continuous, online recording of bilateral physiological pupil responses. The system uses an infra red (IR) light-emitting diode (LED) as its light source and an IR sensitive camera for image capture. Image acquisition and processing is achieved using a PC equipped with specialized image acquisition hardware and development software (LabVIEW, National Instruments Corporation, Austin, TX). Software is currently under development to extract the pupillary and gaze information from both eyes in real time. The extraction is achieved through experimentation with various image processing techniques such as thresholding, pixel erosion/dilation, and edge detection.

Conclusion: This system will allow the real-time retinal illuminance for each eye to be calculated and directly related to electroretinographic measures. In addition, pupil information can be used to set

more objective criteria of adequate fixation during evoked potential recording.

Colour specificity of the motion after-effect

E. Laviers and D. McKeefry

Department of Optometry, University of Bradford, Richmond Road, Bradford BD7 1DP, UK

Purpose: It has been demonstrated that a motion after-effect (MAE) can be both induced and nulled using isoluminant chromatic stimuli (Cavanagh and Favreau, 1985; Derrington and Badcock, 1985; Mullen and Baker, 1985). It has also been suggested that, at low velocities at least, the motion-processing pathway is sensitive to the chromaticity of motion stimuli (Hawken *et al.*, 1994, Gegenfurtner and Hawken, 1995, 1996; Burr *et al.*, 1998; McKeefry, 2001). Therefore, it would follow that the MAE would display some degree of colour selectivity. To investigate the colour selectivity of the MAE, we used a 2AFC motion-nulling paradigm to measure the strength of the MAE induced using isoluminant adapting stimuli modulated along the cardinal chromatic axes in MBDKL colour space and isoluminant test stimuli modulated along a number of different chromatic axes. We hypothesised that the MAE would be greatest when the adapting and test stimulus were modulated along the same axis, and weakest when test and adapting stimuli were modulated along orthogonal axes.

Methods: Subjects adapted to a sinusoidal grating drifting to the left at 2 deg s^{-1} and subsequently viewed a test grating of variable velocity and direction (i.e. left or rightward motion) then made a choice as to whether the test grating drifted towards the left or the right. The test velocity at which the MAE was nulled was recorded as the MAE strength. All stimuli were presented at equal multiples of contrast detection threshold.

Results: The MAE was strongest when the test stimulus was modulated along the same chromatic axis as the adapting stimulus and MAE strength showed the general trend of decreasing with increasing deviation of the test axis from that of the adapting stimulus.

Conclusion: The results confirm our hypothesis that the MAE is colour selective, for these conditions.

References

Burr, D. C., Fiorentini, A. and Morrone, C. (1998) Reaction time to motion onset of luminance and chromatic gratings is determined by perceived speed. *Vision Res.* **38,** 3681–3690.

Cavanagh, P. and Favreau, O. E. (1985) Color and luminance share a common motion pathway. *Vision Res.* **25,** 1595–1601.

Derrington, A. M. and Badcock, D. R. (1985) The low level motion system has both chromatic and luminance inputs. *Vision Res.* **25,** 1879–1884.

Gegenfurtner, K. R. and Hawken, M. J. (1995) Temporal and chromatic properties of motion mechanisms. *Vision Res.* **35,** 1547–1563.

Gegenfurtner, K. R. and Hawken, M. J. (1996) Interaction of motion and color in the visual pathways. *Trends Neurosci.* **19,** 394–401.

Hawken, M. J. and Gegenfurtner, K. R. and Tang, C. (1994) Contrast dependence of colour and luminance motion mechanisms in human vision. *Nature* **367,** 268–270.

McKeefry, D. J. (2001) Chromatic visual evoked potentials elicited by fast and slow motion onset. *Colour Res. and Appl.* **26,** S145–S149.

Mullen, K. T. and Baker, C. L. (1985) A motion aftereffect from an isoluminant stimulus. *Vision Res.* **25,** 685–688.

Repeatability of the Complete Ophthalmic Analysis System (COAS®) on determining higher order aberrations on model eyes

A. Cerviño, S. L. Hosking, S. A. Naroo and M. C. M. Dunne

Neurosciences Research Institute, Aston University, Birmingham B4 7ET, UK

Purpose: Evaluating the repeatability of the Complete Ophthalmic Analysis System (COAS®, WaveFront Sciences, Albuquerque, NM, USA) on the determination of higher order aberrations of model eyes.

Method: Twelve model eyes were examined with the COAS. Two sessions of 10 measurements each, as well as another session of 10 more measurements without refocusing, were performed. Values obtained were analysed to assess repeatability of the instrument, variations on the intrasession and intersession repeatability, as well as those induced by human manipulation during the focusing procedure.

Results: Root mean square (RMS) of the confidence interval (CI) obtained for the whole sample was reduced to 1.10% of the mean value. High correlation was obtained between the repeatability obtained from two measurements and that obtained from ten consecutive measurements ($r = 0.950$; $p < 0.001$; 95% CI for $r = 0.7755$ to 0.9898) with the values not being significantly different (mean difference: 0.0258, S.D.: 0.1005, 95% CI: −0.0514 to 0.1031, $p = 0.4628$; paired t-test), suggesting a high performance of the instrument. When refocusing, up to four measurements are needed to get a correlation above 0.500 ($r = 0.5715$, $p = 0.1080$; 95% CI for $r = -0.1493$ to 0.8957) and for the values not to be significantly different (mean difference: −0.0175, S.D.: 0.0499, 95% CI: −0.0558 to 0.0209, $p = 0.3246$; paired t-test), suggesting that at least four measurements are needed to get a reliable value. Comparison of values obtained in two sessions (refocusing for each measurement) shows variable correlation for the different eyes, suggesting a non-constant human factor in the manipulation of the instrument.

Conclusions: The COAS wavefront sensor shows good performance with high repeatability. However, the comparability of results diminishes significantly due to human manipulation of the instrument, and there is variability between sessions. This suggests a need for improving the reference for focusing, so that the whole image capture procedure is less clinician-dependent.

Diurnal variation of corneal sensitivity and thickness

A. M. Ntola and P. J. Murphy

School of Optometry and Vision Sciences, Cardiff University, Cardiff CF10 3NB, UK

Aim: To assess the diurnal pattern of change in corneal sensitivity (CS) and corneal thickness (CT).

Methods: Twenty Caucasian subjects were recruited (males = 7, females = 13, age = 23.7 ± 3.18 years). Subjects with any ocular condition known to affect CS were excluded. Ethical approval was obtained and subjects were asked to sign a consent form prior to participating. Central CS was assessed using the non-contact corneal aesthesiometer (NCCA) and Cochet-Bonnet aesthesiometer (C-BA). The NCCA stimulates the cold C fibres, while the C-BA stimulates the Aδ mechano-sensors. CT was measured using the Haag-Streit optical pachometer. All measurements were taken on the left eye, which was patched overnight. The patch was removed 5 min before measurements began, to create a standard point for all subjects. Measurements were taken every hour from 8 AM to 12 PM, and then every 2 h from 2 PM to 10 PM. The order of measurements was randomised at each time period. To assess patient training with the NCCA, seven subjects were re-measured on a second day.

Results: A significant diurnal change in CS was found with the NCCA, with sensitivity being lower in the morning and higher in the evening (ANOVA, $p = 0.0285$). No significant change was found using the C-BA (ANOVA, $p = 0.0545$). With CT, a significant change was found from 8 AM to 12 PM (ANOVA, $p = 0.0401$), but no significant change was found from 2 PM to 10 PM (ANOVA, $p = 0.9693$). A significant correlation between the first and second measurements, for the re-test subgroup of NCCA was found ($r^2 = 0.9637$).

Conclusions: The NCCA was able to detect the diurnal variation in sensitivity of the C-fibres. The C-BA was unable to detect any variation, because of its truncated stimulus range. CT decreased through the day, having an inverse relationship with CS ($r^2 = 0.6910$). Measurement of corneal sensitivity with the NCCA has only a small learning component.

Acknowledgements

AMN is supported by a Greek State Foundation Scholarship (IKY).

Vernier acuity in children with Down's syndrome

N. R. Bromham, J. M. Woodhouse and Ff. M. John
Department of Optometry and Vision Sciences, Cardiff University, Cardiff CF10 3NB, UK

Purpose: In typically developing children, vernier acuity is finer than grating or optotype acuity. Offsets smaller than foveal cone width can be detected, thus vernier acuity is termed a hyperacuity. Vernier acuity reflects cortical visual processing and should be more sensitive than other measures to anomalous development of the visual cortex. While anomalies of the visual cortex are well documented in Down's syndrome (DS) their impact on vision in DS is unclear. This study aimed to measure vernier acuity in DS.

Methods: The subject groups consisted of 34 children with DS and 19 controls aged between 2.5 and 14 years. Two computer-generated vertical bars were presented on each trial, one bar contained abutting vernier offsets and the other was straight. The child's task was to point to the vernier stimulus. After a training phase, thresholds were obtained using a 2AFC staircase. Probit analysis was used to determine the threshold. Optotype acuity (OA) was measured using age appropriate optotype acuity tests.

Results: Analysis of covariance, with age as the covariate, indicated poorer vernier acuity in the DS than in the control group, $F_{(1,52)} = 11.414$, $p = 0.001$. Regression analysis suggested vernier acuity improved with age in the control group but not in the DS group. Taking 30 arcsec as the hyperacuity limit, eight control children and no child with DS showed hyperacuity. Vernier was superior to optotype acuity for 22 of 34 children in the DS group and for 15 of 16 controls (OA data were missing for three controls).

Conclusions: While children with DS often had better vernier than optotype acuity, no children with DS showed hyperacuity (but foveal cone spacing is not yet known in DS). Vernier thresholds did not improve with age in the DS group. The results are consistent with the idea of a neural sensory deficit in DS.

Comparison of S-cone electroretinogram and colour vision in subjects with diabetes mellitus

K. E. Mortlock,[a] *Z. Chiti,*[a,b] *N. Drasdo,*[a] *D. R. Owens*[c] *and R. V. North*[a]
[a]School of Optometry and Vision Sciences, Cardiff University, Cardiff, CF10 3NB, UK
[b]Department of Anatomy, MRC Centre for Synaptic Plasticity, Bristol University, Bristol BS8 1TD, UK
[c]Diabetes Research Unit, University of Wales College of Medicine, Cardiff CF14 4XN, UK

Purpose: Tritanopic colour vision defects are an established finding in diabetes mellitus (DM). Objective examination using the S-cone electroretinogram has revealed a selective reduction of the S-cone b-wave amplitude, even in those with no diabetic retinopathy (NDR). This study aims to investigate the S-cone electroretinogram and colour vision in a group of subjects with either NDR or minimal background retinopathy (BDR).

Methods: Twenty-one subjects with type 1 DM (10 NDR, 11 BDR), 32 subjects with type 2 DM (21 NDR, 11 BDR) and 42 age-matched controls participated in the study. All subjects completed the Desaturated D15 monocularly. Silent substitution S-cone electroretinograms were recorded using a 535 and 450 nm wavelength stimulus, matched to be equiluminant for the M-cones, alternating in a square wave at 4.16 Hz. Presented over a high luminance 650 nm background, this stimulus elicits a S-cone electroretinogram with minimal intrusion from the L/M-cones and rods.

Results: The S-cone electroretinogram and D-15 total error score (TES) were not significantly different from controls in the NDR group. The TES and implicit time of the a- and b-waves of the S-cone electroretinogram were significantly increased in the BDR group compared with the controls; b-wave implicit time and TES were also significantly increased compared with the NDR group.

Conclusions: Neither colour vision nor the electroretinogram detected retinal dysfunction in those with NDR. While both identified dysfunction in those with BDR, colour vision testing is simpler to administer clinically. The electroretinogram may, however, be useful in indicating the retinal locus of colour vision defects in DM.

An excess of with-the-rule astigmatism in high hyperopes and high myopes

J. E. Farbrother and J. A. Guggenheim
School of Optometry and Vision Sciences, Cardiff University, Cardiff CF10 3NB, UK

Purpose: Against-the-rule (ATR) astigmatism has been shown to be a risk factor for subsequent myopia development. In this study, we evaluated the relationship between astigmatic axis and the level of spherical ametropia.

Methods: Cross-sectional data for a cohort of about 90 000 subjects attending 19 optometric practices in the north of England were analysed. Initially, the relationship between astigmatic axis and cylinder power, and between axis and sphere power, were examined in 21 40 and 21 30 year olds, respectively, to control for the effects of age. Multivariate logistic regression analysis was performed using data for all compound astigmats in the cohort to explore the effect of sphere power, cylinder power, age and sex on the odds of subjects having either ATR or with-the-rule (WTR) astigmatism.

Results: There was a highly significant excess of WTR astigmats in the high myopes compared with the low myopes ($p < 0.00001$). A parallel increase in WTR astigmatism was also found for high hypermetropes ($p = 0.002$). The odds of having WTR astigmatism were increased if subjects were young or had a high cylinder power (both, $p < 0.00001$). ATR astigmatism occurred more often with increasing age and in subjects with lower spherical ametropia (both, $p < 0.00001$). Indeed, for 21–30-year-old subjects with less than two dioptres of myopia, ATR occurred more often than WTR astigmatism.

Conclusion: Astigmatic axis was found to be related to the level of ametropia, with both a higher spherical component or higher cylinder power increasing the odds of astigmatism being WTR. Low ametropes, particularly myopes, were more likely to have axes ATR.

Acknowledgements

The authors are extremely grateful to John W. Welsby (Conlons Opticians) and Robert Ward (Relcon Software) for providing anonymised optometric practice data. This research was funded by grant SCIAD 015 from the National Eye Research Centre.

Development of a practical spatio-temporal contrast sensitivity test: interim estimates of normative data

S. Malihi, K. E. Mortlock, N. Bromham, R. V. North and N. Drasdo
School of Optometry and Vision Sciences, Cardiff University, Cardiff CF10 3NB, UK

Purpose: Many studies have used simple tests of contrast sensitivity in patients with diabetes mellitus and glaucoma. The aim of this study is to evaluate a method which, while being clinically practicable, provides a more complete assessment of the extent of retinal damage and disability by the use of an increased range of spatiotemporal stimuli. The preliminary normative data is presented.

Methods: Thirteen healthy volunteers (aged 38–80 years) participated in the study. Visual field (24-2 SITA Standard) and FDT (Frequency Doubling Technology) (Full Threshold C-20) were measured. Spatiotemporal contrast sensitivity was assessed at spatial frequencies of 0.025, 0.5 and 10 c/deg at temporal frequencies of 2.17, 6.50 and 21.66 Hz. The stimuli were vertical sinusoidal gratings, generated by a VSG 2/5 (Cambridge Research Systems Ltd, Rochester, Kent, UK) and presented either on a monitor or back projected with minimal distortion on a curved diffusing screen using a video

projector. A rapid adaptive psychophysical threshold test paradigm, QUEST, was used to determine contrast threshold.

Results: The mean contrast threshold values at spatial frequency of 0.025 c/deg and temporal frequencies of 2.17, 6.50 and 21.66 Hz were 3.028, 1.172 and 3.594% respectively. The mean contrast threshold values at spatial frequency of 0.5 c/deg and temporal frequencies of 2.17, 6.50 and 21.66 Hz were 1.211, 0.532 and 2.601% respectively and the mean contrast threshold values at spatial frequency of 10 c/deg and temporal frequencies of 2.17, 6.50 and 21.66 Hz were 6.304, 8.441 and 39.572% respectively.

Conclusions: Our experiment has demonstrated that this technique is a practical possibility for the assessment of visual function for observers over an extended age range.

Acknowledgement

K. E. Mortlock is supported by the Wellcome Trust.

Contrast sensitivity as well as visual acuity is reduced in infants and children with Down's syndrome: are all fine discriminations compromised in Down's syndrome?

Ff. M. John,[a] *N. R. Bromham,*[b] *J. M. Woodhouse*[b] *and T. R. Candy*[a]

[a]Department of Optometry, University of Indiana, Bloomington, IN, USA

[b]School of Optometry and Vision Sciences, Cardiff University, Cardiff CF10 3NB, UK

Purpose: Infants and children with Down's syndrome typically show reduced visual acuity and contrast sensitivity when tested using conventional behavioural techniques. These results may reflect sensory deficits of optical or neural origin, or a loss of performance in later mechanisms responsible for generating the behavioural response. The purpose of the present study was to compare objective acuity and contrast sensitivity measurements recorded using visual-evoked potentials (VEP), with behavioural clinical tests, in a group of children with Down's syndrome and a group of controls. The goal was to determine whether children with Down's syndrome demonstrate reduced performance in VEP recordings from the first stages of the response pathway.

Methods: The subject group comprised 58 children with Down's syndrome and 44 control children, aged 3 months to 14.15 years. Visual acuity and contrast thresholds were measured using both steady-state, swept VEP and behavioural techniques.

Results: Group differences in visual acuity and contrast sensitivity were analysed using ANCOVA with age as a covariate. Visual acuity thresholds were significantly lower in the group with Down's syndrome than in the control group. This was true for both VEP, $F(1,73) = 23.62$, $p < 0.001$, and behavioural measures, $F(1,86) = 49.32$, $p < 0.001$. The Down's syndrome group also had reduced contrast sensitivity when compared with the controls, for VEP contrast sensitivity $F(1,55) = 15.66$, $p < 0.01$, and behavioural contrast sensitivity $F(1,64) = 10.54$, $p = 0.02$. The group differences remained even when children with ophthalmological anomalies were excluded from the analysis.

Conclusions: Reduced visual acuity and contrast sensitivity in the Down's syndrome group support the idea of an underlying sensory deficit in the Down's syndrome visual system.

The influence of cognition on oculomotor and cardiovascular function*

L. N. Davies, J. S. Wolffsohn and B. Gilmartin

Neurosciences Research Institute, Aston University, Birmingham B4 7ET, UK

*Winner of the Cambridge Research Systems Sponsored Poster Prize.

Purpose: Autonomic control of accommodation incorporates responses to retinotopic and spatiotopic stimuli, the former comprising optical parameters such as retinal blur, the latter non-optical parameters such as perceived distance and cognition. Using concurrent measures of accommodation (with constant retinotopic stimuli) and systemic cardiovascular function, we investigated whether there is a correlation between ocular and systemic responses to variations in cognitive demand.

Methods: Ten subjects aged 19–39 years (mean: 23.3 ± 4.8 years) were rendered functionally emmetropic with conventional soft contact lenses (Acuvue daily disposables; Johnson & Johnson Healthcare, Jacksonville, FL, USA). Subjects monocularly viewed stationary numerical digits (at 3D accommodative demand) in random order between 1 and 100 (displayed on a 5 × 4 cm LCD screen). The cognitive task consisted of a two-alternative forced choice paradigm, where subjects responded when the number was between 25 and 74 inclusive. Cognitive demand was varied by altering the speed of presentation, and correct response rate for a range of presentation speeds calculated. From the results, five cognitive levels of increasing difficulty (corresponding to 0.1 s slower than 100% correct, 87.5, 75, 62.5% and 0.1 s faster than 50% correct) were employed in a random order. Five 20-s continuous objective recordings of the accommodative response measured with the open-view Shin-Nippon SRW5000 were obtained for each cognitive level, while simultaneous measurement of heart rate was recorded with a piezo-electric finger pulse transducer for 5 min. Fourier transformation of the inter-heartbeat interval allowed the relative parasympathetic and sympathetic components of the autonomic response to be assessed.

Results: Increasing the cognitive demand led to a significant reduction in the accommodative response (by −0.38 ± 0.14 D; $F = 5.37$, $p < 0.005$). Mean heart period showed a significant reduction with increasing levels of workload ($F = 11.21$, $p < 0.0005$) and a positive correlation with accommodative response ($r^2 = 0.96$, $p < 0.001$). Fourier analysis of the inter-heartbeat intervals showed that the sympathetic nervous system dominates with higher levels of workload.

Conclusions: The data demonstrate a significant reduction in accommodative response with increasing cognitive demand that is positively correlated with a sympathetic bias in systemic cardiovascular profile. The findings suggest that concomitant measures of cardiovascular function can provide systematic monitoring of the effect of cognition on accommodative response.

Acknowledgement

LND is supported by an EPSRC and BAe Systems CASE award.

Design of an electrophysiological technique able to investigate the optimum light level required to suppress the rod system

J. A. Cumiskey, K. E. Mortlock, R. V. North and N. Drasdo

School of Optometry and Vision Sciences, Cardiff University, Cardiff CF10 3NB, UK

Purpose: It has been hypothesised by Arden *et al.* (1998) that retinal hypoxia due to the high oxygen consumption of rod photoreceptors during dark adaptation may be a significant factor in the development of diabetic retinopathy. It has therefore been suggested that in order to reduce the oxygen demand to the retina subjects with diabetes may benefit from sleeping with the lights on. We report the development of an electrophysiological technique, employing the simultaneous cone-rod electroretinogram, to investigate further the optimum light level required to suppress the rods.

Methods: Electroretinograms were recorded monocularly using DTL fibres from seven healthy controls, mean age 24 years (range 21–48). Signals were amplified, averaged and band-pass filtered using a Medelec Sapphire[II] 4E system (Oxford Instruments, Witney, Oxfordshire,

UK). To obtain optimum separation of the cone and rod responses, a red (peak 655 nm) 5 ms flash, was presented at 1.3 Hz over a range of stimulus intensities (0.022–0.264 cds m^{-2}), following 20min dark adaptation and with pupil dilation. In order to mimic conditions of sleep, this was repeated through closed eyelids and without pupil dilation. Finally, background illumination was increased in order to determine the optimum level required to saturate the rod response.

Results: Our technique elicits a clear response from the cone and rod systems simultaneously in the dark adapted eyes of a group of control subjects. Dim ambient illumination suppressed the rod response, whilst the cone response remained intact.

Conclusions: From our preliminary data it appears that levels of 30 lux or less saturate or significantly reduce the rod response, which is presumed to be associated with a marked reduction in oxygen demand.

Reference

Arden G.B., Wolf J.E., Tsang, Y. (1998) Does dark adaptation exacerbate diabetic retinopathy? Evidence and a linking hypothesis. *Vision Res.* **38,** 1723–1729.

The human tear film: sample recovery after collection

M. Esmaeelpour and P. J. Murphy

School of Optometry and Vision Sciences, Cardiff University, Cardiff CF10 3NB, UK

Introduction: The pre-ocular tear film is a fluid with a complex composition and a dynamic structure that has many essential functions for the health of the ocular surface. Any disturbance in the tear film results in loss of stability and dry eye disease and a carefully targeted treatment is difficult. However, the neonate tear film shows a surprisingly high stability and a low blink rate (Lawrenson and Murphy, 2002). Current knowledge about the neonate tear film is limited and further studies of its physiology are needed to explain the observed quality. Less invasive and time-consuming tear collection methods are required for the evaluation of neonates and infants.

Purpose: A sample collection technique needs to be developed that determines materials with good absorbance and extraction properties. Further optimal centrifugation operating modes and possible effects of delayed processing need to be determined.

Methods: Six materials were selected polyester and cellulose acetate rods, polyvinyl alcohol and cellulose sponges, viscose towels, and Schirmer paper strips. Three different solutions–two high viscosity eye drops and saline were extracted from the absorbent materials. By measurement of the extracted volume different centrifugation parameters, such as spin duration and speed were tested. Finally many variations of factors, which can alter the extracted volume, such as temperature in the centrifuge, sample volume, receptor size, disinfecting, and delays of 1 h and 7 days, were tested and analysed.

Results: The polyester and cellulose acetate rods and the viscose towel had optimal extraction rates. Centrifugation can be carried out at a setting of 3 min, 14000 rpm and 4°C. Delays enhance the extraction. The small material size and shape helps to obtain more solution out of the rods and altering the sample volume does not make a significant difference. Disinfection had no influence on the structure of the materials.

Discussion: Although the optimal materials were chosen by their extraction rates, we noticed a good absorption when samples were prepared. They need to be tested for the effect of collection on the ocular surface and the effect of extraction on subsequent tear analysis. The extracted amounts were reasonably high so that they might be useful to collect samples for different tear analysis methods in neonates, such as protein analysis, osmolality and ferning testing.

Reference

Lawrenson, J.G. and Murphy P.J. (2002) The relationship between blink parameters, tear film stability and corneal sensitivity in neonates and infants. *Cont. Lens. Ant. Eye.* **25,** 208.

Expression of RhoA mRNA during human corneal transplant rejection

A. Benavente,[a] *J. A. Dixon,*[a] *A. B. Tullo*[b] *and M. C. Hillarby*[a,b]

[a]Academic Department of Ophthalmology, University of Manchester, Manchester M13 9PL, UK

[b]Manchester Royal Eye Hospital, Manchester M13 9WH, UK

Purpose: To investigate the mRNA expression of RhoA, a GTPase protein shown to play key roles in immune regulation and apoptosis, during human corneal transplantation.

Methods: A total of 117 blood samples were assessed, 39 of which had successful grafts, and 23 samples showed at least one rejection episode. Fifty-five blood samples were taken as controls showing no ocular conditions. Semi-quantitative analysis was undergone through RT-PCR. One-tailed *t*-test for two samples assuming unequal variances was used to determine the significance of the frequency difference between these groups ($\alpha = 0.05$).

Results: A down-regulation in the mRNA expression of the gene under study was found in the rejecting samples after comparing it to that from successful corneal grafting ($p = 0.024$), whereas the tendency of the rejecting group towards down-regulation was not found to be statistically significant after its comparison with the control group ($p = 0.09$). The difference in expression of RhoA in patients whose condition leading to surgery was herpes simplex keratitis (HSK) was also statistically significant compared with those without HSK ($p = 0.002$).

Conclusion: As the Rho family of GTPases have been proved to take part in the induction of apoptosis, these results might link the low levels of RhoA found in rejectors with a suppression of the apoptotic mechanism against the inflammatory cells that enter the cornea during human allotransplantation, and which would therefore lead to a rejection episode.

Paxillin expression during corneal transplant rejection

B. Huntjens,[a] *J. A. Dixon,*[a] *A. B. Tullob*[b] *and M. C. Hillarby*[a,b]

[a]Academic Department of Ophthalmology, University of Manchester, Manchester M13 9PL, UK

[b]Manchester Royal Eye Hospital, Manchester M13 9WH, UK

Purpose: To investigate the mRNA expression of paxillin, a focal adhesion protein that recruits adhesion- and growth factor-mediated signals from the extracellular matrix, during human corneal transplantation. Paxillin has previously been shown to play a role in corneal wound repair.

Methods: A total of 125 blood samples were assessed, 45 of which had successful corneal grafts and 25 samples showing at least one corneal rejection episode. The remaining 55 blood samples were used as normal controls, showing no ocular abnormalities. Semi-quantitative analysis was performed by RT-PCR. One-tailed *t*-test for two samples assuming unequal variances was used to determine the significance of the frequency difference between all groups.

Results: mRNA expression of paxillin was found to be significantly down-regulated in the rejecting samples compared with controls ($p = 0.019$). However, no significant difference was found between controls and the non-rejecting group or between subjects in the non-rejecting and rejecting group. Paxillin expression was also found to be significant altered between rejecting and controls or non-rejecting subjects, when age, gender, and surgical risk were compared between these groups.

Conclusion: Our results and previous findings indicate an important role for paxillin during corneal transplant rejection. Low levels of paxillin expression could be responsible for a decreased corneal wound healing response in human allografts, leading to a rejection episode.

Repeatability and reproducibility of macular thickness measurements using the OCT 3 system

H. L. Workman and S. L. Hosking

Neurosciences Research Institute, Aston University, Birmingham B4 7ET, UK

Purpose: Optical coherence tomography (OCT) is a non-contact and non-invasive imaging method employing low-coherence interferometry to produce high depth resolution cross-sectional images of ocular tissue. The aim of this study is to determine the within-visit repeatability and between-visit reproducibility of the OCT 3 (Model 3000; Carl-Zeiss Ophthalmic Systems Inc, Humphrey Division, Dublin, CA, USA).

Methods: Macular thickness measurements were obtained at each of two visits using multiple radial line scans, 6 mm in length, centred through the fixation point of 20 normal control subjects (58.9 ± 13.1 years). Retinal thickness analysis software produced a circular map comprising nine sectors depicting average retinal thickness. Coefficient of repeatability (CoR1) and coefficient of variation (CoV) were used to determine the repeatability of measures within a visit, while coefficient of reproducibility (CoR2) and intraclass correlation coefficients (ICC) were used to determine the reproducibility of measures between visits.

Results: The within-visit CoV ranged from 1.19 to 2.36% (mean 1.64%). CoR1 ranged from 1.19 to 2.36 (mean 1.64 ± 0.39). CoR2 ranged from 1.72 to 4.67 (mean 2.87 ± 1.12). ICCs for between-visit reproducibility ranged from 77 to 97% (mean 91%).

Conclusion: Measurements of macular thickness made with the OCT 3 in normal subjects are both highly repeatable and reproducible. OCT 3 represents a valuable clinical method by which to diagnose and monitor macular pathologies.

Ophthal. Physiol. Opt. 2005 **25:** 464–475

Abstracts

British Congress of Optometry and Vision Science (BCOVS) meeting held at University of Bradford, UK, 7th–8th April 2005

Keynote Addresses

Myopia: a growing problem

B. Gilmartin

School of Life and Health Sciences, Aston University, Birmingham, UK

Myopia is invariably a long-term condition characterised by a high and increasing prevalence (around 25 and 75% of young adolescents in, respectively, industrialised societies of the West and Far East) and is recognised as a significant ocular problem by the World Health Organisation. Myopia occurs when the refractive components of the anterior segment of the eye fail to compensate for excessive growth of the posterior vitreous chamber: essentially the eye outgrows its refractive capability. The consensus is that sustained degradation of central retinal image quality can induce myopia by derailing normal homeostatic mechanisms regulating the eye growth. Hyperopic defocus produced by accommodative lag at near is considered to be a major source of degradation and is consistent with the well-documented association between myopia and near work. An account will be given of the application of new measurement techniques to the biometry of the myopic eye: wavefront aberration devices have identified complex variations in retinal image quality with accommodation and refractive error; partial coherent interferometry now provides high-resolution, non-contact alternatives to ultrasound biometry. A novel recent development is the use of Magnetic Resonance Imaging for 3-dimensional whole-eye representation of eye shape and volume.

Does amblyopia have a future?

B. T. Barrett

Department of Optometry, University of Bradford, Bradford, UK

Amblyopia is a curious condition because it is easier to define in terms of the clinical features which are not present than it is to define those which are! Although research in amblyopia has a long, and often colourful, history, debate continues about the precise nature and causes of this condition. For example, the clinical dogma is that most human amblyopias are caused by strabismus and/or anisometropia. There is, however, a significant and growing literature that directly challenges this *causal* hypothesis. What, then, is the root cause of the visual loss if it is not strabismus or anisometropia? A number of recent studies have claimed that many 'amblyopic' eyes exhibit subtle structural defects raising the possibility that the condition may be less prevalent that we think. These controversial findings will be considered alongside the results from several recently published, large-scale investigations into the efficacy of amblyopia therapy. The intention is to seek an answer to the following question: *does the future look bright for the condition that we call 'amblyopia' and the treatment we administer for it?*

Environmental control of refractive state is conserved in all vertebrates

J. Sivak and W. Shen

School of Optometry, University of Waterloo, Ontario, Canada

The objective of this research was to determine if it is possible to induce form deprivation myopia in fish as well as to investigate the role of the lens in refractive error development. Tilapia (*Oreochromis niloticus*), about 4 months old and from 26 to 63 g, was divided into three groups. Translucent goggles were directly sutured over the right eye for 4 weeks to induce form deprivation myopia while the left eye served as an untreated contralateral control. Refractive state was measured by retinoscopy. Ocular dimensions were determined from frozen sections and with ultrasound biomicroscopy, while a scanning laser system was used to determine the optical quality of excised lenses. All the deprived fish eyes developed significant amounts of myopia ranging from −3.75 to −26.25 diopters (D), with the average amounting to −10.27 ± 1.14 D, after 4 weeks of form deprivation treatment. Eye dimension measurements show that the vitreous and anterior chambers of the treated eye are significantly longer axially than those of the contralateral eyes. No significant change in optical quality was found between lenses of the myopic and non-myopic eyes. The fish recovered completely from the myopia 5 days after the goggle was removed. These results indicate that although lower vertebrates are capable of lifelong growth, their eyes are susceptible to form deprivation myopia. Thus, the visual environment is an important factor controlling ocular development in lower vertebrates, as well as in higher ones, and eye development is not strictly genetically determined. This study also indicates that lens growth and optical development are largely independent from the refractive development of the whole eye.

Oral Presentations

Objective assessment of accommodative function in children with cerebral palsy

J. F. McClelland[a,b], *A. J. Jackson*[b,a], *J. Parkes*[c], *N. Hill*[d] *and K. J. Saunders*[a,b]

[a]School of Biomedical Sciences, University of Ulster, Coleraine, UK

[b]Ophthalmology, Royal Group of Hospitals, Belfast, UK

[c]School of Biomedical Sciences, Queen's University, Belfast, UK

[d]Children's Services, South and East Belfast Community Trust, Belfast, UK

Purpose: To assess ocular accommodation using objective techniques in children with different sub-types and severities of cerebral palsy (CP).

Method: Ninety-four subjects with CP (aged 4–15 years) were recruited via the Northern Ireland CP Register (NICPR) (Parkes *et al.*, 2001). The NICPR contains information regarding the CP sub-type and severity of all children in Northern Ireland diagnosed with CP. Whilst wearing appropriate refractive correction, accommodative function was assessed using the clinical judgement technique (CJ) and dynamic retinoscopy (DR). Using DR, accommodation was assessed at three different accommodative demands (4D, 6D and 10D) (McClelland and Saunders 2003, 2004). Using the CJ technique, pupil responses were graded as present, reduced or absent (if no discernable response was present). Subjects with ocular pathology, as determined by direct ophthalmoscopy (excluding nystagmus), were excluded from the present study ($n = 1$). Data regarding the subject's neurological status were derived from the NICPR.

Results: It was possible to assess accommodative function with 88 subjects (93.6%) using DR and 92 subjects (97.9%) using the CJ technique. Using DR, 51.5% of subjects with CP demonstrated reduced accommodation. The CJ technique demonstrated normal pupil responses in 55 subjects, reduced pupil reactions in 22 subjects and no discernable response in 15 subjects. Results from both techniques demonstrated children with ataxic or dyskinetic CP, more severe motor impairments and more severe intellectual impairments were at a significantly increased risk of accommodative dysfunction (ANOVA $p < 0.05$). Statistical analysis demonstrated a significant association between the results obtained using DR and the CJ technique (ANOVA $p < 0.001$).

Conclusions: Both the CJ technique and DR provide useful methods of detecting accommodative dysfunction in children with CP. CP significantly impacts upon ocular accommodation in children. These findings have implications for the optometric care of children with CP and inform our understanding of the role of different areas of the brain in visual development.

References

McClelland, J. F. and Saunders, K. J. (2003) The repeatability and validity of dynamic retinoscopy in assessing the accommodative response. *Ophthal. Physiol. Opt.* **23**, 243–250.

McClelland, J. F. and Saunders, K. J. (2004) Accommodative lag using dynamic retinoscopy: age norms for school-age children. *Optom. Vis. Sci.* **81**, 929–933.

Parkes, J., Dolk, H., Hill, N. and Pattenden, S. (2001) Cerebral palsy in Northern Ireland: 1981–93. *Paediatr. Perinat. Epidemiol.* **15**, 278–286.

Reconciling the results of genetic and epidemiological studies of myopia

J. A. Guggenheim[a], *Seang M. Saw*[b], *R. Pong-Wong*[c] *and C. S. Haley*[c]

[a]School of Optometry and Vision Sciences, Cardiff University, UK

[b]Departments of Community Occupational Family Medicine and Ophthalmology, National University of Singapore, and the Singapore Eye Research Institute, Singapore

[c]Department of Genetics and Biometry, Roslin Institute, UK

Purpose: Epidemiology studies aiming to identify environmental risk factors causing predisposition to myopia have had only limited success: the proportion of the variance that has been explained (R^2) in the best studies is ~12–13%. As genetic factors have been included in these models (for example, in the form of parental myopia status) and the heritability of refractive error is high, we investigated how this apparently paradoxical situation could arise.

Methods: Simulation studies were carried out to explore the power of the conventional epidemiological study design, as a function of the level of heritability.

Results: When the heritability of refractive error is high, the conventional study design was only able to explain a limited proportion of the total variance, even if full account was taken of all relevant environmental risk factors. Additionally, the young age of study subjects, the classification of refractive error as a categorical variable, and the presence of *gene* × *gene*, or *gene* × *environment* interactions would also decrease power.

Conclusions: For populations in which the heritability of refractive error is high, a low R^2 value may result from the study design not capturing a significant proportion of the variation due to genetic factors. For populations in which the heritability of refractive error is low, a low R^2 value is more likely to be caused by unidentified environmental risk factors. The power to detect environmental (and genetic) risk factors should be improved by study designs that capture both genetic and environmental sources of variance.

Audiovisual asynchrony judgements – adaptation negates effect of viewing distance

J. Heron[a], *D. Whitaker*[a] *and P. V. McGraw*[b]

[a]Department of Optometry, University of Bradford, Bradford, UK

[b]School of Psychology, University of Nottingham, Nottingham, UK

Purpose: Recent evidence suggests that, despite the differential velocities of light and sound in air, observers recalibrate the arrival time of sound signals across a range of viewing distances to maintain the perception of synchrony (Sugita and Suzuki, 2003). This view is, however, controversial (Lewald and Gusky, 2003). Adaptation to audiovisual (AV) asynchrony shifts the observer's point of subjective simultaneity (PSS) in the direction of the adapted asynchrony (Fujisaki *et al.*, 2004). We investigate the effect of this adaptation process in synchrony perception across viewing distance.

Methods: Point of subjective simultaneity was measured as a function of viewing distance. Observers made temporal order judgments (TOJs) as to 'which came first – sound (white noise 'click' delivered via speaker) or vision (circular white disk)'. TOJs were made with and without adaptation to the asynchrony arising from viewing distance.

Results: We found no evidence for an automatic distance-dependent recalibration of sound arrival times. However, given a period of adaptation to the AV asynchrony arising at a particular viewing distance, observers displayed a progressive shift in their PSS closer to zero.

Conclusions: Observers are able to recalibrate their perception of AV synchrony across viewing distance provided they are given an initial adaptation period.

References

Fujisaki, W., Shimojo, S., Kashino, M. and Nishida, S. (2004) Recalibration of audiovisual simultaneity. *Nature Neurosci.* **7**, 773–778.

Lewald, J. and Gusky, R. (2003) Auditory-visual temporal integration as a function of distance: no compensation for sound-transmission time in human perception. *Neurosci. Lett.* **357**, 119–122.

Sugita, Y. and Suzuki, Y. (2003) Implicit estimation of sound-arrival time. *Nature*, **421**, 911.

Deficits in the 'on-line' control of reaching and grasping actions in adults with reduced binocular vision

S. Grant, D. Melmoth, M. J. Morgan and A. L. Finlay

Department of Optometry and Visual Science, City University, London, UK

Purpose: We compared the speed and accuracy of reaching and grasping actions made under binocular or monocular viewing conditions by normal and by stereodeficient (SD) adults.

Methods: Hand movements to objects of different size and location were recorded using a 3D motion-capture system (ProReflex, Qualisys Medical AB, Gothenburg, Sweden). Profiles of the wrist velocity, spatial path and grip aperture were examined for on-line errors, and key dependent measures of the movement kinematics were analysed.

Results: The results showed that both subject groups executed their movements more efficiently under binocular control than when using monocular vision: removing binocular information increased the durations of the terminal reach and object manipulation phases, increased the occurrence of 'on-line' corrections during these phases, and led to poorer grip scaling at the point of object contact. The binocular performance of the SD subjects was, however, significantly worse than that of the normal adults on all of these measures, especially among those with the most severe reductions in binocular stereoacuity.

Conclusions: Our data support an earlier proposal (Morgan, 1989) that binocular disparity processing is normally utilized to control the actions of the hand as it approaches, contacts and lifts solid objects.

Reference

Morgan, M.J. (1989) Stereopsis – vision of solid objects. *Nature* **339**, 101–103.

Structural and functional progressive damage in open angle glaucoma

C. Hudson[a], *J. M. Wild*[a] *and I. A. Cunliffe*[b]
[a]School of Optometry and Vision Sciences, Cardiff University, Cardiff, UK
[b]Department of Ophthalmology, Birmingham Heartlands Hospital, Birmingham, UK

Purpose: To evaluate the presence of, and any relationship between, structural and functional progression in open angle glaucoma (OAG).

Methods: Data for the study were obtained from a longitudinal prospective investigation that took place at Birmingham Heartlands Hospital between 1997 and 2005. Twelve patients with OAG and nine patients with high-risk ocular hypertension (OHT) had each been followed up for approximately 77 months using Heidelberg Retinal Tomography (HRT) and threshold perimetry with the Humphrey Field Analyzer (HFA) on one randomly designated eye of each patient. Evidence for structural progression was assessed using the HRT Change Probability Map and for functional progression with the Glaucoma Probability Analysis.

Results: Three patients (2 OAG and 1 OHT) showed progressive change to the visual field and optic nerve head combined. Six patients (4 OAG and 2 OHT) showed progressive ONH change with no detectable change in the visual field. Six patients (4 OAG and 2 OHT) showed progressive visual field change with no detectable change to the ONH. Six patients (2 OAG and 4 OHT) showed no evidence of progressive change to the ONH or visual field.

Conclusion: The results indicate tbat it is necessary to undertake both structural and functional assessment in the follow-up of patients with OAG and OHT.

Changes in colour perception with retinal eccentricity

D. McKeefry[a], *N. Parry*[b] *and I. Murray*[c]
[a]Department of Optometry, University of Bradford, Bradford, UK
[b]Vision Science Centre, Manchester Royal Eye Hospital, Manchester, UK
[c]Faculty of Life Sciences, The University of Manchester, UK

Purpose: When a coloured stimulus is moved from the fovea to more eccentric retinal positions, there are changes in its perceived hue and saturation. In this series of experiments, we were interested in determining how retinal eccentricity influences the perception of colour across a wide range of chromatic stimuli incorporating spectral as well as non-spectral regions of colour space.

Methods: Perceived shifts in chromaticity of test stimuli presented on a cathode ray tube at different retinal eccentricities up to 24° were measured by comparing them with a probe of 1° eccentricity. Photometrically isoluminant probe and test pairs were flashed for 380 ms on a 12.5 cd m^{-2} white background. Twelve to 24 probe chromaticities were equally spaced around a hue circle in MBDKL colour space. Perceived hue shift was measured as an orientation change in this colour space using a same-different paradigm to generate psychometric functions.

Results: The perceived shifts in hue that are observed as coloured stimuli fall on more peripheral regions of the retina are not uniform across colour space. Whilst certain hues undergo large perceived shifts in their appearance, others remain largely invariant with increasing retinal eccentricity. In terms of colour matching, increasing the stimulus size does not make peripheral colour vision exactly fovea-like. Increasing the size may restore all the normal colour categories but the distortions in colour matching for regions of colour space are still in evidence.

Conclusions: The perception of colour in certain regions of colour space is distorted in the peripheral retina. This is not simply an effect of stimulus size but is likely to be a result of physiological factors operating in the peripheral retina.

The evaluation of the peripheral corneal thickness with ultrasound-based and scanning slit methods

S. Jonuscheit, M. J. Doughty and N. F. Button
Department of Vision Sciences, Glasgow Caledonian University, Glasgow, UK

Purpose: To assess the corneal thickness (CT) with ultrasonic (US) and scanning-slit pachymetry at central, mid-peripheral, and peripheral sites and compare the outcome of both instruments.

Methods: Single point measurements were obtained at the centre, the mid-periphery (3 mm radius from centre), and the periphery (4–4.5 mm from centre) of 16 healthy subjects (mean age 32.5 ± 10.5 years, range 20–58 years). Scanning-slit Orbscan measurements were taken first followed by ultrasonic pachymetry.

Results: Ultrasonic pachymetry readings were 0.519 ± 0.034 mm, 0.555 ± 0.035 mm, and 0.595 ± 0.044 mm (mean ± SD) for centre, mid-periphery, and periphery, respectively. Orbscan readings were higher with 0.578 ± 0.038 mm, 0.655 ± 0.035 mm, and 0.704 ± 0.035 mm (mean ± SD) without a correction factor. The difference between Orbscan and US measurements ranged from 8–16% (11 ± 2% mean ± SD), 12–25% (18 ± 4%), and 1–30% (18 ± 7%) for central, mid-peripheral, and peripheral locations, respectively. The application of the default correction factor (0.92) reduced the original Orbscan measurements by 8%. The corrected corneal thickness values were 0.531 ± 0.035 mm, 0.602 ± 0.033 mm, and 0.647 ± 0.032 mm. Mid-peripheral CT readings were thus 7% greater on average than central readings by US but 13% greater with the Orbscan. A similar difference (22% vs 15%) was noted for Orbscan and US, respectively, for peripheral readings.

Conclusion: The thickness of the human cornea gradually increases towards the periphery but US and Orbscan devices yield different results. The default correction factor of 0.92 of the Orbscan is not ideal to bring Orbscan measurements into accordance with US results for the entire cornea and so should be abandoned.

Development of the 'Optometric Anxiety Scale'

H. Walters[a], *K. Greenland*[b] *and T. Margrain*[a]
[a]School of Optometry and Vision Sciences, Cardiff University, Cardiff, UK
[b]Cardiff School of Social Sciences, Cardiff University, Cardiff, UK

Purpose: In stark contrast to the wealth of knowledge and understanding about patient anxiety within primary healtb care, almost nothing is known about anxiety in optometric practice. The aim of this research was to develop an 'Optometric Anxiety Scale'; a tool that may be used to quantify patient anxiety within an optometric setting. Such a tool may be used to assess the ability of various interventions to reduce patient anxiety.

Methods: On the basis of information from focus groups, published literature about anxiety, and discussions with optometrists, an 83-item, five response option (strongly agree to strongly disagree) questionnaire was developed and piloted on 348 young adults. The validity of the responses was assessed and principal component analysis (PCA) was performed to identify the principal factors, each including questions

with a high degree of internal consistency. The resulting shorter 30-item questionnaire was piloted in optometric practice.

Results: One hundred and fifty-six questionnaires were completed in two different optometric practices. The resulting data were evaluated using SPSS V.11. Items with positive valence were recoded, so that a high value represented higher anxiety. Reliability analysis of all the questions revealed very good internal consistency (Cronbach alpha coefficient: 0.94). PCA and evaluation of a screenplot suggested the presence of four strong factors with eigenvalues exceeding 1 i.e. the patient–practitioner relationship, concern about health of the eyes, contact lenses and responding to test questions. Construct validity was assessed, including correlation of items with a criterion variable. Two items from each of the strongest factors as revealed by PCA were selected for the final questionnaire. This resulted in the 8-item, five response option (strongly agree to strongly disagree) 'Optometric Anxiety Scale'.

Conclusions: The 'Optometric Anxiety Scale' is a short self-report questionnaire that may be used to evaluate patient anxiety in optometric practice. The questionnaire is currently being validated and test–retest reliability evaluated.

Functional magnetic resonance imaging evidence for the neural representation of faces

G. Loffler[a], *G. Yourganov*[b], *F. Wilkinson*[b] *and H. R. Wilson*[b]

[a]Department of Vision Sciences, Glasgow Caledonian University, Glasgow, UK

[b]Center for Vision Research, York University, Toronto, Canada

Purpose: At the highest levels of the primate form vision pathway in inferior temporal cortex, neurons respond selectively to highly complex object forms such as faces. Functional magnetic resonance imaging (fMRI) studies on humans have revealed a cortical area, the fusiform face area (FFA) that is also specialized for face processing. It has been hypothesized that faces are represented in a multi-dimensional space with individual faces encoded by their direction and distance from the mean face, and psychophysical data support this view. The aim of this study was to investigate this hypothesis by recording fMRI signals from FFA as a function of varying facial geometry (head shape, hair line, internal feature size and placement).

Methods: We presented synthetic faces and modified their facial geometry (defined by how much a face differed from the population mean). The FFA was localised individually in each observer by contrasting the activation to grey-scale photographs of faces from houses. Subsequent measurements were focused within this region of interest. The Blood Oxygenation Level Dependent (BOLD) signal was measured using a 4T, whole body MRI system. Voxel volume was $3 \pm 3 \pm 6$ mm collected using a T2*-weighted, interleaved echo-planar imaging (EPI) acquisition. Subjects engaged in a modified one-back same-different task during scanning.

Results: Data indicate that the BOLD signal increases as a sigmoid function of geometric distance from the mean face. Furthermore, fMRI adaptation indicates that the same neural population responds to all geometric variation in a single direction from the mean.

Conclusion: These results provide direct support for a neural face space and have strong implications for how faces are computed and, more generally, how they are represented in human cortex.

Comparison of the topographical distributions of first- and second-order motion-onset visual evoked potentials

E. G. Laviers and D. J. McKeefry

Department of Optometry, University of Bradford, Bradford, UK

Purpose: The processing pathway of luminance (first-order) motion has been extensively documented but the mechanisms governing motion defined by properties other than luminance (second-order) are less well understood, and it is unclear whether first- and second-order stimuli are processed by a common or by segregated motion pathway(s). Here, we compare the topographical distribution of first- and second-order motion-onset visual evoked potentials (VEPs) in order to locate the visual areas responsible for the processing of each stimulus type.

Methods: Motion-onset VEPs were recorded from five electrode sites located at Oz and at four locations (T1–T4) lateral to Oz at intervals of 5% of the head circumference. The stimuli were either achromatic luminance-modulated sinusoidal gratings or contrast-modulated 'beat' gratings, and responses were recorded over a range of velocities and contrasts. Amplitudes were measured peak to peak (N2–P2) for four subjects.

Results: N2–P2 amplitudes generated by both the first- and second-order stimuli were maximal at lateral electrode locations (T1/T2). This result was observed at all velocities and contrasts tested.

Conclusion: The similar topographical distribution of the first- and second-order stimuli suggests a common mechanism for the processing of luminance and contrast-defined motion.

Internal noise in artificial scotomas

P. Mihaylov[a], *V. Manahilov*[a], *W. A. Simpson*[b] *and N. Strang*[a]

[a]Department of Vision Sciences, Glasgow Caledonian University, Glasgow, UK

[b]Simulation Modelling Section, DRDC Toronto, Toronto, Ontario, Canada

Purpose: When presented with a homogeneous grey patch surrounded by a dynamic noise background, subjects report that the perceptual artificial scotoma fades and is filled in by the dynamic noise from the surround. When the background is switched off, observers report perception of a prolonged patch of twinkling noise in the non-stimulated area (Ramachandran and Gregory, 1991). These phenomena might be related to active neural processes induced by the surrounding stimulation, increasing the level of internal noise within the visual system. To test this suggestion, we employed the equivalent noise approach in conjunction with the artificial scotoma paradigm. The experiments are designed to quantify directly the processes underlying our perception of twinkling noise in the non-stimulated area.

Methods: Observers were presented with Gaussian dynamic noise and a grey patch of 1.5° radius centred at the fixation point. They detected a foveal Gabor patch of 4 c deg^{-1} (SD 15 min of arc) embedded in Gaussian dynamic noise. Using a two interval forced choice method and a staircase procedure, contrast thresholds for detecting the test stimulus were measured in filling-in and after filling-in conditions.

Results: The detection threshold increased as the scotoma noise density increased. These functions were shifted to higher contrast levels as the surrounding noise density increased. Observers' performance was analysed by a model for detecting visual patterns. Sampling efficiency, additive internal noise and internal noise induced by surrounding noise, were taken into account. The results show that in filling-in conditions, the surrounding noise induces an internal noise component, which is higher than that obtained in after filling-in conditions. In addition, the level of the additive internal noise is higher for after filling-in conditions than for filling-in conditions.

Conclusions: Dynamic noise may be transferred into internal noise over distances longer than the receptive field size. The differences in additive internal noise levels for different experimental conditions suggest that there is a relationship between the additive and the induced internal noise components.

Reference

Ramachandran, V.S. and Gregory, R.L. (1991) Perceptual filling-in of artificially induced scotomas in human vision. *Nature* **350**, 699–702.

Perceived speed of colour and luminance grating stimuli

M. Burton and D. McKeefry
Department of Optometry, University of Bradford, Bradford, UK

Purpose: The existence of different contrast matching functions at slow and fast speeds has led to the proposal that the speeds of slowly moving chromatic and luminance grating stimuli are governed by separate processing pathways (Hawken *et al.*, 1994). In this study, we re-examine the extent of independence between colour and luminance contrast and their influence on perceived speed at low and high stimulus velocities.

Methods: Perceived speed of a luminance ($L + M$), a red-green ($L - M$) and a blue-yellow [$S - (L + M)$] 1 cycle deg^{-1} sinusoidal grating of variable contrast was matched against an achromatic, 2.5% contrast, 1 cycle deg^{-1} sinusoidal grating at low and high velocities. Perceived speed was also matched for a ($L - M$) control against a ($L - M$) test and for an $S - (L + M)$ control against an $S - (L + M)$ test. The ($L + M$) to ($L + M$) match was then repeated in the presence of a high contrast, variable velocity modifier grating, either side of the test grating, which was modulated along ($L + M$), ($L - M$) and $S - (L + M)$ axes.

Results: The perceived speed of chromatic and luminance stimuli, matched as a function of detection threshold, exhibits identical speed matching functions at low and high velocities. In addition, the presence of a high contrast chromatic or achromatic modifier grating has an equal influence on the perceived speed of the control achromatic grating.

Conclusions: The perception of speed of luminance and chromatic gratings is not analysed within independent pathways, even at low stimulus speeds, but calculated via a large, contrast-influenced, chromatically independent sampling area.

Reference

Hawken, M.J., Gegenfurtner, K.R. and Tang, C. (1994) Contrast dependence of colour and luminance motion mechanisms in human vision. *Nature* **367**, 268–270.

Poster Presentations

Short-wavelength resolution acuity in age-related maculopathy: selective damage and 'normal' vision

R. S. Anderson[a], *R. O. Beirne*[a], *M. B. Vidinova*[a] *and U. Chakravarthy*[b]
[a]Vision Science Research Group, University of Ulster at Coleraine, N. Ireland, Ireland
[b]Ophthalmology and Vision Science, Queen's University of Belfast, N. Ireland, Ireland

Purpose: Previous studies have indicated that measurements of short wavelength sensitive (SWS) grating acuity can be used to estimate the density of the small bistratified class of ganglion cells across the human retina. How is SWS resolution affected in age-related maculopathy (ARM), especially when a patient displays central retinal changes but otherwise normal vision by conventional testing methods?

Methods: A total of 88 subjects (32 males, 56 females; 51–87 years, mean 71.4 ± 8.2 years) took part in the study. All subjects were tested using conventional visual acuity, contrast sensitivity and colour vision methods and graded into seven grades of age-related macular appearance ranging from completely normal (grade 0), through different grades of ARM (Grades 1–5), to clinically significant AMD (grade 6). Resolution acuity was measured using both achromatic and blue-on-yellow gratings at four locations 6° from the fovea.

Results: Achromatic resolution acuity was poor at distinguishing between subjects with ARM and those with normal retinal appearance. It was also unable to distinguish between different groups of ARM subjects. However, SWS resolution acuity was significantly lower in subjects with some ARM than those with none ($p = 0.002$) and there was a significant difference between most of the ARM groups ($p < 0.001$). Interestingly, the chromatic/achromatic resolution ratio was also significantly lower in subjects with ARM indicating a selective loss of the SWS pathway in these subjects.

Conclusion: Short wavelength sensitive resolution (and hence small bistratified ganglion cell density) appears to be reduced in many subjects with early ARM long before they would be classified as clinically 'pathological'. Such a test may be useful to predict which patients will go on to suffer AMD at a later date.

Determination of refractive error with wavefront analysers

A. Cervino, S. L. Hosking, S. A. Naroo and B. Gilmartin
School of Life and Health Sciences, Aston University, Birmingham, UK

Purpose: To assess the accuracy of two current wavefront analysers (WAs) in determining refractive error in non-cyclopleged eyes, compared with a previously validated standard binocular open-view autorefractor, and examine whether mydriasis and cycloplegia using topical instillation of antimuscarinic agents should be employed.

Methods: Eighty eyes from 40 subjects were examined with the Shin-Nippon SRW-5000 open-view infra-red autorefractor (Ajinomoto Trading Inc., Tokyo, Japan); and the OPD-scan (dynamic-skiascopy principle-based; Nidek, Gamagori, Japan) and WASCA (Hartmann-Shack principle-based; Carl Zeiss Meditec, Jena, Germany) WAs under low illumination conditions. Subjects were young adult optometry students (19 men, 21 women; mean age 20.8 ± 2.5 years old) whose sphere refractive errors ranged from +1.5D to –9.75D (mean –2.11 ± 3.09D) and up to 1.75 cylinder (mean 0.02 ± 0.79D). Three readings were collected by the same examiner with each instrument without the use of an antimuscarinic agent.

Results: High levels of correlation were found between WAs and SRW-5000 data for mean spherical equivalent (MSE): OPD, $r = 0.959$, $p = 0.000$; WASCA, $r = 0.981$, $p = 0.000$. Mean differences, level of significance and limits of agreement indicated significantly more negative MSEs found with WAs: OPD, 0.406 ± 0.768D (0.235 to 0.580), $p = 0.000$; WASCA, 0.511 ± 0.550D (0.390 to 0.634), $p = 0.000$; but no statistically significant differences for the astigmatic components J0 and J45 (0.040 ± 0.385D and –0.046 ± 0.477D for the OPD; and –0.102 ± 0.282D and –0.015 ± 0.373D for the WASCA, respectively). Bland–Altman dispersion plots showed a trend for the MSE to be relatively more negative with the WAs as the baseline level of myopia decreased.

Conclusion: Given that instrument myopia is a well-established phenomenon under relatively enclosed viewing conditions such as those present in the WAs used in this study, it is concluded that this phenomenon accounts principally for the mean MSE discrepancy of approximately 0.50 D more myopia found with WA refraction compared with SRW-5000 refraction. As instrument myopia is attributed to a surfeit of accommodation, the data imply therefore that stable and accurate refraction with WAs would be facilitated by the use of antimuscarinic agents, particularly for lower levels of myopia.

The effect of blur adaptation on accommodation accuracy and near-work-induced transient myopia (NITM)

M. P. Cufflin, C. A. Hazel and E. A. H. Mallen
Department of Optometry, University of Bradford, Bradford, UK

Purpose: Blur adaptation, or the improvement in unaided distance acuity following a period without refractive correction, has been documented in myopes and defocused emmetropes. Closed-loop accommodation responses have been shown to vary with refractive error. This study investigates how adapting to defocus affects these responses in myopes and emmetropes.

Methods: Accommodation responses during a 10 min near task (4 D), and post-near task accommodation regression functions were recorded for 10 emmetropes and 10 myopes, aged 18–25 years. Two conditions (adapted and non-adapted) were compared. For the

adapted condition, subjects viewed broadcast television for 45 min at a distance of 4 m with +1.75 DS added to their optimum distance refraction. Defocus was then removed and accommodation measures immediately taken using a Shin-Nippon SRW-5000 autorefractor. For the non-adapted condition, accommodation measures were taken without a prior period of defocus.

Results: Blur adaptation produced a mean improvement in VA of 0.24 ± 0.07logMAR and 0.14 ± 0.04logMAR for myopes and emmetropes, respectively. There was a trend for the near-task lag of accommodation to be greater following blur adaptation, however, this did not reach significance in either the myopic ($p = 0.05$) or the emmetropic subjects ($p = 0.05$). Repeated measures ANOVAS showed that blur adaptation did not significantly affect the speed of the closed-loop post-task regression, for either myopes ($p = 0.36$) or emmetropes ($p = 0.23$).

Conclusion: Blur adaptation had no significant effect on the accuracy of the accommodation response to a near task, or the closed-loop post-task accommodative regression (NITM), in either myopes or emmetropes.

Myopes show increased accommodative microfluctuations at low target luminance levels

M. Day, D. Seidel, N. C. Strang and L. S. Gray
Department of Vision Sciences, Glasgow Caledonian University, Glasgow, UK

Purpose: The aim of this study is to examine the effect of target luminance on the accommodation microfluctuations in emmetropes and myopes.

Methods: Thirty-six [12 emmetropic (EMM) and 24 myopic (MYO)] healthy young adult volunteers (mean ± SD age: 22.5 ± 4.45 years) with <0.75 D of astigmatism participated with informed consent in the study. Subjects viewed a Maltese cross target through a +5 D Badal lens at a vergence equal to their dark focus (DF) level of accommodation. Accommodation microfluctuations were measured in DF conditions and while viewing the target at luminances of 0.002 cd m^{-2}, 0.2 cd m^{-2}, 6 cd m^{-2} and 600 cd m^{-2}. Accommodation was measured continuously over a period of 2 min using a Shin-Nippon SRW-5000 (Ajinomoto Trading Inc., Tokyo, Japan) infrared autorefractor at a sampling rate of 52 Hz. All myopic subjects were fully corrected with mid-water (58%) content thin soft contact lenses (Acuvue, Johnson & Johnson, Jacksonville, FL, USA).

Results: Overall, the myopic group had significantly larger (ANOVA $F_{1,180} = 16.763$, $p < 0.001$) microfluctuations than the emmetropic group. Increases in the magnitude of the microfluctuations with reducing luminance occurred in both subject groups and the microfluctuations increased more in the myopic subjects (ANOVA EMM: $F_{4,60} = 3.348$, $p < 0.001$; MYO: $F_{4,60} = 25.632$, $p < 0.001$). Subjects who had a larger size of microfluctuations in the high luminance condition also had larger microfluctuations in the two lowest luminance conditions (Pearson Correlation, 600 cd m^{-2} vs DF: $R^2 = 0.49$, $p = 0.001$; 600 cd m^{-2} vs 0.002 cd m^{-2}: $R^2 = 0.52$, $p = 0.001$). Frequency analysis showed that these increases in the magnitude of the microfluctuations were caused by increases in the low frequency components (0.05–0.6 Hz) of the microfluctuations.

Conclusions: Myopic subjects show greater microfluctuations compared with emmetropes. Reducing target luminance produces an increase in the microfluctuations of accommodation in all subjects. This was more pronounced in myopes, which indicates greater instability of the accommodation system when retinal image quality is poor in those subjects.

The effect of crowding bar contrast on contour interaction for letter targets

A. Demberg
Department of Vision Sciences, Glasgow Caledonian University, Glasgow, UK

Purpose: Contour interaction has been shown to be reduced or absent for low contrast letter targets. These findings were obtained with the contrast of both the letters and the crowding bars at the same level. The aim of this study was to examine whether the contrast dependency of contour interaction is determined by the contrast of the letter target or the contrast of the crowding bars.

Methods: Twenty-five visually normal subjects (mean age 22.4 ± 6.4 years) participated with informed consent in the study. Subjects wore their full spectacle correction and had VA of 6/6 or better. A computer-based vision-testing program (TestChart2000, Thomson Software, Potters Bar, Herts, UK) was employed to present single optotypes at six levels of contrast (90, 40, 30, 20, 10 and 5%). Letters were presented on a standard SVGA monitor at a viewing distance of 6 m. The letters were presented with and without crowding bars, and the contrast of the crowding bars was either the same as the letter or fixed at 90% for all levels of letter contrast. Crowded and uncrowded acuity thresholds were determined psychometrically at each contrast level using a forced choice paradigm.

Results: With the crowding bars fixed at 90% contrast, the mean uncrowded VA (–0.14 ± 0.08 logMAR) for the 90% contrast letters was significantly ($p = 0.0001$) higher than the mean crowded VA (–0.02 ± 0.06 logMAR). Similarly the mean uncrowded VA (0.16 ± 0.09 logMAR) for the 5% contrast letters was significantly ($p = 0.0001$) higher than the mean crowded VA (0.27 ± 0.04 logMAR) for that contrast. When the contrast of the crowding bars was the same as the letters, the mean uncrowded VA was not significantly different from the mean crowded VA at all levels of contrast.

Conclusions: Contour interaction is absent at low letter contrasts when the crowding bars have the same contrast as the letters, but contour interaction is present at all levels of letter contrast when the crowding bars are fixed at high contrast. This suggests that the presence of contour interaction is determined by the contrast of the inhibitory surrounding contours.

Jargon-busting in practice

F. Fylan[a,b] *and A. Hepworth*[c]
[a]Department of Health Sciences, University of York, Heslington, UK
[b]Brainbox Research, 143–145 The Headrow, Leeds, UK
[c]Essilor UK, Cooper Road, Thornbury, Bristol, UK

Purpose: Misunderstandings between practitioners and patients in ophthalmic consultations are common, and they influence anxiety, satisfaction, and purchasing decisions. We have explored the factors underlying misunderstandings, and have identified ways in which communication between practitioners and patients can be enhanced.

Methods: We observed interactions between practitioners and patients in eight different practices, and interviewed both practitioners and patients about the observed consultations. Focus groups were held with patients about their experiences of consultations with both optometrists and opticians, and their understanding of the language used during consultations. Explanations of those terms that participants had difficulty understanding were developed, and a questionnaire study was undertaken to assess participants' preferences for these explanations. Participants were assigned randomly to receive a combination of technical, detailed and concise explanations, and were asked to rate how easy to understand, and how relevant to their needs, each explanation was perceived to be.

Results: The eye examination can give rise to anxieties regarding procedures, the detection of pathology, and giving correct answers. Jargon, particularly that used during dispensing, is often misunderstood by patients and can lead to inappropriate expectations and purchasing behaviour. Patients want more information than they commonly receive, in an easy-to-understand form, and good practitioner–patient relationships in which they feel able to ask questions. Information that includes technical language, particularly about lens options, is perceived by patients as being more difficult to understand and less relevant to their needs.

Conclusions: Practitioners' communications skills have a major influence on patients' satisfaction with their consultation and their eyewear purchases. We have used the results of this study to develop jargon-busting communication techniques that can be applied by practitioners to better meet their patients' information needs.

Changes in quality of life after LASIK for myopia

E. Garamendi[a], *K. Pesudovs*[b] *and D. B. Elliott*[a]
[a]Department of Optometry, University of Bradford, Bradford, UK
[b]Department of Ophthalmology, Flinders Medical Centre and Flinders University, Bedford Park, Australia

Purpose: To measure the quality of life (QoL) outcome of pre-presbyopic myopic subjects undergoing LASIK refractive surgery using the Quality of Life Impact of Refractive Correction (QIRC) questionnaire. Additionally, we compared the QoL of pre-surgery subjects to a sample of spectacle and contact lens wearers not considering refractive surgery.

Methods: The validated QIRC questionnaire was prospectively completed by sixty-six patients before and 3 months after LASIK. Patients had myopia >0.50 D (range –0.75 to –10.50 D) and were aged 16–39 years. Subjects were also directly asked to evaluate their QoL after surgery.

Results: Overall QIRC scores improved after LASIK from a mean (±SD) of 40.07 ± 4.30 to 53.09 ± 5.25 ($F_{1,130} = 172.65$, $p < 0.001$). Greater improvements occurred for females (53.83 ± 5.46) than males (49.39 ± 5.94; $F_{1,64} = 9.37$, $p < 0.005$). Overall, 15 of the 20 questions (especially convenience, health concerns and well-being questions) showed significantly improved scores ($p < 0.05$). Subjects who 'strongly agreed' (53.96 ± 4.91, $n = 33$) or 'agreed' (51.78 ± 6.19, $n = 23$) their QoL had improved had significantly higher QIRC scores than those who 'neither agreed nor disagreed' (44.36 ± 4.97, $n = 5$) or 'strongly disagreed' (42.82, $n = 1$) ($F_{1,60} = 11.24$, $p < 0.001$). The matched group not contemplating LASIK scored 42.41 ± 3.89 on QIRC overall.

Conclusions: Large improvements in QIRC QoL scores were found after LASIK for myopia in the majority of subjects, with greater improvements occurring for females. A small number of subjects (4.5%) had decreased QIRC QoL scores and these were associated with complications. People presenting for LASIK had measurably poorer scores than matched subjects not contemplating refractive surgery.

Retinal ganglion cell axons increase their diameters along the rat optic nerve

C. R. C. Guibal and G. E. Baker
Department of Optometry and Visual Science, City University, London, UK

Purpose: The diameter and conduction velocity along mammalian retinal ganglion cell axons are not constant. In ferret, the conduction velocity of the largest axons is twice as fast in the tract as in the nerve (Baker and Stryker, 1990). We investigated the optic nerve and tract in rat to determine whether there is a constant increase along the axons or a step-like change from the nerve to tract.

Method: Six deeply anesthetised rats were perfusion fixed with mixed aldehydes and the diameter of their optic axons was measured at four different locations along the primary visual pathway.

Results: The results show that the mean number of axons with a diameter larger than 2 μm was significantly greater in the tract than the nerve ($t = 3.28$, $p < 0.01$). Also, along the pathway, this number increased gradually (1277.5 intraorbitally in the nerve, 1706.2 intracranially, 2419.3 pre-chiasmatically and 3171.8 in the tract). This increase in diameter was found in all ranges of axons measured and was estimated to reach 20% for the largest axons as they travel from the nerve to the tract.

Conclusion: There is no location along the pathway where a step-like increase in diameter was consistently found.

Reference

Baker, G. E. and Stryker, M. P. (1990) Retinofugal fibers change conduction-velocity and diameter between the optic-nerve and tract in ferrets. *Nature* **344**, 342–345.

Stepping up to a new level: effects of blurring vision in the elderly

K. J. Heasley[a], *J. G. Buckley*[a], *A. Scally*[b], *P. Twigg*[c] *and D. B. Elliott*[a]
[a]Department of Optometry, Vision and Mobility Research Laboratory, University of Bradford, Bradford, UK
[b]Institute of Health Research, School of Health, University of Bradford, Bradford, UK
[c]School of Engineering, Design and Technology, University of Bradford, Bradford, UK

Purpose: To determine the effects of blurring vision, using cataract simulation, on the step negotiation strategy of healthy elderly subjects, through analysis of whole body centre of mass (CM) dynamics and foot clearance parameters.

Methods: Centre of mass dynamics and foot clearance parameters were measured in 12 subjects, seven males and five females, (mean age 72.3 ± 4.17 years). Measurements were then repeated with the presence of the cataract simulation lenses.

Results: In the blurred condition, subjects took 11% longer across all stepping phases ($p < 0.05$) and reduced the mediolateral (but not anterioposterior) displacement of their centre of pressure from 37.6% stance width to 28.3% during the anticipatory phase ($p < 0.01$). Peak mediolateral divergence between the CM and the centre of pressure (CP) (the weighted average of all pressures over the area in contact with the ground) also decreased whilst in the anticipatory phase by 9.8 mm ($p < 0.01$). Toe clearance was found to increase during the blurred trials in both horizontal (28%) and vertical (19%) directions ($p < 0.05$).

Conclusions: This study has highlighted that a twofold safety-driven adaptation occurs when under the influence of visual disturbance such as cataract. Firstly, CM excursion within the base of support was reduced, to increase dynamic stability, and secondly toe clearance, in both horizontal and vertical directions, was increased to reduce the risk of tripping by providing greater room for error.

First- and second-order motion: a comparison of 'windows of visibility'

C. Hutchinson and T. Ledgeway
School of Psychology, University of Nottingham, Nottingham, UK

Purpose: To characterise the spatiotemporal 'window of visibility' for first-order motion (luminance-modulated noise) and three varieties of second-order motion (contrast-modulated, flicker-modulated and spatial length-modulated noise).

Methods: Direction-identification thresholds (the minimum modulation depth producing 79.4% correct performance) were measured for each motion pattern (acuity permitting) over a spatial and temporal frequency range of five octaves (0–16 c deg $^{-1}$; 0–16 Hz, respectively). Threshold values were then converted into modulation sensitivity (the reciprocal of modulation depth at threshold).

Results: There were distinct differences in sensitivity and in the overall shapes of the functions for first- and second-order motion. For second-order motion, the functions corresponding to contrast- and flicker-modulated noise were virtually identical in terms of shape and

sensitivity. However, sensitivity to modulations of spatial length was extremely poor and more low-pass, suggesting that additional strategies, perhaps a feature-based system, may be required for encoding the motion of images of this type.

Conclusions: This study has characterised the spatiotemporal window of visibility for a range of first- and second-order motion patterns. The findings clearly reinforce the notion that first- and second-order motion are encoded separately in human vision but most importantly, the results for second-order motion have demonstrated that all second-order image attributes may not be homogenous or encoded solely by low-level motion-detecting mechanisms within the human visual system.

Temporal changes in the height of the inferior tear meniscus following a blink

M. E. Johnson, C. George and P. J. Murphy
School of Optometry and Vision Sciences, Cardiff University, Cardiff, UK

Purpose: To investigate changes in the height of the inferior tear meniscus following a blink.

Methods: Images of the lower tear meniscus were captured every 2 s for the 10 s immediately following a blink, in 15 subjects (aged 19–26 years), using a video-slitlamp. Fluorescein dye (5 mL of 2%) was used to enhance meniscus visibility. To ensure that measurements were not influenced by the volume of fluorescein solution added to the eye, the experiment was started 5 min after dye instillation. This time interval allowed the height of the tear meniscus to decay back to its habitual level. Recordings made during this period verified that meniscus height was stable prior to data collection.

Results: Tear meniscus height increased following a blink ($p = 0.021$; Friedman test). The rate of increase was not linear, but slowed with time. However, despite its statistical significance, the average change in 10 s was small in comparison with average tear meniscus height and inter-subject variation.

Conclusions: The height of the inferior tear meniscus minimally increases after a blink. Standardisation of the time interval between its assessment and the preceding blink will be advantageous in clinical research trials. However, owing to their small size, these changes are unlikely to be of clinical importance.

The perceived depth of a dot cloud is the centroid of the disparities

D. R. T. Keeble[a], *J. Harris*[b] *and I. Pacey*[a]
[a]Department of Optometry, University of Bradford, Bradford, UK
[b]School of Psychology, University of St Andrews, St Andrews, UK

Purpose: There is an evidence that a number of visual properties such as position and texture orientation (Whitaker *et al.*, 1996; Keeble, *et al.*, submitted) are encoded as the centroid (i.e. mean) of the distribution of the relevant variable. Although the perception of stereoscopic depth has been extensively investigated, little is known about how separate estimates of disparity are combined to produce an overall perceived depth.

Methods: Using base-in prisms mounted on a trial frame and half-images presented on a computer screen, we produced stereoscopic images of dot clouds (e.g. as in Harris and Parker, 1995) with skewed (i.e. asymmetrical) distributions of disparity. Subjects were required to judge in a 2-alternative-forced-choice task whether the dot cloud was in front of, or behind, an adjacent flat plane of dots. Psychometric functions were generated and the point of subjective equality was calculated. Three subjects were employed.

Results: For dot clouds of thickness up to about 6 arc min disparity the perceived depth was close to the centroid for all three subjects, regardless of skew. For thicker clouds, (thicknesses up to 25 arc min were tested), the perceived depth was slightly closer to the subject than the centroid, regardless of skew.

Conclusion: The human visual system integrates depth information vertically for thin surfaces. For thick surfaces, the dots closest to the observer have a higher weighting, presumably due to their greater salience.

References

Harris, J. M. and Parker, A. J. (1995) Independent neural mechanisms for bright and dark information in binocular stereopsis. *Nature* **374**, 808–811.
Keeble, D. R. T., Kingdom, F. A. A. and Morgan, M. J. The perceived orientation of line textures. *J. Vis.* Submitted.
Whitaker, D., McGraw, P. V., Pacey, I. and Barrett, B. T. (1996). Centroid analysis predicts visual localisation of first- and second-order stimuli. *Vision Res.* **36**, 2957–2970.

Effects of global shape on angle discrimination

G. J. Kennedy, H. S. Orbach and G. Loffler
Department of Vision Sciences, Glasgow Caledonian University, Glasgow, UK

Purpose: Previous studies have been inconclusive as to whether angle discrimination can be predicted by a model based on the sensitivity of orientation discrimination mechanisms, or by a model based on specialised mechanisms. However, these studies have assumed that angle discrimination is independent of the overall shape of which the angle forms a part. We aimed to test the validity of this assumption.

Methods: We measured angle discrimination using angles that were parts of different triangular shapes: isosceles triangles (sides forming the angle were of identical length), scalene triangles (sides were of different lengths), and triangles where the length of each side defining the angle was varied randomly across and within trials. Triangles were either defined by an outline or by a dot at the location of each corner. Within trials, we varied the stimulus size (up to $\pm 70\%$) and the overall orientation of the triangles (up to $\pm 10°$), in order to eliminate any cue to the task other than the angle itself. Subjects were asked to judge which of two successively presented angles was more obtuse.

Results: Angle discrimination thresholds, for both outlined and dot triangles, were lowest when the stimuli were isosceles triangles. Performance was poorer by a factor of 2.2 for scalene triangles, and by a factor of 3.2 for the random condition.

Conclusions: These results show that performance in angle discrimination tasks is strongly dependant on the stimulus shape. This implies that geometric angles are computed by mechanisms that are sensitive to the global geometry of the stimulus. Furthermore, our results can explain the inconsistencies found in previous studies of angle discrimination.

Changes in tear physiology and corneal sensitivity after cataract surgery

S. Khanal[a], *A. Tomlinson*[a] *and L. Esakowitz*[b]
[a]Department of Vision Sciences, Glasgow Caledonian University, Cowcaddens Road, Glasgow, UK
[b]Department of Ophthalmology, Royal Alexandra Hospital, Paisley, UK

Purpose: To identify any changes in tear film physiology and corneal sensitivity after cataract surgery (phacoemulsification) and determine the efficacy of tear supplement in the treatment of resulting dry eye symptoms.

Methods: The design of the study was longitudinal, parallel, randomised and single masked. A total of 18 patients (average age 74 years, seven males and 11 females) undergoing phacoemulsification were recruited and divided into three groups of six. The first group was the control, second and third groups were given either saline or tear supplement (Refresh Soothe: Allergan, High Wycombe, Bucks, UK) to use after the surgery. Tear production,

evaporation, structure and osmolality along with corneal sensitivity were measured before, and 3 days, 2 weeks, 1 month and 3 months after the surgery.

Results: Statistically significant detrimental changes were seen in all parameters of tear physiology ($p < 0.005$) and corneal sensitivity threshold ($p = 0.006$) immediately after the surgery. In the 3 months following surgery, a gradual recovery was seen in all of the assessed parameters in all groups. However, none of the values had been restored to baseline in the 3 months. There was no significant difference between the groups using saline or a tear supplement in the improvement of tear physiology and corneal sensitivity after the surgery.

Conclusions: There is deterioration in tear film properties and corneal sensitivity after phacoemulsification. However, a substantial improvement takes place within 3 months of the surgery. Tear supplements may not be required unless the patient has specific complaints of dry eye.

A novel method for measuring vernier acuity at short test distances in children

J. Little, J. S. Lauritzen and K. J. Saunders

Department of Vision Sciences, University of Ulster, Cromore Road, Coleraine, Northern Ireland, Ireland

Purpose: It is accepted that vernier acuity reflects cortical processing (Levi *et al.*, 1985). This has been measured as low as 5.1 s of arc (Li *et al.*, 2000). Such low thresholds combined with the resolution limitations of commercially available cathode ray tubes (CRTs) have necessitated large test distances (around 20 m). As such test distances are problematic for children, we designed a protocol to measure vernier acuity using a CRT at short test distances (1.5 m).

Methods: A total of 74 children aged 5–11 years with visual acuity better than 0.175 LogMAR were tested wearing best correction. Vernier thresholds were calculated using a novel protocol (Little *et al.*, 2005). A modified contrast masking protocol was used to display a sub-pixel offset. Contrast thresholds were obtained using a 2-alternative forced choice (2-AFC) QUEST adaptive staircase procedure, from which equivalent vernier acuity in seconds of arc was calculated. Grating resolution thresholds were measured in seconds of arc using a similar 2AFC procedure.

Results: Thresholds for grating and vernier acuity were obtained from 94.6% of children: vernier thresholds were significantly lower (paired t-test $t = 37.56$, $p = 0.00$). The ratio of grating to vernier thresholds ranged from 3.49 in the youngest subjects, to 2.65 in the oldest. A significant improvement with increasing age was found for grating resolution thresholds. This value was 2.25 s of arc per year (linear regression $r = 0.62$, $p < 0.0001$). Vernier thresholds did not change significantly with age.

Conclusion: The novel testing protocol confirms the notion that Vernier thresholds are lower than grating resolution thresholds, and that Vernier acuity remains stable through ages 5–11, unlike grating acuity.

References

Levi, D. M., Klein, S. A. and Aitsebaomo A. P. (1985) Vernier acuity, crowding and cortical magnification. *Vision Res.* **25**, 963–977.

Li, R. W., Edwards, M. H. and Brown, B. (2000) Variation in Vernier acuity with age. *Vision Res.* **40**, 3775–3781.

Little, J., Lauritzen, J. S., and Saunders, K. J. (2005) A novel computer-based method for measuring Vernier acuity at short test distances. *Invest. Ophthalmol. Vis. Sci.* **46**: (Abstract No. 5647).

Central corneal thickness and its association with diagnostic indicators of glaucoma

G. T. Mahalingam, I. E. Pacey, J. M. Gilchrist and J. B. Ares-Gomez

Department of Optometry, University of Bradford, Bradford, UK

Purpose: A low central corneal thickness (CCT) has been associated with an increased risk of developing glaucomatous optic nerve head (ONH) damage and an increased rate of progression in established glaucoma. This study aimed to investigate the relationship between CCT and previously identified diagnostic indicators for glaucoma.

Methods: A cross-sectional study of 39 clinically normal controls and 19 patients with primary open angle glaucoma (POAG) was undertaken. The ophthalmic examination included: CCT measurement using ultrasound pachymetry, ONH tomography (Top SS Topographic Scanning System: Laser Diagnostics Technologies, San Diego, CA, USA), nerve fibre layer thickness measurement using scanning laser polarimetry (GDxVCC: Carl Zeiss Meditec, Jena, Germany) and axial length measurement using partial coherence interferometry (IOL Master, Carl Zeiss Meditec). Data from the right eye of the controls and from the eye with the greatest visual field defect of the patients with glaucoma were analysed.

Results: In the control group, there was no significant relationship between the variation in CCT and the measured variables with the exception of cup-disc (CD) ratio for which a thin CCT was associated with a smaller CD ratio ($p = 0.011$). This is opposite to the relationship found in the patients with glaucoma whereby a thin CCT was associated with a larger CD ratio ($p = 0.017$). The slopes of these two regression functions were significantly different ($p < 0.001$). Similar significant differences ($p < 0.001$) in regression functions between the groups were found for other ONH and nerve fibre layer measures.

Conclusion: In controls, there was little evidence of significant association between CCT and diagnostic indicators for glaucoma. In patients with glaucoma, however, a low CCT was associated with greater severity of glaucomatous damage.

Failure to consider the extrafoveal contrast deficit leads to excessive spatial scaling

D. R. Melmoth[a] *and J. M. Rovamo*[b]

[a]Department of Optometry and Visual Science, City University, London, UK

[b]School of Optometry and Vision Sciences, Cardiff University, Cardiff, UK

Purpose: To determine whether 'double-scaling', i.e. scaling of both size *and* contrast dimensions, provides a more accurate explanation of letter perception across the visual field than spatial scaling alone.

Methods: Contrast sensitivities for letter identification were measured over a range of stimulus sizes and retinal locations to determine whether qualitative or quantitative differences exist in extrafoveal performance. E_2 values, which quantify the retinal eccentricity at which stimulus size and contrast must double to maintain foveal performance levels, were calculated.

Results: As previously reported, extrafoveal low-contrast letter recognition shows two quantitative deficits relative to the fovea. One reflects a change in local spatial scale, which becomes systematically coarser with increasing retinal eccentricity due to a dramatic decrease in cortical processing resources in peripheral vision. Compensation for this requires spatial magnification of stimuli. The other extrafoveal deficit is a size-independent decrease in the utilisation of contrast energy, stemming from reduced efficiency relative to an ideal observer. Compensation for this requires increased stimulus contrast. Scaling extrafoveal data according to spatial and contrast E_2 values revealed that this 'double-scaling' returns a much larger spatial E_2 value than if the data are *only* spatially scaled, as has previously been done. This means stimuli need less magnification in peripheral vision. Furthermore, the data are more accurately scaled to the foveal data curve by using double-scaling.

Conclusions: 'Double-scaling' quantifies the simultaneous but independent changes in local spatial *and* contrast scales across the visual field. Moreover, when combined with the appropriate contrast-scaling factor for a given eccentricity, much less spatial magnification is needed. This indicates that spatial scaling alone, when contrast scaling is also actually needed, may have produced artificially small E_2 values

for visual tasks, and may help explain the large range of spatial E_2 values previously reported for different tasks.

Loss of positional information when tracking multiple moving dots: attentional capacity vs working memory

S. Narasimhan, S. P. Tripathy and B. T. Barrett
Department of Optometry, University of Bradford, Bradford, UK

Purpose: To investigate the relative roles of attention and visual working memory in multiple object tracking.

Methods: Thresholds were measured for identifying the direction of deviation in a single bilinear trajectory (target) in the presence and absence of other linear undeviating trajectories (distractors). All trajectories moved from the left half to the right half of the screen along fixed random orientations. In the first experiment, the stimuli were presented over several frames while in the second experiment the equivalent information was presented within a single frame. In both the experiments, the distractor trajectories terminated at the vertical mid-line of the display, while the target trajectory alone continued on the right half of the display having undergone a deviation at the vertical mid-line. Set-size effects were studied by varying, between blocks, the number of distractor trajectories presented.

Results: If attentional capacity is the limiting factor in this task, we expect that set-size effects should be more pronounced when the information is presented in a single frame compared with when it is distributed over multiple frames. Deviation thresholds rose steeply when the number of distractors was increased from zero (typical threshold = 2°) to three (threshold typically over 20°) when the trajectory information was distributed across multiple frames. However, contrary to the above prediction, deviation thresholds remained relatively unchanged in single frame presentations as the number of distractors was increased. Observers had no difficulty in detecting the direction of deviation of the target trajectory even when the number of distractor trajectories was increased to nine.

Conclusions: Our results suggest that the set-size effects in the current multiple object-tracking task arise from limitations of working memory and not attentional capacity.

The effect of simulated visual function loss on reaching and grasping movements

S. Pardhan, C. Gonzalez-Alvarez and A. Subramanian
Department of Optometry and Ophthalmic Dispensing, Anglia Polytechnic University, East Road, Cambridge, UK

Purpose: Although vision plays an important role in guiding the hand to reach and grasp an object, very few studies have investigated how visual deficits affect these movements. This study aims to study the effect of simulated visual impairment on prehensile indices of reaching and grasping.

Methods: Ten volunteers with normal vision (mean age 24.5 years) were recruited. Subjects were instructed to pick up a cylindrical object under normal viewing conditions, and in the presence of positive blur (+3.00 DS and +6.00 DS). A motion analysis system (Vicon 460: Oxford Metrics Ltd, Oxford, UK) was used to record and reconstruct 3D hand and finger movements. The transport component was assessed by measuring maximum wrist velocity, time to maximum velocity (expressed as a percentage of the total time) and total movement time. The grasp component was measured as the maximum grip aperture.

Results: Repeated measures ANOVA revealed that, as the level of blur increased, maximum wrist velocity decreased ($p < 0.05$). Maximum grip aperture and the relative time taken to reach maximum velocity increased with lower visual acuity ($p < 0.05$).

Conclusions: Reduced vision affects both the transport and grasp components of reaching and grasping, as well as the organisation of these movements. This has clinical implications for low vision patients.

Acknowledgement: Supported by the College of Optometrists and RDS grant (Anglia Polytechnic University).

The effect of changing stimulus parameters on reading in dyslexics and controls

C. S. Porter and C. M. Dickinson
Faculty of Life Sciences, University of Manchester, Manchester, UK

Purpose: To determine the effects of changing stimulus parameters on reading rate in dyslexic and control adults. The dyslexic subjects had used coloured overlays (or Precision Tinted Spectacles) for at least 1 year and these had been prescribed on the basis of anomalous visual effects and/or an improvement in the reading rate with the Wilkins Rate of Reading Test (Wilkins *et al.*, 1996).

Methods: Reading rate was measured in 70 subjects (35 control, 35 dyslexic) under eight different experimental conditions using variations of the Wilkins Rate of Reading Test. (1) Normal rate of reading: black text on white background. (2) White text on a black background (3) Brightfield magnifier, (4) Visual Tracking Magnifier (VTM) (5) Typoscope (6) Text 1.7x bigger (7) Text in narrow columns (8) Using the preferred coloured overlay.

Results: The controls read faster than the dyslexics in all experimental conditions ($p < 0.01$). The control group had their reading slowed by the VTM and Brightfield magnifiers ($p < 0.001$) and by the typoscope ($p = 0.005$) and narrow columns ($p < 0.001$). There was no statistical difference in the reading speed for any of the other conditions. The dyslexic group had an improvement in their reading speed with the coloured overlay ($p < 0.001$). There was no statistical difference in reading speed for any of the other conditions for dyslexic subjects.

Conclusion: Coloured overlays are of benefit to some dyslexics as a way to improve reading speed. The Visual Tracking Magnifier does not benefit dyslexics with reading.

Reference

Wilkins, A. J., Jeanes, R. J., Pumfrey, P. D. and Laskier, M. (1996) Rate of reading test: its reliability, and its validity in the assessment of the effects of coloured overlays. *Ophthal. Physiol. Opt.* **16**, 491–497.

Investigation of candidate loci for familial non-syndromic human strabismus

A. Rice[a,b], *F. Cassidy*[b], *G. A. Williams*[b], *J. Hoole*[c], *E. Sheridan*[d], *I. G. Simmons*[c], *C. Toomes*[b], *B. T. Barrett*[a], *D. B. Elliott*[a] *and C. Inglehearn*[b]
[a]Department of Optometry, University of Bradford, Bradford, UK
[b]Molecular Medicine Unit, St James's University Hospital, Leeds, UK
[c]Eye Department, St James's University Hospital, Leeds, UK
[d]Clinical Genetics, St James's University Hospital, Leeds, UK

Purpose: Strabismus (squint) is a misalignment of the visual axes affecting approximately 2–5% of the population. Twin and family studies suggest a substantial genetic component, especially for esotropia (an inward deviation) in Caucasians. However, the association of strabismus with a variety of chromosomal abnormalities and with prematurity and birth trauma suggests genetic complexity and an environmental component to causation. To date, no genes have been implicated in concomitant strabismus, but one susceptibility locus, STBMS1, on chromosome 7p22, has been described.

Methods: We have ascertained over 100 families with two or more individuals affected by esotropia and/or hyperopia (greater than or equal to +1.50 D). Thus far, we have sampled a panel of 74 Caucasian individuals from 10 pedigrees, including four larger families. In this panel, we carried out a preliminary linkage screen of several candidate loci. Markers were tested covering the STBMS1 locus, the whole of chromosome 21 and loci on chromosomes 8p23 and 15q26. Chromosome 21 markers were tested as Down syndrome children have a higher incidence of esotropia with an accommodative element, compared with those children with strabismus associated with other syndromes. The 8p23 and 15q26 markers were tested because of an observation of two siblings with esotropia carrying a balanced 8p:15q translocation.

Results: None of the families reveal a pattern of inheritance consistent with linkage to the susceptibility locus, STBMS1; however, most of the families examined were too small to give definitive exclusion. Neither do any of the other markers tested show statistically significant evidence of linkage.

Conclusions: These data do not support the existence of a major susceptibility locus for esotropia in association with hyperopia on chromosome 7p. Consequently, these results provide further evidence of genetic heterogeneity.

Corneal neuropathy in keratoconus and contact lens wearers

L. Simo[a], *C. O'Donnell*[a] *and C. Tromans*[b]

[a]University of Manchester, PO Box 88, Manchester, UK

[b]Department of Optometry, Manchester Royal Eye Hospital, Oxford Road, Manchester, UK

Background: Corneal nerves play a vital role in the maintenance of a healthy corneal epithelium. Transient loss of corneal sensitivity occurs in rigid gas permeable (RGP) and soft contact lens wearers but relatively little is known about corneal nerve structure and function in keratoconic patients. Controversy often exists as to whether the corneal scarring seen in keratoconus is related to the necessity of RGP contact lens wear or to the unknown aetiology of the disease.

Case reports: Three cases are presented to illustrate the possible differences in corneal nerve structure and function in controls, RGP contact lens wearers and keratoconic patients. Nerve appearance was assessed using a ConfoScan 3 confocal microscope (Nidek Co., Gamagori, Japan). Nerve function was assessed using contact and non-contact corneal aesthesiometry. Slit lamp biomicroscopy, topographical ultrasonic pachometry and videokeratoscopy were performed to indicate the severity of the keratoconus and to enable comparisons between subjects.

Results: Confocal images revealed a higher level of tortuosity and reflectivity in the nerves of the keratoconic patient compared with the other subjects. Nerve diameter and orientation was also found to be different. Corneal sensitivity was decreased in the RGP contact lens wearer and in the keratoconic subject compared with the control subject. As expected, central corneal thickness was similar in the normal subject and the RGP contact lens wearer but was reduced in the keratoconic patient.

Conclusions: The changes in nerve structure as observed using confocal microscopy (increased thickness, tortuosity, reflectivity and orientation) in the keratoconic patient may explain why on slit lamp examination the corneal nerves appeared much more visible. A better understanding of the corneal nerve structure and function in keratoconic patients could assist in diagnosis and management of the condition.

Direction discrimination in random dot kinematograms: effect of dot density, displacement size and coherence level

N. Syed, S. P. Tripathy and M. J. Cox

Department of Optometry, University of Bradford, Bradford, UK

Purpose: When detecting direction of motion in random dot kinematograms (RDKs), threshold coherence is independent of dot densities (Downing and Movshon, 1989; Barlow and Tripathy, 1997), but the maximum displacement limit is dependent on dot density (Eagle and Rogers, 1997). In estimating threshold coherence, displacement size is fixed at an optimal level, whereas in estimating maximum displacement limit, coherence is typically 100%. We investigate the effect of dot density and displacement size on motion detection performance at different coherence levels.

Methods: In experiment 1, we investigated the effect of varying dot density (0.13–26.67 dots deg^{-2}) and displacement size (1–100 arc min) on the direction discrimination performance at coherence of 30%. In experiment 2, experiment 1 was repeated but for displacement sizes 50–200 arc min at 100% coherence. In experiment 3, we varied the coherence for each displacement (1–100 arc min) so that performance was 80–90% correct for the lowest dot density at each displacement.

Results: At 30% coherence, the effect of dot density on performance is minimal; at 100% coherence performance dropped rapidly as the dot density increased; at variable coherence, for high coherence levels performance was affected by dot densities. As predicted by the correspondence noise hypothesis, performance is affected by large displacements and high coherence levels (Tripathy and Barlow, 2001).

Conclusion: Under appropriate conditions, each of the factors, dot density, displacement size and coherence level can affect motion direction discrimination performance.

References

Barlow, H. and Tripathy, S. P. (1997) Correspondence noise and signal pooling in the detection of coherent visual motion. *J. Neurosci.* **17**, 7954–7966.

Downing, C. J. and Movshon, J. A. (1989) Spatial and temporal summation in the detection of motion in stochastic random dot displays. *Invest. Ophthalmol. Vis. Sci.* **30**, 72.

Eagle, R. A. and Rogers, B. J. (1997) Effects of dot density, patch size and contrast on the upper spatial limit for direction discrimination in random-dot kinematograms. *Vision Res.* **37**, 2091–2102.

Tripathy, S. P. and Barlow, H. B. (2001) Unified theory for threshold coherence and D_{max} in random dot kinematograms. *Perception* **30**, 32.

Three presentations of monocular vision loss, secondary to Hollenhorst plaque formation, leading to the diagnosis of carotid artery disease

M. E. Trego[a,b] *and J. M. Pagani*[a,c]

[a]Pennsylvania College of Optometry, Philadelphia, PA, USA

[b]School of Optometry and Vision Sciences, Cardiff University, Cardiff, UK

[c]Nemours Health Clinic, Wilmington, DE, USA

Background: Carotid artery disease is estimated to affect 30% of persons over age 50. Risk factors include hypertension, cigarette smoking, hyperlipidemia and diabetes mellitus. Symptoms ascribed to carotid artery lesions with stenosis of the artery or plaque formation include monocular vision loss, transient ischemic attacks and ischemic strokes. Patients can present with monocular vision loss as their initial symptom.

Case reports: Three patients from a geriatric clinic in Wilmington, Delaware presented with different complaints of vision loss with similar overall outcomes. Patient A was an 87-year-old female who presented with blurry vision on extreme left head turn. Dilated left fundus examination revealed a Hollenhorst plaque. Carotid Doppler examination revealed 50–79% left internal carotid stenosis with no hemodynamic stenosis of the right internal carotid. Patient B was a 78-year-old female who presented with a right superior altitudinal defect and transient vision loss in the right eye. Dilated right fundus examination revealed a Hollenhorst plaque. Carotid Doppler examination revealed 50–79% carotid stenosis in both the left and right

internal carotids. Patient C was an 84-year-old man who complained of a right superior altitudinal visual field defect. Dilated right fundus examination revealed a Hollenhorst plaque. Carotid Doppler examination revealed 50–79% carotid stenosis in both the left and right internal carotids.

Conclusions: These three presentations reveal that through proper management of patients over 50 years of age who present with chief complaints of monocular vision loss, a differential diagnosis of carotid artery disease must be considered. Patients who exhibit Hollenhorst plaques are at an increased risk for both cardiovascular and cerebrovascular disease. Appropriate measures for confirming a diagnosis include Doppler ultrasound imaging and magnetic resonance angiography. Invasive surgical techniques such as carotid angioplasty and carotid endarterectomy may be recommended.

The effect of attentional load on perimetric thresholds

K. Weaver, I. E. Pacey and D. R. T. Keeble
Department of Optometry, University of Bradford, Bradford, UK

Purpose: It is well known that changing the attentional load in a psychophysical task will frequently change the threshold. This study investigated the effect on the threshold and threshold variability of directing attention in a perimetric examination.

Methods: Attention was manipulated during a perimetric examination by reducing the area in which a stimulus could occur. This was achieved using a custom program of the Humphrey Field Analyser 750 (Carl Zeiss Meditec, Dublin, CA, USA) to test the stimulus locations within each quadrant. Standardised instructions informed the patient which quadrant was being examined on each occasion. All four quadrants and a complete Program 30–2 test were performed in a balanced order design and repeated at a second visit. The Full Threshold strategy was used for all examinations. Data from the four quadrant tests were compared with the corresponding quadrants of the complete 30–2 central field test for a group of healthy young and for a group of healthy elderly volunteers.

Results: The overall mean sensitivity of the quadrant tests was 0.66 dB higher than that for the complete 30–2 test (repeated measures ANOVA: $p < 0.0001$). For the quadrant tests, the between-subject threshold variability for the individual stimulus locations was reduced by on average eight percent in the elderly group and by 10 percent in the younger group. In addition, the combined test duration of the quadrant tests was on average 1 min 3 s quicker than for the Full Field test ($p < 0.0001$). There was no significant difference in the test–retest variability between the full field and quadrant tests for either age group.

Conclusion: When perimetry is performed by combining a series of reduced area tests, thus reducing attentional load, the mean sensitivity is higher, threshold variability is reduced and the combined test takes less time than when the whole central field is examined. This has the potential to improve the ability to detect variations from normality.